

**DESIGN, SYNTHESIS, AND EVALUATION OF DENDRIMERS BASED ON
MELAMINE AS DRUG DELIVERY VEHICLES**

A Dissertation

by

JONG DOO LIM

Submitted to the Office of Graduate Studies of
Texas A&M University
in partial fulfillment of the requirements for the degree of

DOCTOR OF PHILOSOPHY

August 2007

Major Subject: Chemistry

**DESIGN, SYNTHESIS, AND EVALUATION OF DENDRIMERS BASED ON
MELAMINE AS DRUG DELIVERY VEHICLES**

A Dissertation

by

JONG DOO LIM

Submitted to the Office of Graduate Studies of
Texas A&M University
in partial fulfillment of the requirements for the degree of

DOCTOR OF PHILOSOPHY

Approved by:

Chair of Committee,	Eric E. Simanek
Committee Members,	Brian T. Connell
	Francois P. Gabbai
	Allison R. Ficht
Head of Department,	David H. Russell

August 2007

Major Subject: Chemistry

ABSTRACT

Design, Synthesis, and Evaluation of Dendrimers Based on Melamine as Drug Delivery Vehicles. (August 2007)

Jong Doo Lim, B.S., Korea University;

M.S., Korea University

Chair of Advisory Committee: Dr. Eric E. Simanek

A variety of dendrimers based on melamine are designed, synthesized, and evaluated for drug delivery systems. The synthesis of a dendrimer, including multiple copies of four orthogonally reactive groups, is described. The three groups on the surface are nucleophilic and include four free hydroxyl groups, four *tert*-butyldiphenylsilyl (TBDPS) ether groups, and sixteen amines masked as *tert*-butoxycarbonyl (BOC) groups. The core of the dendrimer displays two electrophilic monochlorotriazines. The dendrimer above is further manipulated for *in vivo* biodistribution: incorporation of the reporting groups Bolton-Hunter and DOTA (1,4,7,10-tetraazacyclododecane-1,4,7,10-tetraacetic acid); PEGylation for biocompatibility and size tuning. In preliminary biodistribution studies, dendrimers circulate in the blood for a longer time as the molecular weight increases, which is important to passively target tumor tissues via the EPR effect. Also, high uptake by the tumor tissues was observed in mice bearing prostate cancer xenografts.

A drug delivery vehicle for the anticancer agent paclitaxel is described. This drug delivery vehicle contains sixteen molecules of paclitaxel via acid-labile ester linkage,

two Bolton-Hunter groups, and sixteen monochlorotriazine groups for PEGylation. The in vitro drug release studies shows faster release of paclitaxel at lower pH in PBS.

DEDICATION

To Injeong

ACKNOWLEDGEMENTS

I especially thank my advisor, Dr. Eric Simanek, for giving me the opportunity to explore the dendritic world and for his kind guidance. He has always been supportive of my research, offering both insightful advice and smiles.

My thanks also goes to my committee members, Dr. Francois Gabbai, Dr. Allison Rice-Ficht, and Dr. Brian Connell for their support and comments.

I am grateful to Dr. Xiankai Sun, Yi Guo, and Mai Lin at UT Southwestern for the biodistribution data of the third chapter.

I must thank my first advisor Dr. Hogyu Han for his support, guidance, and enjoyable conversations about chemistry and life.

A hearty thanks to the whole Simanek group filled with friendly people and great chemists. Current members: Dr. Abdellatif Chouai, Karlos Moreno, Hannah Crampton, Meredith Mintzer, and Vincent Venditto. Former members: visiting professor Yoshikazu Kitano, Dr. Hui-Ting Chen, Dr. Emily Hollink, and Susan Hatfield.

I am indebted to my parents who have continued to support and encourage me throughout my entire life. Without their care, I couldn't have gotten this far. To my sister Miseon, thank you for everything you shared with me.

My final thanks goes to my lovely wife, Injeong. With your endless support and love, my life at home and work has been full of joy and energy.

TABLE OF CONTENTS

	Page
ABSTRACT	iii
DEDICATION	v
ACKNOWLEDGEMENTS	vi
TABLE OF CONTENTS	vii
LIST OF FIGURES	ix
LIST OF SCHEMES	xi
LIST OF TABLES	xii
 CHAPTER	
I INTRODUCTION	1
Dendrimers: Concepts, Types, and Syntheses	1
Drug Delivery Vehicles	8
II SYNTHESIS OF A DENDRIMER WITH FOUR ORTHOAGONALLY REACTIVE GROUPS	16
Introduction	16
Results and Discussion	18
Conclusions	23
Experimental	23
General Procedures	23
Experimental Procedures	23

CHAPTER	Page
III POST-SYNTHETIC MANIPULATIONS OF A MELAMINE DENDRIMER AND IN VIVO BIODISTRIBUTION	30
Introduction	30
Results and Discussion	32
Post-Synthetic Manipulations of 1	32
Preliminary In Vivo Biodistribution Studies	36
Conclusions	42
Experimental	42
General Procedures	42
Experimental Procedures	43
IV SYNTHESIS AND CHARACTERIZATION OF A DENDRIMER BASED ON MELAMINE THAT RELEASES PACLITAXEL	51
Introduction	51
Results and Discussion	53
Part 1. Synthesis of Dendrimer 1	54
Part 2. Synthesis of the Paclitaxel Conjugate	55
Part 3. Synthesis of Dendrimers 2-4	57
Part 4. Characterization	58
Part 5. In Vitro Studies of Paclitaxel Release	62
Conclusions	64
Experimental	64
General Procedures	64
Experimental Procedures	65
V SUMMARY	75
REFERENCES	77
APPENDIX A	84
APPENDIX B	112
APPENDIX C	136
VITA	172

LIST OF FIGURES

FIGURE	Page
1.1	Divergent and convergent synthetic routes to dendrimers 2
1.2	Architecture of dendrimers: (a) PPI; (b) PAMAM; (c) polyester; (d) triazine-based dendrimer 3
1.3	Relative reactivity of various amines for the substitution of a monochlorotriazine 7
1.4	Polymeric architectures for therapeutics 7
1.5	Polymer-drug conjugates to passively target tumor tissues via EPR effect and cellular uptake by endocytic internalization 9
1.6	The design of drug delivery system using dendrimers 10
1.7	A library of dendrimers based on melamine used in cytotoxicity studies 12
1.8	Drug-polymer conjugates with a variety of linkers: (a) 5-fluoro-2'-deoxyuridine-polymer conjugate with acetal linkage; (b) FA-MTX-PAMAM conjugate; (c) poly(RCOOH- <i>co</i> -BA- <i>co</i> -PDSA)- drug conjugate; (d) doxorubicin-HPMA conjugate 13
2.1	Dendrimer 1 in atomic and schematic detail 18
2.2	Mass spectrograms of 2-9, and 1 acquired by ESI-TOF or MALDI-TOF MS 22
3.1	Copper (II) complexing macrocyclic chelators 30
3.2	Potential post-synthetic manipulation of 1 31
3.3	MALDI-TOF mass spectra of 8 and 12 35
3.4	GPC traces of PEGylated dendrimers containing Bolton-Hunter (a) or DOTA groups (b) 35
3.5	Time-concentration plot of dendrimers in the blood 36

FIGURE	Page
3.6 Two-compartment open model kinetics following intravenous injection	38
3.7 Biodistribution data of ^{125}I -labeled dendrimers	39
3.8 Coronal PET images of a ^{124}I -labeled dendrimer in a tumor-bearing mouse	40
3.9 Post-PET biodistribution data of a ^{124}I -labeled dendrimer (~17 kDa) in nude mice with PC-3-Luc xenografts at 48 h post-injection	41
4.1 ^1H NMR assignment and integration of 2 in the expanded region 4.8 to 8.2 ppm	58
4.2 The MALDI-TOF spectrum of 2	59
4.3 The analytical GPC chromatogram obtained using 0.1 M NaNO_3 (aq) as an eluent with a RI detector	60
4.4 ^1H NMR of the PEGylated paclitaxel conjugates 4a and 4b purified from dialysis	61
4.5 Paclitaxel release from 4a and 4b in PBS buffers (pH 4.0, 5.5, and 7.4) at 37 °C and a HPLC chromatogram showing paclitaxel released from the conjugates	63

LIST OF SCHEMES

SCHEME	Page
1.1 Synthesis of dendrimers: (a) G2 PAMAM by a divergent route and (b) G2 polyether by a convergent route	5
2.1 Synthesis of 1	20
3.1 Synthesis of PEGylated dendrimers with Bolton-Hunter reagent	32
3.2 Synthesis of PEGylated dendrimers with DOTA	33
4.1 Summary of the chemistries reported including paclitaxel conjugation and PEGylation	53
4.2 Synthesis of a precursor dendrimer for drug conjugation	54
4.3 Modifications of paclitaxel	56

LIST OF TABLES

TABLE		Page
1.1	Drug-polymer conjugates and micelles in clinical trials	8
3.1	A library of dendrimers (2-7) for biodistribution study	34
3.2	Pharmacokinetic data of the ¹²⁵ I-radiolabeled dendrimers	37
4.1	Analysis and characterization of 4a and 4b	62

CHAPTER I

INTRODUCTION

The unique properties of dendrimers, which are rarely found in conventional polymers, have captured the intense attention of many researchers over decades: multivalency, a well-defined globular structure, mono or low polydispersity, large internal space for host-guest interactions, and availability of multiple functionalities. Due to such properties, dendrimers have been investigated for a variety of applications such as catalysis, medical diagnostics, sequestration of small molecules, and drug delivery.¹⁻¹⁵ In this study we focus on the development of potent drug delivery vehicles, exploring dendrimers based on 1,3,5-triazine building blocks.

Dendrimers: Concepts, Types, and Syntheses

The term dendrimer was originated from the Greek *dendron* (tree or branch) and *meros* (part) by the analogy of its structure. The dendritic structure is composed of a core, an interior shell, and a multivalent periphery. The core and interior shell is well protected from the surroundings by the periphery, providing microenvironments to encapsulate guest molecules, such as hydrophobic drugs and catalysts. The multivalent periphery is very useful to introduce synthetic or biological entities to the polymeric system for diverse purposes.

This dissertation follows the style and format of *Journal of the American Chemical Society*.

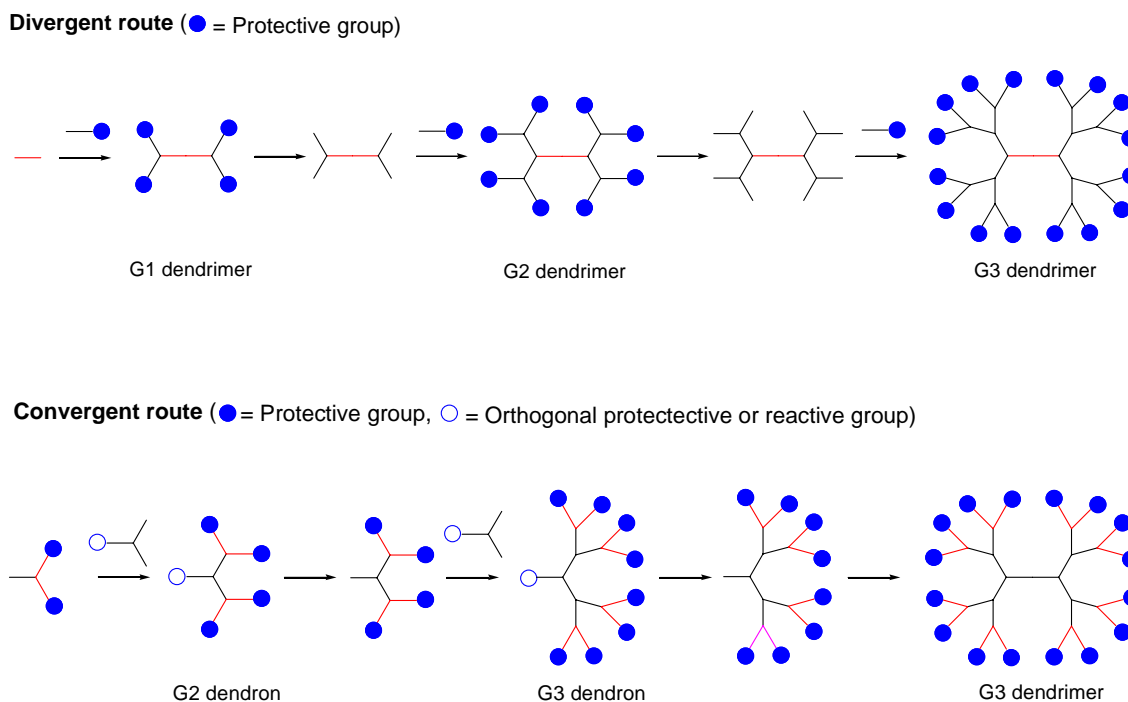


Figure 1.1. Divergent and convergent synthetic routes to dendrimers.¹⁶

Though the highly branched globular polymer seems woven and complicated, it actually displays symmetrical and repetitive architecture, which can be stepwise constructed by reiterative reactions with functional monomers. The synthesis of dendrimers is conducted in two different ways, either divergently or convergently (Figure 1.1). In the divergent synthesis,¹⁷ dendrimers are synthesized from the core to the surface step by step. Polypropylene imines (PPI) and polyamidoamines (PAMAM) are well-known and commercially available dendrimers synthesized in this route. On the other hand, in the convergent approach¹⁸ developed by Frechét *et al.*, the dendrimer is synthesized from the surface as the starting point and ended up at the core. Generally, the convergent synthetic approach facilitates purification process due to the smaller

number of the reactive sites as well as the incorporation of multiple functional groups on the periphery, while the divergent approach is useful for the synthesis of high generation dendrimers and large-scale synthesis.

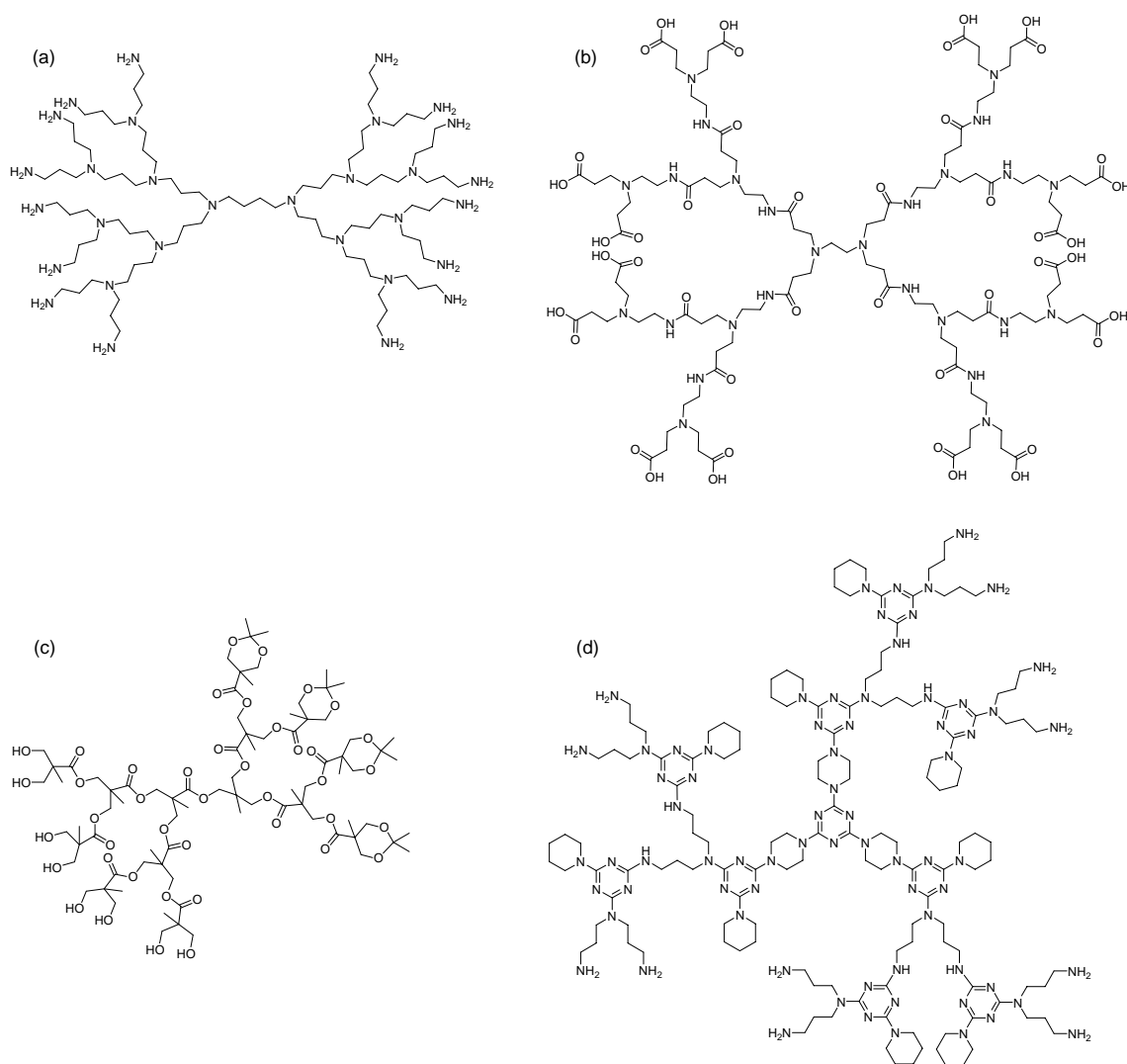


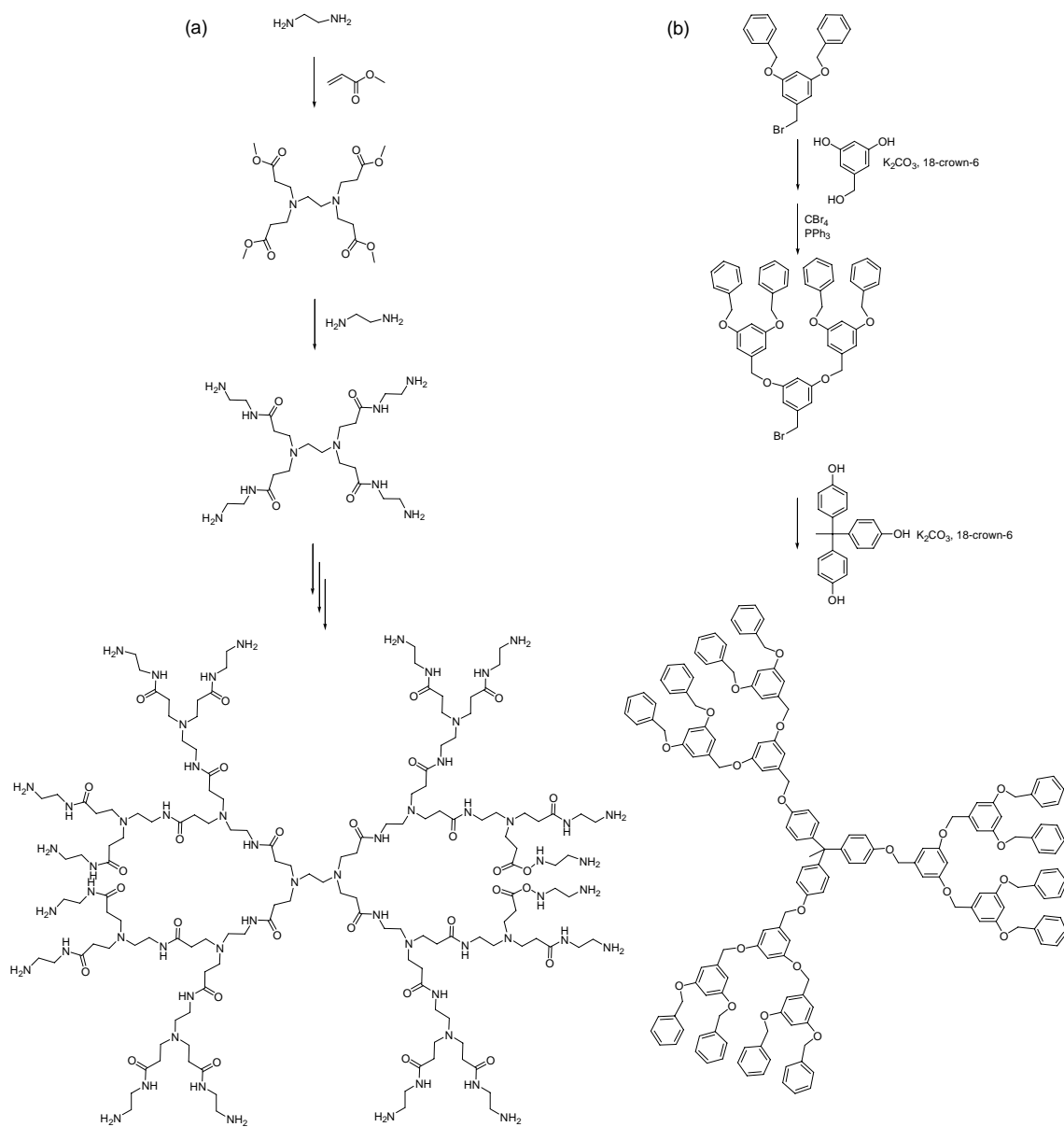
Figure 1.2. Architecture of dendrimers: (a) PPI; (b) PAMAM; (c) polyester; (d) triazine-based dendrimer.

Figure 1.2 shows the dendritic architecture broadly being used for diverse applications. PPI structures developed mainly by Vögtle and Meijer^{19,20} can be constructed by Michael addition of 1,4-diaminobutane to acrylonitrile and the subsequent reduction of the nitriles to primary amines. The iterative reaction process can be repeated to produce higher generation dendrimers. However, more defects and higher polydispersity are often observed in the synthesis of high generation PPI due to a large number of reactive sites on the surface.

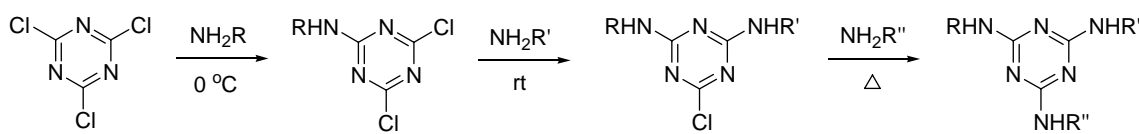
Tomalia's PAMAM dendrimers²¹⁻²³ have been most widely investigated and commercially available. PAMAM can be prepared from a diamine by divergent growth (Scheme 1.1). The first intermediate, star PAMAM (CO₂Me)₄, is synthesized from Michael addition of 1,2-diaminoethane to methyl acrylate. The reaction of the resulting intermediate with the excess of 1,2-diaminoethane gives the tetraamine-terminated PAMAM. The iterative reactions are needed to produce higher generation PAMAM dendrimers.

The bow-tie design by Gillies and Fréchet is based on polyesters.^{24,25} Two polyester dendrons are covalently linked. One dendron has free hydroxyl groups for the attachment of poly(ethylene oxide) (PEO) and the other dendron has acetal protecting groups for further manipulation such as drug conjugation and radiolabeling. Another Fréchet-type dendrimer is based on polyethers and prepared by convergent growth (Scheme 1.1). The polyether dendrimers that derive from the 3,5-dihydroxybenzyl alcohol group have been investigated for diverse purposes: self-assembling, catalysis, light harvest, and encapsulation.²⁶⁻³¹

Scheme 1.1. Synthesis of dendrimers: (a) G2 PAMAM by a divergent route and (b) G2 polyether by a convergent route



The 1,3,5-triazines broadly used for preparation of herbicides are also employed to the synthesis of dendrimers.³²⁻⁵⁰ The advantages of triazine dendrimers mainly derive from their synthetic versatility. Chlorines on the triazine ring can be stepwise substituted with various nucleophiles via the mechanism of nucleophilic aromatic substitution. The differential reactivity of triazine chlorides on nucleophiles can be further regulated with reaction temperature.³³ For instance, dichlorotriazines can be obtained from the reaction of cyanuric chloride ($C_3N_3Cl_3$) with a nucleophilic amine (RNH_2) at low temperature. Subsequent reaction with another amine ($R'NH_2$) at room temperature can afford monochlorotriazines. The excess amount of amines or high reaction temperature is often required to substitute the chlorine of monochlorotriazine. Thus, the differential reactivity of chlorotriazine derivatives allows us to prepare compositionally diverse dendrimers with high purity and simplicity.^{34,35}



Mackay and Simanek³³ demonstrated the chemoselective reactivity of a variety of amines with a monochlorotriazine. The 2-chloro-4,6-dimorpholino-1,3,5-triazine was used to conduct the competition reactions. Figure 1.3 shows relative substitution rates in the competition reactions of various amines with the monochlorotriazine.

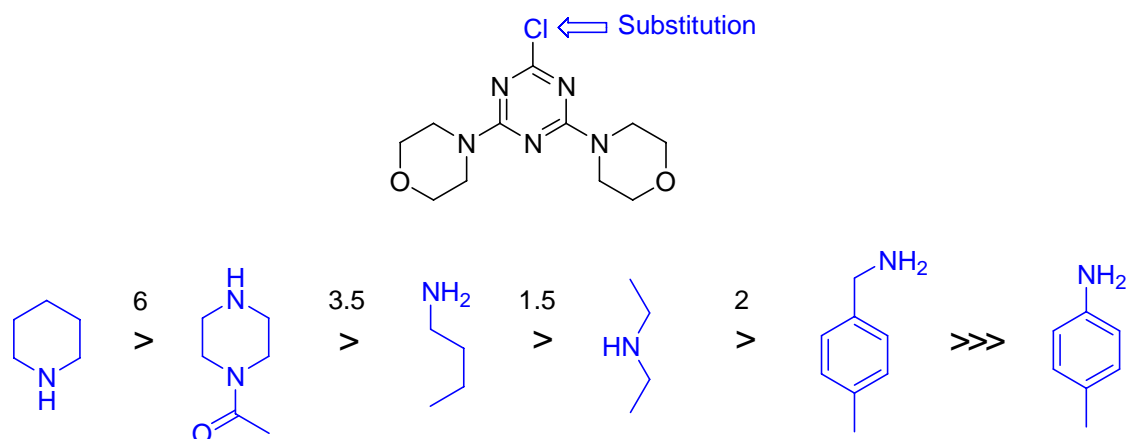


Figure 1.3. Relative reactivity of various amines for the substitution of a monochlorotriazine.³³

The chemoselective reactivity of triazine chlorides and amine nucleophiles gives a variety of benefits for the synthesis of dendrimers, including multi-functional groups on the surface, single-pot synthesis, precise control on the dendritic composition and structure, and facile postsynthetic manipulation.

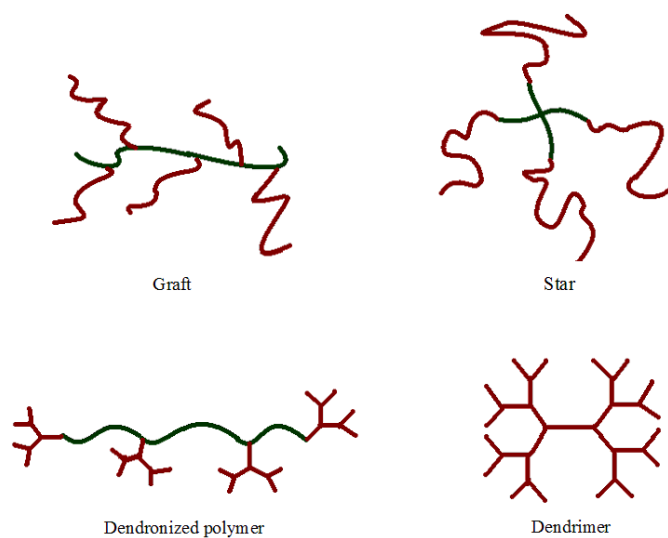


Figure 1.4. Polymeric architectures for therapeutics.

Drug Delivery Vehicles

Polymeric architecture including stars, grafts, dendronized polymers, and dendrimers has been explored to develop delivery-vehicles for therapeutic agents (Figure 1.4).^{10,13,14,51-57} Globular multi-functional dendrimers are more versatile as drug-carriers, compared to linear mono-functional polymers. However, such dendrimers are often challengeable to synthesize and hardly available in the market. As a result, most of drug-polymer conjugates in clinical trials were prepared by using linear or graft polymers (Table 1.1).^{14,58}

Table 1.1. Drug-polymer conjugates and micelles in clinical trials.

Compound	Linker	Status of development
doxorubicin-HPMA copolymer (PK1)	amide	phase II
galactosamine-doxorubicin-HPMA copolymer (PK2)	amide	phase I/II
doxorubicin-aspartic acid-PEG micelle (NK911)	amide/free drug	phase I
paclitaxel-HPMA copolymer (PNU166945)	ester	phase I
paclitaxel-polyglutamate (CT2103)	ester	phase II/III
camptothecin-PEG (Prothecan)	alanine ester	phase II
camptothecin-polyglutamate (CT2106)	ester	phase I
diamineplatinum (II) HPMA copolymer (AP5280)	amide	phase I

Many drugs have obstacles to be directly used in clinical therapy due to low solubility in physiological conditions, instability, low biopermeability, or systemic toxicity. Synthetic/biopolymers have promising characteristics to become efficient drug-

carriers, overcoming such challenges. For example, hydrophilic polymers can be linked to the drug to improve the solubility in aqueous media. Conjugation and encapsulation using polymers are a useful way to shield the drugs from the environment before released at the target area and to reduce toxicity during delivery. Also, cell-penetrating peptides can be employed to the drug-carriers to improve biopermeability.

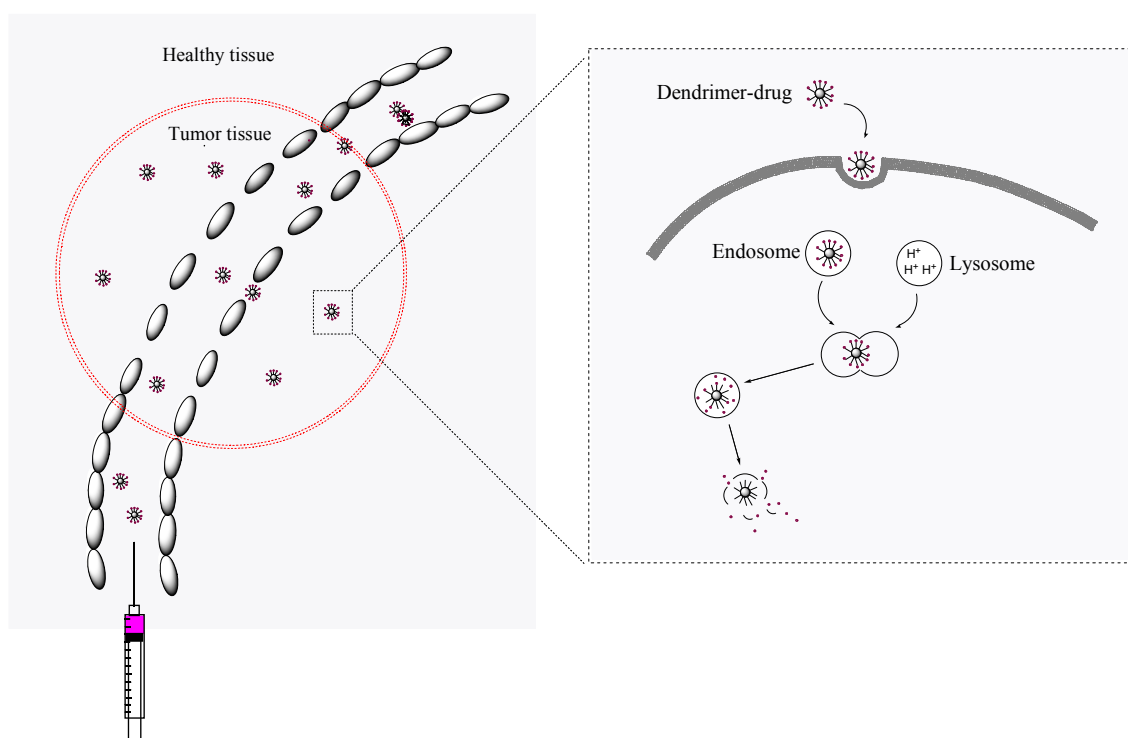


Figure 1.5. Polymer-drug conjugates to passively target tumor tissues via EPR effect and cellular uptake by endocytic internalization.^{14,16}

Another important advantage of polymer-drug conjugates comes from molecular sizes. Maeda and coworkers^{59,60} reported that large macromolecules had a passive selectivity for various types of tumors due to a leaky angiogenic tumor vasculature and the lack of lymphatic drainage, which was termed the enhanced permeability and retention time (EPR) effect (Figure 1.5). Typically, the defective pores of the tumor vasculature show the range of size 200 to 600 nm.⁶¹ By tailoring the size of drugs (over 80% of marketed drugs are smaller than MW 500 Da) with polymers, the drug-polymer conjugates (> 20 kDa) may be efficiently accumulated on the tumor cells with prolonged circulation time in blood, and then internalized into the cell by endocytosis.^{62,63}

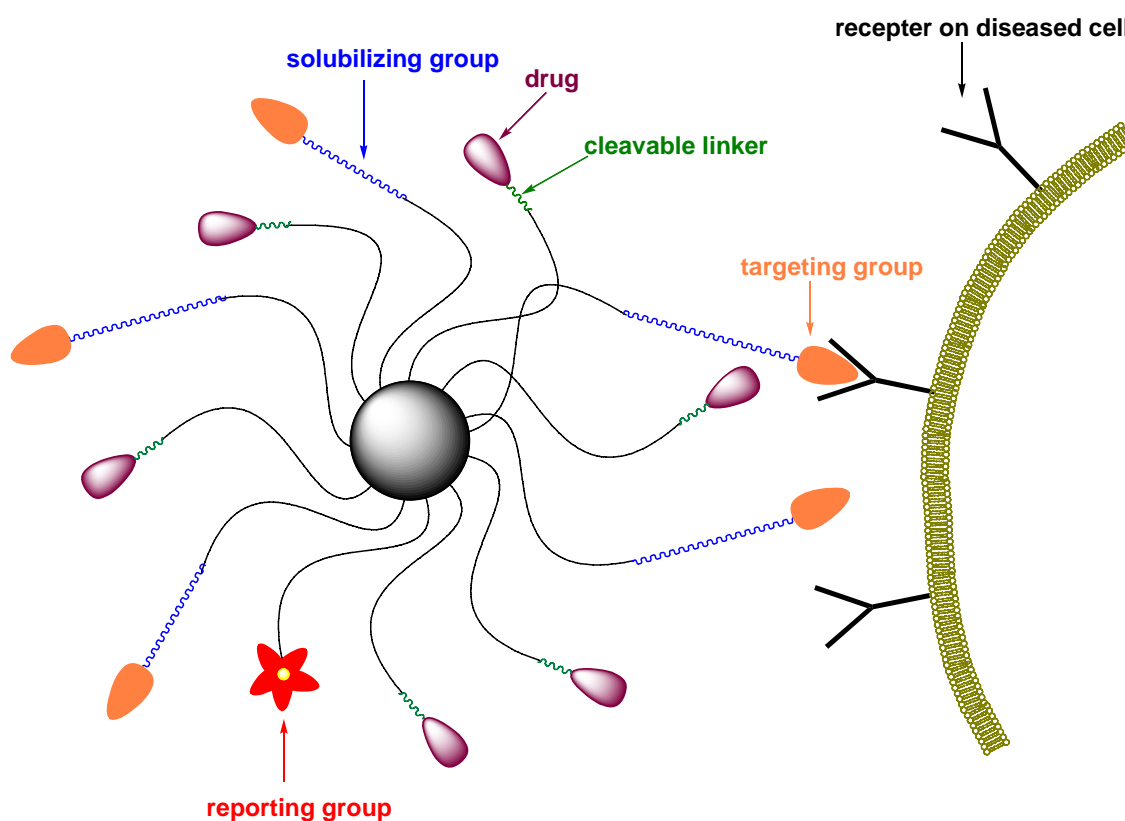


Figure 1.6. The design of drug delivery system using dendrimers.

In order to design efficient drug delivery system, we need to consider the followings (Figure 1.6): biocompatibility (nontoxic, nonimmunogenic, and soluble in physiological conditions), targeting groups, drug loading capacity with controlled release, and reporting tags (radio or fluorescent tags). Dendrimers containing a large number of reactive sites and multiple functional groups are advantageous to incorporate all these molecules of interest.

Recent toxicity studies of cationic (amino-terminated) and anionic (carboxylate-terminated) PAMAM dendrimers have revealed that cationic polymers have a significantly higher cytotoxicity on various cell lines.⁶⁴⁻⁶⁷ The high toxicity of cationic dendrimers is explained by strong interaction between the cationic dendrimer and the negatively charged cell membrane, causing cell lysis. Also, less flexible and globular dendrimers show lower cytotoxicity compared with flexible and linear dendrimers, which can be explained by weaker adherence to cellular surfaces due to less flexibility of globular structures.^{16,68,69} Cytotoxicity studies with dendrimers based on melamine were performed by Chen and Simanek *et al.*^{37,44} As outlined in Figure 1.7, the library of dendrimers comprised of **1-2** (cationic), **3-5** (anionic), and **6** (neutral). While the cationic dendrimers **1** and **2** showed significant cytotoxicity even at low concentrations (< 0.01 mg/mL), the anionic **3**, **4** and **5** showed little cytotoxicity at the same concentrations. The PEGylated dendrimer **6** displayed little cytotoxicity even at high concentrations (0.1-10 mg/mL). Thus, the conjugation of terminal amine groups with PEG chains enhanced biocompatibility of triazine-based dendrimers.

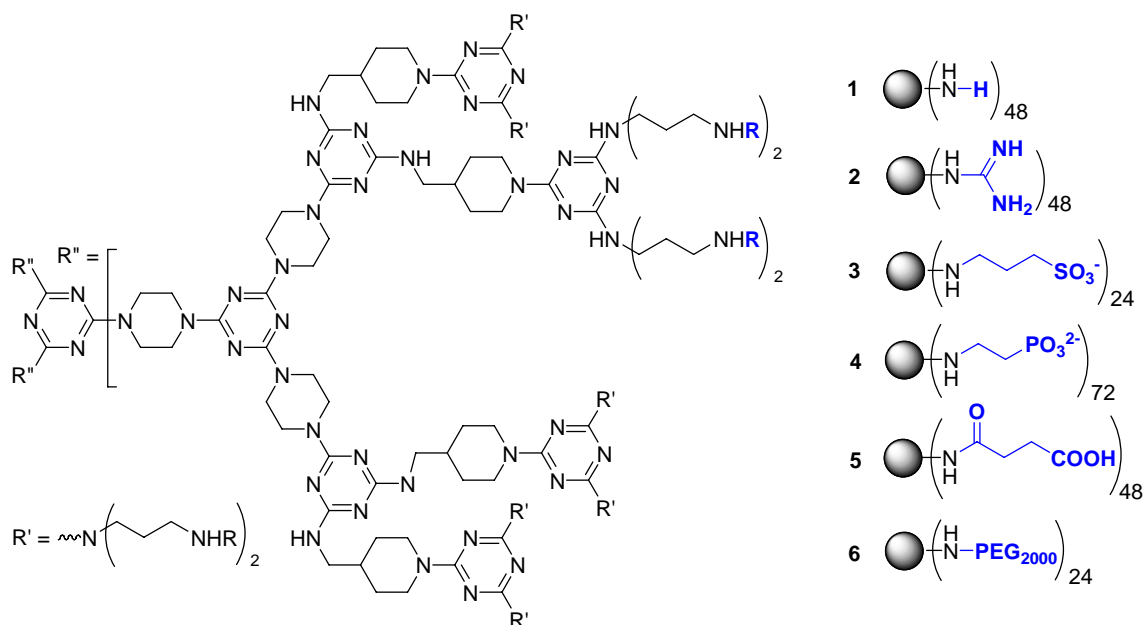


Figure 1.7. A library of dendrimers based on melamine used in cytotoxicity studies.

Two strategies are employed to dendritic drug delivery: encapsulation and conjugation. In research on drug encapsulation by Kono *et al.*,^{70,71} PAMAM dendrimers based on ethylenediamine are used to encapsulate the anticancer drugs, doxorubicin and methotrexate. The acid-base interactions between the drugs and the basic hydrophobic interior of PAMAM dendrimers afforded the high capacity of drug loading and slow release. However, the controlled release of drugs would be a hard problem to solve, since the encapsulation and release of drugs by dendrimers are highly dependable on the structures and compositions of drugs and dendrimers. The alternative drug-dendrimer conjugation will take more advantages of regulating the loading and release of drugs by using desirable linkers. A variety of degradable linkages have been used for drug-

delivery vehicles including acid-labile bonds,⁷²⁻⁷⁹ disulfide,⁸⁰⁻⁸² and enzyme-cleavable bonds⁸³⁻⁸⁵ (Figure 1.8).

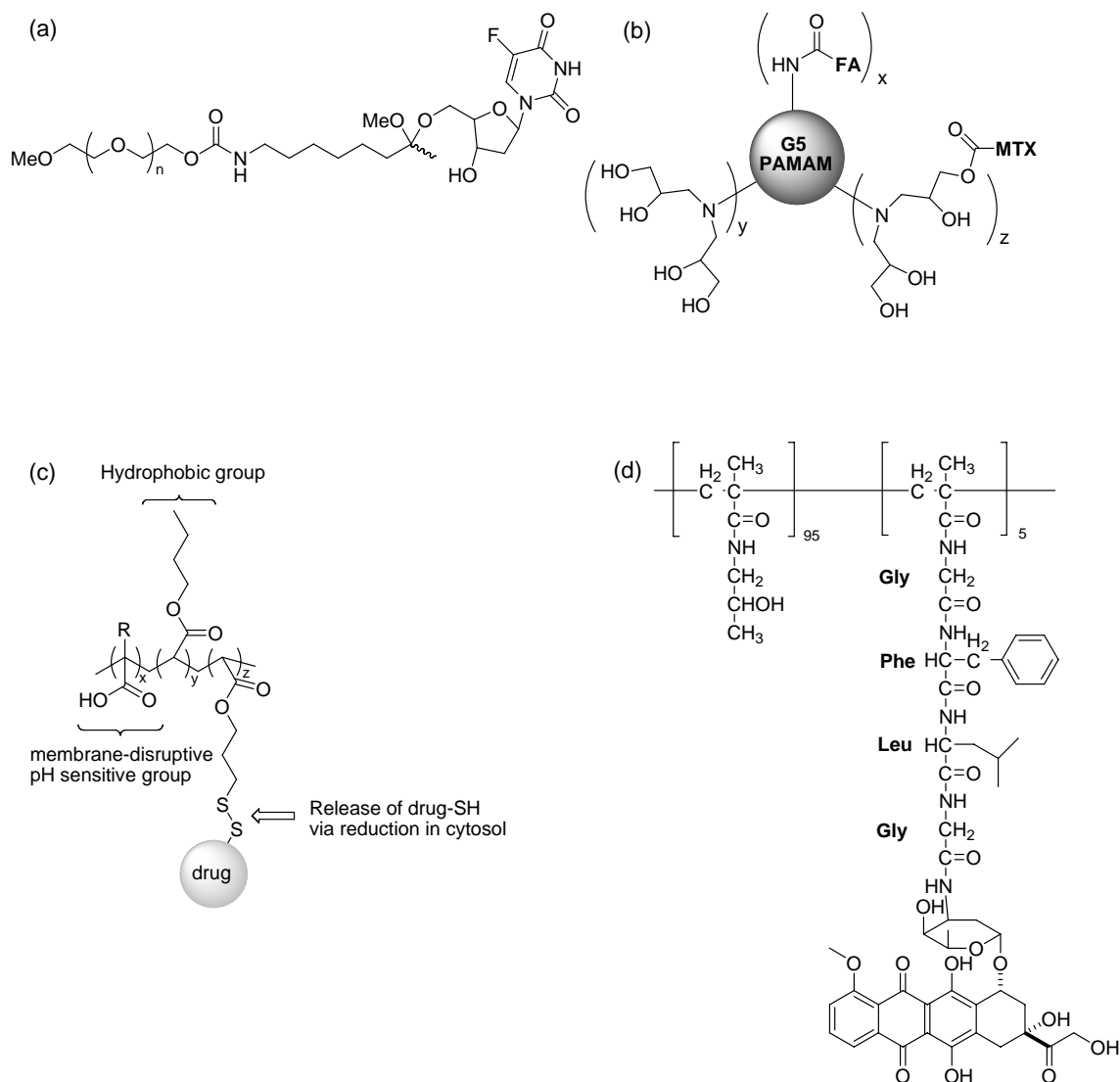


Figure 1.8. Drug-polymer conjugates with a variety of linkers: (a) 5-fluoro-2'-deoxyuridine-polymer conjugate with acetal linkage; (b) FA-MTX-PAMAM conjugate; (c) poly(RCOOH-co-BA-co-PDSA)-drug conjugate; (d) doxorubicin-HPMA conjugate.

Acid labile linkers such as ester, acetal, and hydrazone have been extensively used for drug conjugation, as the drug release can be triggered at the acidic environment (pH 6.5~4.0) of endosome and lysosome during endocytosis. Figure 1.8 (a) shows the anticancer agent 5-fluoro-2'-deoxyuridine that is conjugated to linear PEG via an acetal linker.⁷⁵ Hydrolysis study of the drug-conjugate at pH 5.0 displayed over 90% release of the drug after 10 min incubation at 37 °C. Baker and coworkers⁷⁷ reported a drug-delivery vehicle based on G5 amine-terminated PAMAM dendrimers (Figure 1.8 (b)). Folic acid (FA) was conjugated to the terminal amines as targeting ligands, and the residue of cationic amines were masked by using glycidol to reduce toxicity. The anticancer drug methotrexate (MTX) was then conjugated via ester linkage. The MTX-conjugates with FA effectively killed receptor-expressing cells by receptor-mediated endocytosis.

Recent studies have showed that glutathione (GSH), L- γ -glutamyl-L-cysteinylglycine, is significantly overexpressed in tumor cells of various regions such as breast, lung, ovary, bone marrow, and colon, as compared with the adjacent normal cells.^{86,87} The high level of GSH in many cancer tissues allows us to control drug delivery in more efficient manner by using thiol-disulfide exchange. As shown in Figure 1.8 (c), Hoffman and Stayton *et. al.*⁸² designed pH-responsive and membrane-destabilizing polymers with glutathione-reactive disulfide bonds. The polymer conjugates comprise of three components: pH responsive groups (alkyl acrylic acid monomers), hydrophobic groups (butyl acrylate monomers), and drug carrier groups (pyridyl disulfide acrylate (PDSA) monomers). The polymers are ionized and

hydrophilic at physiological pH, but they become more hydrophobic in acidic endosome, disrupting the membrane to be released into the cytoplasm. Glutathione in the cytosol can accelerate the drug release by reducing the disulfide bond of the conjugates.

Also, Gly-Phe-Leu-Gly peptidyl linkers have been used for the enzymatic cleavage by the lysosomal protease cathepsin B in endocytosis.⁸³ The doxorubicin-HPMA copolymer conjugate (PK1) was the first member of the drug-polymer conjugates in clinical trials (Figure 1.8 (d)). *N*-(2-hydroxypropyl) methacrylamide (HPMA) copolymer extensively used for polymer therapeutics was conjugated to the anticancer drug doxorubicin (about 8 wt%) by using the tetrapeptidyl linker. In phase I evaluation, the maximum tolerated dose (MTD) of PK1 was 320 mg/m² doxorubicin equivalents, which was a fivefold increase relative to free doxorubicin.^{58,88,89}

In the following chapters, the design and synthesis of dendrimers with orthogonal functional groups are discussed, and followed by post-synthetic manipulations and in vivo biodistribution studies. A drug delivery vehicle for the anticancer drug paclitaxel is also addressed.

CHAPTER II

SYNTHESIS OF A DENDRIMER WITH FOUR ORTHOGONALLY REACTIVE GROUPS*

Introduction

We, and the drug-delivery community, have been intrigued by dendrimers for use as drug delivery vehicles.¹⁰⁻¹⁴ These highly branched, globular macromolecules present well-defined (often uniquely monodisperse) structures, a large number of reactive surface groups, and may afford passive selectivity for tumors based on the enhanced permeability and retention time (EPR) effect.⁵⁹ Much of the molecular details for optimizing these vehicles to function in the complex environment presented by an organism is poorly understood, but advances are being made by numerous investigators each favoring a specific subclass of dendrimers including polyesters,²⁴ poly(amidoamines),⁷⁹ poly(propylene imines),⁹⁰ and poly(amides).⁹¹ We favor triazines linked by diamines.³²⁻⁴⁵ The systematic replacement of chlorine atoms around the triazine ring of cyanuric chloride offers tremendous potential for compositional diversity and a hydrophobic interior for sequestering hydrophobic drugs.

Here, we employ control over composition to synthesize a dendrimer with four different groups of reactive sites. We envision that these sites will be used for

*Reproduced in part with permission from “Toward the next-generation drug delivery vehicle: Synthesis of a dendrimer with four orthogonally reactive groups” by Jongdoo Lim and Eric E. Simanek. *Mol. Pharm.* **2005**, *2*, 273-277. Copyright 2005 American Chemical Society.

i) conjugating drugs, ii) enhancing solubility and biocompatibility (PEGylation), iii) presenting biodistribution tags, and iv) displaying targeting ligands.

In our previous studies, we reported the synthesis of versatile dendrimer with five different functional groups, including free hydroxyls, levulinic acid esters, *tert*-butyldiphenylsilyl (TBDPS) ethers, pyridyl disulfide (PyrSSR) groups, and *tert*-butyloxycarbonate (BOC) protected amines.³⁴ The choice of these groups derived from Wong's orthogonally-protected sugars.⁹² This original, orthogonally reactive dendrimer, however, suffered from three issues that limited its potential role as a building block for manipulation. First, the levulinic acid ester groups and the pyridyldisulfides were not as chemically robust as the other protecting groups during the dendrimer synthesis. Accordingly, yields for reactions involving these groups were lower (~80%) compared with manipulations of the intermediate containing the other groups (>95%). Second, the dendrimer was more complex than necessary; only four unique groups of sites are believed to be required. Third, too many of the orthogonal groups were hydroxyl groups which are less reactive and less selective than the electrophilic triazines incorporated here. Here we describe a dendrimer, **1**, with four groups that are amenable for post-synthetic manipulation (Figure 2.1) that incorporates both nucleophilic and electrophilic sites. We envision that this dendrimer will serve as the basis for future studies of biodistribution and efficacy in tumor-bearing animals.

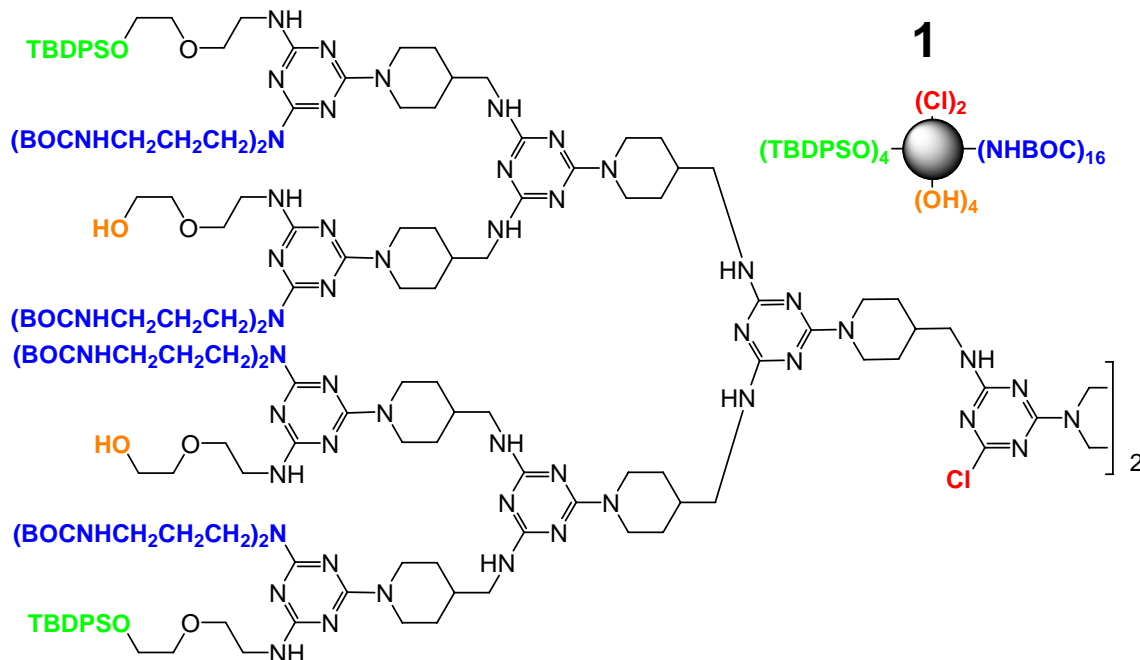


Figure 2.1. Dendrimer **1** in atomic and schematic detail.

Results and Discussion

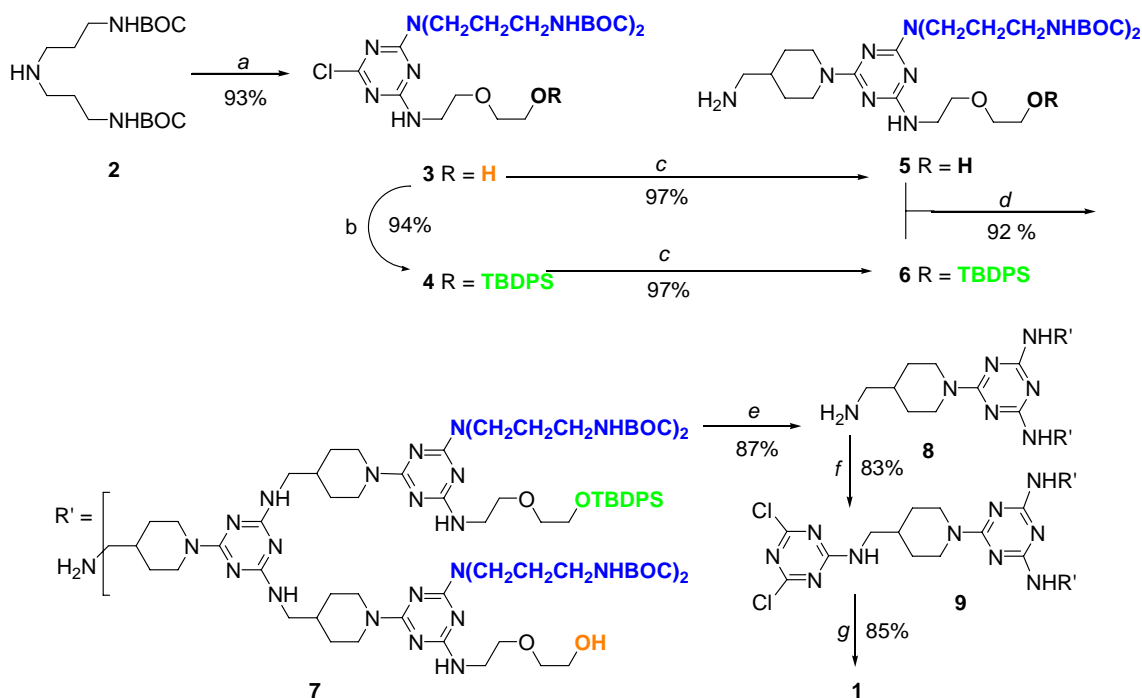
Dendrimer **1** was synthesized using a strategy similar to that of the original dendrimer described by our group.³⁴ This new dendrimer has a total of twenty-six reactive sites for manipulation. This architecture represents the current generation of dendrimers that we are exploring for drug delivery. Such a vehicle will carry a cargo of drugs linked by biolabile, covalent bonds, ligands for targeting, poly(ethylene glycol) (or PEG) for biocompatibility and tuning size which in turn affects circulation time and excretion route, and a beacon that indicates location. The hydroxyl groups are subject to acylation directly, or upon cleavage of the silyl ethers with tetrabutylammonium fluoride (TBAF) for further manipulation. The BOC groups can be unmasked to provide amines

amenable to multiple manipulation strategies. All three of these groups were present in the previous generation vehicle. However, here the levulinic esters and pyridyl disulfide groups have been replaced with monochlorotriazines. These groups react efficiently with amine nucleophiles: we have invested significant energies in the study of such groups and find that cyclic secondary amines are well suited to for this reaction.³³

The synthesis of dendrimer **1** is outlined in Scheme 2.1 and employs the convergent strategy¹⁸ in which the surface groups are elaborated iteratively toward the core group. Intermediate **2** is prepared by protecting the primary amines of 3,3'-diaminodipropylamine with BOC-ON.⁹³ Subsequent reactions with cyanuric chloride and 2-(2-aminoethoxy)ethanol respectively will produce monochlorotriazine **3**, which can selectively react with the secondary amine of 4-(aminomethyl)piperidine (4-AMP) to yield **5**. Using TBDPSCI, the free hydroxyl group of **3** is protected to afford **4**, and then reacted with 4-AMP to give **6**. The synthesis of **7** is conducted in a single-pot reaction by first reacting **6** with cyanuric chloride. The reaction is followed by adding **5** and then completed with the addition of 4-AMP. In a similar way, intermediate **7** is sequentially reacted with cyanuric chloride and then 4-AMP to give **8**. Dendrimer **1** was prepared in two steps from **8** through the intermediate dichlorotriazine **9** and subsequent dimerization with piperazine. The synthesis is executed in seven linear (8 total) steps from **2** to give the target dendrimer in 55% overall yield from the protected triamine. The route as described can be used to prepare moderate quantities of material. For example, intermediate **8** is useful for this dendrimer and related structures: it has been

prepared on 20 g scale. This effort takes between 7 and 8 days at this scale. The final dendrimer has been prepared on 6g scale.

Scheme 2.1. Synthesis of **1**^a



^a Reagents and conditions: (a) cyanuric chloride, DIPEA, THF, 0 °C, 2h; then 2-(2-aminoethoxy)ethanol with CH₃OH, rt, 24h; (b) TBDPS-Cl, imidazole, DIPEA, THF, rt, 4h; (c) 4-(aminomethyl)piperidine, THF, rt, 8h; (d) cyanuric chloride, DIPEA, THF, 0 °C, 2h; then **5**, rt, 24h; then 4-(aminomethyl)piperidine, 24h; (e) cyanuric chloride, DIPEA, THF, rt, 48h; then 4-(aminomethyl)piperidine, rt, 24h; (f) cyanuric chloride, DIPEA, THF, 0 °C, 5h; (g) piperazine, DIPEA, THF:CH₃OH=7:1, 0 °C to rt, 48h.

The synthesis is followed by mass spectrometry and NMR spectroscopy. Mass spectrometry is particularly valuable (Figure 2.2). With rare exception, the reaction proceeds spot-to-spot conversion as judged by thin layer chromatography and yields products that appear to be single compounds after chromatography. The mass spectra show lines corresponding to the protonated material and sodium and potassium ion adducts. Ladders of lines corresponding to loss of BOC groups that occur presumably during the ionization process are often observed for larger species. Doubly charged species are observed in the spectrogram of **1**, which are isotopically resolved adducts with H^+ , Na^+ , and K^+ as well as fragment peaks corresponding to loss of one and two BOC groups.

NMR spectroscopy also is diagnostic for the reactions, but interpretation is hampered by opportunities for the existence of slowly interconverting rotamers derived from hindered rotation about the triazine-NHR bond. These rotamers manifest themselves as broad lines in the proton NMR traces and often as double-lines in the ^{13}C NMR traces. Replacement of the chlorine atoms of monochlorotriazines with 4-(aminomethyl)piperidine typically simplifies the spectrum due presumably to either the reduction of rotamer number or the dissipation in the magnitude of the C-Cl dipole.

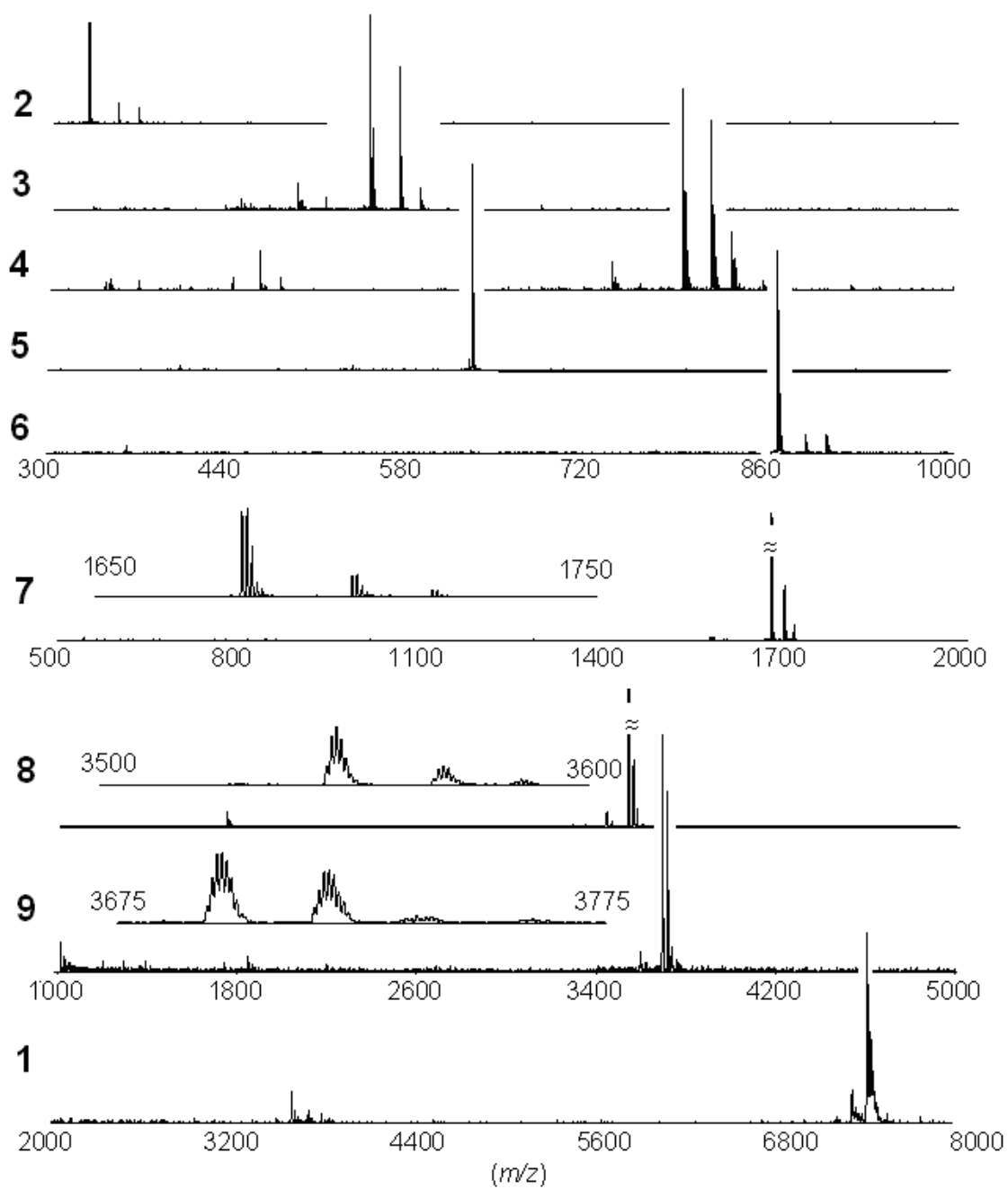


Figure 2.2. Mass spectrograms of **2-9**, and **1** acquired by ESI-TOF or MALDI-TOF MS.

Conclusions

We have prepared a versatile dendrimer with four orthogonally reactive groups: monochlorotriazine, free hydroxyl, TBDPS and BOC groups. Each of the functional surface groups can be readily utilized to improve solubility in physiological conditions, load drugs, link ligands or antibodies for targeting specific diseased cells and attach imaging agent for biodistribution assay. All of the synthetic steps are well established to afford the moderate scale preparation of the target.

Experimental

General Procedures

Chemicals were purchased from Aldrich and Acros and used without further purification. All solvents were ACS grade and used without further purification. NMR spectra were recorded on a Varian Mercury 300 MHz or Inova 500 MHz spectrometer in CDCl₃, MeOH-d₄, or CDCl₃:MeOH-d₄ (10:1). All mass spectral analyses were carried out by the Laboratory for Biological Mass Spectrometry at Texas A&M.

Experimental Procedures

Intermediate 2. A solution of BOC-ON (30.0 g, 122 mmol) in THF (150 mL) was added dropwise to an ice-bath cooled solution of 3,3'-diaminodipropylamine (8.5 mL, 60.9 mmol) and DIPEA (30mL, 172 mmol) in THF (150 mL). After the addition was complete, the reaction mixture was stirred for 4 h at room temperature, and the solvent was then removed by reduced-pressure evaporation. The residue was dissolved in dichloromethane and extracted with 5% NaOH (aq). The organic layer was dried over

MgSO₄ and then evaporated under vacuum. The resulting thick oil was precipitated from dichloromethane and petroleum ether to give **2** (17.1 g, 85%) as a white solid. ¹H NMR (300 MHz, CDCl₃) δ 3.21 (q, 4H), 2.66 (t, *J* = 6.5 Hz, 4H), 1.66 (m, 4H), 1.44 (s, 18H); ¹³C NMR (75 MHz, CDCl₃) δ 156.26, 79.13, 47.54, 39.05, 29.86, 28.55; MS (ESI-TOF) calcd for C₁₆H₃₃N₃O₄ 331.25, found 332.27 (M+H)⁺.

Intermediate 3. A reaction solution of **2** (5.0 g, 15.1 mmol) and DIPEA (8.0 mL, 46.0 mmol) in THF (150 mL) was cooled in a salt/ice-bath before cyanuric chloride (2.78 g, 15.1 mmol) was added. The solution was stirred for 2 h at low temperature. Subsequently, 2-(2-aminoethoxy)ethanol (3.0 mL, 30.0 mmol) and methanol (25 mL) were added to the reaction mixture. The reaction solution was stirred for 24 h. Following removal of the salts by filtration, the solution was evaporated under vacuum. The residue was dissolved in dichloromethane and washed with brine. The organic layer was dried over MgSO₄ and then evaporated under vacuum. The crude product was purified by silica gel chromatography (ethyl acetate:hexane = 3:1) to afford **3** (7.8 g, 93%). ¹H NMR (300 MHz, CDCl₃) δ 3.71 (br m, 2H), 3.62-3.47 (m, 10H), 3.07 (br m, 4H), 1.71 (m, 4H), 1.42 (s, 18H); ¹³C NMR (75 MHz, CDCl₃) δ 168.73, 165.46, 165.12, 156.29, 156.08, 79.40, 78.98, 72.54, 69.58, 69.38, 61.70, 44.14, 43.68, 41.17, 40.84, 38.38, 37.76, 36.95, 28.52, 28.25, 28.00, 27.88; MS (ESI-TOF) calcd for C₂₃H₄₂ClN₇O₆ 547.29, found 548.31 (M+H)⁺.

Intermediate 4. A solution of **3** (2.5 g, 4.6 mmol), TBDPS-Cl (1.4 mL, 5.3 mmol), imidazole (250 mg, 3.7 mmol), and DIPEA (0.90 mL, 5.2 mL) in THF (50 mL) was stirred for 4 h at room temperature and the solvent was then removed by reduced-

pressure evaporation. The residue was dissolved in dichloromethane, washed with brine, dried over MgSO_4 and evaporated under vacuum. The crude compound was purified by silica gel chromatography (ethyl acetate:hexane = 1:1) to give **4** (3.4 g, 94%) as a white solid. ^1H NMR (300 MHz, CDCl_3) δ 7.67 (m, 4H), 7.40 (m, 6H), 3.79 (m, 2H), 3.62-3.46 (m, 10H), 3.07 (br m, 4H), 1.73 (m, 4H), 1.44 (s, 9H), 1.42 (s, 9H), 1.05 (s, 9H); ^{13}C NMR (75 MHz, CDCl_3) δ 168.93, 165.50, 165.26, 156.31, 156.02, 135.68, 133.62, 129.81, 127.80, 79.34, 78.98, 72.52, 72.34, 69.84, 69.52, 63.50, 43.85, 43.51, 41.00, 37.55, 36.90, 28.56, 27.96, 27.79, 26.92, 26.68, 19.29; MS (MALDI-TOF) calcd for $\text{C}_{39}\text{H}_{60}\text{ClN}_7\text{O}_6\text{Si}$ 785.41, found 786.44 ($\text{M}+\text{H}$) $^+$.

Intermediate 5. Intermediate **3** (2.9 g, 5.3 mmol) was dissolved in THF (50 mL) and 4-aminomethyl piperidine (2.0 mL, 16.6 mmol) was added. The solution was stirred for 8 h at room temperature and then evaporated under vacuum. The residue was dissolved in dichloromethane, washed with brine, dried over MgSO_4 , and evaporated under vacuum. The product was purified by silica gel chromatography (dichloromethane:methanol = 7:1 with 1% NH_4OH) to give **5** (3.2 g, 97%) as a white solid. ^1H NMR (300 MHz, CDCl_3) δ 4.69 (br, 2H), 3.69 (t, $J = 4.5$ Hz, 2H), 3.58-3.55 (m, 10H), 3.02 (br s, 4H), 2.75 (t, $J = 12.2$, 2H) 2.57 (d, $J = 6.3$ Hz, 2H), 1.75-1.65 (m, 6H), 1.54 (br, 1H), 1.40 (s, 18H), 1.09 (m, 2H); ^{13}C NMR (75 MHz, CDCl_3) δ 165.96, 165.46, 164.58, 155.99, 78.83, 72.37, 69.97, 61.34, 47.71, 43.16, 42.11, 40.47, 39.44, 38.35, 37.03, 29.67, 28.44, 27.67; MS (MALDI-TOF) calcd for $\text{C}_{29}\text{H}_{55}\text{N}_9\text{O}_6$ 625.43, found 626.59 ($\text{M}+\text{H}$) $^+$.

Intermediate 6. Intermediate **4** (3.0 g, 3.84 mmol) was dissolved in THF (50 mL) and 4-aminomethyl piperidine (1.4 mL, 11.6 mmol) was added. The solution was stirred for 8 h at room temperature and then evaporated under vacuum. The residue was dissolved in dichloromethane, washed with brine, dried over MgSO₄, and evaporated under vacuum. The product was purified by silica gel chromatography (dichloromethane:methanol = 7:1 with 1% NH₄OH) to give **6** (3.1 g, 93%) as a white solid. ¹H NMR (500 MHz, CDCl₃) δ 7.68 (m, 4H), 7.39 (m, 6H), 4.73 (br, 2H), 3.79 (t, *J* = 5.3 Hz, 2H), 3.60-3.56 (m, 10H), 3.04 (br s, 4H), 2.77 (t, *J* = 11.3, 2H) 2.60 (d, *J* = 6.5 Hz, 2H), 1.76-1.69 (m, 6H), 1.55 (br, 1H), 1.42 (s, 18H), 1.11 (m, 2H), 1.04 (s, 9H); ¹³C NMR (125 MHz, CDCl₃) δ 166.12, 165.77, 164.86, 156.13, 135.69, 133.74, 129.72, 127.75, 79.05, 72.35, 70.26, 63.50, 47.97, 43.32, 42.14, 40.73, 39.74, 37.28, 36.96, 29.85, 28.61, 27.66, 27.04, 26.92, 26.79, 19.28; MS (MALDI-TOF) calcd for C₄₅H₇₃N₉O₆Si 863.55, found 864.54 (M+H)⁺.

Intermediate 7. Cyanuric chloride (404 mg, 2.19 mmol) was added to an ice-bath cooled solution of **6** (1.893 g, 2.19 mmol) and DIPEA (1.4 mL, 8.0 mmol) in THF (50 mL). The solution was stirred for 4 h at 0 °C before a THF solution (20 mL) of **5** (1.403 g, 2.24 mmol) was added. The solution was stirred for 24 h at room temperature. After the addition of 4-aminomethyl piperidine (3.0 mL, 25.0 mmol), the solution was stirred for an additional 24 h at room temperature and evaporated under vacuum. The residue was dissolved in dichloromethane, washed with brine, dried over MgSO₄, and evaporated under vacuum. The crude product was purified by silica gel chromatography (dichloromethane:methanol = 7:1 with 1% NH₄OH) to give **7** (3.4 g, 92%). ¹H NMR

(300 MHz, CDCl₃) δ 7.67 (m, 4H), 7.38 (m, 6H), 4.72 (br, 6H), 3.79 (t, J = 5.1 Hz, 2H), 3.73 (t, J = 4.4 Hz, 2H), 3.59-3.55 (m, 20H), 3.28 (br, 4H), 3.05 (br, 8H), 2.78-2.69 (br m, 8H), 1.77-1.70 (br m, 17H), 1.41 (s, 36H), 1.17 (m, 6H), 1.04 (s, 9H); ¹³C NMR (75 MHz, CDCl₃) δ 166.03, 165.78, 165.62, 164.86, 164.70, 156.15, 135.72, 133.77, 129.75, 127.78, 79.08, 72.37, 70.29, 70.15, 63.51, 61.76, 47.50, 46.28, 46.19, 43.33, 43.26, 42.43, 40.75, 38.90, 37.27, 30.03, 29.83, 28.63, 27.83, 26.95, 19.31; MS (MALDI-TOF) calcd for C₈₃H₁₃₉N₂₃O₁₂Si 1678.07, found 1679.27 (M+H)⁺.

Intermediate 8. Cyanuric chloride (170 mg, 0.922 mmol) was added to a solution of **7** (3.139 g, 1.87 mmol) and DIPEA (0.6 mL, 3.4 mmol) in THF (80 mL). The solution was stirred for 48 h at room temperature. After the addition of 4-aminomethyl piperidine (1.5 mL, 12.5 mmol), the solution was stirred for an additional 24 h, and then evaporated under vacuum. The residue was dissolved in dichloromethane, washed with brine, dried over MgSO₄, and evaporated under vacuum. The product was purified by silica gel chromatography (dichloromethane:methanol = 7:1 with 1% NH₄OH) to give **8** (2.85 g, 87%) as a white solid. ¹H NMR (500 MHz, CDCl₃) δ 7.67 (m, 8H), 7.37 (m, 12H), 4.70 (br, 14H), 3.79 (t, J = 5.3 Hz, 4H), 3.72 (br, 4H), 3.58-3.55 (m, 40H), 3.26 (br, 12H), 3.05 (br, 16H), 2.75 (br, 16H), 1.76-1.69 (br m, 37H), 1.41 (s, 72H), 1.16 (br, 14H), 1.03 (s, 18H); ¹³C NMR (125 MHz, CDCl₃) δ 165.83, 164.80, 156.14, 135.69, 133.74, 129.73, 127.76, 79.05, 72.42, 72.35, 70.27, 70.13, 63.49, 61.66, 46.14, 43.31, 43.24, 42.35, 40.73, 40.64, 37.20, 36.97, 30.01, 29.75, 28.62, 27.80, 26.93, 19.29; MS (MALDI-TOF) calcd for C₁₇₅H₂₈₉N₅₁O₂₄Si₂ 3545.25, found 3546.19 (M+H)⁺.

Intermediate 9. Cyanuric chloride (62 mg, 0.336 mmol) was added to an ice-bath cooled solution of **8** (800 mg, 0.226 mmol) and DIPEA (174 μ L, 1.0 mmol) in THF (20 mL). The reaction solution was stirred for 5 h at 0 °C and then evaporated under vacuum. The residue was dissolved in dichloromethane, washed with brine, dried over MgSO₄, and evaporated under vacuum. The crude product was purified by silica gel chromatography (ethyl acetate to dichloromethane:methanol = 8:1) to give **9** (690 mg, 83%) as a white solid. ¹H NMR (500 MHz, CDCl₃) δ 7.67 (m, 8H), 7.36 (m, 12H), 4.68 (br, 14H), 3.78 (t, *J* = 5.0 Hz, 4H), 3.70 (br, 4H), 3.57-3.54 (m, 40H), 3.24 (br, 14H), 3.03 (br, 16H), 2.73 (br, 14H), 1.72-1.68 (br, 37H), 1.39 (s, 72H), 1.14 (br, 14H), 1.02 (s, 18H); ¹³C NMR (125 MHz, CDCl₃) δ 170.83, 166.02, 164.73, 156.07, 135.61, 133.65, 129.66, 127.69, 78.96, 72.38, 72.26, 70.18, 63.42, 61.59, 46.78, 46.17, 43.20, 42.22, 40.66, 40.55, 37.18, 36.88, 29.95, 29.59, 28.55, 27.72, 26.86, 19.21; MS (MALDI-TOF) calcd for C₁₇₈H₂₈₈Cl₂N₅₄O₂₄Si₂ 3692.19, found 3693.14 (M+H)⁺.

Dendrimer 1. A solution of piperazine (3.2 mg, 0.0371 mmol) and DIPEA (40 μ L, 0.232 mmol) in methanol (1 mL) was added dropwise to an ice-bath cooled solution of **9** (300 mg, 0.0812 mmol) in THF (6 mL). The solution was warmed to room temperature, stirred for 48 hr, and then evaporated under vacuum. The residue was dissolved in dichloromethane, washed with brine, dried over MgSO₄, and evaporated under vacuum. The crude product was purified by silica gel chromatography (ethyl acetate to dichloromethane:methanol = 8:1) to give **1** (233 mg, 85%) as a white solid. ¹H NMR (500 MHz, CDCl₃) δ 7.66 (m, 16H), 7.33 (m, 24H), 4.69 (br, 28H), 3.84 (br, 8H), 3.78 (t, *J* = 5.3 Hz, 8H), 3.71 (br, 8H), 3.58-3.55 (m, 80H), 3.25 (br, 28H), 3.04 (br, 32H), 2.74

(br , 28H), 1.73-1.68 (br , 74H), 1.40 (s, 144H), 1.15 (br, 28H), 1.03 (s, 36H); ^{13}C NMR (125 MHz, CDCl_3) δ 165.80, 164.78, 164.67, 156.10, 135.65, 133.69, 129.69, 127.73, 78.99, 72.41, 72.30, 70.22, 70.15, 63.45, 61.64, 46.23, 43.22, 42.28, 40.69, 40.59, 37.18, 36.94, 29.99, 29.75, 28.59, 27.78, 26.89, 19.24; MS (MALDI-TOF) calcd for $\text{C}_{360}\text{H}_{584}\text{Cl}_2\text{N}_{110}\text{O}_{48}\text{Si}_4$ 7398.51, found 7399.18 ($\text{M}+\text{H}$) $^+$.

CHAPTER III

POST-SYNTHETIC MANIPULATIONS OF A MELAMINE DENDRIMER AND

IN VIVO BIODISTRIBUTION

Introduction

A variety of radiolabels are commonly used as molecular beacons due mostly to their sensitivity: ^{14}C , ^{32}P , ^{35}S , iodine isotopes, and ^3H .⁹⁴ ^{125}I is one of the most effective markers used in biodistribution study.⁹⁵ The radioactive iodine is highly sensitive, relatively safe (low γ energy emission). In addition, the target molecule can be easily labeled by radioactive iodine and stored for a while (60 day half-life). The radioiodination method developed by Bolton and Hunter utilizes 3-(4-hydroxyphenyl)propionyl groups.⁹⁶ The tyrosyl residue is very useful for iodination at the ortho position of the hydroxyl group. Positron emission tomography (PET) images can be also obtained with ^{120}I ($t_{1/2} = 1.4$ h, β^+ 56%) or ^{124}I ($t_{1/2} = 4.18$ d, β^+ 22%).^{94,97}

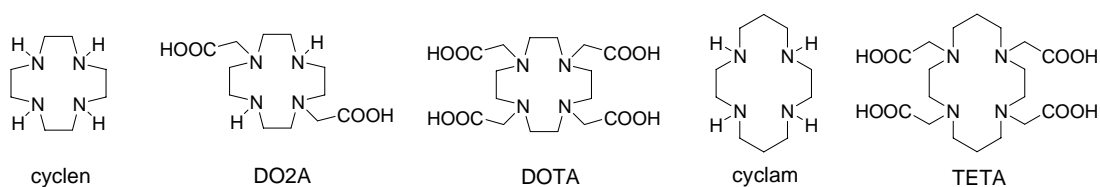


Figure 3.1. Copper (II) complexing macrocyclic chelators.

A variety of Radiometals are used in PET: ^{64}Cu ($t_{1/2} = 12.7$ h, β^+ 19%), ^{66}Ga ($t_{1/2} = 9.5$ h, β^+ 56%), ^{86}Y ($t_{1/2} = 14.7$ h, β^+ 33%).⁹⁸⁻¹⁰⁰ Figure 3.1 shows macrocyclic chelators

for Cu (II).¹⁰⁰ These radiometal chelating ligands can be incorporated into dendrimers to non-invasively produce 2- or 3-dimensional images during in vivo biodistribution.

Polyethylene glycol (PEG) is non-toxic, hydrophilic, and approved for clinical applications by FDA. The PEGylation of dendrimers is widely used to enhance the solubility in physiological conditions and to tailor the molecular size.

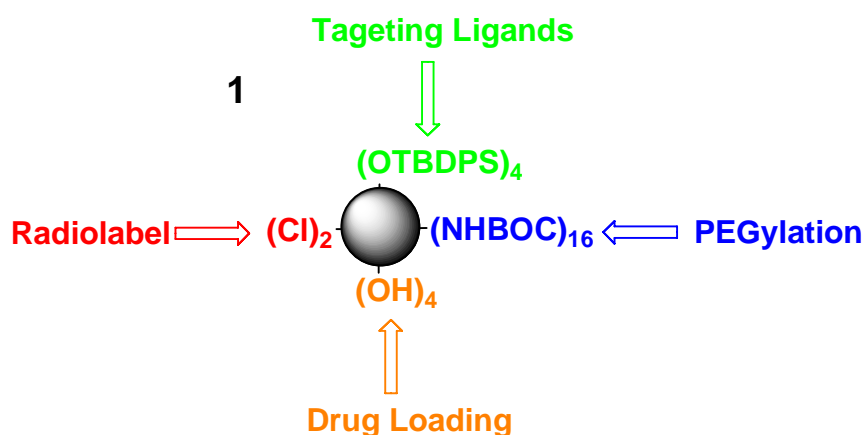


Figure 3.2. Potential post-synthetic manipulation of **1**.

Dendrimer **1** has potential for diverse biological applications due to its orthogonally reactive functional groups (Figure 3.2). In this study, we modify **1** by using two monochlorotriazine groups at the core and sixteen Boc-protected amine groups on the surface. The chlorine atoms are substituted with Bolton-Hunter type group or DOTA (1,4,7,10-tetraazacyclododecane-1,4,7,10-tetraacetic acid) ligand for biodistribution study and PET, respectively. After unmasking Boc groups, PEGylation is conducted by using the free amines. Potentially, the free hydroxyl and TBDPS ether groups can be further

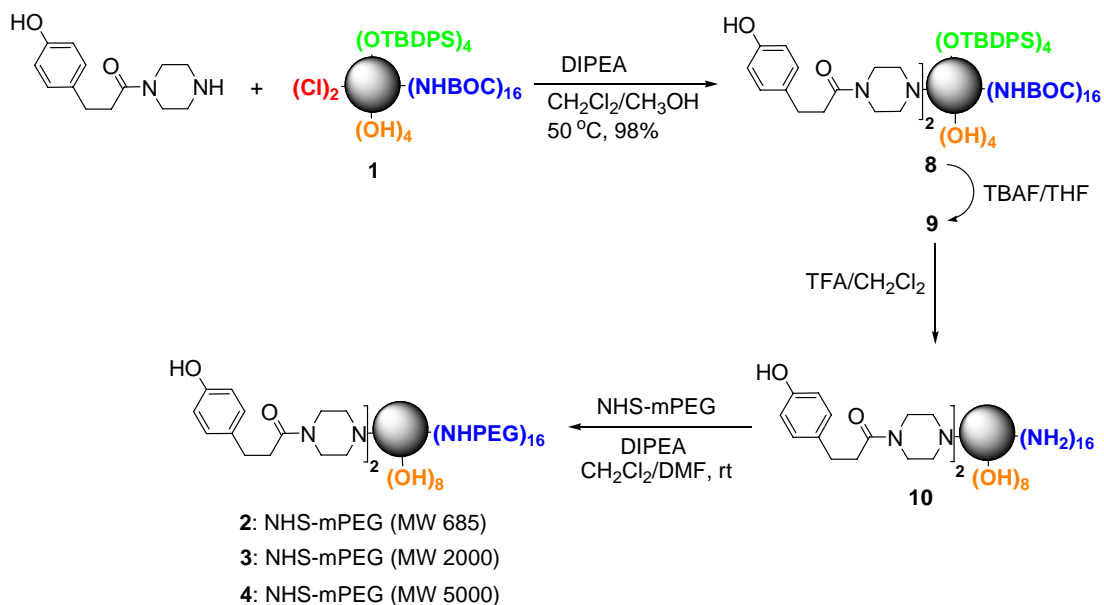
manipulated for drug conjugation and the attachment of targeting ligands. Preliminary biodistribution studies are also described here.

Results and Discussion

Post-Synthetic Manipulations of 1

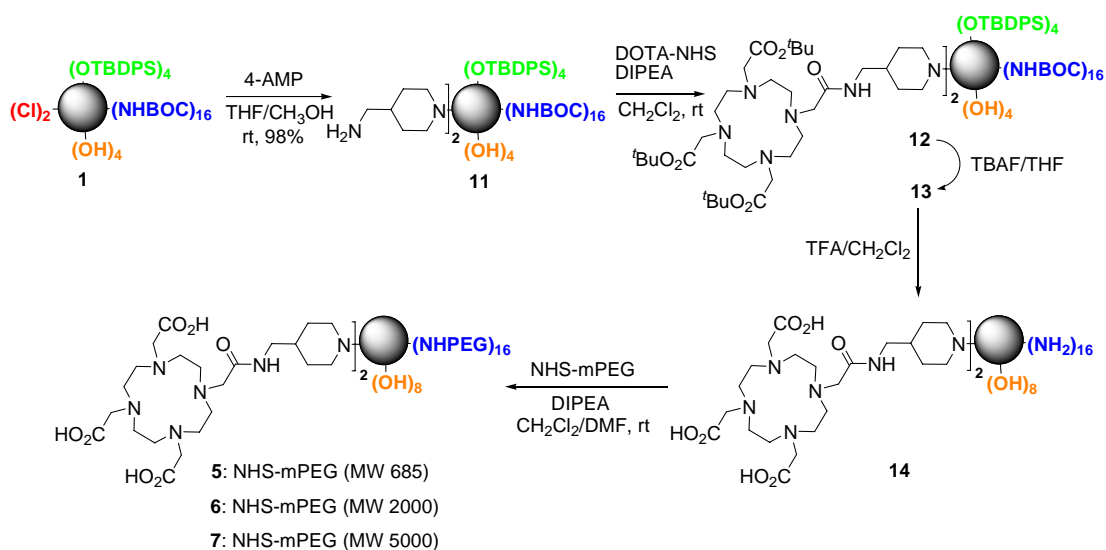
The synthesis of PEGylated dendrimers containing Bolton-Hunter groups is outlined in Scheme 3.1. The Bolton-Hunter type reagent is prepared in the treatment of BOC-piperazine with 3-(4-hydroxyphenyl)propionic acid using PyBOP as a coupling agent in DMF.^{35,101} After the deprotection of the Boc group with trifluoroacetic acid (TFA), the nucleophilic Bolton-Hunter reagent is almost quantitatively incorporated to give **8**.

Scheme 3.1. Synthesis of PEGylated dendrimers with Bolton-Hunter reagent.



The TBDPS ether groups of **8** is deprotected by using tetrabutylammonium fluoride (TBAF) in THF to afford **9**, and then followed by treatment with TFA to produce **10**. The Amines of **10** are pegylated with the different sizes of NHS-mPEG (MW 685, 2000 and 5000 respectively). The PEGylated dendrimers **2**, **3**, and **4** are purified by dialysis in deionized water.

Scheme 3.2. Synthesis of PEGylated dendrimers with DOTA.



The synthesis of PEGylated dendrimers containing DOTA groups is outlined in Scheme 3.2. Dendrimer **1** is reacted with the secondary amine of 4-aminomethyl piperidine (4-AMP) to give **11**, and then followed by reaction with the NHS ester of a protected DOTA group to produce **12**. The excess/decomposed DOTA-NHS ester reagents are removed by dialysis after the PEGylation step. Dendrimer **12** is treated with TBAF, and followed by reaction with TFA to give the deprotected dendrimer

14. PEGylation is carried out to afford **5**, **6**, and **7**. The small MW impurities including free PEG are removed by dialysis purification in deionized water. Table 3.1 shows a library of dendrimers for biodistribution study. Dendrimers **2** to **7** have the range of MW about 11 to 82 kDa with the two types of reporting groups, Bolton-Hunter (BH) and DOTA.

Table 3.1. A library of dendrimers (**2-7**) for biodistribution study.

dendrimer	MW (Da) (MALDI-TOF)	reporting group	solubilizing group
2	11200	BH	PEG 685
3	30400	BH	PEG 2000
4	73400	BH	PEG 5000
5	11600	DOTA	PEG 685
6	28800	DOTA	PEG 2000
7	82100	DOTA	PEG 5000

MALDI-TOF MS is very useful to follow the synthesis of dendrimers (Figure 3.3). The mass ion peak of **8** containing BH groups was observed at 7794.11 $[M + H]^+$ (the calculated exact mass: 7794.83). The mass ion of DOTA-dendrimer **12** was observed at 8668.07 $[M + H]^+$ (the calculated exact mass: 8663.52). The PEGylated dendrimers (**2-7**) are analyzed using GPC in 0.1 M NaNO₃ (aq) with a refractive index (RI) detector (Figure 3.4).

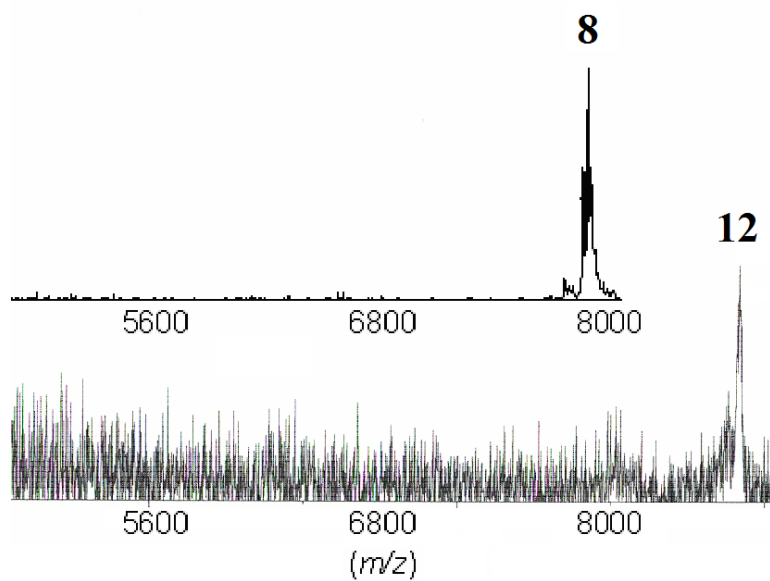


Figure 3.3. MALDI-TOF mass spectra of **8** and **12**.

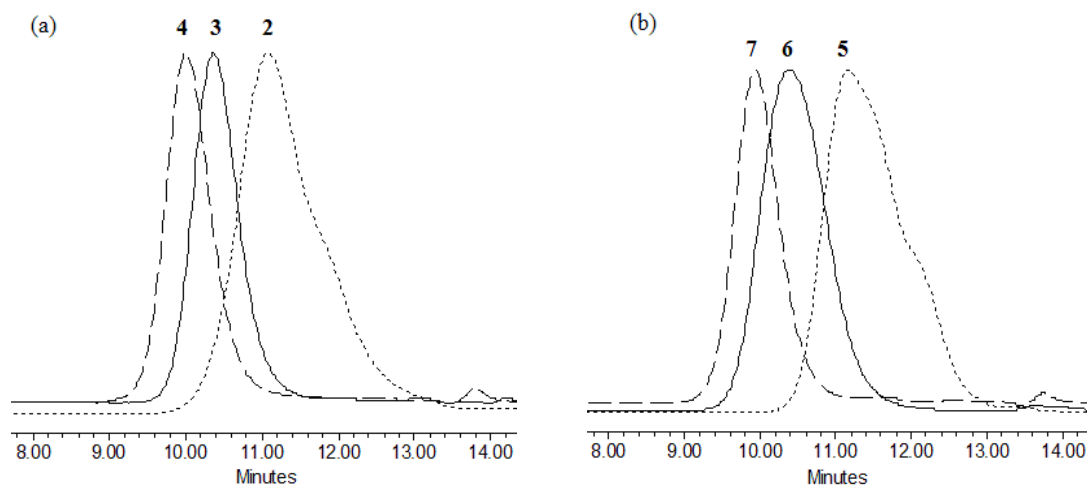


Figure 3.4. GPC traces of PEGylated dendrimers containing Bolton-Hunter (a) or DOTA groups (b).

Preliminary In Vivo Biodistribution Studies

Preliminary biodistribution studies were performed in collaboration with Dr. Xiankai Sun's group at UT Southwestern Medical Center. BH-dendrimers **2**, **3**, and **4** are used to investigate biodistribution profiles that may depend on the molecular weight, composition, and structure of dendrimers. Radioiodination is conducted by using Iodogen (1,3,4,6-tetrachloro-3 α ,6 α -diphenylglycouril), an effective oxidation reagent and Na¹²⁵I in 0.1 N NaOH.^{102,103} After purification and analysis of ¹²⁵I-labeled dendrimers, dendrimer solutions (100 μ L, 6 μ Ci per mouse) are intravenously administered to healthy male BALB/c mice (four mice per group). The mice are sacrificed at the scheduled time points (30 min, 1 h, 4 h, 24 h, and 48 h post-injection). Blood, heart, lungs, liver, spleen, kidneys, fat, muscle, intestines, stomach, and thyroid are weighed, and the radioactivity of each organ is quantified.

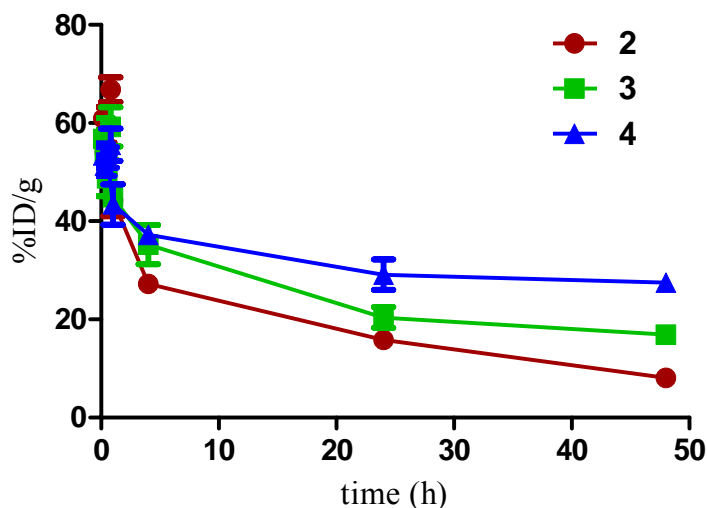


Figure 3.5. Time-concentration plot of dendrimers in the blood.

As shown in Figure 3.5, the percent injected dose per gram tissue (%ID/g) in the blood was higher with increasing MW of dendrimers: **2** (8.12 ± 1.64 %ID/g, MW 11200

Da), **3** (16.95 ± 1.64 %ID/g, MW 30400 Da), and **4** (27.50 ± 1.73 %ID/g, MW 73400 Da) at 48 h post-injection of ^{125}I -labeled dendrimers, respectively. The pharmacokinetic data (Table 3.2) are obtained from the two-compartment open model (Figure 3.6).^{24,104} The distribution half-lives ($t_{1/2\alpha}$) of dendrimers to other organs displayed similar patterns (**2**: 48.1 min, **3**: 45.4 min, and **4**: 52.1 min), while the elimination half-lives ($t_{1/2\beta}$) and $\text{AUC}_{0 \rightarrow \infty}$ values were significantly increased in higher MW of dendrimers: **2** (1593.5 min, 1188.9 %ID·h/g), **3** (2547.2 min, 2159.2 %ID·h/g), and **4** (6010.5 min, 5379.6 %ID·h/g), respectively.

Table 3.2. Pharmacokinetic data of the ^{125}I -radiolabeled dendrimers.

Dendrimer	Half-lives (min)		$\text{AUC}_{0 \rightarrow \infty}$ (%ID·h/g) ^a
	$t_{1/2\alpha}$	$t_{1/2\beta}$	
2	48	1600	1200
3	45	2500	2200
4	52	6000	5400

^a $\text{AUC}_{0 \rightarrow \infty}$ equals the area under the %ID/g of blood curve from zero to infinite time.

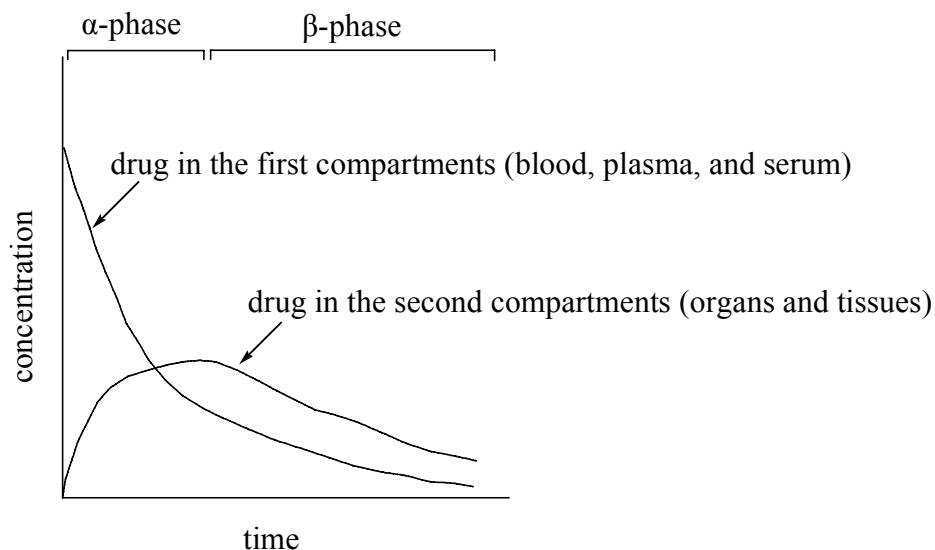


Figure 3.6. Two-compartment open model kinetics following intravenous injection.

Figure 3.7 shows the biodistribution results of dendrimers in the excretory organs: liver, lungs, spleen, and kidneys. Accumulation in the liver was observed with all the dendrimers. With decreasing the PEG chain length, the cellular uptake in the liver was increased presumably because the iodinated phenol groups at the core could be more easily recognized by receptors with less shielding.²⁴ The biodistribution of dendrimers in other organs displayed similar patterns regardless of the MW.

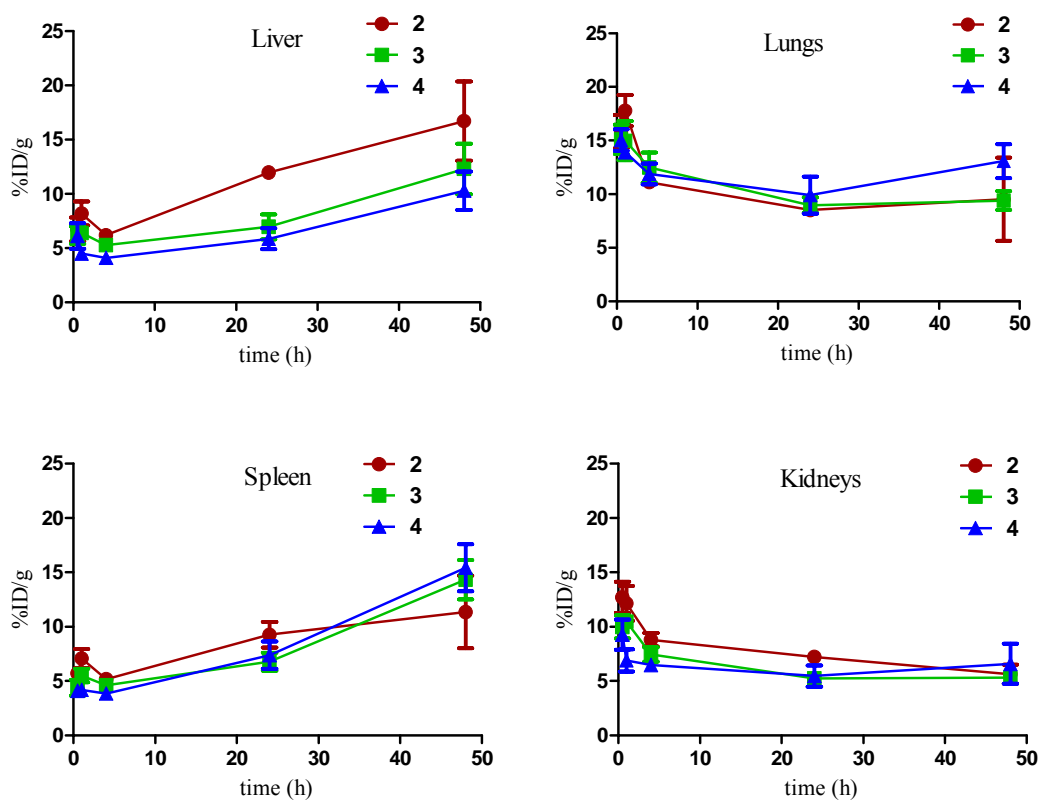


Figure 3.7. Biodistribution data of ^{125}I -labeled dendrimers.

In addition, preliminary biodistribution studies were carried out with tumor-bearing mice. The dendrimer (MW ~ 17 kDa) used in this study was obtained from the reaction of **10** with activated PEG (750 Da) that was prepared by treating methoxypolyethylene glycol with 4-nitrophenyl chloroformate using pyridine in dichloromethane. Prostate cancer cells (PC-3-Luc) were injected subcutaneously into the right flank of each male nude mouse. ^{125}I -labeled samples were prepared by using the same method described. As shown in coronal PET images (Figure 3.8), dendrimer accumulation in the tumor tissues

slowly occurred, indicating the passive targeting via EPR effect. At 48 h post-injection of the dendrimer, the uptake ratios of tumor to muscle and blood were respectively 5.7 and 3.3 (Figure 3.9).

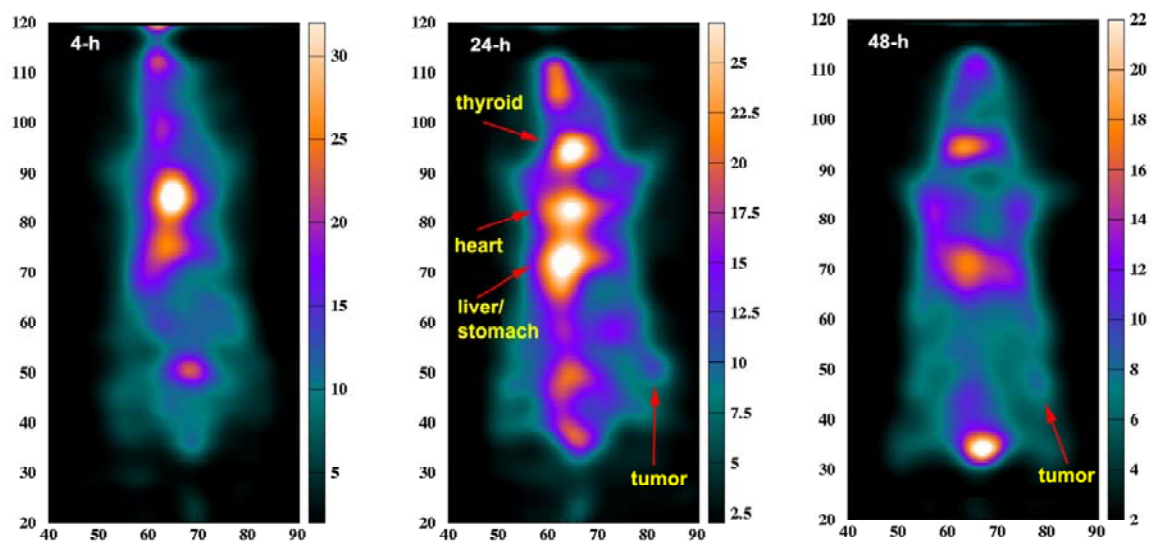


Figure 3.8. Coronal PET images of a ^{124}I -labeled dendrimer in a tumor-bearing mouse. The injection dose was 727 μCi . The imaging acquisition time was 40 – 90 min. The imaging intensity is not on the same scale.

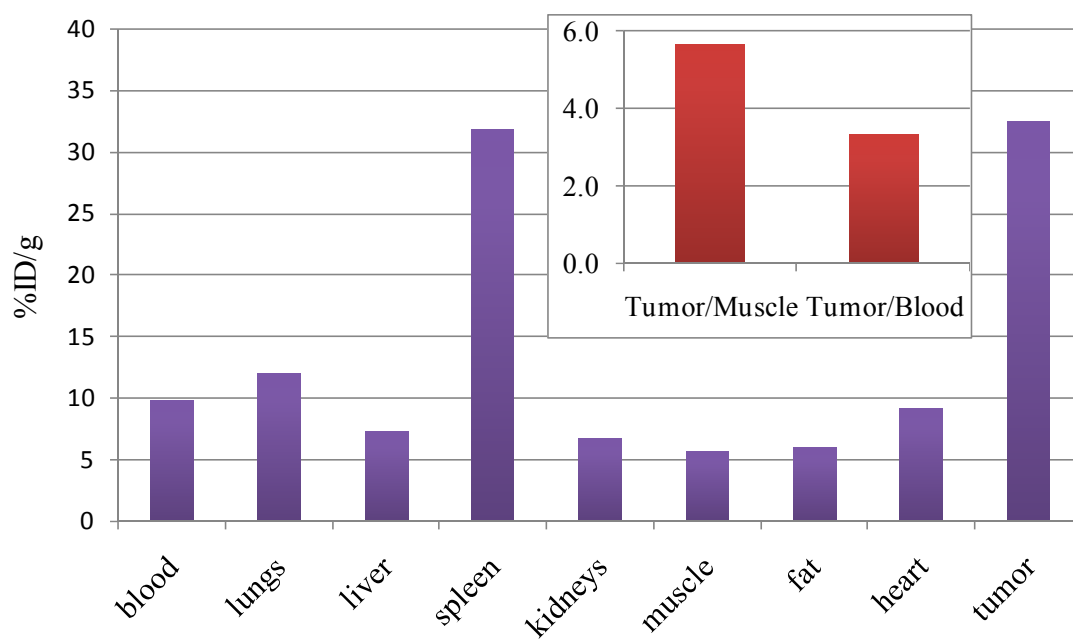


Figure 3.9. Post-PET biodistribution data of a ^{124}I -labeled dendrimer (~ 17 kDa) in nude mice with PC-3-Luc xenografts at 48 h post-injection.

Conclusions

We described post-synthetic manipulations and preliminary biodistribution studies using a versatile dendrimer with four orthogonally reactive groups. Reporting groups including BH and DOTA were incorporated by using monochlorotriazine groups. PEGylation was performed to improve the solubility in physiological conditions, tailoring the molecular size. Free hydroxyl and TBDPS ether groups can be potentially employed to other biological applications such as drug conjugation and the attachment of ligands. In preliminary biodistribution studies of **2**, **3**, and **4**, higher MW dendrimers displayed longer circulation times in the blood. Slow tumor accumulation was observed even for a relatively small dendrimer (MW ~17 kDa) in mice bearing prostate cancer xenografts. The complete biodistribution studies using all the dendrimers (**2-7**) are being pursued.

Experimental

General Procedures

NHS-mPEGs were purchased from Nektar Therapeutics and Quanta BioDesign. DOTA-mono-NHS-tris (*t*-Bu) ester was purchased from Macrocyclics. All other chemicals were purchased from Aldrich and Acros and used without further purification. All solvents were ACS grade and used without further purification. Dialysis membranes were purchased from Spectrum Laboratories, Inc. Size exclusion chromatography (SEC) was carried out using a Waters Delta 600 system and a Waters 2414 refractive index detector. A Suprema 10 micron GPC analytical

column (1000 Å, 8 x 300 mm) was used with 0.1 M NaNO₃ as the eluent and a flow rate of 1 mL/min. NMR spectra were recorded on a Varian Mercury 300 MHz or Inova 500 MHz spectrometer in CDCl₃, MeOH-d₄, or CDCl₃:MeOH-d₄ (10:1). All mass spectral analyses were carried out by the Laboratory for Biological Mass Spectrometry at Texas A&M.

Experimental Procedures

Bolton-Hunter-BOC-piperazine. 1-BOC-piperazine (0.56 g, 3.0 mmol) and DIPEA (0.8 mL, 4.6 mmol) were added to a solution of 3-(4-hydroxyphenyl)propionic acid (0.50 g, 3.0 mmol) and PyBOP (1.72 g, 3.3 mmol) in DMF (10 mL). The solution was stirred for 12 h at room temperature. The reaction mixture was poured into 50 mL of 0.5 M KHSO₄ (aq) and extracted with ethyl acetate. The organic layer was washed with Sat. NaHCO₃ (aq), dried over MgSO₄, and then evaporated under vacuum. The crude product was purified by silica gel chromatography (ethyl acetate:hexane = 3:1) to afford a white hygroscopic solid (1.0 g, 99%). ¹H NMR (300 MHz, CDCl₃) δ 7.07 (dd, *J* = 6.5, 2.0, 2H), 6.76 (dd, *J* = 6.5, 2.3, 2H), 3.58 (t, *J* = 5.3 Hz, 2H), 3.39-3.31 (m, 6H), 2.90 (t, *J* = 7.8 Hz, 2H), 2.60 (t, *J* = 7.7 Hz, 2H), 1.46 (s, 9H); ¹³C NMR (75 MHz, CDCl₃) δ 171.75, 155.24, 154.67, 131.67, 129.42, 115.50, 80.67, 45.47, 43.08, 41.53, 35.31, 30.77, 28.36; MS (ESI-TOF) calcd for C₁₈H₂₆N₂O₄ 334.19, found 335.19 (M+H)⁺.

Bolton-Hunter-piperazine. Trifluoroacetic acid (10 mL) was added to an ice-bath cooled solution of the modified Bolton-Hunter reagent (1.0 g, 2.99 mmol) in dichloromethane (10 mL). The solution was warmed to room temperature and stirred for 4 h. The solution was concentrated under vacuum to give a TFA salt. ¹H NMR (300

MHz, MeOH-d₄) δ 7.04 (dd, $J = 6.6, 2.1, 2\text{H}$), 6.72 (dd, $J = 6.5, 2.0, 2\text{H}$), 3.78 (t, $J = 5.0$ Hz, 2H), 3.65 (t, $J = 5.0$ Hz, 2H), 3.11 (t, $J = 5.1$ Hz, 2H), 2.97 (t, $J = 5.0$ Hz, 2H), 2.82 (t, $J = 7.5$ Hz, 2H), 2.66 (t, $J = 7.1$ Hz, 2H); ¹³C NMR (75 MHz, MeOH-d₄) δ 173.71, 156.94, 132.63, 130.61, 116.29, 44.28, 43.64, 39.38, 35.41, 31.74; MS (ESI-TOF) calcd for C₁₃H₁₈N₂O₂ 234.14, found 235.12 (M+H)⁺.

Dendrimer 8. A solution of the modified Bolton-Hunter reagent salt (180 mg) in methanol (2 mL) was added to a solution of **1** (150 mg, 0.020 mmol) and DIPEA (0.4 mL, 2.3 mmol) in dichloromethane (1 mL). The solution was stirred for 48 h at 50 °C and the solvent was then removed by reduced-pressure evaporation. The residue was dissolved in dichloromethane, washed with brine, dried over MgSO₄ and evaporated under vacuum. The compound was purified by silica gel chromatography (dichloromethane:methanol = 10:1) to give **8** (155 mg, 98%) as a white solid. ¹H NMR (500 MHz, CDCl₃+MeOH-d₄) δ 7.97 (dd, $J = 7.8, 1.3, 16\text{H}$), 7.68 (m, 24H), 7.32 (d, $J = 8.0, 4\text{H}$), 7.04 (d, $J = 7.5, 4\text{H}$), 4.98 (br, 28H), 4.10-3.85 (m, 120H), 3.56 (br, 28H), 3.34 (br, 32H), 3.17 (t, $J = 7.3$ Hz, 4H), 3.07 (br, 28H), 2.92 (br, 4H), 2.08-2.01 (br, 74H), 1.71 (s, 144H), 1.46 (br, 28H), 1.33 (s, 36H); ¹³C NMR (125 MHz, CDCl₃+MeOH-d₄) δ 171.74, 166.18, 165.82, 165.35, 164.81, 164.48, 156.34, 155.22, 135.41, 133.40, 131.40, 129.51, 129.24, 127.51, 115.22, 79.08, 72.20, 72.09, 69.98, 69.78, 63.23, 61.16, 45.93, 45.49, 43.05, 42.86, 42.53, 41.42, 40.36, 40.26, 37.08, 36.80, 35.21, 30.73, 30.06, 29.73, 29.49, 29.18, 28.75, 28.23, 27.52, 26.60, 18.97; MS (MALDI-TOF) calcd for C₃₈₆H₆₁₈N₁₁₄O₅₂Si₄ 7794.83, found 7794.11 (M+H)⁺.

Dendrimer 9. Dendrimer **8** (1.30 g, 0.167 mmol) was dissolved in THF (40 mL). 1.0 M TBAF (1 mL, 1.0 mmol in THF) was added at 0 °C. The solution was warmed to room temperature and stirred under nitrogen overnight. The solvent was removed by reduced-pressure evaporation. The residue was dissolved in dichloromethane, washed with brine, dried over MgSO₄ and evaporated under vacuum. The deprotected TBDPS was removed by silica gel chromatography (ethyl acetate to dichloromethane:methanol = 8:1) to give **9** (1.05 g, 92%) as a white solid. MS (MALDI-TOF) calcd for C₃₂₂H₅₄₆N₁₁₄O₅₂ 6842.36, found 6845.32 (M+H)⁺.

Dendrimer 10. Trifluoroacetic acid (10 mL) was added to an ice-bath cooled solution of **9** (1.0 g) in dichloromethane (10 mL). The solution was warmed to room temperature and stirred for 24 h. The solution was concentrated under vacuum to give a TFA salt. The residue was dissolved in methanol and neutralized by adding triethylamine, and then evaporated under vacuum to afford **10** as a white solid. MS (MALDI-TOF) calcd for C₂₄₂H₄₁₈N₁₁₄O₂₀ 5241.52, found 5244.63 (M+H)⁺.

Dendrimer 11. A solution of 4-(aminomethyl)piperidine (0.50 g, 4.38 mmol) in methanol (4 mL) was added to a solution of **1** (0.35 g, 0.0473 mmol) in THF (16 mL). The solution was stirred for 24 h at room temperature, and then evaporated under vacuum. The residue was dissolved in dichloromethane, washed with brine, dried over MgSO₄, and evaporated under vacuum. The crude product was purified by silica gel chromatography (dichloromethane:methanol = 7:1) to give **11** (0.35 g, 98%) as a white solid. ¹H NMR (500 MHz, CDCl₃) δ 7.67 (m, 16H), 7.38 (m, 24H), 4.70 (br, 32H), 3.79 (t, *J* = 5.0 Hz, 8H), 3.74 (m, 16H), 3.57 (m, 80H), 3.27 (br, 28H), 3.05 (br, 32H), 2.76

(br, 36H), 1.77-1.70 (br, 80H), 1.41 (s, 144H), 1.16 (br, 32H), 1.04 (s, 36H); ^{13}C NMR (125 MHz, $\text{CDCl}_3+\text{MeOH-d}_4$) δ 165.56, 164.86, 164.10, 156.29, 134.95, 132.94, 129.09, 127.07, 78.42, 71.73, 71.63, 69.54, 69.44, 62.87, 60.53, 45.46, 42.71, 39.91, 39.81, 36.98, 36.60, 29.36, 27.53, 25.96, 18.41; MS (MALDI-TOF) calcd for $\text{C}_{372}\text{H}_{610}\text{N}_{114}\text{O}_{48}\text{Si}_4$ 7554.79, found 7576.12 (M+H) $^+$.

Dendrimer 12. DOTA-mono-NHS-tris (*t*-Bu) ester (100 mg, 0.123 mmol) in dichloromethane (2 mL) was added to a solution of **11** (130 mg, 0.0172 mmol) and DIPEA (0.1 mL, 0.58 mmol) in dichloromethane (5 mL). The solution was stirred under nitrogen for 24 h at room temperature. The reaction solution was poured into 15 mL of 5% NaOH (aq) and extracted with dichloromethane. The organic layer was washed with brine, dried over MgSO_4 , and then evaporated under vacuum to give **12** as a white solid. MS (MALDI-TOF) calcd for $\text{C}_{428}\text{H}_{710}\text{N}_{122}\text{O}_{62}\text{Si}_4$ 8663.52, found 8668.07 (M+H) $^+$.

Dendrimer 13. Dendrimer **12** (200 mg, 0.023 mmol) was dissolved in THF (10 mL). 1.0 M TBAF (1 mL, 1.0 mmol in THF) was added at 0 $^\circ\text{C}$. The solution was warmed to room temperature and stirred under nitrogen overnight. The solvent was removed by reduced-pressure evaporation. The residue was dissolved in dichloromethane, washed with brine, dried over MgSO_4 and evaporated under vacuum. The deprotected TBDPS was removed by silica gel chromatography (ethyl acetate to dichloromethane:methanol = 8:1) to give **13** (165 mg) as a white solid. MS (MALDI-TOF) calcd for $\text{C}_{364}\text{H}_{638}\text{N}_{122}\text{O}_{62}$ 7711.05, found 7752.79 (M+H) $^+$.

Dendrimer 14. Trifluoroacetic acid (5 mL) was added to an ice-bath cooled solution of **13** (150 mg) in dichloromethane (5 mL). The solution was warmed to room temperature and stirred for 24 h. The solution was concentrated under vacuum to give a TFA salt. The residue was dissolved in methanol and neutralized by adding triethylamine, and then evaporated under vacuum to give **14**. MS (MALDI-TOF) calcd for $C_{260}H_{462}N_{122}O_{30}$ 5773.84, found 5785.86 (M+H)⁺.

Dendrimer 2. A solution of **10** (20 mg) and DIPEA (0.1 mL, 0.58 mmol) in DMF (1 mL) was added to a solution of NHS-mPEG (MW 685, 44 mg, 0.064 mmol) in dichloromethane (1 mL). The solution was stirred under nitrogen for 24 h at room temperature. The reaction solution was dialyzed to remove DMF against distilled water using a Spectra/Por regenerated cellulose membrane (MWCO: 3.5 kDa) for 24 h, and then the solution was evaporated under vacuum. The residue was dissolved in deionized water and filtered. The filtrate was purified to remove low molecular weight impurities using a Spectra/Por cellulose ester membrane (MWCO: 10 kDa) in deionized water for 48 h. The deionized water was changed every 12 h. The dialyzed solution was evaporated under vacuum to afford **2** as a colorless solid. The resulting compound was analyzed by size exclusion chromatography. MS (MALDI-TOF) calcd for 16 PEG species 14360.24, found 11184.91 (M+H)⁺.

Dendrimer 3. A solution of **10** (12 mg) and DIPEA (0.1 mL, 0.58 mmol) in DMF (1 mL) was added to a solution of NHS-mPEG (MW 2000, 67 mg, 0.034 mmol) in dichloromethane (1 mL). The solution was stirred under nitrogen for 24 h at room temperature. The reaction solution was dialyzed to remove DMF against distilled water

using a Spectra/Por regenerated cellulose membrane (MWCO: 3.5 kDa) for 24 h, and then the solution was evaporated under vacuum. The residue was dissolved in deionized water and filtered. The filtrate was purified to remove low molecular weight impurities using a Spectra/Por cellulose ester membrane (MWCO: 10 kDa) in deionized water for 5 days. The deionized water was changed every 12 h. The dialyzed solution was evaporated under vacuum to afford **3** as a white solid. The resulting compound was analyzed by size exclusion chromatography. MS (MALDI-TOF) calcd for 16 PEG species 35400.24, found 30423.46 (M+H)⁺.

Dendrimer 4. A solution of **10** (12 mg) and DIPEA (0.1 mL, 0.58 mmol) in DMF (1 mL) was added to a solution of NHS-mPEG (MW 5000, 191 mg, 0.038 mmol) in dichloromethane (1 mL). The solution was stirred under nitrogen for 24 h at room temperature. The reaction solution was dialyzed to remove DMF against distilled water using a Spectra/Por regenerated cellulose membrane (MWCO: 3.5 kDa) for 24 h, and then the solution was evaporated under vacuum. The residue was dissolved in deionized water and filtered. The filtrate was purified to remove low molecular weight impurities using a Spectra/Por cellulose ester membrane (MWCO: 50 kDa) in deionized water for 5 days. The deionized water was changed every 12 h. The dialyzed solution was evaporated under vacuum to afford **4** as a white solid. The resulting compound was analyzed by size exclusion chromatography. MS (MALDI-TOF) calcd for 16 PEG species 83400.24, found 73408.90 (M+H)⁺.

Dendrimer 5. A solution of **14** (20 mg) and DIPEA (0.1 mL, 0.58 mmol) in DMF (1 mL) was added to a solution of NHS-mPEG (MW 685, 44 mg, 0.064 mmol) in

dichloromethane (1 mL). The solution was stirred under nitrogen for 24 h at room temperature. The reaction solution was dialyzed to remove DMF against distilled water using a Spectra/Por regenerated cellulose membrane (MWCO: 3.5 kDa) for 24 h, and then the solution was evaporated under vacuum. The residue was dissolved in deionized water and filtered. The filtrate was purified to remove low molecular weight impurities using a Spectra/Por cellulose ester membrane (MWCO: 10 kDa) in deionized water for 48 h. The deionized water was changed every 12 h. The dialyzed solution was evaporated under vacuum to afford **5** as a colorless solid. The resulting compound was analyzed by size exclusion chromatography. MS (MALDI-TOF) calcd for 16 PEG species 14892.56, found 11620.48 (M+H)⁺.

Dendrimer 6. A solution of **14** (12 mg) and DIPEA (0.1 mL, 0.58 mmol) in DMF (1 mL) was added to a solution of NHS-mPEG (MW 2000, 67 mg, 0.034 mmol) in dichloromethane (1 mL). The solution was stirred under nitrogen for 24 h at room temperature. The reaction solution was dialyzed to remove DMF against distilled water using a Spectra/Por regenerated cellulose membrane (MWCO: 3.5 kDa) for 24 h, and then the solution was evaporated under vacuum. The residue was dissolved in deionized water and filtered. The filtrate was purified to remove low molecular weight impurities using a Spectra/Por cellulose ester membrane (MWCO: 10 kDa) in deionized water for 5 days. The deionized water was changed every 12 h. The dialyzed solution was evaporated under vacuum to afford **6** as a white solid. The resulting compound was analyzed by size exclusion chromatography. MS (MALDI-TOF) calcd for 16 PEG species 35932.56, found 28811.69 (M+H)⁺.

Dendrimer 7. A solution of **14** (12 mg) and DIPEA (0.1 mL, 0.58 mmol) in DMF (1 mL) was added to a solution of NHS-mPEG (MW 5000, 191 mg, 0.038 mmol) in dichloromethane (1 mL). The solution was stirred under nitrogen for 24 h at room temperature. The reaction solution was dialyzed to remove DMF against distilled water using a Spectra/Por regenerated cellulose membrane (MWCO: 3.5 kDa) for 24 h, and then the solution was evaporated under vacuum. The residue was dissolved in deionized water and filtered. The filtrate was purified to remove low molecular weight impurities using a Spectra/Por cellulose ester membrane (MWCO: 50 kDa) in deionized water for 5 days. The deionized water was changed every 12 h. The dialyzed solution was evaporated under vacuum to afford **7** as a white solid. The resulting compound was analyzed by size exclusion chromatography. MS (MALDI-TOF) calcd for 16 PEG species 83932.56, found 82070.03 (M+H)⁺.

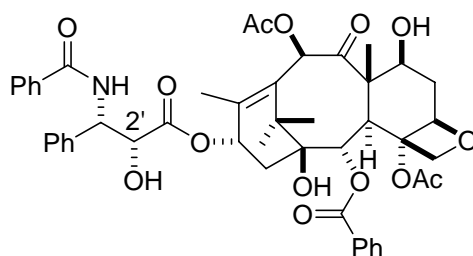
CHAPTER IV
SYNTHESIS AND CHARACTERIZATION OF A DENDRIMER BASED ON
MELAMINE THAT RELEASES PACLITAXEL

Introduction

To date, various types of polymers have been investigated as drug delivery systems.¹⁴ Examples include grafts,^{51,52} stars,⁵³ multivalent polymers,⁵⁴ block copolymers,⁵⁵ dendronized polymers,⁵⁶ and dendrimers.^{10,13,24,37,79} Dendrimers are promising as drug-delivery vehicles by virtue of the following characteristics: multivalency; a well-defined and large globular structure; mono- or low polydispersity; amenability to postsynthetic manipulation. We, and others, believe that dendrimers may surmount some of the barriers to chemotherapy including poor solubility of some agents in physiological conditions, high systemic toxicity, poor bioavailability, and low stability. Through rational design, dendrimers might shift in vivo pharmacokinetics of the drug, accelerate cellular uptake, prolong plasma half-life, and even specifically target the diseased cells either actively (via ligands) or passively (via the enhanced permeability and retention (EPR) effect^{59,60} resulting from a leaky vasculature and the lack of lymphatic drainage in solid tumor tissues).

We have chosen paclitaxel as our illustrative drug for four reasons. First, paclitaxel is a clinically relevant broad spectrum anticancer agent useful for treating tumors of the ovaries, breast, head and neck, lung, and AIDS-related Kaposi's sarcoma.¹⁰⁵ Second, it faces significant solubility challenges: its low solubility in water (< 0.1 µg/mL). Third, it

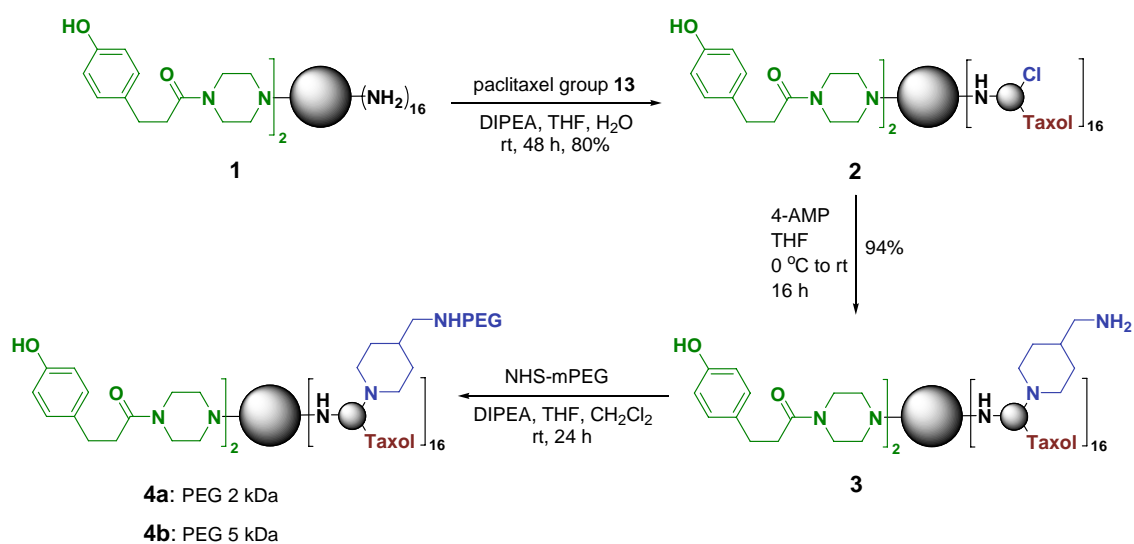
is amenable to synthetic manipulations (through esterification of the 2'-hydroxyl group) that provide a mechanism for conjugation and release. Finally, the target molecules can be compared to a variety of delivery vehicles have been described including emulsions,¹⁰⁶ micelles,^{107,108} liposomes,¹⁰⁹ nanoparticles,¹¹⁰ and other dendrimers.^{111,112}



The chemistry that we describe here is cartooned in Scheme 4.1. The methods and strategies employed in the synthesis of dendrimer derive from our previous efforts.³²⁻⁴⁵ In summary, chlorine atoms on triazine rings are substituted in a stepwise fashion with amine nucleophiles. The benefits of this chemistry derive from the compositional diversity which is often a challenge in conventional polymers and other types of dendrimers. Dendrimer **1** possesses groups amenable to radioiodination.⁹⁶ Subsequently, **1** is reacted with a paclitaxel-containing group to provide **2**. PEGylation is achieved in two steps. Reaction of the poly(monochlorotriazine) dendrimer **2** with 4-aminomethylpiperidine affords nucleophile for acylation with PEG groups that vary in size. Here, two different PEG-NHS esters are employed to obtain products **4a** and **4b**. PEGylation is a convenient mechanism to convey biocompatibility and solubility to the hydrophobic triazine dendrimer while simultaneously allowing us to tailor its size, and

accordingly, its biodistribution times and fates. By employing PEG chains with molecular weights 2 and 5 kDa, by weight the vehicles **4a** and **4b** are 30% and 18% drug, 52% and 71% PEG, and only 18% and 11% triazine dendrimer. In addition to details of synthesis and characterization of these molecules, we also report on paclitaxel release.

Scheme 4.1. Summary of the chemistries reported including paclitaxel conjugation and PEGylation.



Results and Discussion

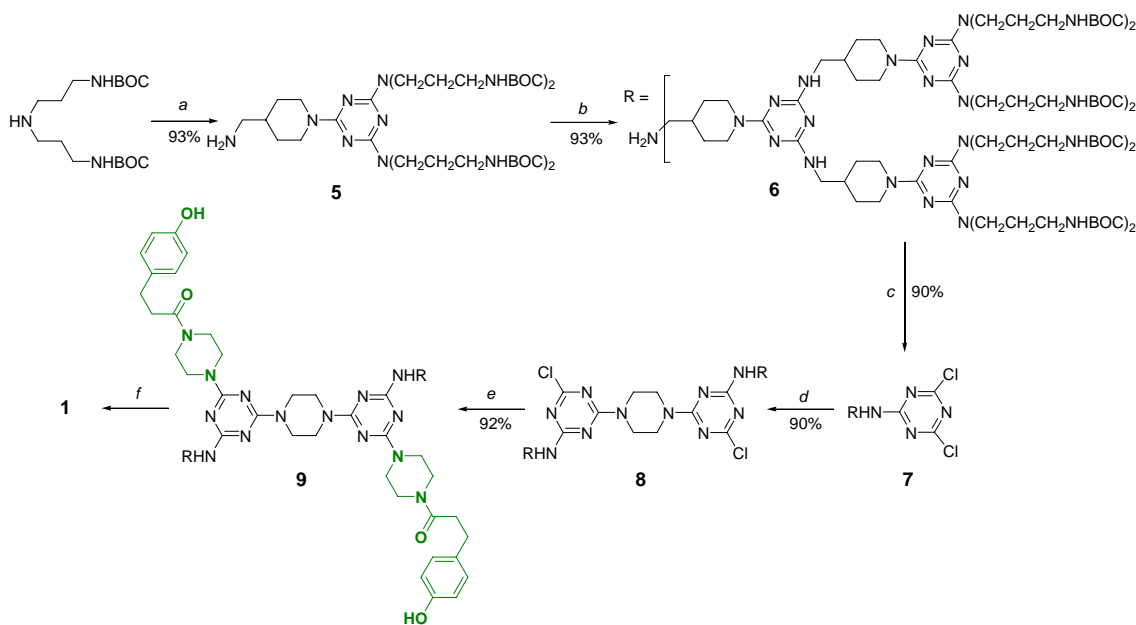
The results and discussion section are divided into five parts. The first three sections describe the synthesis of dendrimer **1**, the paclitaxel-conjugate, and targets **2-4**. The

fourth part addresses characterization. The fifth part describes release of paclitaxel from these conjugates.

Part 1. Synthesis of Dendrimer 1

Dendrimer **1** (Scheme 4.2) presents sixteen amines on the surface and two Bolton-Hunter-like groups at the core.

Scheme 4.2. Synthesis of a precursor dendrimer for drug conjugation.^a



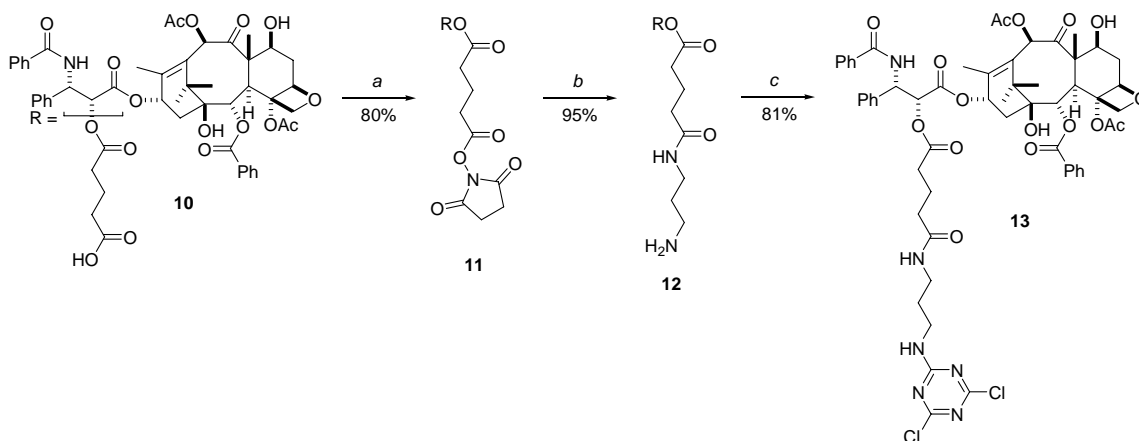
^a Reagents and conditions: (a) cyanuric chloride, DIPEA, THF, 0°C to rt, 24 h; then 4-AMP, rt, 24 h; (b) cyanuric chloride, DIPEA, THF, 0°C to rt, 24 h; then 4-AMP, rt, 24 h; (c) cyanuric chloride, DIPEA, THF, 0°C , 2 h; (d) piperazine, DIPEA, THF, CH_3OH , 0°C to rt, 24 h; (e) modified Bolton-Hunter, DIPEA, CH_2Cl_2 , CH_3OH , 40°C , 48 h; (f) TFA, CH_2Cl_2 , CH_3OH , 0°C to rt, 12 h.

The target was synthesized using a convergent route.¹¹³ Intermediate **5** is prepared in one pot by the reaction of cyanuric chloride with 2 equiv. of the Boc-protected triamine⁹³ and subsequent reaction with the secondary amine of 4-aminomethyl piperidine (4-AMP). Elaboration of **5** to **6** proceeds in a similar way: cyanuric chloride is first reacted with 2 equiv. of **5**, and followed by the addition of 4-AMP. Dichlorotriazine **7** was obtained by reacting **6** with cyanuric chloride. Dimerization of **7** with piperazine yields **8**. The radioiodination group (prepared as previously reported)^{35,101} was incorporated to give **9**. Finally, the BOC groups of **9** were quantitatively removed using trifluoroacetic acid (TFA). Overall, **1** is synthesized from the protected amine in 64% yield in six linear steps.

Part 2. Synthesis of the Paclitaxel Conjugate

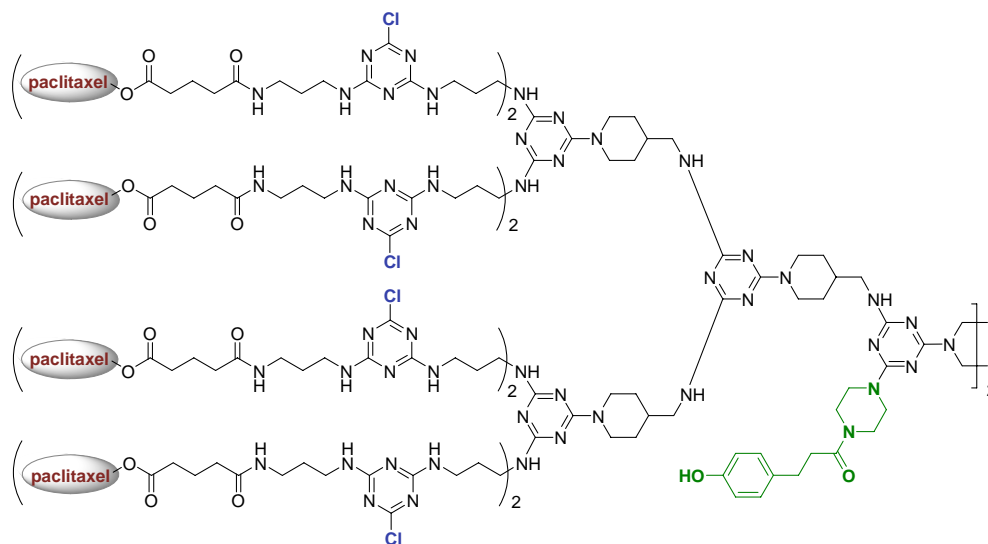
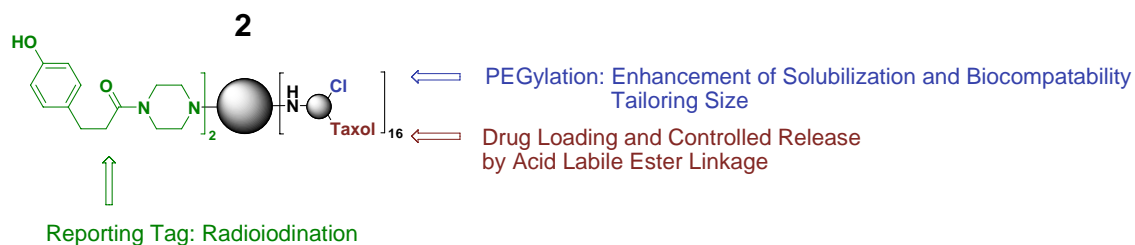
Our modification strategy for the covalent attachment of paclitaxel to dendrimer **1** follows the precedent esterification of the 2'-hydroxyl group.^{76,114} While both glutaric and succinic esters have been pursued, Safavy and coworkers¹¹⁴ reported that the glutaric ester-linked conjugates displayed better antitumor activity compared to the succinic ester-linked conjugate. Our strategy rests on the preparation of a dichlorotriazine modified with paclitaxel that could be used to react with the amines of **1**, giving sixteen monochlorotriazines to be utilized for further modification. The chemistry employed is outlined in Scheme 4.3.

Scheme 4.3. Modifications of paclitaxel^a



^a Reagents and conditions: (a) SDPP, TEA, CH₃CN, rt, 6 h; (b) 1,3-diaminopropane, TEA, CH₂Cl₂, 0 °C, 30 min; (c) cyanuric chloride, DIPEA, THF, 0 °C, 1 h.

The conjugate is prepared in four steps in 60% overall yield. Paclitaxel is reacted with glutaric anhydride in the presence of pyridine to give 2'-glutarylpaclitaxel **10**. Paclitaxel-NHS ester **11** is obtained by reaction of **10** with *N*-succinimidyl diphenylphosphate (SDPP).¹¹⁵ The paclitaxel-NHS ester is treated with excess of 1,3-diaminopropane at low temperature to afford the amine **12**. The linear, flexible diamine was chosen to reduce steric hindrance. Finally, the reaction of amine **12** with cyanuric chloride using DIPEA as a base yields the paclitaxel-dichlorotriazine **13**.



Part 3. Synthesis of Dendrimers 2-4

Scheme 4.1 describes the reaction of dendrimer **1** with **13** to give **2**. The resulting poly(monochlorotriazine) dendrimer undergoes nucleophilic aromatic substitution with 4-AMP to afford **3**. The sixteen primary amines of **3** were not fully pegylated due to steric hindrance. Accordingly, PEGylation with NHS-mPEGs 2 and 5 kDa gives **4a** (MW ~46 kDa for 14 PEG chains) and **4b** (MW ~77 kDa for 12 PEG chains), respectively.

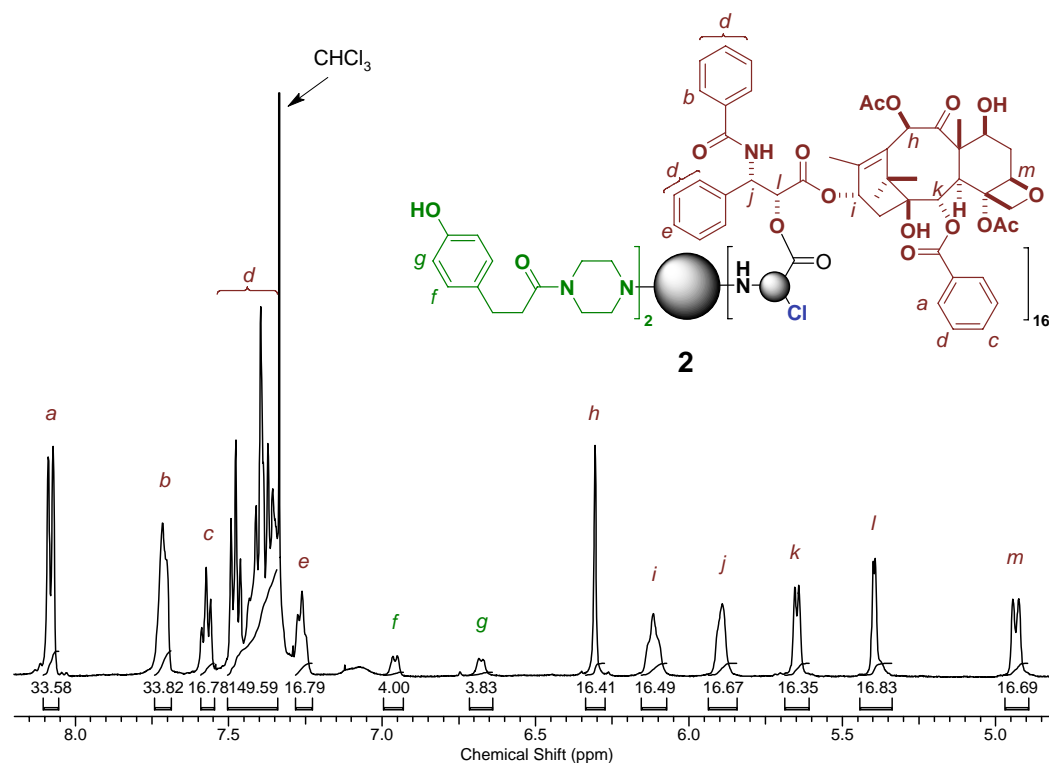


Figure 4.1. ¹H NMR assignment and integration of **2** in the expanded region 4.8 to 8.2 ppm. The spectrum was obtained in CDCl₃:MeOH-d₄ (10:1).

Part 4. Characterization

With the exception of reactions involving **1-4**, most reactions are readily monitored by thin layer chromatography. NMR spectroscopy and mass spectrometry are useful over the entire range of targets. Intermediates **5-13** provide satisfactory NMR and mass spectra data. Gel permeation chromatography (GPC) was used to follow the PEGylated dendrimers. The MALDI-TOF MS of the Boc-protected dendrimers, **5** to **9**, was consistent with single chemical entities: these spectra showed peaks derived from a single compound corresponding to $[M + H]^+$, $[M + Na]^+$, and $[M + Ka]^+$ with ladder peaks from loss of BOC groups during the ionization.

NMR spectroscopy was particularly useful to follow modification of paclitaxel. Figure 4.1 shows the assignment and integration of the spectrum confirm that up to 16 molecules of paclitaxel are conjugated to **2**. Obtaining consistent MALDI-TOF mass spectra from the hydrophobic dendrimer **2** was challenging: We believe those conditions that were optimal for ionization also led to fragmentation at the labile 2'-hydroxyl group. The spectrum in Figure 4.2 shows a good agreement between the calculated exact mass 21038 and the observed mass 21114 (m/z). The ladder peaks occurring in the lower mass region can be attributed to either degraded analytes (loss of paclitaxel due to the labile ester link) from high laser intensity or incomplete reaction of the dichlorotriazine.

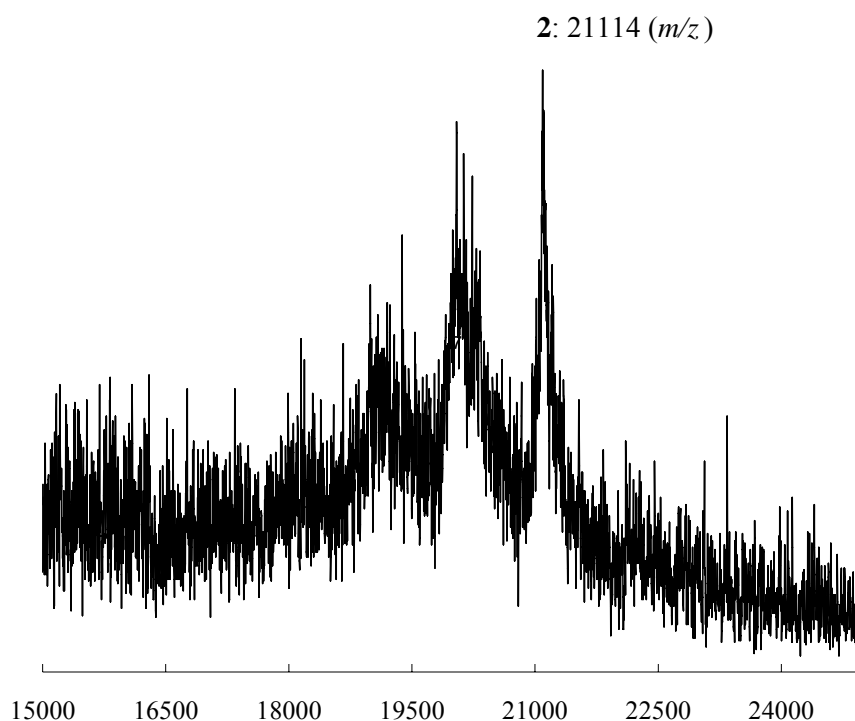


Figure 4.2. The MALDI-TOF spectrum of **2**.

The PEGylated paclitaxel-dendrimer conjugates **4a** and **4b** were analyzed with GPC, ^1H NMR, and MALDI-TOF MS. The PEGylated dendrimers are readily soluble in aqueous media allowing purification by dialysis. The dendrimers were analyzed using GPC in 0.1 M NaNO_3 (aq) with a refractive index (RI) detector (Figure 4.3). ^1H NMR spectroscopy was also used to characterize the drug conjugates. The spectra shown in Figure 4.4 display each peak of the aromatic rings of paclitaxel (7.25-8.09 ppm), the radioiodination group (respectively, 6.68 and 6.96 ppm for ortho and meta protons), and the PEG chains (~ 3.6 ppm). The molecular weight was determined by MALDI-TOF MS: 46100 Da for **4a** and 77400 Da for **4b**. This corresponds to macromolecules that are 30% (**4a**) and 18 wt % (**4b**) paclitaxel.

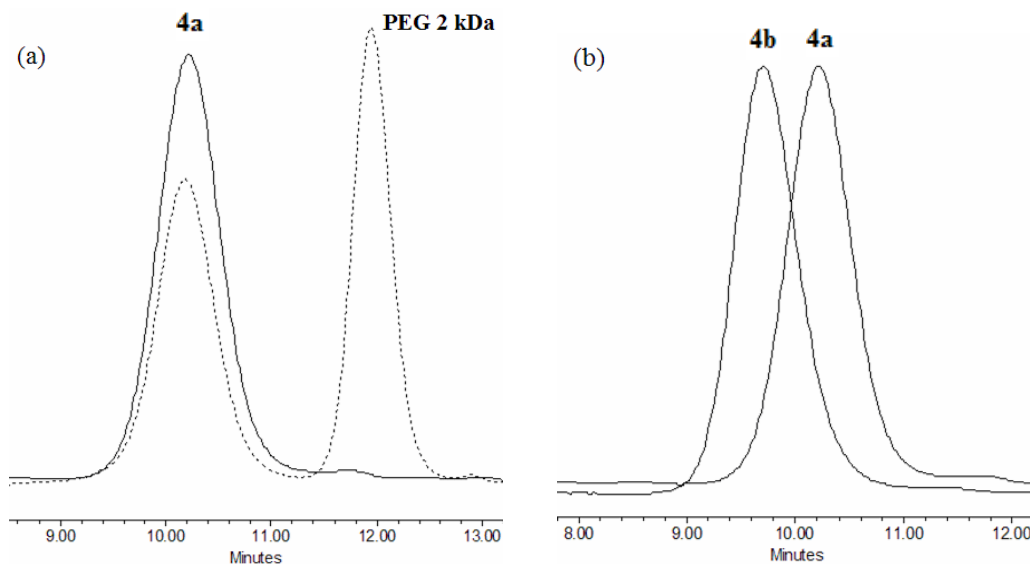


Figure 4.3. The analytical GPC chromatogram obtained using 0.1 M NaNO_3 (aq) as an eluent with a RI detector: (a) before (dotted line) and after (solid line) dialysis purification of **4a**; (b) GPC traces of **4a** and **4b**.

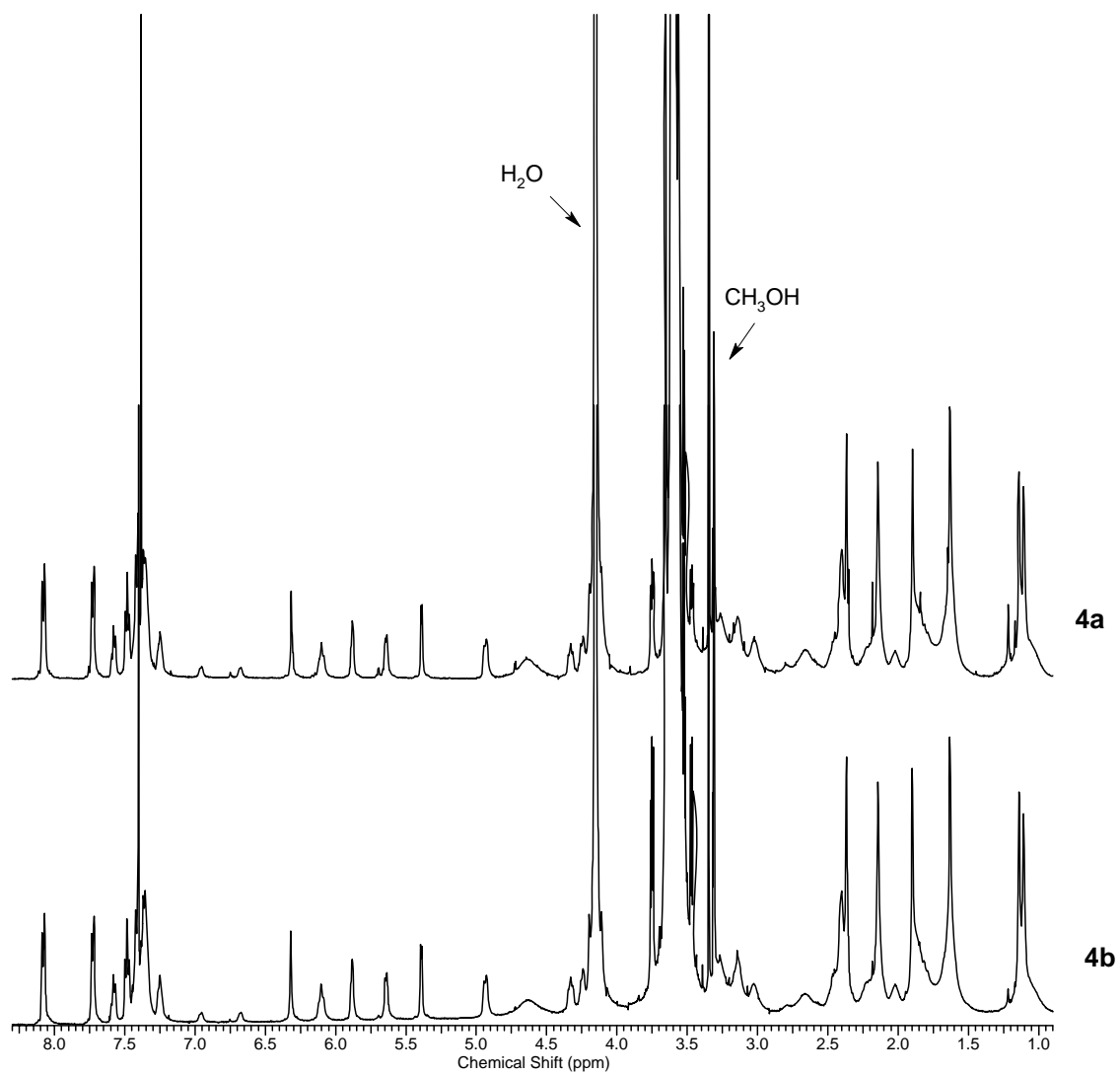


Figure 4.4. ¹H NMR of the PEGylated paclitaxel conjugates **4a** and **4b** purified from dialysis. The spectra were obtained in CDCl₃:MeOH-d₄ (10:1).

The polydispersity index (PDI) M_w/M_n was determined by GPC using THF as the eluent with polystyrene standards (Table 4.1). Both dendrimers showed very low PDIs (1.01-1.02). GPC analysis of dendrimer **4a** in THF showed a peak corresponding to dimer (2M), which was not observed in aqueous eluent such as 0.1 M NaNO₃. We are currently investigating the source of this dimerization.

Table 4.1. Analysis and characterization of **4a** and **4b**.

product	MW (Da) (MALDI-TOF)	M_n^a	PDI (M_w/M_n) ^a	wt % drug loading
4a	46100	82200 (2M)	1.02	30%
4b	77400	61300	1.01	18%

^a Determined by GPC in THF using polystyrene standards.

Part 5. In Vitro Studies of Paclitaxel Release

In vitro release of paclitaxel from **4a** and **4b** was evaluated using phosphate buffered saline (PBS) at the different pH (4.0, 5.5, and 7.4). The samples were prepared at the concentration of 0.2 mg/mL in microcentrifuge tubes and incubated at 37 °C with occasional vortexing.

To quantify paclitaxel released, the samples were extracted with HPLC grade diethyl ether at the scheduled time respectively. After evaporating solvent, the sample was dissolved in 1 mL of ethanol. The amount of released paclitaxel was determined by measuring absorbance at 227 nm with the extinction coefficient $\epsilon = 3.13 \times 10^4 \text{ M}^{-1} \text{ cm}^{-1}$.¹¹⁶ Release of paclitaxel was confirmed by HPLC analysis (Figure 4.5) using a mobile phase of 60% acetonitrile and 40% water at a flow rate of 1 mL/min with Symmetry C18

column (5 μm , 4.6 x 250 mm, Waters). The released paclitaxel was eluted at 6.84 min and detected at 227 nm. Figure 4.5 shows the release of paclitaxel from the conjugates was faster at lower pH due to the acid-labile ester linkage. Though both drug conjugates showed the same pattern of pH-dependent release, **4b** with longer PEG chains released the drug faster than **4a** at the same pH. Overall, the rates of release were similar to those reported by Jing and coworkers in a micellar block copolymer.¹¹⁷ After 3 d incubation, the percent drug releases of **4a** were respectively 25%, 19%, and 8% at the pH 4.0, 5.5, and 7.4, while those of **4b** were respectively 33%, 24%, and 14%.

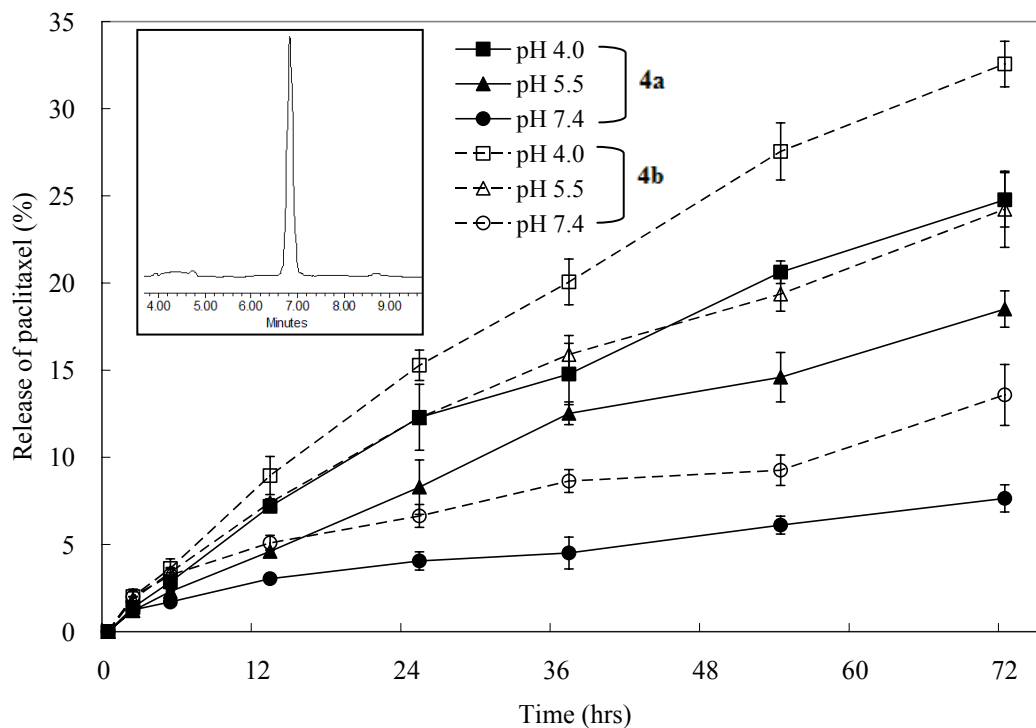


Figure 4.5. Paclitaxel release from **4a** and **4b** in PBS buffers (pH 4.0, 5.5, and 7.4) at 37 °C and a HPLC chromatogram showing paclitaxel released from the conjugates.

Conclusions

Here, we have described a drug-delivery vehicle, **2** that is installed with Bolton-Hunter as biodistribution tag, paclitaxel with the ester linkage for controlled release, and monochlorotriazine groups to be PEGylated for aqueous solubilization and size tuning. The precursor dendrimer **1** was prepared at 64% overall yield from the bisprotected amine, and the modification of paclitaxel was proceeded in four steps with 60% overall yield. The analysis and characterization of **2** showed that the drug conjugate contained up to 16 molecules of paclitaxel indicating fully coupling of **1** with the modified drug. After PEGylation, we obtained two dendrimers **4a** and **4b** with about MW 46 and 77 kDa respectively. In addition, the high paclitaxel payloads (up to 30 wt %) via the ester linkage can maximize the drug efficacy on the targeted cells, while reduce the toxicity during in vivo delivery of the drug. The in vitro drug release study of **4a** and **4b** revealed that paclitaxel was released faster at lower pH, indicating hydrolysis of the acid-labile ester link. Biological evaluation including in vivo biodistribution and toxicity studies will be performed in due course as well as the efficacy test with tumor models.

Experimental

General Procedures

Paclitaxel (Taxol) was purchased from LC Laboratories or CEC. NHS-mPEGs were purchased from Nektar Therapeutics or Quanta BioDesign. All other chemicals were purchased from Aldrich and Acros and used without further purification. All solvents were ACS grade or HPLC grade and used without further purification.

Dialysis membranes were purchased from Spectrum Laboratories, Inc. Size exclusion chromatography (SEC) was carried out using a Waters Delta 600 system and a Waters 2414 refractive index detector. A Suprema 10 micron GPC analytical column (1000 Å, 8 x 300 mm) was used with 0.1 M NaNO₃ as the eluent and a flow rate of 1 mL/min. SEC analysis for the PDI was carried out using a Viscotek I-MBMMW-3078 mixed bed column and a triple detector system including a Model VE3580 RI detector. Polystyrene standards were used for calibration, and THF was used as the eluent at a flow rate of 1 mL/min. NMR spectra were recorded on a Varian Mercury 300 MHz or Inova 500 MHz spectrometer in CDCl₃, or CDCl₃:MeOH-d₄ (10:1). All mass spectral analyses were carried out by the Laboratory for Biological Mass Spectrometry at Texas A&M.

Experimental Procedures

2'-Glutarylpaclitaxel 10. Paclitaxel (0.50 g, 0.585 mmol) was added to a solution of glutaric anhydride (0.60 g, 5.25 mmol) in pyridine (7 mL). The solution was stirred under nitrogen for 4 h at room temperature, and then evaporated *in vacuo*. The residue was stirred in water (20 mL) for 30 min and extracted with dichloromethane. The organic layer was washed three times with brine, dried over MgSO₄, and evaporated under vacuum. The crude product was purified by silica gel chromatography (washed with dichloromethane and eluted with ethyl acetate) to give a white solid (0.55 g, 97%). ¹H NMR (300 MHz, CDCl₃) δ 8.14 (dd, *J* = 8.0, 1.5, 2H), 7.73 (dd, *J* = 8.4, 1.5, 2H), 7.61 (t, *J* = 7.5 Hz, 1H), 7.53-7.31 (m, 10H), 6.29 (s, 1H), 6.26 (t, *J* = 9.0, 1H), 5.99 (dd, *J* = 9.3, 3.0, 1H), 5.68 (d, *J* = 7.2, 1H), 5.49 (d, *J* = 3.0, 1H), 4.98 (dd, *J* = 9.5, 2.1, 1H),

4.44 (dd, $J = 10.7, 6.5$ 1H), 4.31 (d, $J = 8.7$, 1H), 4.19 (d, $J = 8.1$, 1H), 3.81 (d, $J = 7.2$, 1H), 2.56 (m, 1H), 2.47 (s, 3H), 2.45-2.39 (m, 3H), 2.34 (t, $J = 7.5$ Hz, 2H), 2.22 (s, 3H), 2.17 (m, 1H), 1.94 (s, 3H), 1.91-1.84 (m, 3H), 1.67 (s, 3H), 1.23 (s, 3H), 1.13 (s, 3H); ^{13}C NMR (75 MHz, CDCl_3) δ 203.95, 176.28, 172.05, 171.44, 170.02, 168.31, 167.71, 167.12, 142.82, 136.96, 133.84, 133.71, 133.01, 132.19, 130.40, 129.35, 129.25, 128.90, 128.85, 128.65, 127.32, 126.68, 84.58, 81.25, 79.15, 76.68, 75.75, 75.26, 74.36, 72.27, 72.05, 58.63, 52.92, 45.72, 43.33, 35.68, 32.79, 32.42, 26.95, 22.84, 22.29, 20.98, 19.82, 14.95, 9.74; MS (MALDI-TOF) calcd for $\text{C}_{52}\text{H}_{57}\text{NO}_{17}$ 967.36, found 990.56 ($\text{M}+\text{Na}$) $^+$..

Paclitaxel-NHS ester 11. First, *N*-succinimidyl diphenylphosphate (SDPP) was prepared from the reaction of diphenyl chlorophosphate (2.68 g, 10 mmol), *N*-hydroxysuccinimide (1.16 g, 10 mmol), and triethylamine (2.0 mL, 14 mmol) in dichloromethane (40 mL). The reaction solution was stirred under nitrogen for 2 h at room temperature, filtered, and evaporated. The residue was dissolved in ethyl acetate, washed three times with brine, dried over MgSO_4 , and then evaporated under vacuum to give SDPP (2.90 g, 84%). A solution of SDPP (0.28 g, 0.81 mmol) in acetonitrile (10 mL) was added to a solution of **10** (0.52 g, 0.54 mmol) and triethylamine (0.315 mL, 2.21 mmol) in acetonitrile (10 mL). The solution was stirred under nitrogen for 6 h at room temperature and concentrated under vacuum. The residue was purified by silica gel chromatography (ethyl acetate:hexane = 5:2) to give **11** as a white solid (0.46, 80%). ^1H NMR (300 MHz, CDCl_3) δ 8.14 (d, $J = 6.9$, 2H), 7.71 (d, $J = 6.9$, 2H), 7.61 (t, $J = 7.5$ Hz, 1H), 7.54-7.33 (m, 10H), 6.30 (s, 1H), 6.28 (t, $J = 8.4$, 1H), 5.98 (dd, $J = 9.3, 3.0$, 1H), 5.69 (d, $J = 7.5$, 1H), 5.48 (d, $J = 3.0$, 1H), 4.99 (d, $J = 8.4$, 1H), 4.45 (dd, $J = 10.7,$

6.2 (1H), 4.32 (d, $J = 7.8$, 1H), 4.21 (d, $J = 8.7$, 1H), 3.82 (d, $J = 7.2$, 1H), 2.91-2.51 (m, 8H), 2.49 (s, 3H), 2.38 (t, $J = 7.5$ Hz, 2H), 2.23 (s, 3H), 2.21-2.02 (m, 3H), 1.95 (s, 3H), 1.86 (m, 1H), 1.68 (s, 3H), 1.24 (s, 3H), 1.14 (s, 3H); MS (MALDI-TOF) calcd for $C_{56}H_{60}N_2O_{19}$ 1064.38, found 1087.14 (M+Na)⁺.

Paclitaxel-diaminopropane 12. A solution of **11** (720 mg, 0.68 mmol) in dichloromethane (20 mL) was slowly added to an ice-bath cooled solution of 1,3-diaminopropane (350 mg, 4.72 mmol) and triethylamine (120 μ L, 0.84 mmol) in dichloromethane (100 mL). The solution was stirred under nitrogen for 30 min at 0 °C. The solution was washed three times with brine, dried over MgSO₄, and then evaporated *in vacuo* to give a white solid (660 mg, 95%). ¹H NMR (300 MHz, CDCl₃+MeOH-d₄) δ 8.09 (d, $J = 6.9$, 2H), 7.72 (d, $J = 7.2$, 2H), 7.58 (t, $J = 7.2$ Hz, 1H), 7.50-7.45 (m, 3H), 7.40-7.35 (m, 6H), 7.29 (m, 1H), 6.31 (s, 1H), 6.12 (t, $J = 8.4$, 1H), 5.90 (d, $J = 3.6$, 1H), 5.66 (d, $J = 7.2$, 1H), 5.40 (d, $J = 3.9$, 1H), 4.95 (d, $J = 7.5$, 1H), 4.34 (dd, $J = 11.0$, 6.8, 1H), 4.27 (d, $J = 8.4$, 1H), 4.21 (d, $J = 8.4$, 1H), 3.76 (d, $J = 6.9$, 1H), 3.15 (t, $J = 6.6$ Hz, 2H), 2.58 (t, $J = 6.9$, 2H), 2.51 (t, $J = 7.2$, 2H), 2.46-2.41 (m, 3H), 2.37 (s, 3H), 2.28 (m, 1H), 2.17 (s, 3H), 2.10 (m, 1H), 1.90 (s, 3H), 1.88-1.79 (m, 3H), 1.64 (s, 3H), 1.54 (m, 2H), 1.16 (s, 3H), 1.11 (s, 3H); ¹³C NMR (75 MHz, CDCl₃) δ 203.88, 172.48, 172.29, 171.32, 170.21, 168.77, 167.43, 167.02, 142.45, 137.16, 133.81, 133.78, 133.07, 132.08, 130.38, 129.44, 129.21, 128.86, 128.73, 128.62, 127.45, 126.87, 84.58, 81.25, 79.13, 76.59, 75.63, 75.20, 74.28, 72.17, 71.99, 58.55, 53.12, 46.23, 45.74, 43.38, 37.93, 35.85, 35.73, 35.20, 33.04, 26.95, 22.87, 22.42, 21.15, 21.01, 14.93, 9.84; MS (MALDI-TOF) calcd for $C_{55}H_{65}N_3O_{16}$ 1023.44, found 1024.21 (M+H)⁺.

Paclitaxel-dichlorotriazine 13. A solution of cyanuric chloride (135 mg, 0.73 mmol) in THF (5 mL) was added to an ice-bath cooled solution of **12** (650 mg, 0.64 mmol) and DIPEA (250 μ L, 1.42 mmol) in THF. The solution was stirred for 1 h at 0 °C and concentrated *in vacuo*. The residue was dissolved in dichloromethane, washed three times with brine, dried over MgSO₄, and then evaporated. The crude product was purified by silica gel chromatography (ethyl acetate:dichloromethane:methanol = 8:8:1) to give a white solid (610 mg, 81%). ¹H NMR (300 MHz, CDCl₃+MeOH-d₄) δ 8.10 (d, *J* = 7.2, 2H), 7.75 (d, *J* = 6.9, 2H), 7.61 (t, *J* = 7.5 Hz, 1H), 7.53-7.37 (m, 9H), 7.29 (m, 1H), 6.34 (s, 1H), 6.14 (t, *J* = 8.7, 1H), 5.91 (dd, *J* = 9.2, 4.1, 1H), 5.67 (d, *J* = 7.2, 1H), 5.42 (d, *J* = 4.2, 1H), 4.96 (d, *J* = 7.5, 1H), 4.35 (dd, *J* = 10.8, 6.6, 1H), 4.28 (d, *J* = 8.1, 1H), 4.21 (d, *J* = 8.4, 1H), 3.78 (d, *J* = 7.2, 1H), 3.38 (t, *J* = 6.6 Hz, 2H), 3.18 (t, *J* = 6.6 Hz, 2H), 2.52-2.44 (m, 3H), 2.39 (s, 3H), 2.31-2.22 (m, 3H), 2.18 (s, 3H), 2.07 (m, 1H), 1.93 (s, 3H), 1.89 (m, 3H), 1.70 (m, 2H), 1.66 (s, 3H), 1.17 (s, 3H), 1.14 (s, 3H); ¹³C NMR (75 MHz, CDCl₃+MeOH-d₄) δ 203.81, 173.59, 172.34, 170.78, 170.17, 169.82, 169.28, 169.01, 168.77, 166.41, 165.44, 141.48, 136.54, 136.51, 133.68, 133.35, 133.04, 131.75, 129.90, 129.38, 128.83, 128.38, 128.34, 127.11, 126.72, 84.42, 80.90, 77.71, 76.33, 75.48, 74.78, 74.03, 71.84, 71.20, 57.97, 53.02, 45.78, 43.10, 38.11, 36.06, 35.67, 35.05, 34.54, 32.58, 28.35, 26.20, 22.32, 21.67, 20.66, 20.49, 14.21, 9.45; MS (MALDI-TOF) calcd for C₅₈H₆₄Cl₂N₆O₁₆ 1170.38, found 1193.00 (M+Na)⁺.

Intermediate 5. A solution of cyanuric chloride (1.24 g, 6.72 mmol) in THF (20 mL) was added to an ice-bath cooled solution of BisBoctriamine (4.50 g, 13.6 mmol) and DIPEA (4.4 mL, 24.9 mmol) in THF (50 mL). The solution was stirred for 1h at 0

°C, warmed to room temperature, and then reacted for 24 h. After the addition of 4-aminomethyl piperidine (3.0 mL, 26.3 mmol), the solution was stirred for an additional 24 h at room temperature and evaporated under vacuum. The residue was dissolved in dichloromethane, washed with brine, dried over MgSO₄, and then evaporated under vacuum. The crude product was purified by silica gel chromatography (dichloromethane:methanol = 8:1 with 1% NH₄OH) to give **5** (5.30 g, 93%) as a white solid. ¹H NMR (500 MHz, CDCl₃+MeOH-d₄) δ 4.69 (d, *J* = 13.0, 2H), 3.51 (br, 8H), 3.04 (br, 8H), 2.78 (t, *J* = 11.8 Hz, 2H), 2.56 (d, *J* = 6.5, 2H), 1.72 (br, 10H), 1.58 (br, 1H), 1.39 (s, 36H), 1.11 (ddd, *J* = 24.8, 12.5, 4.0, 2H); ¹³C NMR (75 MHz, CDCl₃) δ 165.48, 164.85, 156.09, 79.01, 47.91, 43.40, 43.14, 42.41, 39.70, 38.10, 37.19, 29.78, 28.55, 27.97; MS (MALDI-TOF) calcd for C₄₁H₇₇N₁₁O₈ 851.60, found 852.55 (M+H)⁺.

Intermediate 6. A solution of cyanuric chloride (379 mg, 2.05 mmol) in THF (20 mL) was added to an ice-bath cooled solution of **5** (3.50 g, 4.11 mmol) and DIPEA (1.4 mL, 7.92 mmol) in THF (50 mL). The solution was stirred for 1 h at 0 °C, warmed to room temperature, and then reacted for 24 h. After the addition of 4-aminomethyl piperidine (3.0 mL, 26.3 mmol), the solution was stirred for an additional 24 h at room temperature and evaporated under vacuum. The residue was dissolved in dichloromethane, washed with brine, dried over MgSO₄, and evaporated under vacuum. The crude product was purified by silica gel chromatography (dichloromethane:methanol = 8:1 with 1% NH₄OH) to give **6** (3.60 g, 93%) as a white solid. ¹H NMR (500 MHz, CDCl₃+MeOH-d₄) δ 4.67 (d, *J* = 12.5, 6H), 3.49 (br, 16H), 3.23 (br, 4H), 3.04 (br, 16H), 2.76 (m, 6H), 2.56 (d, *J* = 6.5, 2H), 1.74 (br, 24H), 1.60 (br,

1H), 1.39 (s, 72H), 1.12 (m, 6H); ^{13}C NMR (75 MHz, CDCl_3) δ 165.55, 164.92, 156.19, 79.15, 46.20, 43.40, 42.64, 38.18, 37.39, 29.98, 29.77, 28.63, 28.11; MS (MALDI-TOF) calcd for $\text{C}_{91}\text{H}_{165}\text{N}_{27}\text{O}_{16}$ 1892.29, found 1892.98 ($\text{M}+\text{H}$) $^+$.

Intermediate 7. A solution of cyanuric chloride (330 mg, 1.79 mmol) in THF (10 mL) was added to an ice-bath cooled solution of **6** (2.91 g, 1.54 mmol) and DIPEA (0.5 mL, 2.80 mmol) in THF (50 mL). The solution was stirred for 3 h at 0 °C and evaporated under vacuum. The residue was dissolved in dichloromethane, washed with brine, dried over MgSO_4 , and evaporated under vacuum. The crude product was purified by silica gel chromatography (ethyl acetate:hexane = 3:1) to give **7** (2.84 g, 90%) as a white solid. ^1H NMR (500 MHz, $\text{CDCl}_3+\text{MeOH}-d_4$) δ 4.67 (d, $J = 12.0$, 6H), 3.49 (br, 16H), 3.31 (br, 2H), 3.24 (br, 4H), 3.05 (br, 16H), 2.78 (t, $J = 12.0$, 6H), 1.74 (br, 25H), 1.39 (s, 72H), 1.16 (br, 6H); ^{13}C NMR (75 MHz, CDCl_3) δ 171.05, 170.00, 166.29, 165.58, 164.93, 156.18, 79.15, 46.31, 43.38, 42.76, 38.21, 37.50, 36.34, 29.97, 29.57, 28.63, 28.21; MS (MALDI-TOF) calcd for $\text{C}_{94}\text{H}_{164}\text{Cl}_2\text{N}_{30}\text{O}_{16}$ 2039.23, found 2040.13 ($\text{M}+\text{H}$) $^+$.

Intermediate 8. A solution of piperazine (30.4 mg, 0.353 mmol) and DIPEA (300 μL , 1.70 mmol) in methanol (3 mL) was added dropwise to an ice-bath cooled solution of **7** (1.44 g, 0.707 mmol) in THF (15 mL). The solution was warmed to room temperature, stirred for 24 hr, and then evaporated under vacuum. The residue was dissolved in dichloromethane, washed with brine, dried over MgSO_4 , and evaporated under vacuum. The crude product was purified by silica gel chromatography (dichloromethane:methanol = 9:1) to give **8** (1.30 g, 90%) as a white solid. ^1H NMR (300 MHz, $\text{CDCl}_3+\text{MeOH}-d_4$) δ 4.67 (d, $J = 12.0$, 12H), 3.82 (br, 8H), 3.49 (br, 32H),

3.25 (br, 12H), 3.04 (br, 32H), 2.78 (t, $J = 11.9$, 12H), 1.73 (br, 50H), 1.39 (s, 144H), 1.17 (br, 12H); ^{13}C NMR (75 MHz, $\text{CDCl}_3+\text{MeOH-d}_4$) δ 169.58, 168.62, 165.22, 164.67, 164.24, 156.42, 79.04, 45.95, 43.09, 42.63, 38.88, 37.81, 37.07, 36.76, 29.70, 28.85, 28.15, 27.74; MS (MALDI-TOF) calcd for $\text{C}_{192}\text{H}_{336}\text{Cl}_2\text{N}_{62}\text{O}_{32}$ 4092.59, found 4093.96 ($\text{M}+\text{H}$) $^+$.

Dendrimer 9. A solution of the modified Bolton-Hunter reagent salt (300 mg) in methanol (2 mL) was added to a solution of **8** (300 mg, 0.073 mmol) and DIPEA (0.4 mL, 2.3 mmol) in dichloromethane (1 mL). The solution was stirred for 48 h at 40 °C and the solvent was then removed by reduced-pressure evaporation. The residue was dissolved in dichloromethane, washed with brine, dried over MgSO_4 and evaporated under vacuum. The crude compound was purified by silica gel chromatography (ethyl acetate:dichloromethane:methanol = 10:10:1) to give **9** (300 mg, 92%) as a white solid. ^1H NMR (300 MHz, $\text{CDCl}_3+\text{MeOH-d}_4$) δ 7.00 (d, $J = 8.7$, 4H), 6.72 (d, $J = 8.4$, 4H), 4.68 (br, 12H), 3.77 (br, 24H), 3.49 (br, 32H), 3.30 (br, 12H), 3.03 (br, 32H), 2.86-2.73 (m, 16H), 2.60 (t, $J = 7.4$, 4H), 1.71 (br, 50H), 1.38 (s, 144H), 1.17 (br, 12H); ^{13}C NMR (75 MHz, $\text{CDCl}_3+\text{MeOH-d}_4$) δ 171.85, 166.21, 165.24, 164.85, 164.70, 156.46, 155.20, 131.36, 129.21, 115.19, 79.08, 46.06, 45.58, 43.42, 42.99, 41.40, 37.85, 37.14, 36.39, 35.21, 30.68, 29.68, 28.95, 28.19, 27.78; MS (MALDI-TOF) calcd for $\text{C}_{218}\text{H}_{370}\text{N}_{66}\text{O}_{36}$ 4488.92, found 4491.07 ($\text{M}+\text{H}$) $^+$.

Dendrimer 1. Trifluoroacetic acid (3 mL) was added to an ice-bath cooled solution of **9** (300 mg, 0.067 mmol) in dichloromethane (3 mL). Methanol (1 mL) was added to the solution. The solution was warmed to room temperature and stirred for 12 hr. The

solution was concentrated under vacuum to give a TFA salt and neutralized with triethylamine. MS (MALDI-TOF) calcd for $C_{138}H_{242}N_{66}O_4$ 2888.08, found 2889.19 (M+H)⁺.

Dendrimer 2. A solution of **1** (80 mg, 2.77×10^{-2} mmol) in water (3 mL) and THF (7 mL) was slowly added to a solution of **13** (660 mg, 0.563 mmol) and DIPEA (200 μ L, 1.13 mmol) in THF (20 mL). The solution was stirred for 48 h at room temperature and evaporated under vacuum. The residue was dissolved in dichloromethane, washed with brine, dried over $MgSO_4$, and evaporated under vacuum. The crude product was purified by silica gel chromatography (washed with ethyl acetate:dichloromethane:methanol = 8:8:1 and eluted with dichloromethane:methanol = 8:1) to give **2** (468 mg, 80%) as a white solid. The excess or unreacted paclitaxel-dichlorotriazine was recovered from the purification and reused. ¹H NMR (500 MHz, $CDCl_3+MeOH-d_4$) δ 8.08 (d, $J = 7.5$, 32H), 7.72 (br, 32H), 7.57 (t, $J = 7.3$, 16H), 7.49-7.34 (m, 144H), 7.27 (br, 16H), 6.96 (d, $J = 7.5$, 4H), 6.68 (d, $J = 6.5$, 4H), 6.31 (s, 16H), 6.12 (br, 16H), 5.89 (br, 16H), 5.65 (d, $J = 6.5$, 16H), 5.40 (d, $J = 3.0$, 16H), 4.93 (d, $J = 9.0$, 16H), 4.61 (br, 12H), 4.34 (br, 16H), 4.25 (d, $J = 8.0$, 16H), 4.19 (d, $J = 8.0$, 16H), 3.75 (d, $J = 6.5$, 16H), 3.62-3.13 (br m, 164H), 2.76 (br, 16H), 2.56 (br, 4H), 2.48-2.37 (br m, 96H), 2.27-2.06 (br m, 112H), 1.90-1.64 (br m, 226H), 1.19 (br, 12H), 1.15 (s, 48H), 1.11 (s, 48H); ¹³C NMR (125 MHz, $CDCl_3+MeOH-d_4$) δ 203.90, 173.27, 172.43, 171.81, 170.88, 169.91, 168.82, 165.26, 164.87, 141.70, 141.61, 136.67, 133.75, 133.45, 133.17, 131.84, 130.03, 129.49, 129.29, 128.94, 128.51, 128.44, 127.22, 126.83, 115.27, 84.49, 81.04, 77.88, 76.44, 75.60, 74.91, 74.13, 71.95, 71.38, 58.13, 53.09, 45.85, 43.21, 38.00, 37.49, 36.62, 35.79,

35.21, 34.88, 32.74, 29.57, 29.26, 28.72, 27.23, 26.39, 22.47, 21.85, 20.80, 20.74, 20.65, 14.38, 9.61; MS (MALDI-TOF) calcd for $C_{1066}H_{1250}Cl_{16}N_{162}O_{260}$ 21038.46, found 21113.59 (M+Na)⁺.

Dendrimer 3. A solution of 4-aminomethylpiperidine (23 μ L, 0.20 mmol) in THF (5 mL) was added to an ice-bath cooled solution of **2** (60 mg, 2.85×10^{-3} mmol) in THF (10 mL). The solution was warmed to room temperature and stirred under nitrogen for 16 h. After the dilution with chloroform (20 mL), the solution was washed two times with brine, dried over $MgSO_4$, and evaporated under vacuum to give **3** (60 mg, 94%) as a white solid. MS (MALDI-TOF) calcd for $C_{1162}H_{1458}N_{194}O_{260}$ 22288.68, found 22302.19 (M+H)⁺.

Dendrimer 4a. A solution of NHS-mPEG (MW 2 kDa, 146 mg, 7.3×10^{-2} mmol) in dichloromethane (5 mL) was added to a solution of **3** (68 mg, 3.1×10^{-3} mmol) and DIPEA (30 μ L, 0.17 mmol) in dichloromethane (5 mL) and THF (10 mL). The solution was stirred under nitrogen for 24 h at room temperature and concentrated *in vacuo*. The residue was dissolved in deionized water and filtered. The filtrate was purified to remove low molecular weight impurities using a Spectra/Por cellulose ester membrane (MWCO: 25 kDa) in deionized water for 10 days. The deionized water was changed every 12 h. The dialyzed solution was evaporated under vacuum to afford **4a** as a white solid. The resulting compound was analyzed by size exclusion chromatography. MS (MALDI-TOF) PEGylated, found 46100.67 (M+H)⁺.

Dendrimer 4b. A solution of NHS-mPEG (MW 5 kDa, 280 mg, 5.6×10^{-2} mmol) in dichloromethane (5 mL) was added to a solution of **3** (60 mg, 2.7×10^{-3} mmol) and

DIPEA (22 μ L, 0.13 mmol) in dichloromethane (5mL) and THF (10 mL). The solution was stirred under nitrogen for 24 h at room temperature and concentrated *in vacuo*. The residue was dissolved in deionized water and filtered. The filtrate was purified to remove low molecular weight impurities using a Spectra/Por cellulose ester membrane (MWCO: 50 kDa) in deionized water for 10 days. The deionized water was changed every 12 h. The dialyzed solution was evaporated under vacuum to afford **4b** as a white solid. The resulting compound was analyzed by size exclusion chromatography. MS (MALDI-TOF) PEGylated, found 77376.79 (M+H)⁺.

CHAPTER V

SUMMARY

Dendrimers have unique and promising characteristics to be used as drug delivery vehicles: multivalency, functional diversity, a well-defined globular structure, and mono- or low polydispersity. Here, dendrimers based on melamine were investigated to develop potent drug delivery system.

First, a versatile dendrimer with four orthogonally reactive groups was synthesized: two monochlorotriazine groups at the core, four free hydroxyl, four TBDPS ether, and sixteen BOC groups on the surface. The multiple functional groups can be utilized for diverse biological applications including PEGylation, radio-labeling, the attachment of targeting ligands, and drug conjugation.

Second, post-synthetic manipulations of the dendrimer above were carried out, and followed by preliminary biodistribution studies. By using monochlorotriazine groups, the reporting groups, Bolton-Hunter and DOTA were incorporated into the dendrimer. The *in vivo* biodistribution of dendrimers can be evaluated by employing either radioactive iodines or metals. PEGylation provided the enhanced solubility in physiological conditions and tailored the molecular size. We also investigated *in vivo* biodistribution of these modified triazine dendrimers. As expected, dendrimers with longer PEG chains displayed a prolonged plasma circulation time, which was a promising property to passively target the diseased tissues via the EPR effect. High uptake by tumor tissues was found for this melamine dendrimer in tumor-bearing mice.

Finally, a dendrimer including Bolton-Hunter groups, monochlorotriazine groups for PEGylation, and the anticancer agent paclitaxel groups was designed and synthesized. This drug delivery vehicle contains up to 30 wt % paclitaxel (16 molecules per dendrimer) via acid-labile ester linkage. The in vitro paclitaxel release studies displayed that the drug was released faster at lower pH. The complete biological evaluation of the dendritic drug carriers has been being pursued.

REFERENCES

1. Zubia, A.; Cossio, F. P.; Morao, I.; Rieumont, M.; Lopez, X. *J. Am. Chem. Soc.* **2004**, *126*, 5243-5252.
2. Hecht, S.; Fréchet, J. M. J. *Angew. Chem. Int. Ed.* **2001**, *40*, 74-91.
3. Kobayashi, H.; Brechbiel, M. W. *Curr. Pharm. Biotechnol.* **2004**, *5*, 539-549.
4. Wiener, E. C.; Brechbiel, M. W.; Brothers, H.; Magin, R. L.; Gansow, O. A.; Tomalia, D. A.; Lauterbur, P. C. *Magn. Reson. Med.* **1994**, *31*, 1-8.
5. Kobayashi, H.; Brechbiel, M. W. *Mol. Imaging* **2003**, *2*, 1-10.
6. Kobayashi, H.; Saga, T.; Kawamoto, S.; Sato, N.; Hiraga, A.; Ishimori, T.; Konishi, J.; Togashi, K.; Brechbiel, M. W. *Cancer Res.* **2001**, *61*, 4966-4970.
7. Smith, D. K.; Diederich, F. *Chem. Commun.* **1998**, *22*, 2501-2502.
8. Twyman, L. J.; Beezer, A. E.; Esfand, R.; Hardy, M. J.; Mitchell, J. C. *Tetrahedron Lett.* **1999**, *40*, 1743-1746.
9. Zimmerman, S. C.; Wendland, M. S.; Rakow, N. A.; Zharov, I.; Suslick, K. S. *Nature* **2002**, *418*, 399-403.
10. Stiriba, S.-E.; Frey, H.; Haag, R. *Angew. Chem. Int. Ed.* **2002**, *41*, 1329-1334.
11. Aulenta, F.; Hayes, W.; Rannard, S. *Eur. Polym. J.* **2003**, *39*, 1741-1771.
12. Cloninger, M. J. *Curr. Opin. Chem. Biol.* **2002**, *6*, 742-748.
13. Esfand, R.; Tomalia, D. A. *Drug Discovery Today* **2001**, *6*, 427-436.
14. Duncan, R. *Nature Reviews Drug Discovery* **2003**, *2*, 347-360.
15. Tang, M. X.; Szoka, F. C. *Gene Ther.* **1997**, *4*, 823-832.
16. Boas, U.; Heegaard, P. M. H. *Chem. Soc. Rev.* **2004**, *33*, 43-63.
17. Bosman, A. W.; Janssen, H. M.; Meijer, E. W. *Chem. Rev.* **1999**, *99*, 1665-1688.
18. Hawker, C. J.; Fréchet, J. M. J. *J. Am. Chem. Soc.* **1990**, *112*, 7638-7647.
19. Buhleier, E.; Wehner, W.; Vögtle, F. *Synthesis*, **1978**, 155-158.

20. De Brabrande-van den Berg, E. M. M.; Meijer, E. W. *Angew. Chem., Int. Ed.* **1993**, *32*, 1308-1311.
21. Chen, W.; Tomalia, D. A.; Thomas, J. L. *Macromolecules*, **2000**, *33*, 9169-9172.
22. Fréchet, J. M. J.; Tomalia, D. A. *Dendrimers and Other Dendritic Polymers*, Wiley, Chichester, 2001.
23. Tomalia, D. A.; Baker, H.; Dewald, J.; Hall, M.; Kallos, G.; Martin, S.; Roeck, J.; Ryder, J.; Smith, P. *Polym. J.* **1985**, *17*, 117-132.
24. Gillies, E. R.; Dy, E.; Fréchet, J. M. J.; Szoka, F. C. *Mol. Pharm.* **2005**, *2*, 129-138.
25. Gillies, E. R.; Fréchet, J. M. J. *J. Am. Chem. Soc.* **2002**, *124*, 14137-14146.
26. Adronov, A.; Fréchet, J. M. J. *Chem. Commun.* **2000**, 1701-1710.
27. Adronov, A.; Gilat, S. L.; Fréchet, J. M. J.; Ohta, K.; Neuwahl, F. V. R.; Fleming, G. R. *J. Am. Chem. Soc.* **2000**, *122*, 1175-1185.
28. Zimmerman, S. C.; Zeng, F. W.; Reichert, D. E. C.; Kolotuchin, S. V. *Science* **1996**, *271*, 1095-1098.
29. Kawa, M.; Fréchet, J. M. J. *Chem. Mater.* **1998**, *10*, 286-296.
30. Piotti, M. E.; Rivera, F.; Bond, R.; Hawker, C. J.; Fréchet, J. M. J. *J. Am. Chem. Soc.* **1999**, *121*, 9471-9472.
31. Gorman, C. B.; Smith, J. C. *Acc. Chem. Res.* **2001**, *34*, 60-71.
32. Zhang, W.; Tichy, S. E.; Pérez, L. M.; Maria, G.; Lindahl, P. A.; Simanek, E. E. *J. Am. Chem. Soc.* **2003**, *125*, 5086-5094.
33. Steffensen, M. B.; Simanek, E. E. *Org. Lett.* **2003**, *5*, 2359-2361.
34. Steffensen, M. B.; Simanek, E. E. *Angew. Chem. Int. Ed.* **2004**, *43*, 5178-5180.
35. Lim, J.; Simanek, E. E. *Mol. Pharm.* **2005**, *2*, 273-277.
36. Hollink, E.; Simanek, E. E. *Org. Lett.* **2006**, *8*, 2293-2295.
37. Chen, H. T.; Neerman, M. F.; Parrish, A. R.; Simanek, E. E. *J. Am. Chem. Soc.* **2004**, *126*, 10044-10048.
38. Zhang, W.; Simanek, E. E. *Org. Lett.* **2000**, *2*, 843-845.

39. Zhang, W.; Gonzalez, S. O.; Simanek, E. E. *Macromolecules* **2002**, *35*, 9015-9021.
40. Umali, A. P.; Simanek, E. E. *Org. Lett.* **2003**, *5*, 1245-1247
41. Acosta, E. J.; Deng, Y.; White, G. N.; Dixon, J. B.; McInnes, K. J.; Senseman, S. A.; Frantzen, A. S.; Simanek, E. E. *Chem. Mater.* **2003**, *15*, 2903-2909.
42. Zhang, W.; Jiang, J.; Qin, C.; Pérez, L. M.; Parrish, A. R.; Safe, S. H.; Simanek, E. E. *Supramolecular Chem.* **2003**, *15*, 607-616.
43. Zhang, W.; Simanek, E. E. *Tetrahedron. Lett.* **2001**, *42*, 5355-5357.
44. Neerman, M. F.; Chen, H. T.; Parrish, A. R.; Simanek, E. E. *Mol. Pharm.* **2004**, *1*, 390-393.
45. Bell, S. A.; McLean, M. E.; Oh, S.-K.; Tichy, S. E.; Zhang, W.; Corn, R. M.; Crooks, R. M.; Simanek, E. E. *Bioconjugate Chem.* **2003**, *14*, 488-493.
46. Timmerman, P.; Prins, L. J. *Eur. J. Org. Chem.* **2001**, *17*, 3191-3205.
47. Whitesides, G. M.; Simanek, E. E.; Mathias, J. P.; Seto, C. T.; Chin, D.; Mammen, M.; Gordon, D. M. *Acc. Chem. Res.* **1995**, *28*, 37-44.
48. Maciejewski, M.; Bednarek, E.; Janiszewska, J.; Janiszewski, J.; Szczygiel, G.; Zapora, M. *J. Macromol. Sci. Pure Appl. Chem.* **2000**, *37*, 753-783.
49. Verheyde, B.; Dehaen, W. *J. Org. Chem.* **2001**, *66*, 4062-4064.
50. Wu, P.; Feldman, A. K.; Nugent, A. K.; Hawker, C. J.; Scheel, A.; Voit, B.; Pyun, J.; Fréchet, J. M. J.; Sharpless, K. B.; Fokin, V. V. *Angew. Chem. Int. Ed.* **2004**, *43*, 3928-3932.
51. Simon, M.; Wittmar, M.; Bakowsky, U.; Kissel, T. *Bioconjugate Chem.* **2004**, *15*, 841-849.
52. Dautzenberg, H.; Zintchenko, A.; Konak, C.; Reschel, T.; Subr, V.; Ulbrich, K. *Langmuir* **2001**, *17*, 3096-3102.
53. Wang, F.; Bronich, T. K.; Kabanov, A. V.; Rauh, R. D.; Roovers, J. *Bioconjugate Chem.* **2005**, *16*, 397-405.
54. Mammen, M.; Choi, S. -K.; Whitesides, G. M. *Angew. Chem. Int. Ed.* **1998**, *37*, 2754-2794.
55. Zeng, F.; Lee, H.; Allen, C. *Bioconjugate Chem.* **2006**, *17*, 399-409.

56. Gossl, I.; Shu, L.; Schluter, A. D.; Rabe, J. P. *J. Am. Chem. Soc.* **2002**, *124*, 6860-6865.
57. Dennig, J. *Top. Curr. Chem.* **2003**, *228*, 227-236.
58. Haag, R.; Kratz, F. *Angew. Chem. Int. Ed.* **2006**, *45*, 1198-1215.
59. Matsumura, Y.; Maeda, H. *Cancer Res.* **1986**, *6*, 6387-6392.
60. Greish, K.; Fang, J.; Inutsuka, T.; Nagamitsu, A.; Maeda, H. *Clin. Pharmacokinet.* **2003**, *42*, 1089-1105.
61. Nallamothe, R.; Wood, G. C.; Pattillo, C. B.; Scott, R. C.; Kiani, M. F. Moore, B. M.; Thoma, L. A. *AAPS PharmSciTech.* **2006**, *7*, E1-E10.
62. Riezman, H.; Woodman, P. G.; van Meer, G.; Marsh, M. *Cell* **1997**, *91*, 731-738.
63. Wattiaux, R.; Laurent, N.; Conninck, S. W.; Jadot, M. *Adv. Drug Deliv. Rev.* **2000**, *41*, 201-208.
64. Rittner, K.; Benavente, A.; Bompard-Sorlet, A.; Heitz, F.; Divita, G.; Brasseur, R.; Jacobs, E. *Mol. Therapy.* **2002**, *5*, 104-114.
65. Jevprasesphant, R.; Penny, J.; Jalal, R.; Attwood, D.; McKeown, N. B.; D'Emanuele, A. *Int. J. Pharm.* **2003**, *252*, 263-266.
66. El Sayed, M.; Ginski, M.; Rhodes, C.; Ghandehari, H. *J. Controlled Release* **2002**, *81*, 355-365.
67. Malik, N.; Wiwattanapatapee, R.; Klopsch, R.; Lorenz, K.; Frey, H.; Weener, J. W.; Meijer, E. W.; Paulus, W.; Duncan, R. *J. Controlled Release* **2000**, *65*, 133-148.
68. Fischer, D.; Li, Y.; Ahlemeyer, B.; Krieglstein, J.; Kissel, T. *Biomaterials* **2003**, *24*, 1121-1131.
69. Ferruti, P.; Knobloch, S.; Ranucci, E.; Gianasi, E.; Duncan, R. *Proc. Int. Symp. Controlled Rel. Bioact. Mater.* **1997**, 45-46.
70. Kojima, C.; Kono, K.; Maruyama, K.; Takagishi, T. *Bioconjugate Chem.* **2000**, *11*, 910-917.
71. Kono, K.; Liu, M.; Fréchet, J. M. J. *Bioconjugate Chem.* **1999**, *10*, 1115-1121.
72. Kratz, F.; Beyer, U.; Schütte, M. T. *Crit. Rev. Ther. Drug Carrier Syst.* **1999**, *16*, 245-288.

73. De Jesús, O. L. P.; Ihre, H. R.; Gagne, L.; Fréchet, J. M. J.; Szoka, F. C. J. *Bioconjugate Chem.* **2002**, *13*, 453-461.
74. Kratz, F.; Müller-Driver, R.; Hofmann, I.; Drevs, J.; Unger, C. *J. Med. Chem.* **2000**, *43*, 1253-1256.
75. Gillies, E. R.; Goodwin, A. P.; Fréchet, J. M. J. *Bioconjugate Chem.* **2004**, *15*, 1254-1263.
76. Majoros, I. J.; Myc, A.; Thomas, T.; Mehta, C. B.; Baker, J. R. Jr. *Biomacromolecules* **2006**, *7*, 572-579.
77. Patri, A. K.; Kukowska-Latallo, J. F.; Baker, J. R. Jr. *Adv. Drug Deliv. Rev.* **2005**, *57*, 2203-2214.
78. Gillies, E. R.; Fréchet, J. M. J. *Bioconjugate Chem.* **2005**, *16*, 361-368.
79. Quintana, A.; Raczka, E.; Piehler, L.; Lee, I.; Myc, A.; Majoros, I.; Patri, A. K.; Thomas, T.; Mule, J.; Baker, J. R. Jr. *Pharm. Res.* **2002**, *19*, 1310-1316.
80. Saito, G.; Swanson, J. A.; Lee, K. -D. *Adv. Drug Deliv. Rev.* **2003**, *55*, 199-215.
81. Jones, L. R.; Goun, E. A.; Shinde, R.; Rothbard, J. B.; Contag, C. H.; Wender, P. A. *J. Am. Chem. Soc.* **2006**, *128*, 6526-6527.
82. El-Sayed, M. E. H.; Hoffman, A. S.; Stayton, P. S. *J. Controlled Release* **2005**, *104*, 417-427.
83. Satchi, R.; Connors, T. A.; Duncan, R. *Brit. J. Cancer* **2001**, *85*, 1070-1076.
84. Lee, M. -R.; Baek, K. -H.; Jin, H. J.; Jung, Y. -G.; Shin, I. *Angew. Chem. Int. Ed.* **2004**, *43*, 1675-1678.
85. Singer, J. W.; Baker, B.; De Vries, P.; Kumar, A.; Shaffer, S.; Vawter, E.; Bolton, M.; Garzone, P. *Adv. Exp. Med. Biol.* **2003**, *519*, 81-89.
86. Pendyala, L.; Schwartz, G.; Smith, P.; Zdanowicz, J.; Murphy, M.; Hausheer, F. *Cancer. Chemother. Pharmacol.* **2003**, *51*, 376-384.
87. Miller, D. P.; Asomaning, K.; Liu, G.; Wain, J. C.; Lynch, T. J.; Neuberg, D.; Su, L.; Christiani, D. C. *Cancer* **2006**, *107*, 1570-1577.
88. Vasey, P. A.; Kaye, S. B.; Morrison, R.; Twelves, C.; Wilson, P. Duncan, R.; Thomson, A. H.; Murray, L. S.; Hilditch, T. E.; Murray, T.; Burtles, S.; Fraier, D.; Frigerio, E.; Cassidy, J. *Clin. Cancer Res.* **1999**, *5*, 83-94.

89. Loadman, P. M.; Bibby, M. C.; Double, J. A.; Al-Shakhaa, W. M.; Duncan, R. *Clin. Cancer Res.* **1999**, *5*, 3682-3688.
90. Broeren, M. A. C.; van Dongen, J. L. J.; Pittelkow, Michael; Christensen, J. B.; van Genderen, M. H. P.; Meijer, E. W. *Angew. Chem.* **2004**, *43*, 3557-3562.
91. Fuchs, S.; Otto, H.; J., S.; Henklein, P.; Schlueter, A. D. *Chem. Commun.* **2005**, *14*, 1830-1832.
92. Wong, C.-H.; Ye, X.-S.; Zhang, Z. *J. Am. Chem. Soc.* **1998**, *120*, 7137-7138.
93. Westerberg, D. A.; Carney, P. L.; Rogers, P. E.; Kline, S. J.; Johnson, D. K. *J. Med. Chem.* **1989**, *32*, 236-243.
94. Coenen, H. H.; Mertens, J.; Mazière, B. *Radioionidation Reactions for Radio Pharmaceuticals*, Springer, Dordrecht, The Netherlands, 2006.
95. Wilbur, D. S. *Bioconjugate Chem.* **1992**, *3*, 433-470.
96. Bolton, A. E.; Hunter, W. M. *Biochem. J.* **1973**, *133*, 529-539.
97. Adam, M. J.; Wilbur, D. S. *Chem. Soc. Rev.* **2005**, *34*, 153-163.
98. Wu, A. M.; Yazaki, P. J.; Tsai, S.; Nguyen, K.; Anderson, A.; McCarthy, D. W.; Welch, M. J.; Shively, J. E.; Williams, L. E.; Raubitschek, A. A.; Wong, J. Y. C.; Toyokuni, T.; Phelps, M. E.; Gambhir, S. S. *Proc. Natl. Acad. Sci. USA* **2000**, *97*, 8495-8500.
99. Sprague, J. E.; Peng, Y.; Sun, X.; Weisman, G. R.; Wong, E. H.; Achilefu, S.; Anderson, C. J. *Clin. Cancer Res.* **2004**, *10*, 8674-8682.
100. Anderson, C. J.; Welch, M. J. *Chem. Rev.* **1999**, *99*, 2219-2234.
101. Maeda, D.Y.; Berman, F.; Murray, T. F.; Aldrich J. V. *J. Med. Chem.* **2000**, *43*, 5044-5049.
102. Andersson, H.; Lindegren, S.; Bäck, T.; Jacobsson, L.; Leser, G.; Horvath, G. *Acta Oncol.* **1999**, *38*, 323-328.
103. Andersson, H.; Elgqvist, J.; Horvath, G.; Hultborn, R.; Jacobsson, L.; Jensen, H.; Karlsson, B.; Lindegren, S.; Palm, S. *Clin. Cancer Res.* **2003**, *9*, 3914s-3921s.
104. Welling, P. G. *Pharmacokinetics*, Americal Chemical Society, Washington, DC., 1986, pp 213-240.
105. Rowinsky, E. K. *Annu. Rev. Med.* **1997**, *48*, 353-74.

106. Stevens, P. J.; Lee, R. J. *Anticancer Res.* **2003**, *23*, 4927-4932.
107. Lee, S. C.; Huh, K. M.; Lee, J.; Cho, Y. W.; Galinsky, R. E.; Park, K. *Biomacromolecules* **2007**, *8*, 202-208.
108. Shuai, X.; Merdan, T.; Schaper, A. K.; Xi, F.; Kissel, T. *Bioconjugate Chem.* **2004**, *15*, 441-448.
109. Ceruti, M.; Crosasso, P.; Brusa, P.; Arpicco, S.; Dosio, F.; Cattel, L. *J. Controlled Release* **2000**, *63*, 141-153.
110. Zhang, Z.; Feng, S. -S. *Biomaterials* **2006**, *27*, 4025-4033.
111. Ooya, T.; Lee, J.; Park, K. *Bioconjugate Chem.* **2004**, *15*, 1221-1229.
112. Khandare, J. J.; Jayant, S.; Singh, A.; Chandna, P.; Wang, Y.; Vorsa, N.; Minko, T. *Bioconjugate Chem.* **2006**, *17*, 1464-1472.
113. Grayson, S. M.; Frechet, J. M. J. *Chem. Rev.* **2001**, *101*, 3819-3868.
114. Safavy, A.; Georg, G. I.; Velde, D. V.; Raisch, K. P.; Safavy, K.; Carpenter, M.; Wang, W.; Bonner, J. A.; Khazaeli, M. B.; Buchsbaum, D. J. *Bioconjugate Chem.* **2004**, *15*, 1264-1274.
115. Ogura, H.; Nagai, S.; Takeda, K. *Tetrahedron Lett.* **1980**, *21*, 1467-1468.
116. Wenk, M. R.; Fahr, A.; Reszka, R.; Seelig, J. *J. Pharm. Sci.* **1996**, *85*, 228-231.
117. Xie, Z.; Guan, H.; Chen, X.; Lu, C.; Chen, L.; Hu, X.; Shi, Q.; Jing, X. *J. Controlled Release* **2007**, *117*, 210-216.

APPENDIX A
SPECTRA RELEVANT TO CHAPTER II

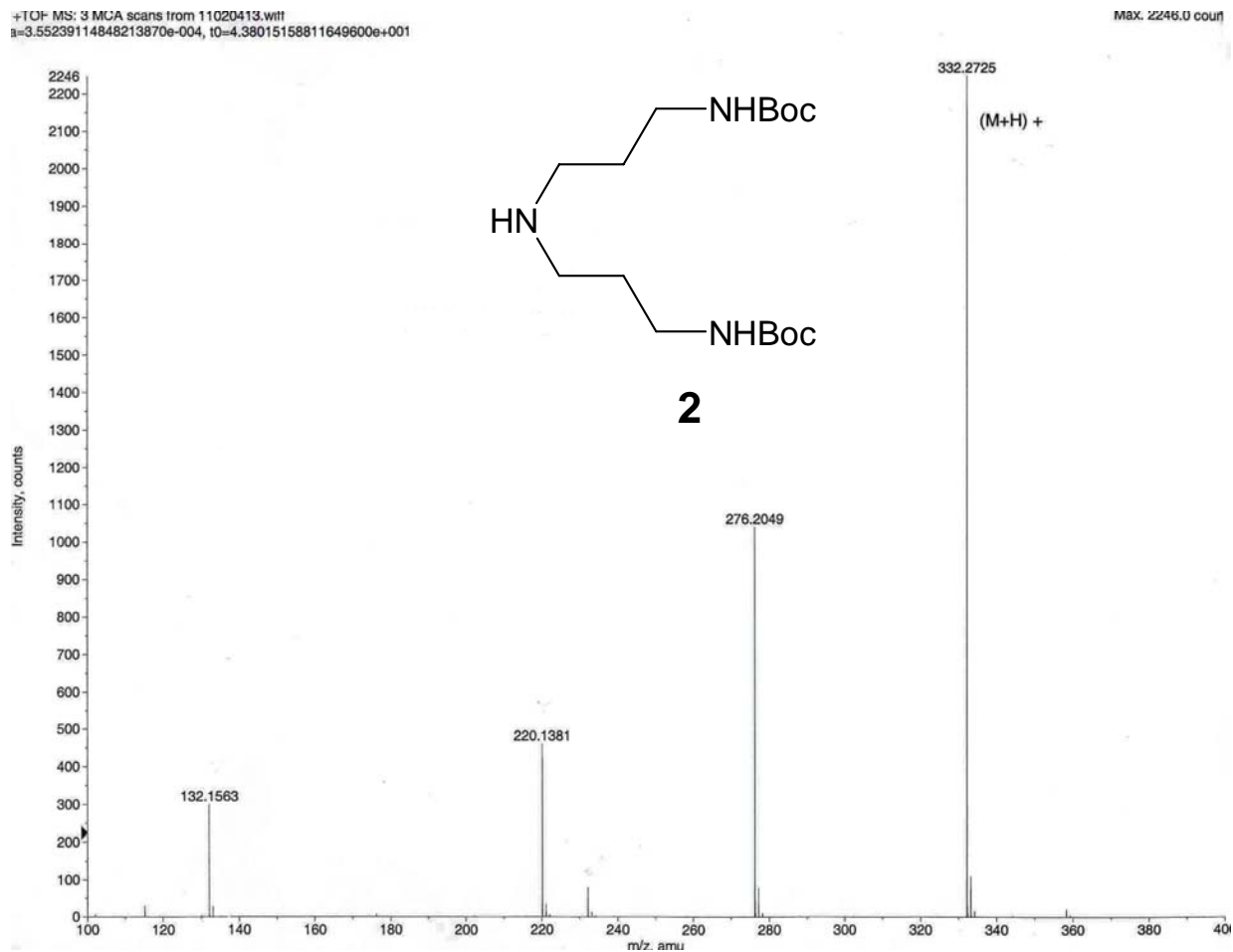


Figure A.1a. The ESI-TOF mass spectrum of **2**.

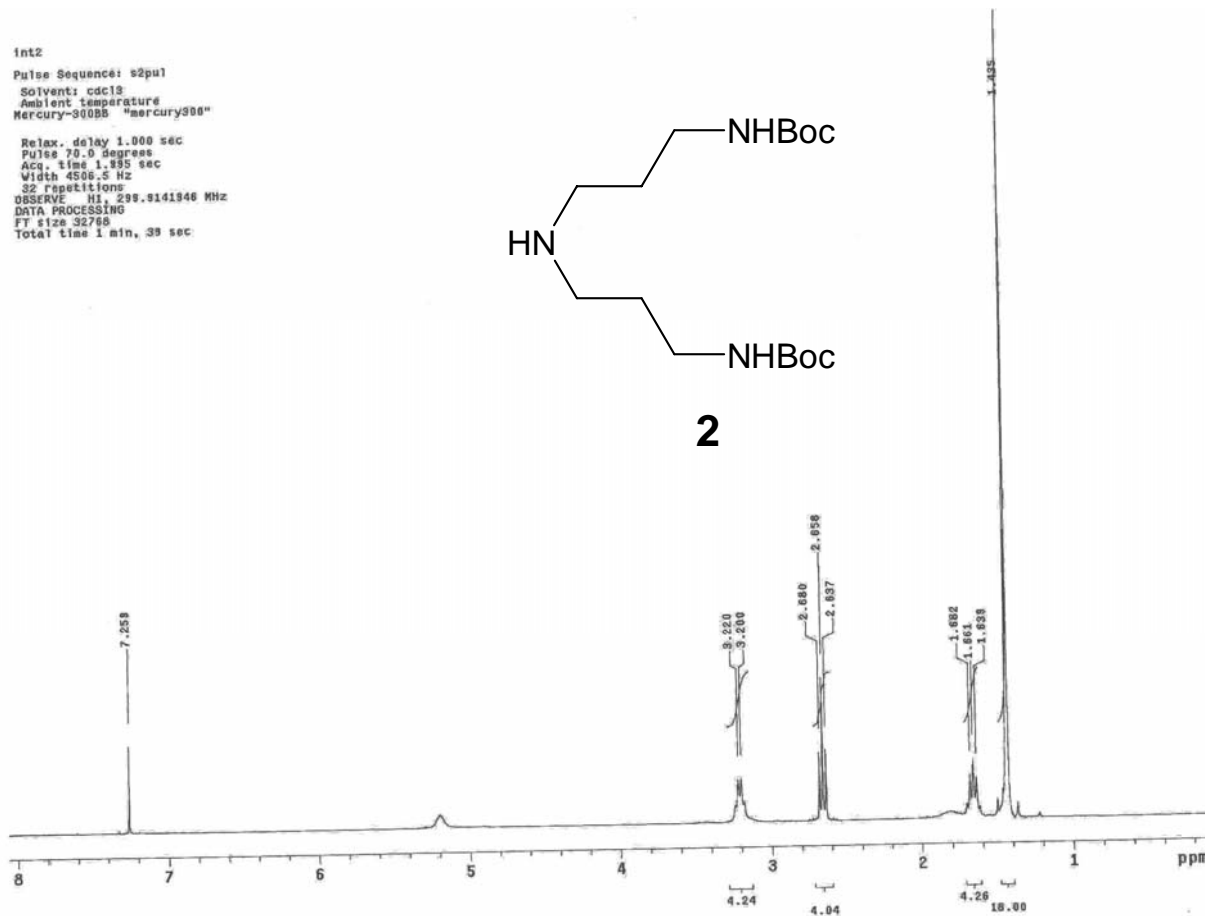


Figure A.1b. The ^1H NMR spectrum of **2**.

int2
Pulse Sequence: s2pu1
Solvent: cdc13
Ambient temperature
User: jdl1m
File: int2carbon
INOVA-500 "nmrsun2"

Pulse 84.8 degrees
Acq. time 1.815 sec
Width 18761.7 Hz
613 repetitions
OBSERVE C13, 75.4134741 MHz
DECOUPLE H1, 299.8156550 MHz
Power 35 dB
continuously on
WALTZ-16 modulated
DATA PROCESSING
Line broadening 1.0 Hz
FT size 131072
Total time 31 min, 7 sec

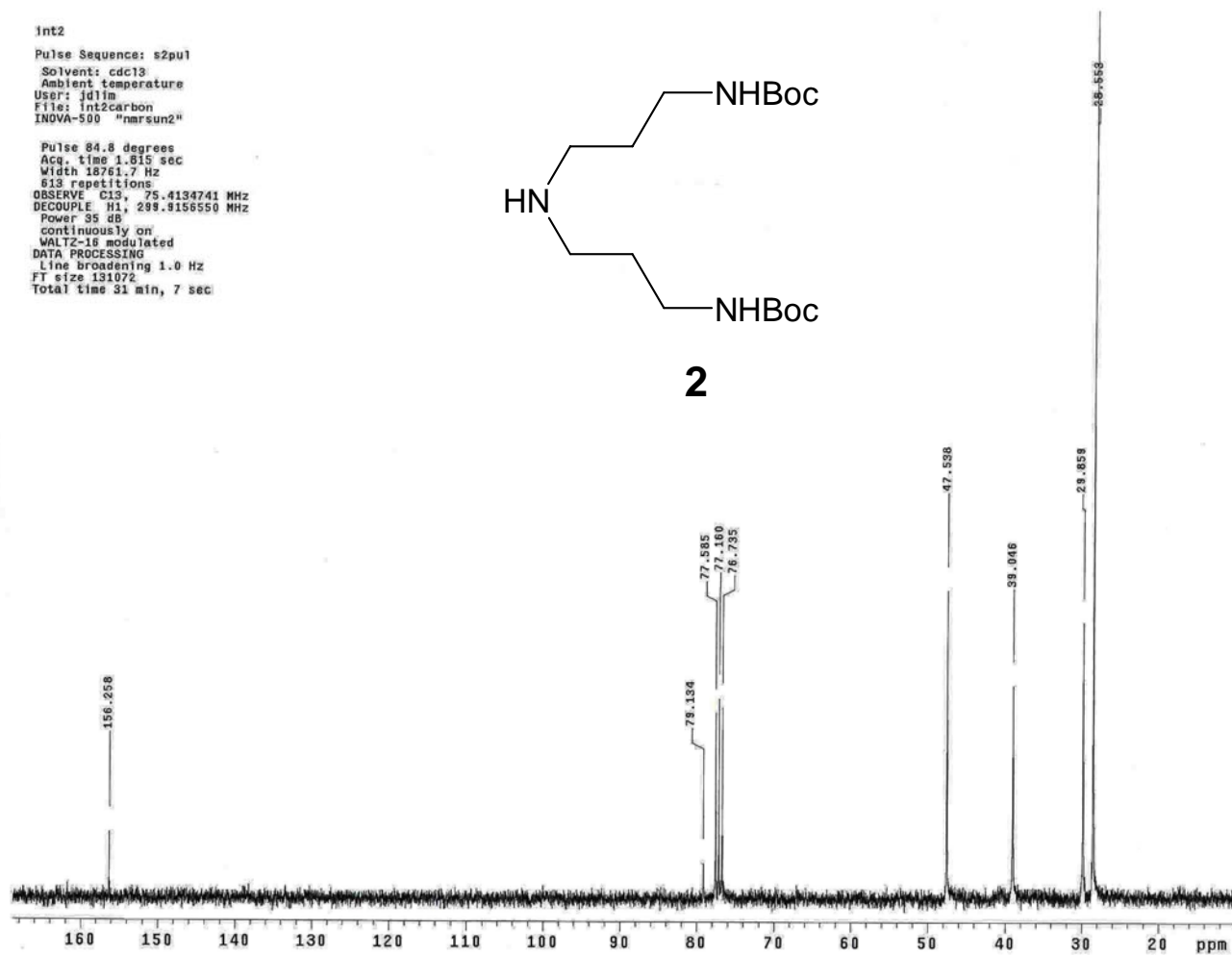


Figure A.1c. The ^{13}C NMR spectrum of 2.

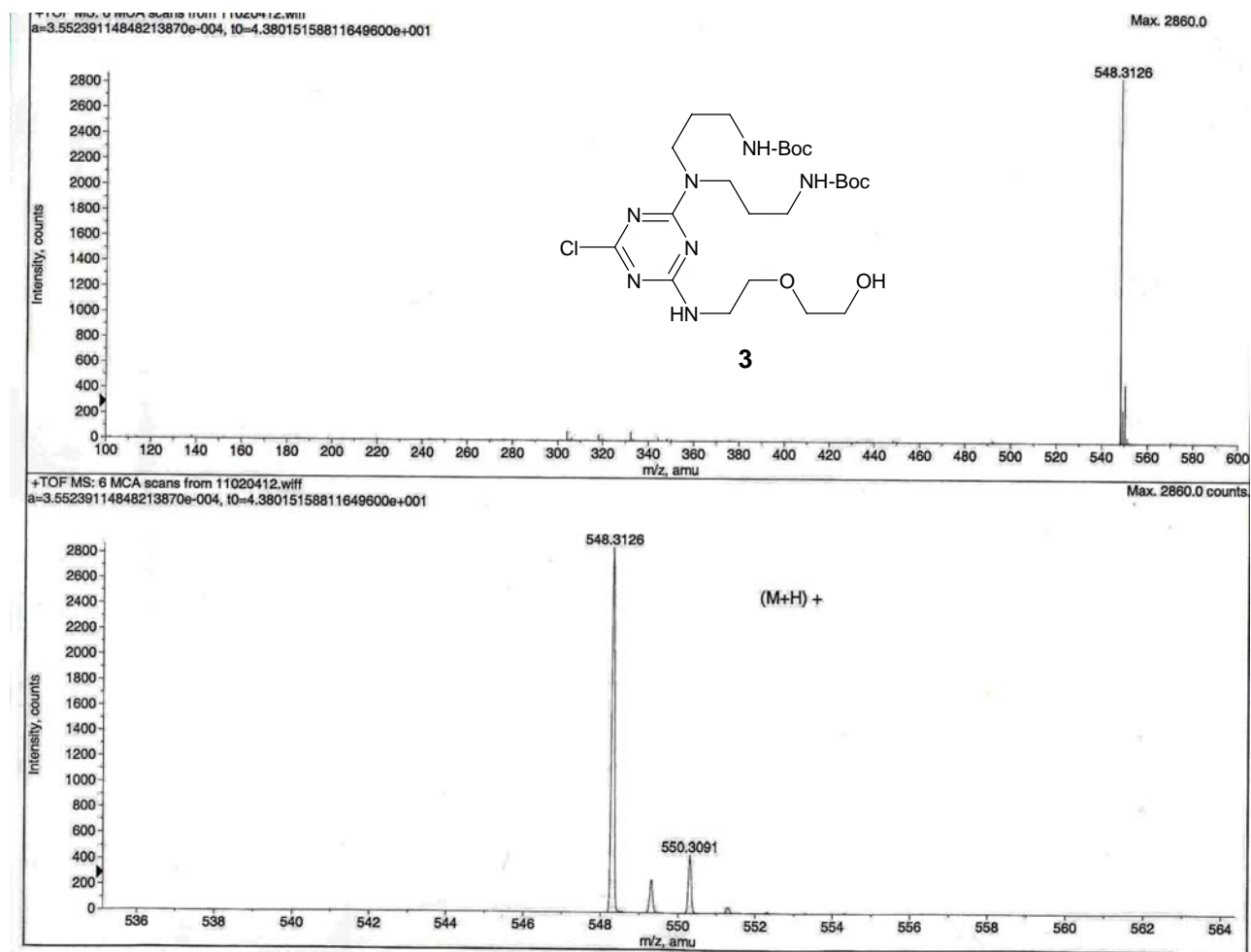


Figure A.2a. The ESI-TOF mass spectrum of **3**.

Int3-2
Pulse Sequence: s2pu1
Solvent: cdc13
Ambient temperature
File: Int3-2
Mercury-300BB "mercury300"

Pulse 67.0 degrees
Acq. time 3.744 sec
Width 4000.0 Hz
32 repetitions
OBSERVE H1, 299.9579356 MHz
DATA PROCESSING
FT size 32768
Total time 2 min, 4 sec

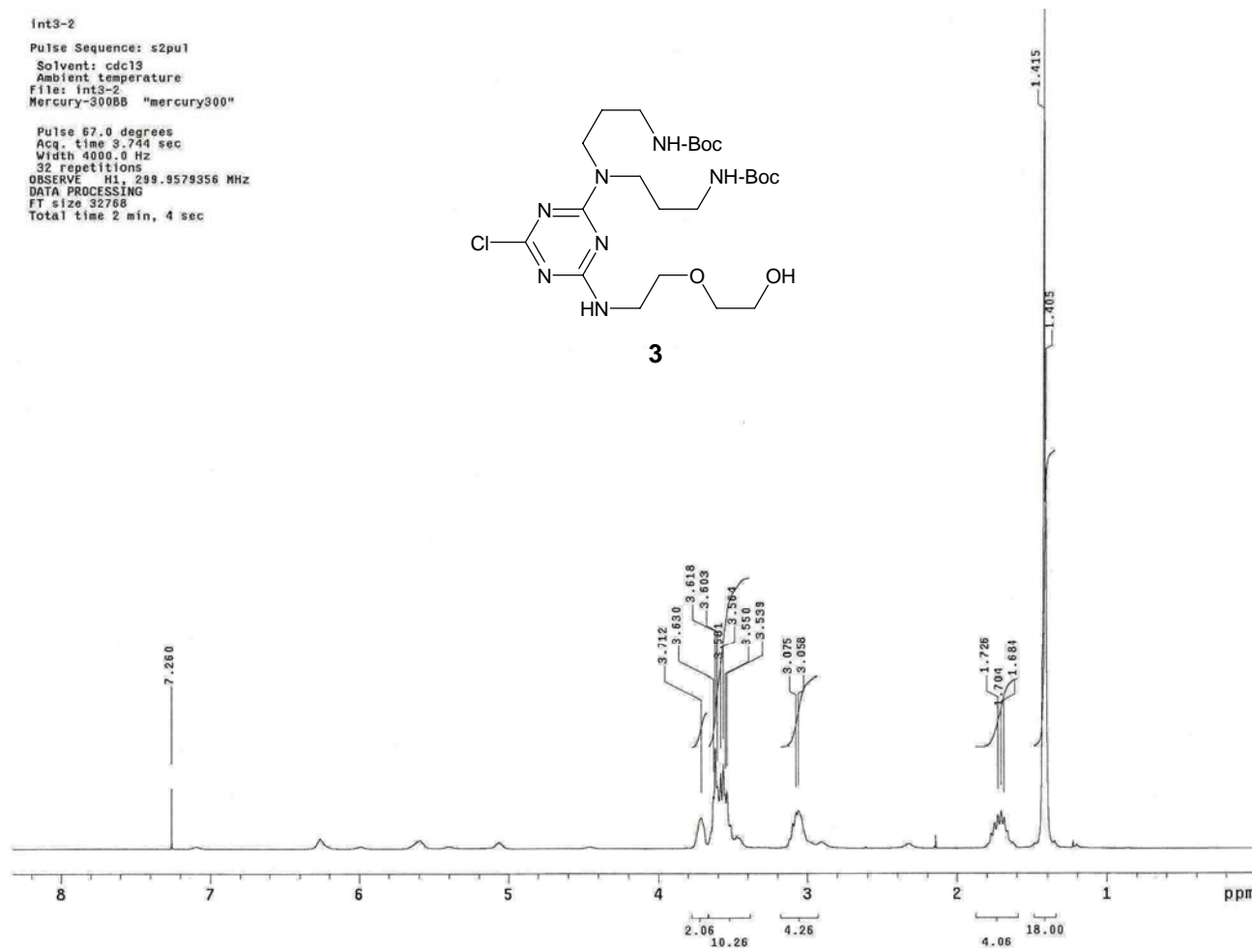
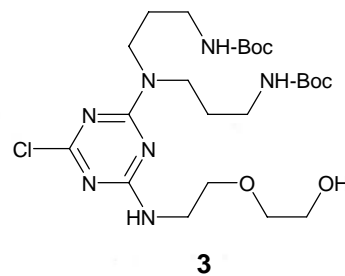


Figure A.2b. The ^1H NMR spectrum of **3**.

int3
Pulse Sequence: s2pu1
Solvent: cdc13
Ambient temperature
User: jdlm
File: int3-2c
INOVA-500 "narsun2"

Pulse 78.0 degrees
Acq. time 1.815 sec
Width 16501.7 Hz
20167 repetitions
OBSERVE C13, 75.4244746 MHz
DECOUPLE H1, 299.3594260 MHz
Power 35 dB
continuously on
WALTZ-16 modulated
DATA PROCESSING
Line broadening 1.0 Hz
FT size 65536
Total time 506 hr, 38 min, 59 sec

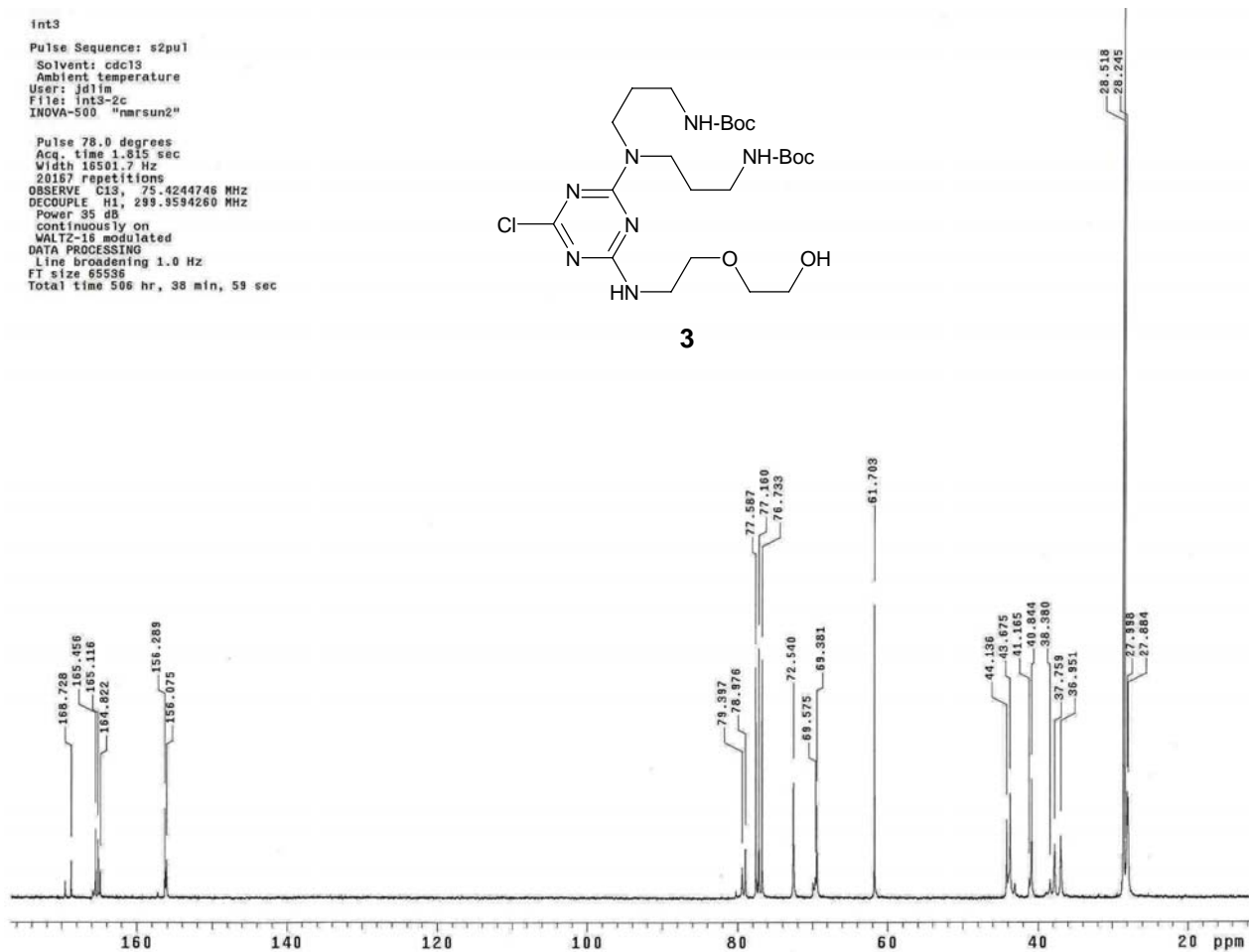
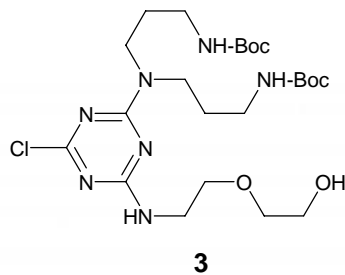


Figure A.2c. The ^{13}C NMR spectrum of **3**.

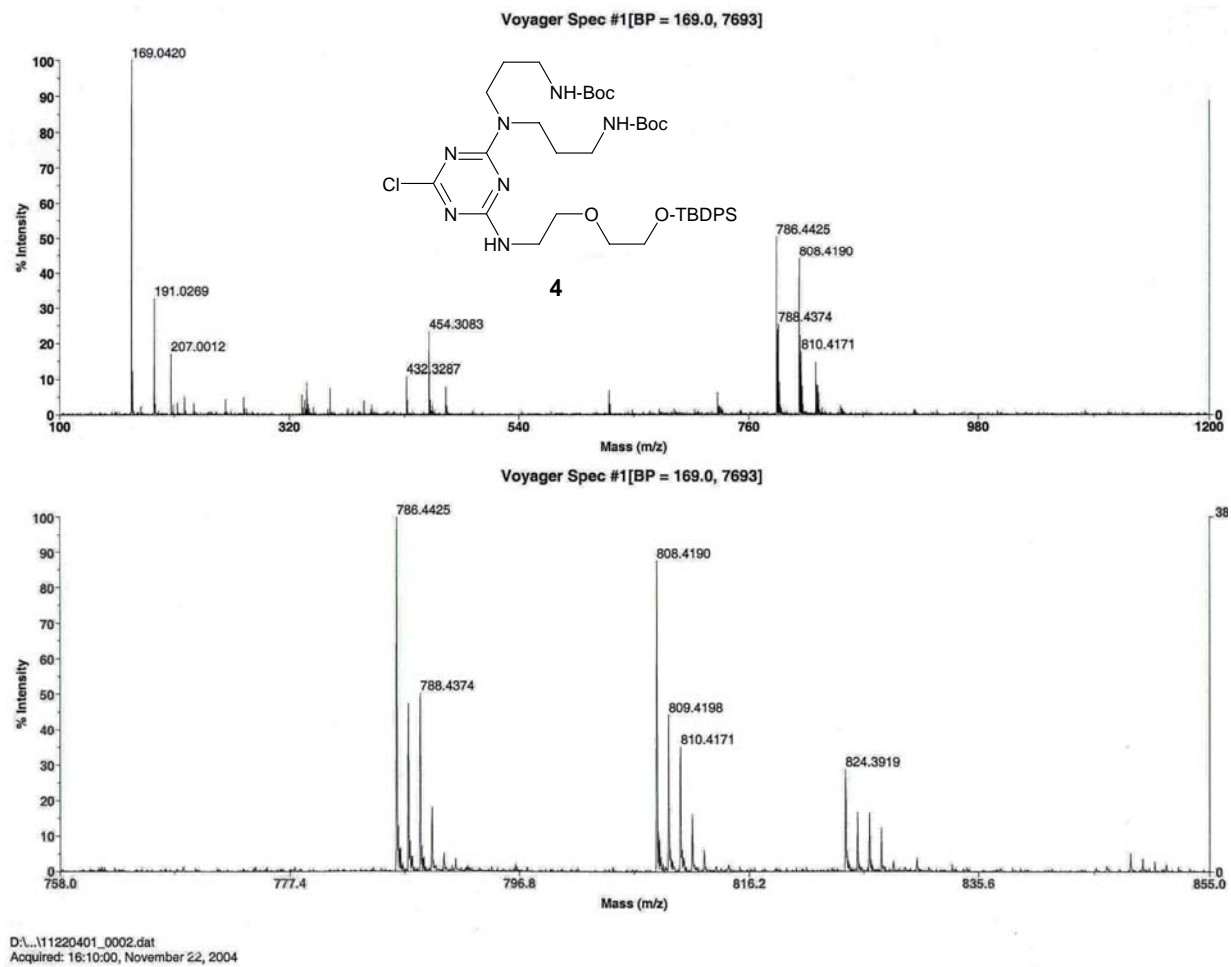


Figure A.3a. The MALDI-TOF mass spectrum of **4**.

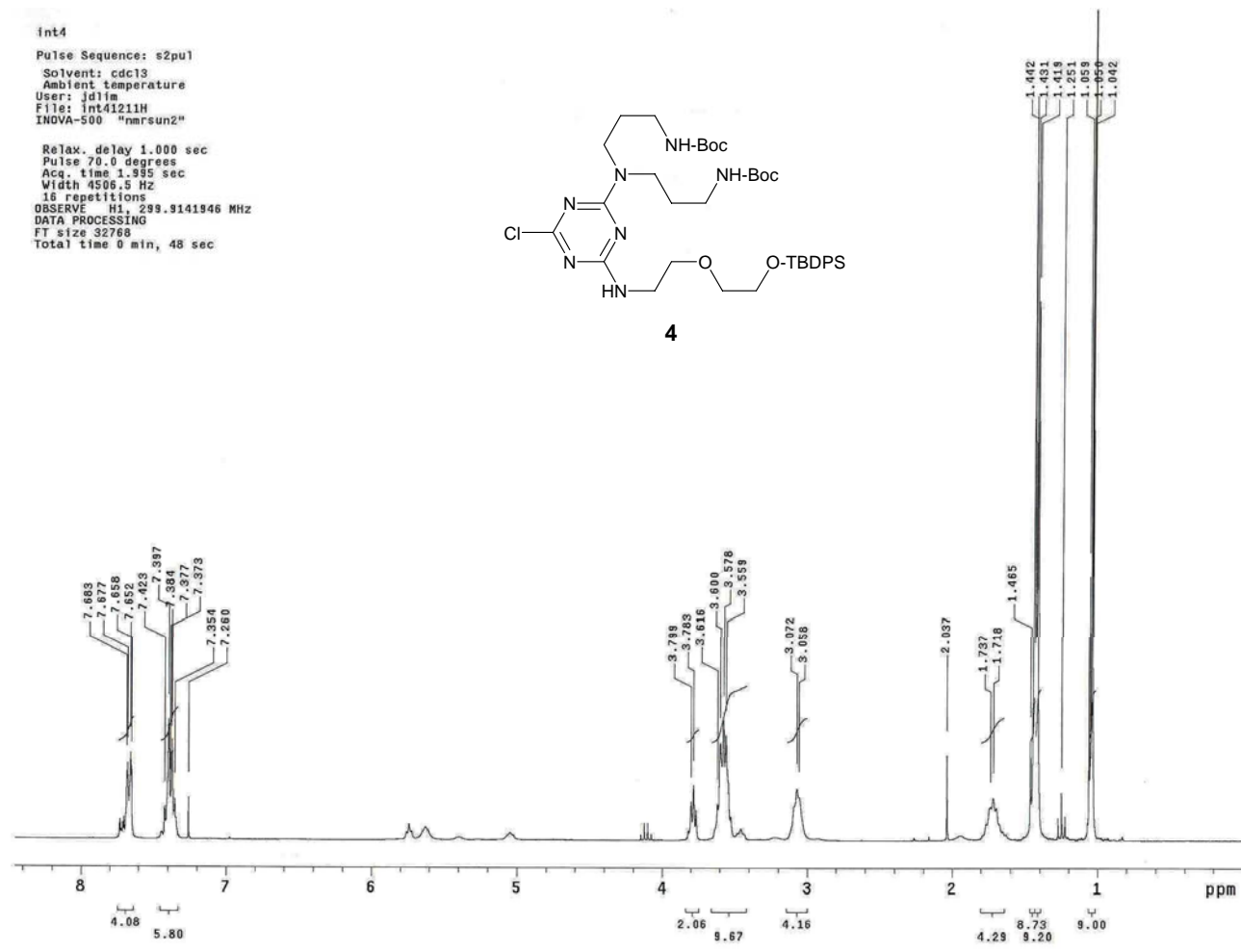


Figure A.3b. The ¹H NMR spectrum of **4**.

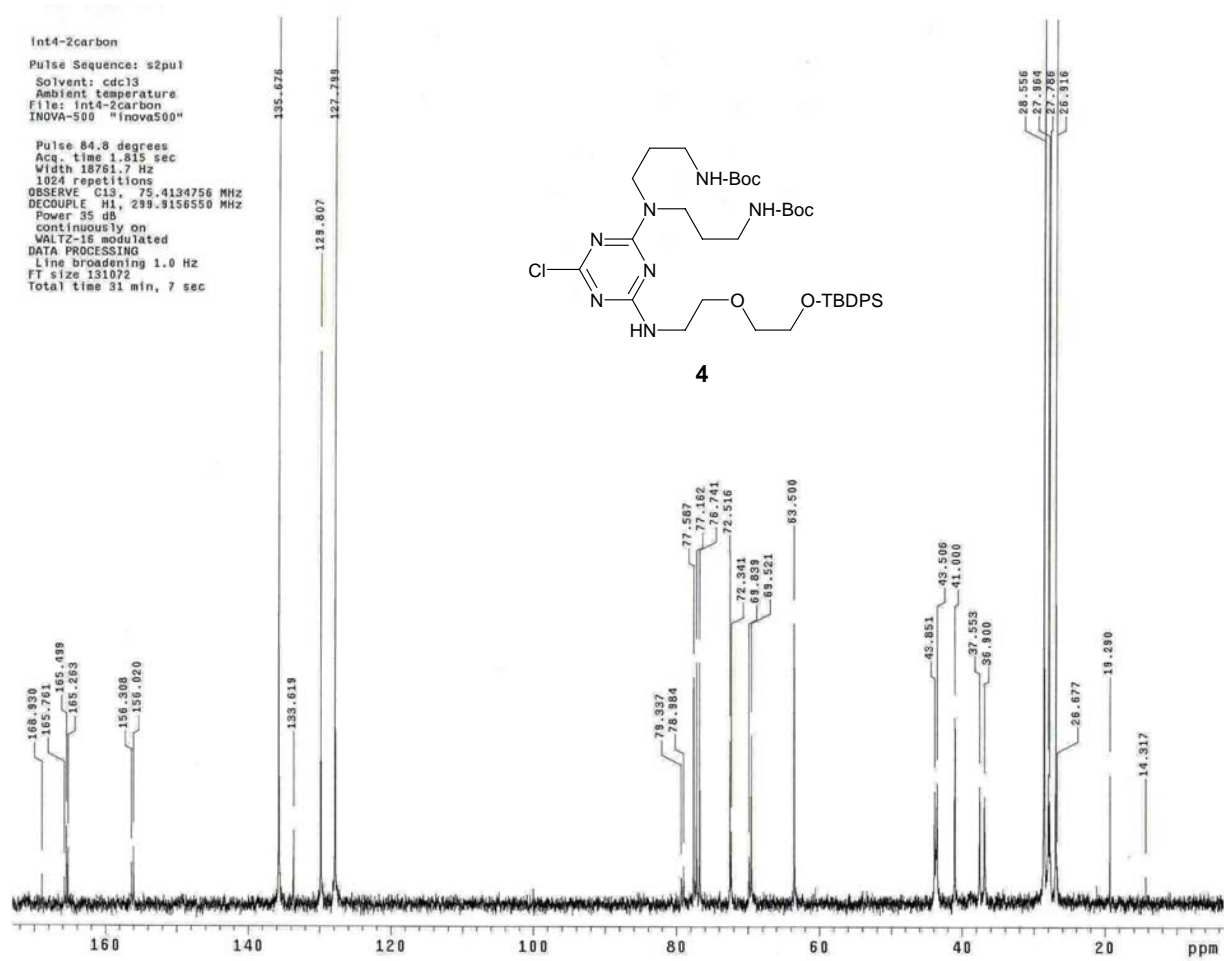


Figure A.3c. The ^{13}C NMR spectrum of **4**.

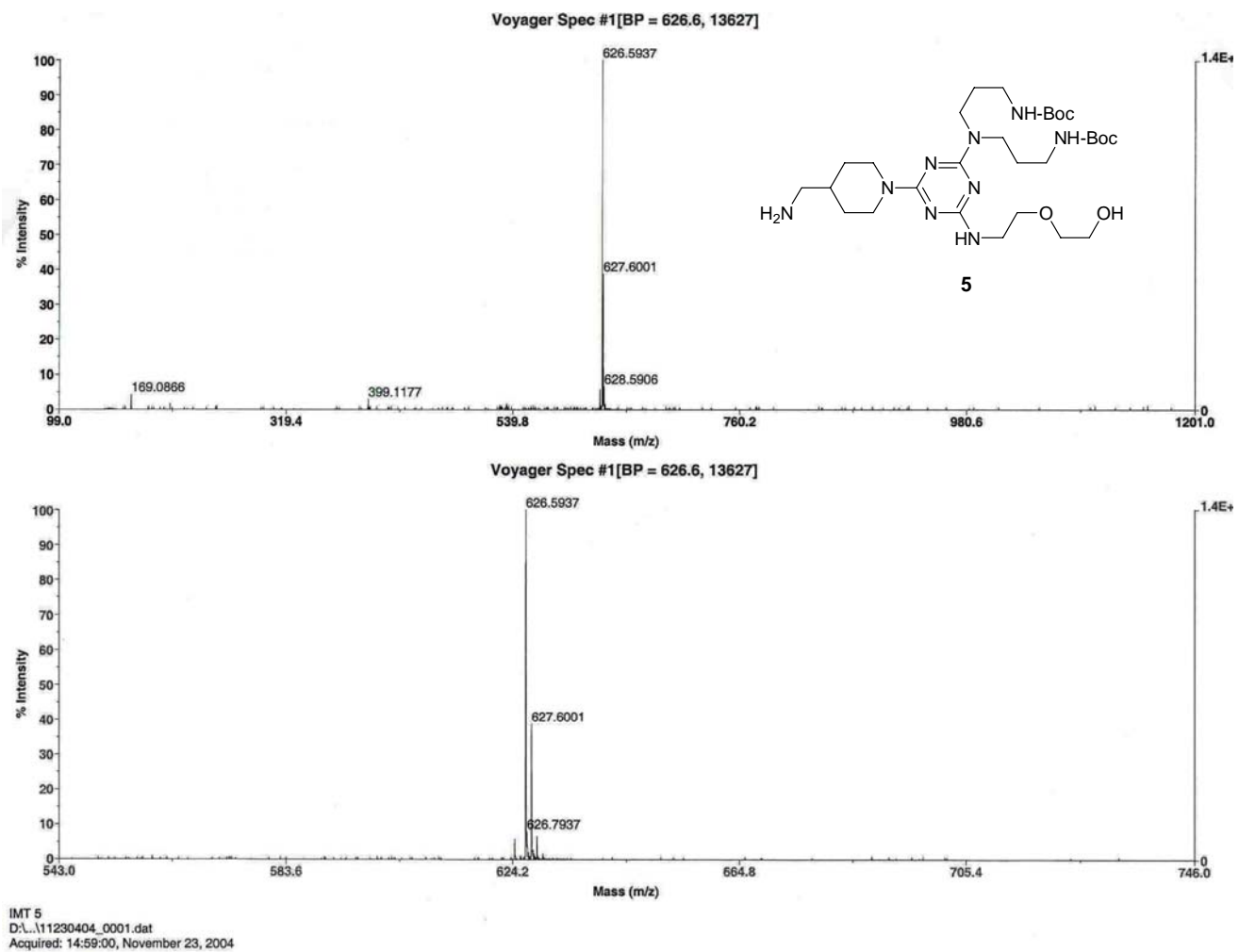


Figure A.4a. The MALDI-TOF mass spectrum of **5**.

int5
Pulse Sequence: s2pu1
Solvent: cdcl3
Ambient temperature
File: int6
INOVA-500 "inova500"
Pulse 67.0 degree
Acq. time 3.744 sec
Width 4000.0 Hz
16 repetitions
OBSERVE H1, 299.3579356 MHz
DATA PROCESSING
F1 size 32768
Total time 1 min, 0 sec

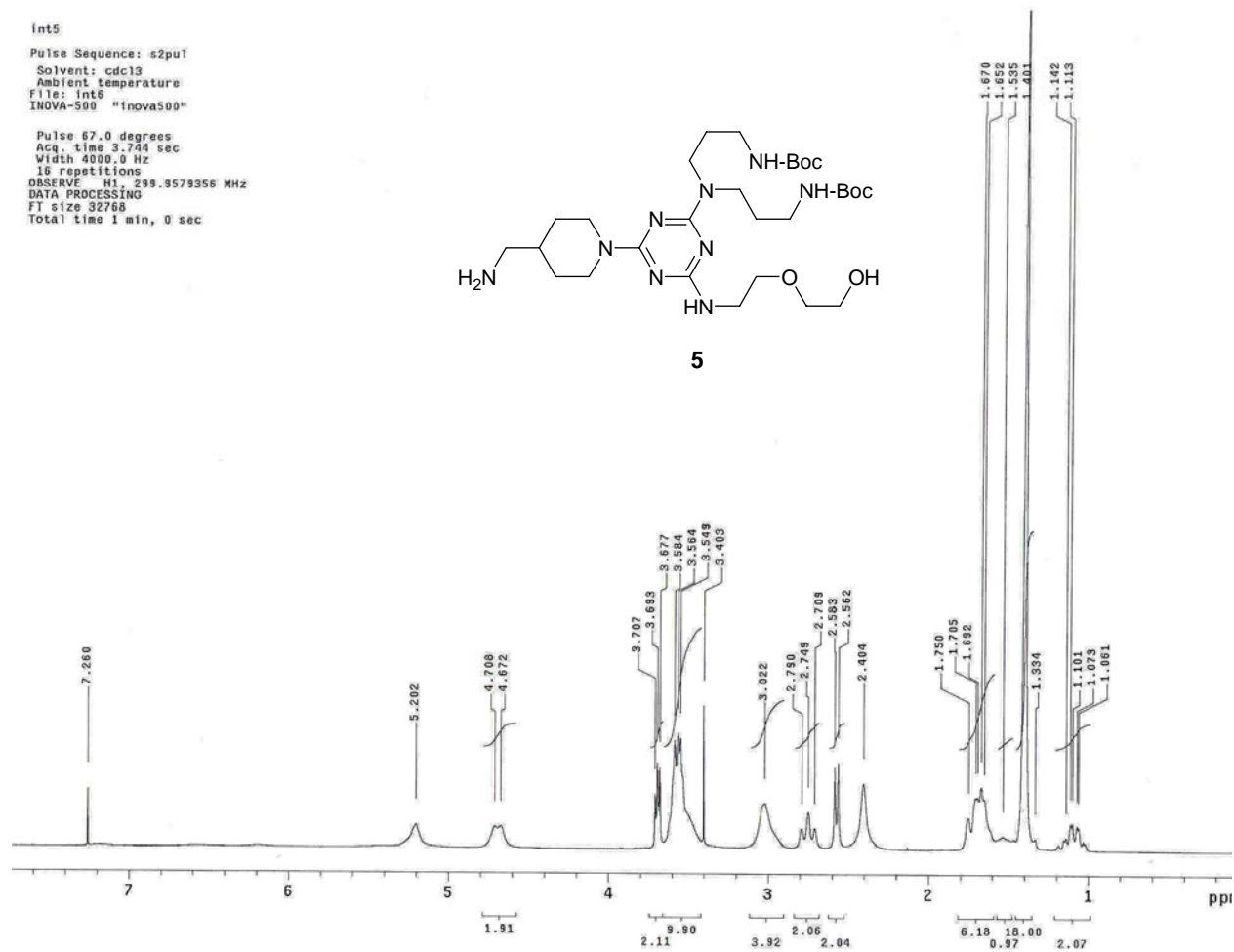
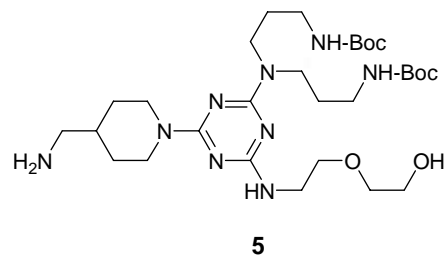


Figure A.4b. The ^1H NMR spectrum of **5**.

int6
 Pulse Sequence: s2pu1
 Solvent: cdcl3
 Ambient temperature
 Mercury-300BB "mercury300"
 Pulse 84.8 degrees
 Acq. time 1.815 sec
 Width 18761.7 Hz
 505 repetitions
 OBSERVE C13, 75.4134844 MHz
 DECOUPLE H1, 299.9156550 MHz
 Power 35 dB
 continuously on
 WALTZ-16 modulated
 DATA PROCESSING
 Line broadening 1.0 Hz
 FT size 131072
 Total time 117 hr, 20 min, 24 sec

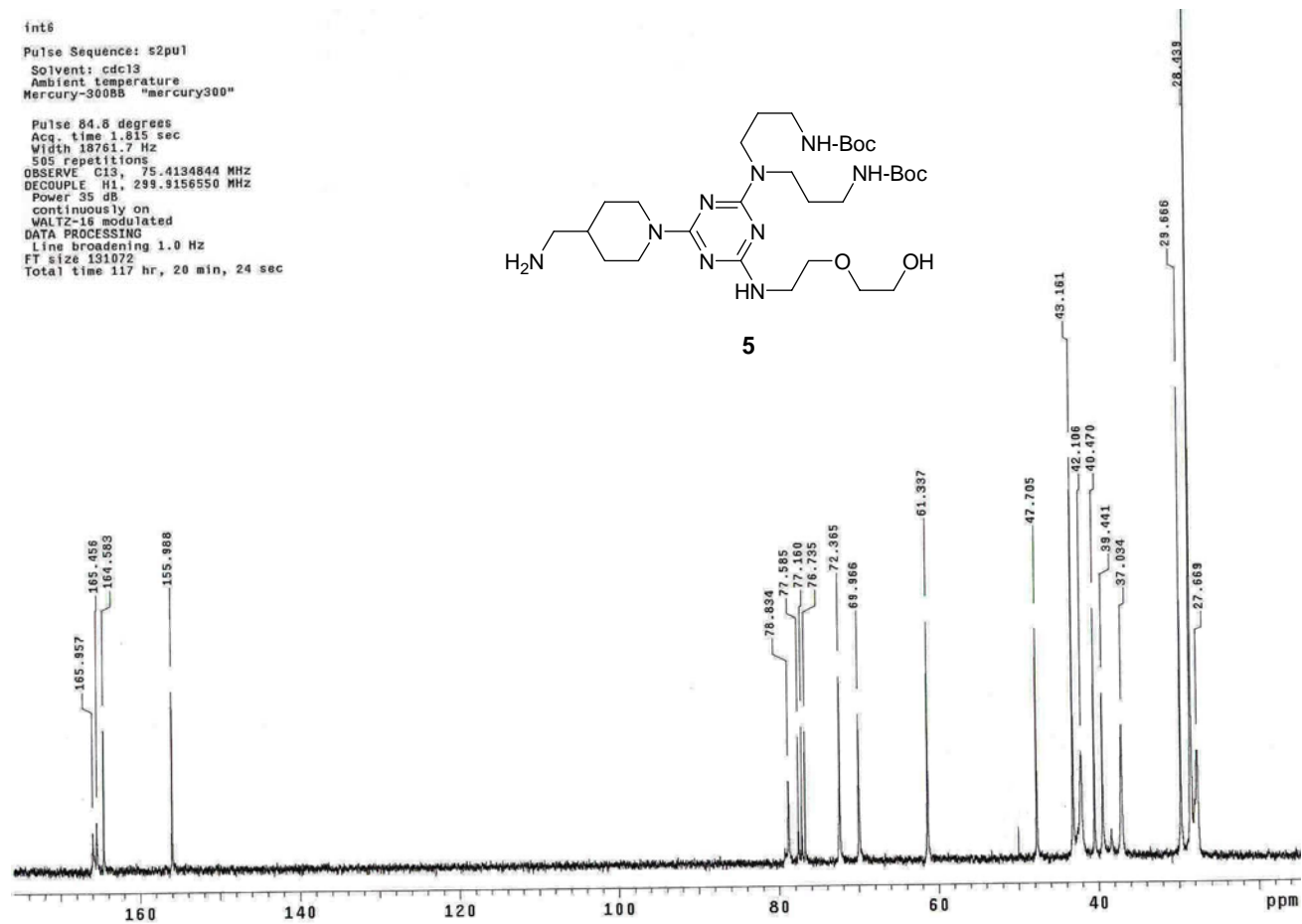
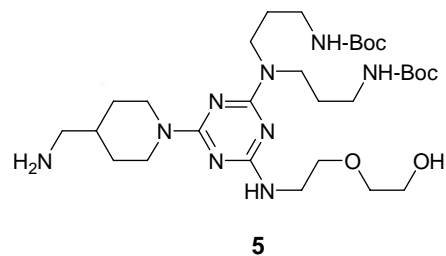


Figure A.4c. The ^{13}C NMR spectrum of **5**.

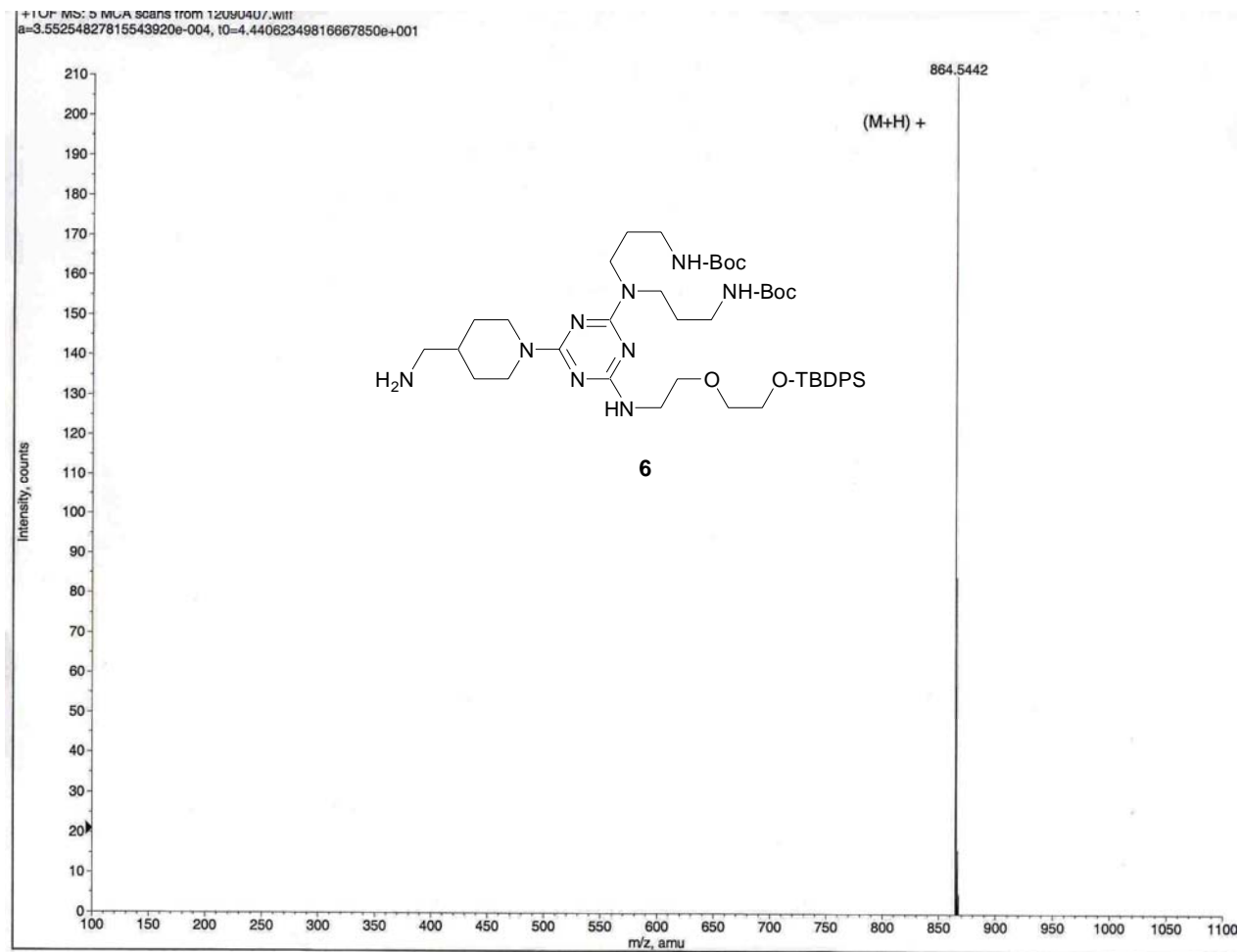


Figure A.5a. The ESI-TOF mass spectrum of **6**.

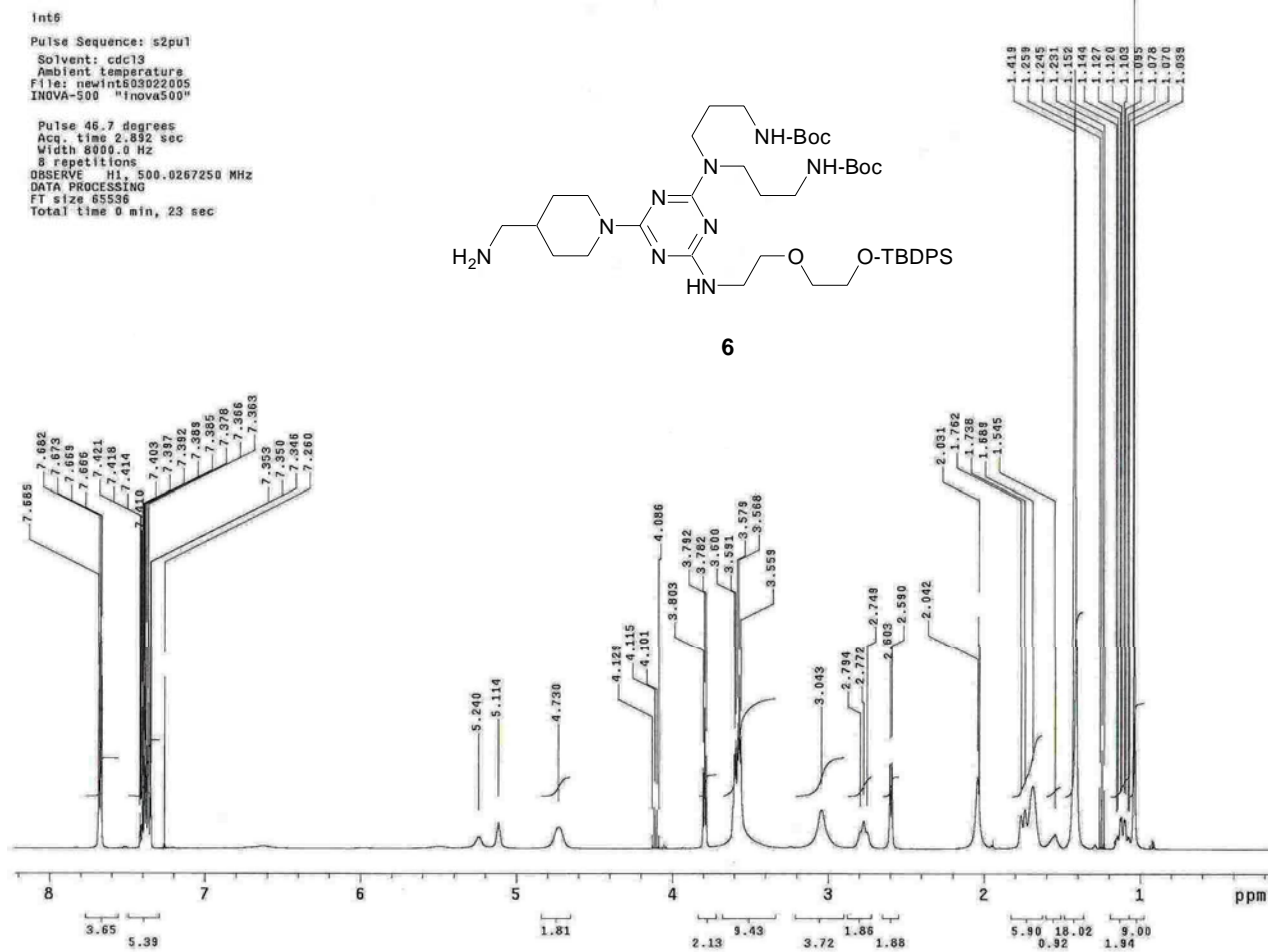


Figure A.5b. The ¹H NMR spectrum of **6**.

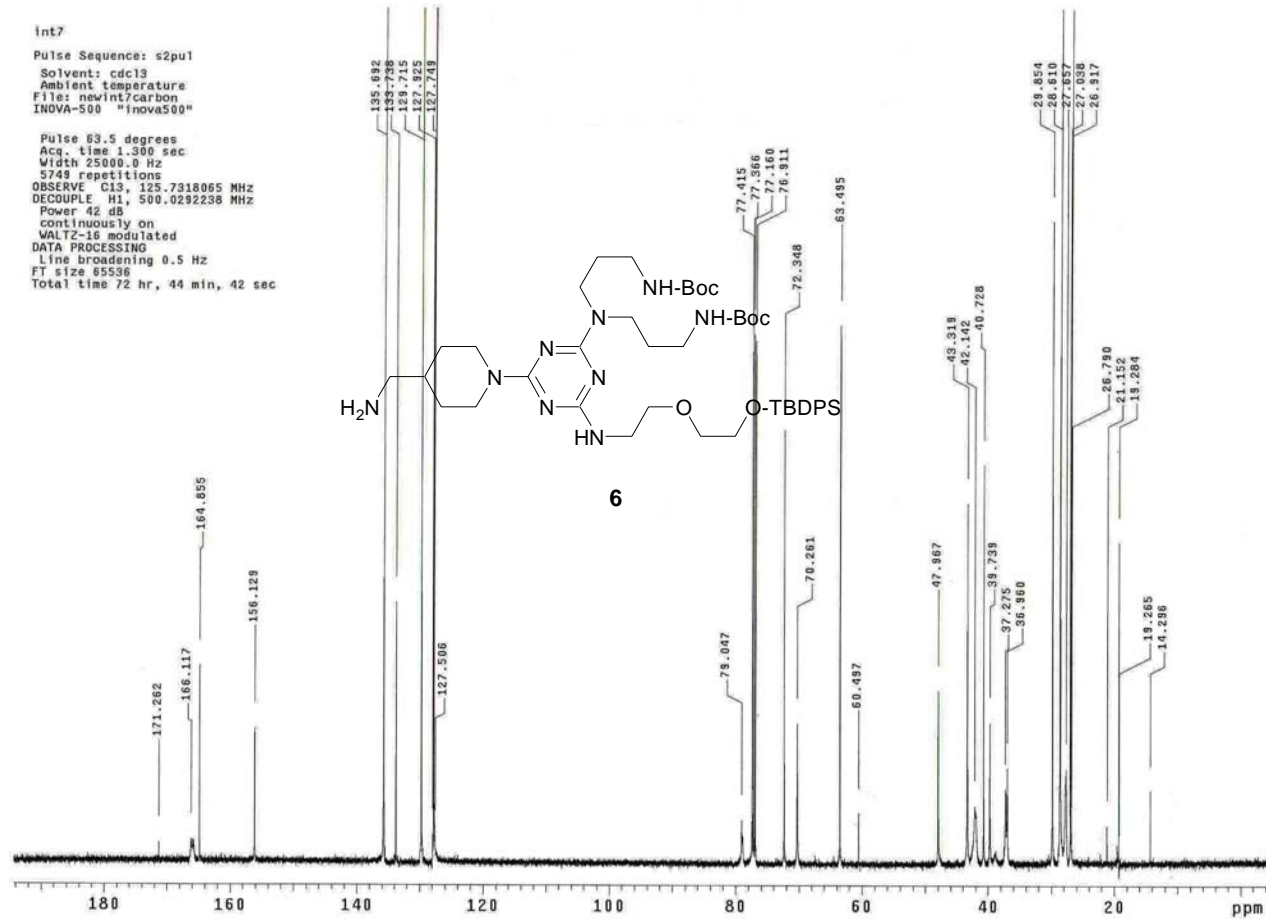


Figure A.5c. The ^{13}C NMR spectrum of **6**.

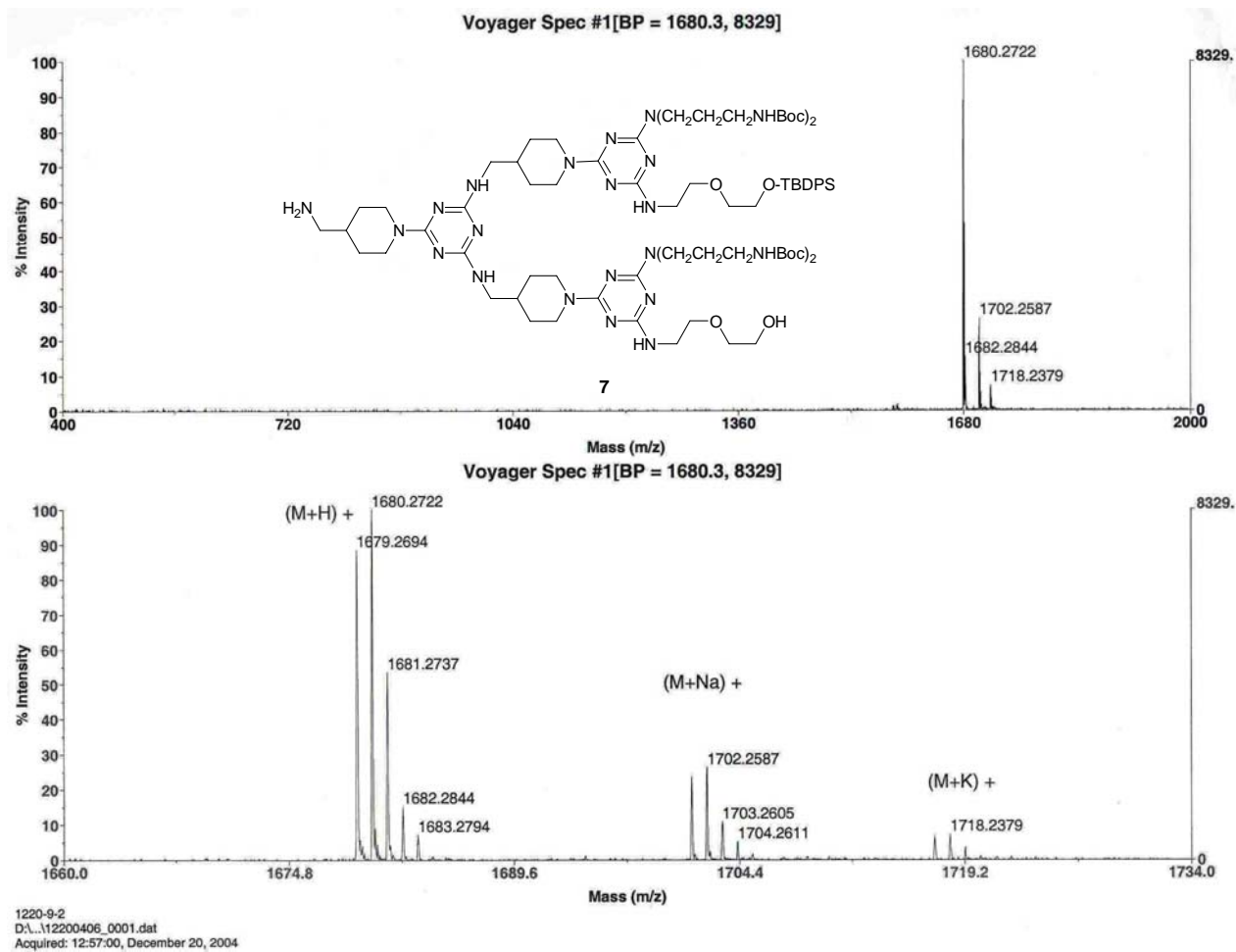


Figure A.6a. The MALDI-TOF mass spectrum of **7**.

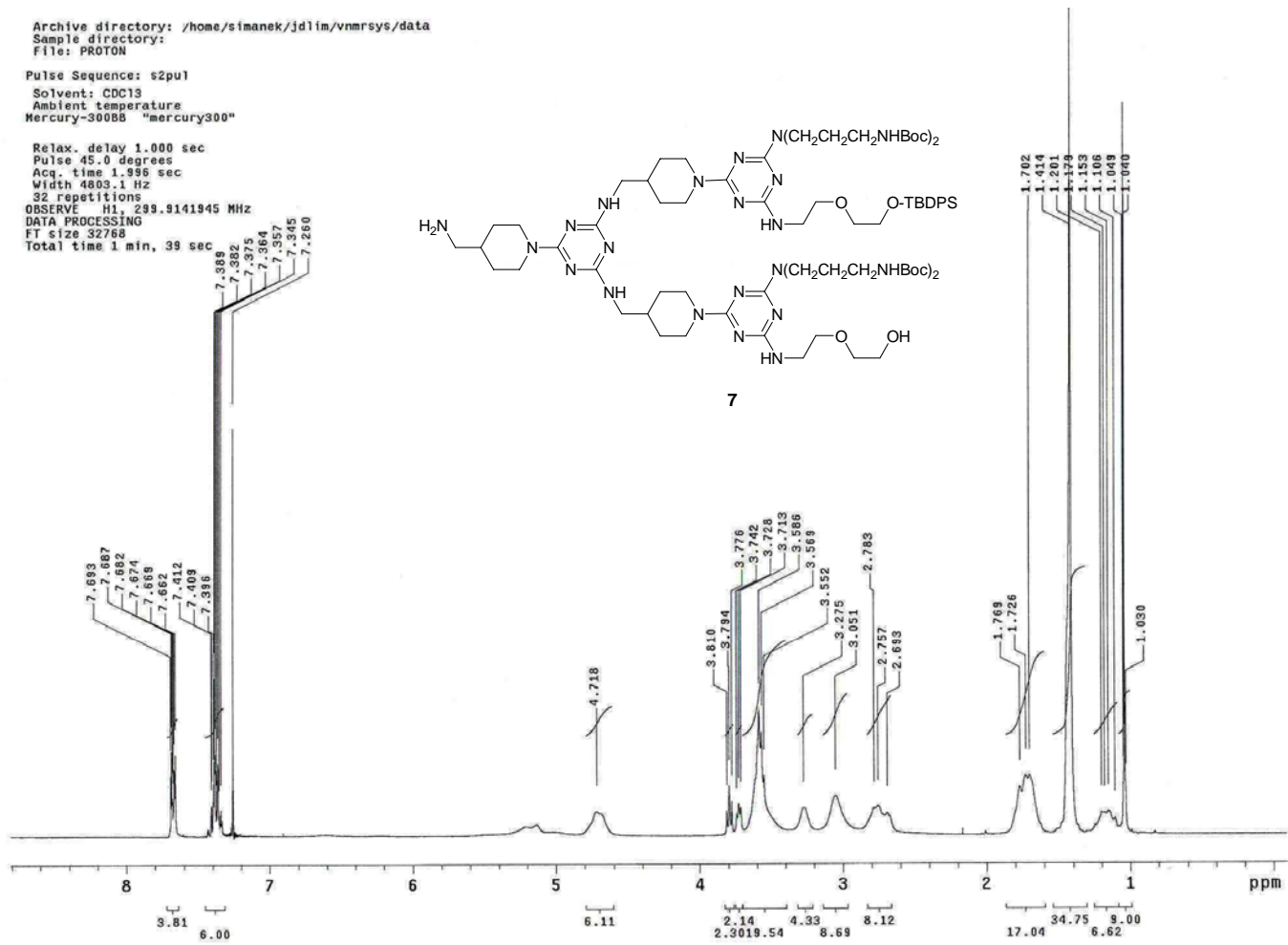


Figure A.6b. The ¹H NMR spectrum of 7.

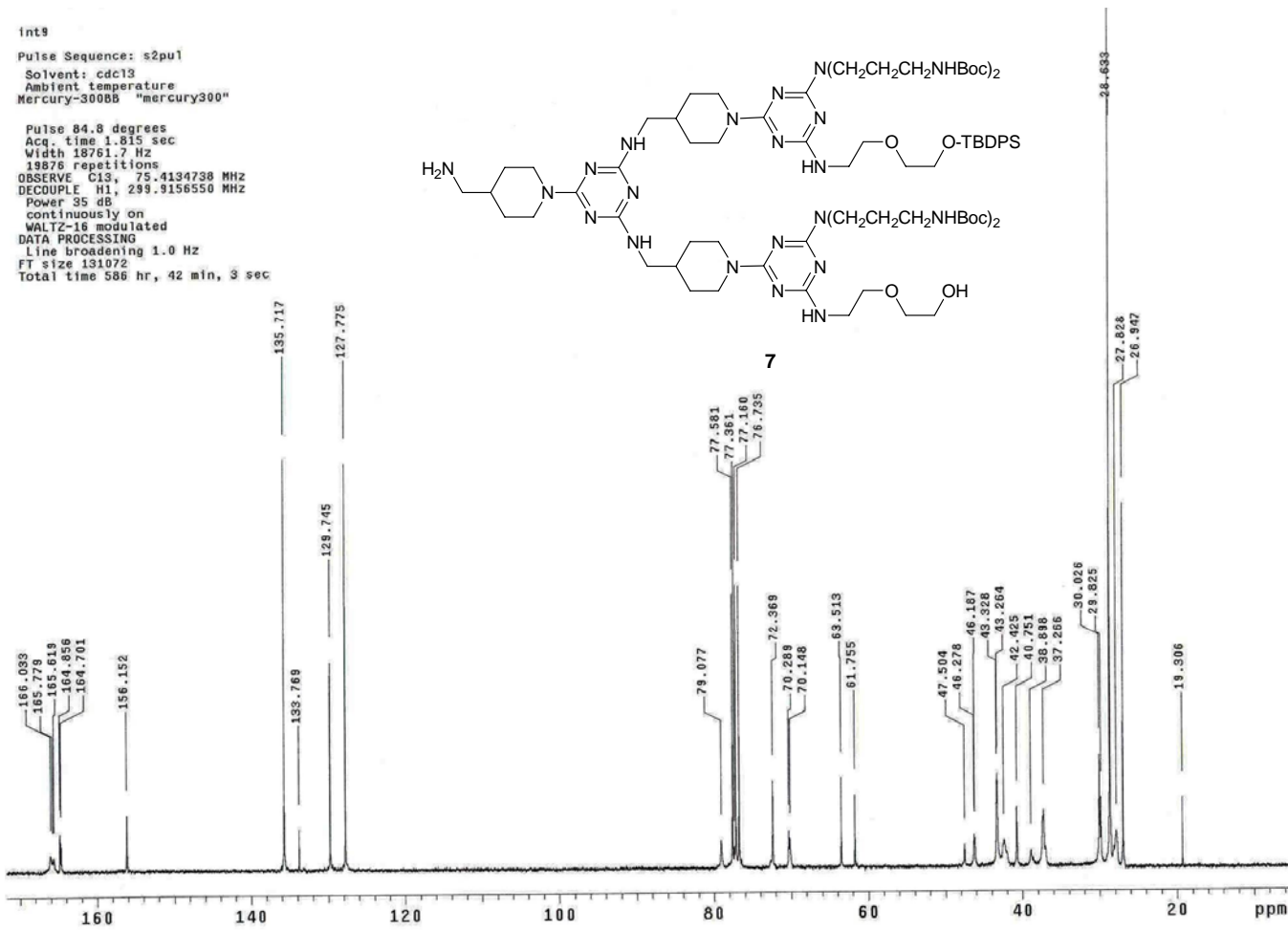


Figure A.6c. The ^{13}C NMR spectrum of **7**.

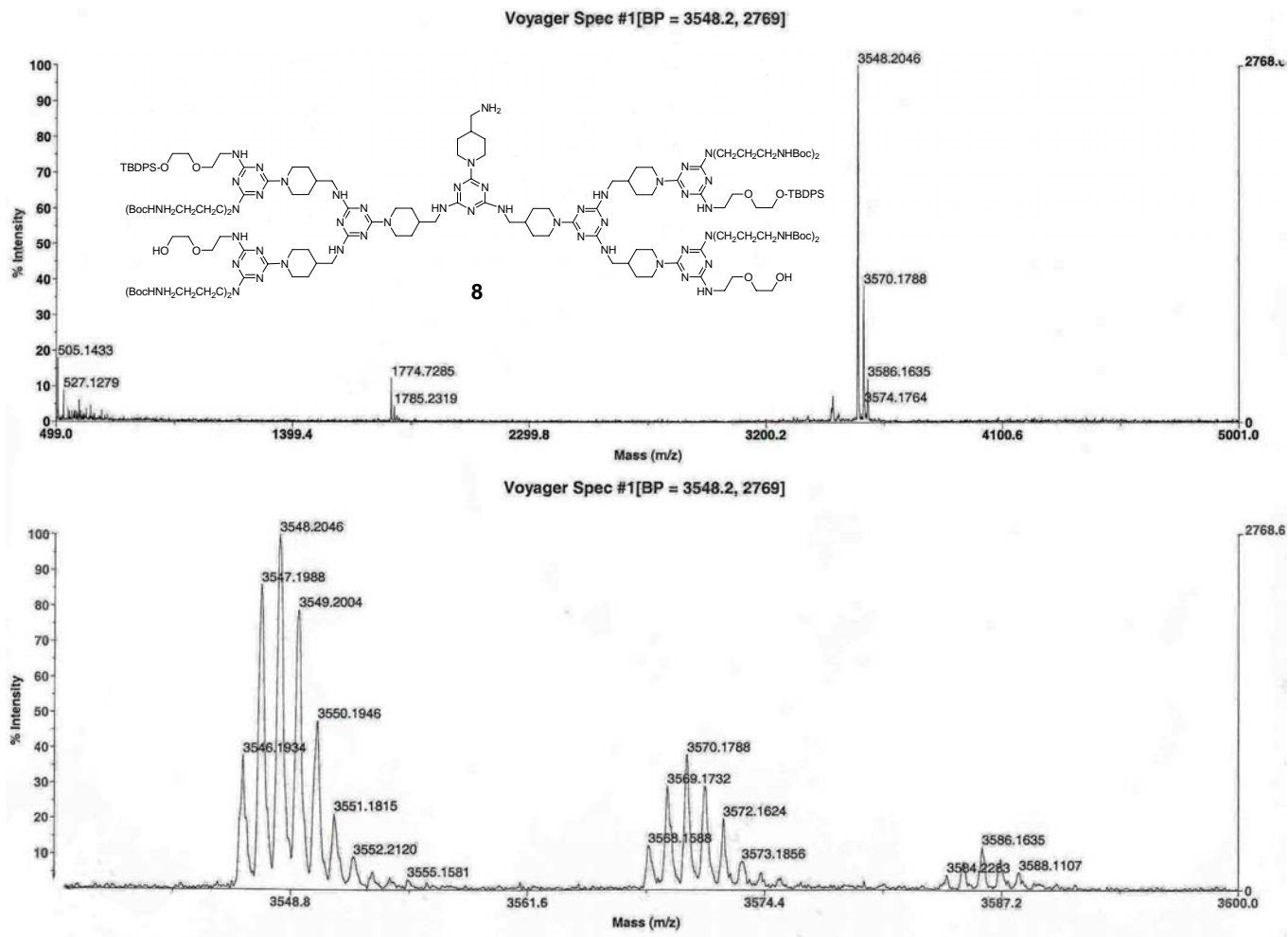


Figure A.7a. The MALDI-TOF mass spectrum of **8**.

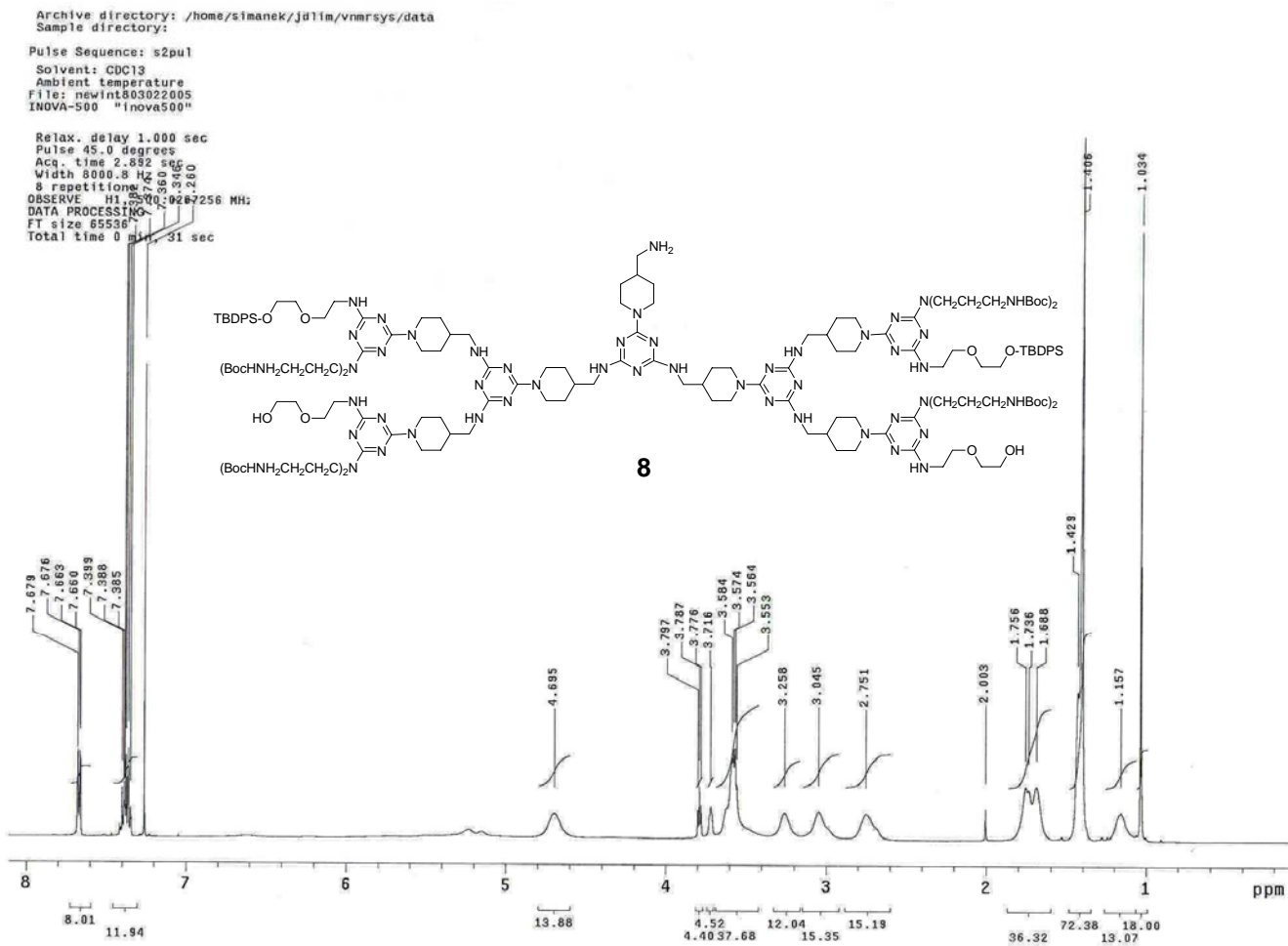


Figure A.7b. The ¹H NMR spectrum of **8**.

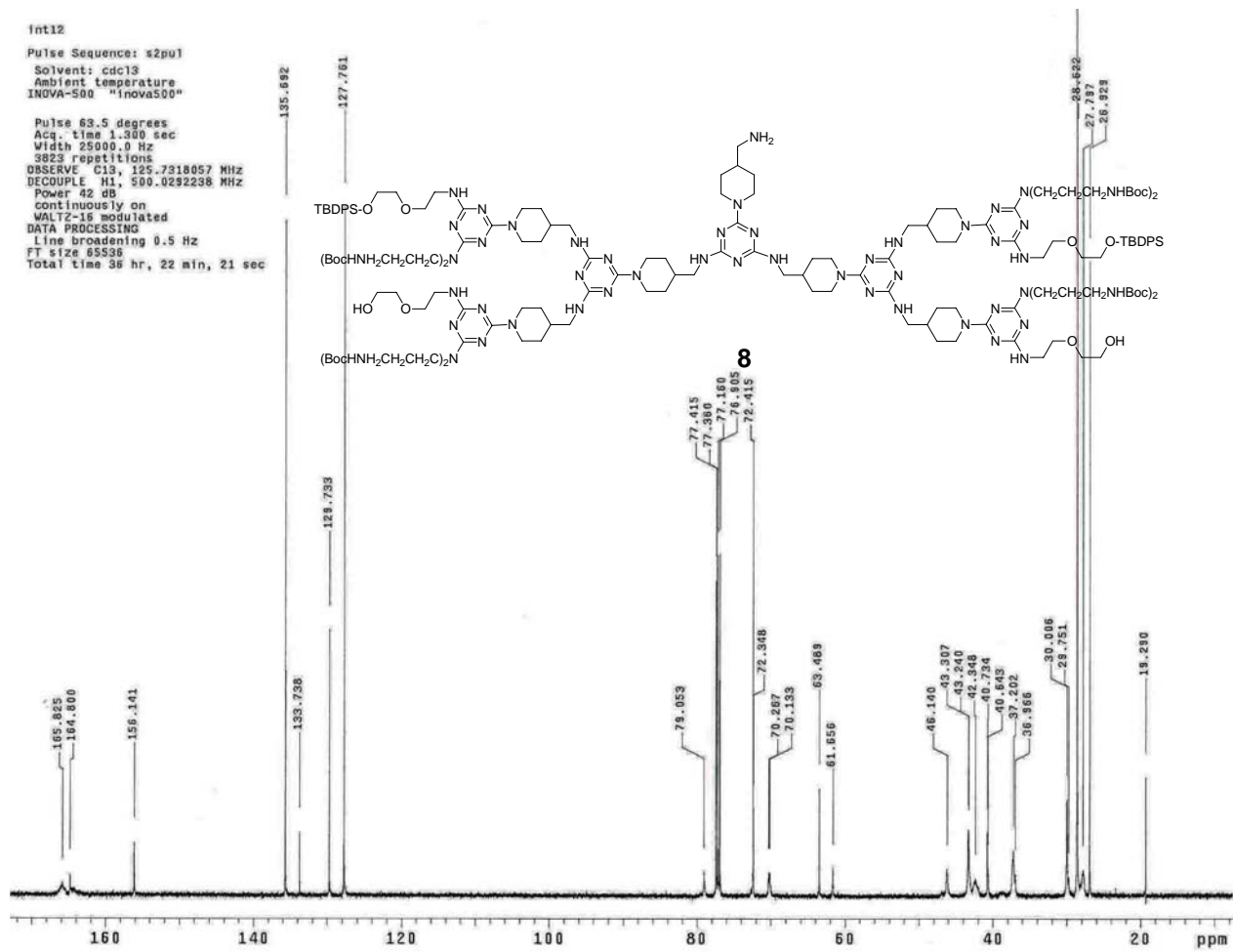


Figure A.7c. The ¹³C NMR spectrum of **8**.

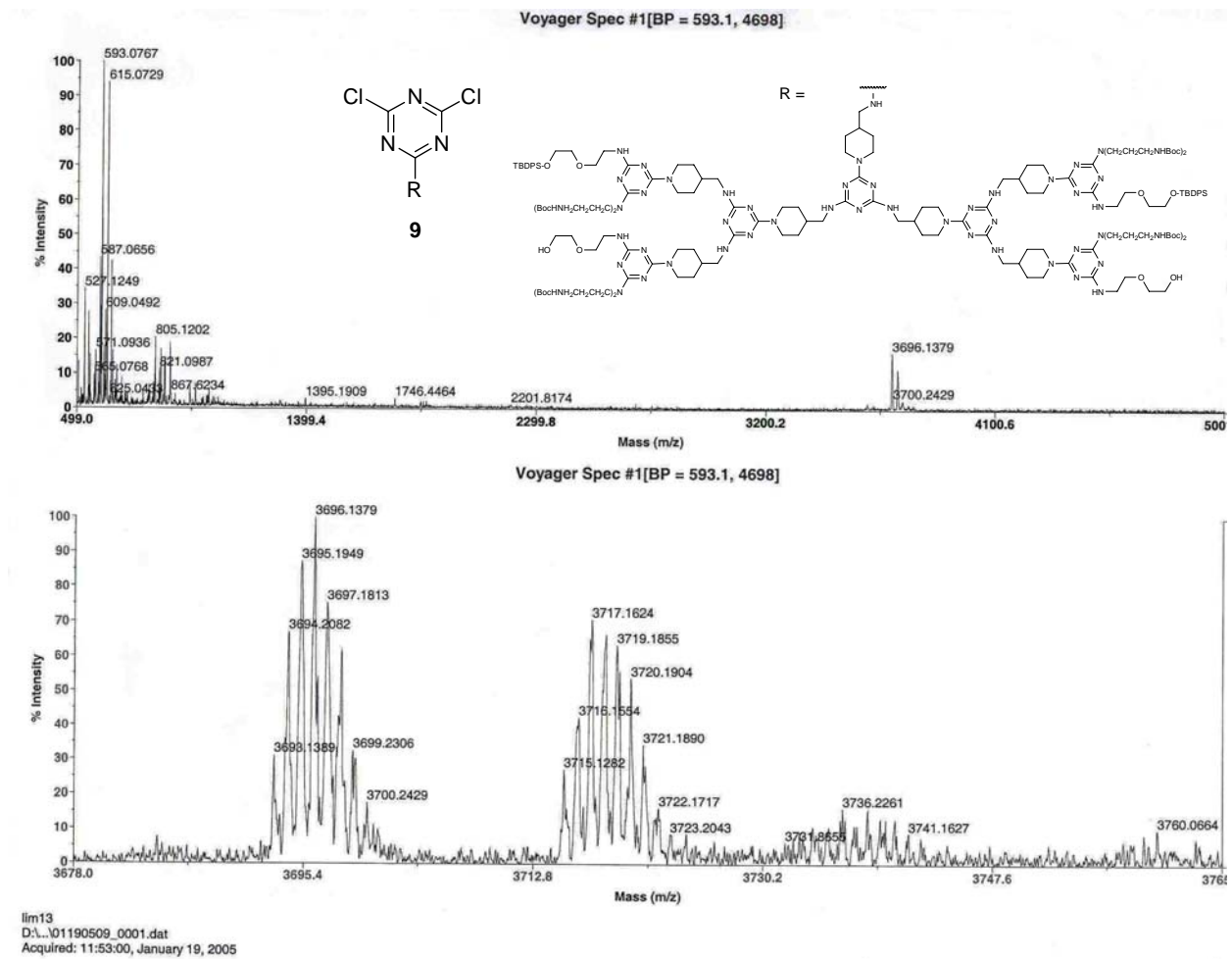


Figure A.8a. The MALDI-TOF mass spectrum of **9**.

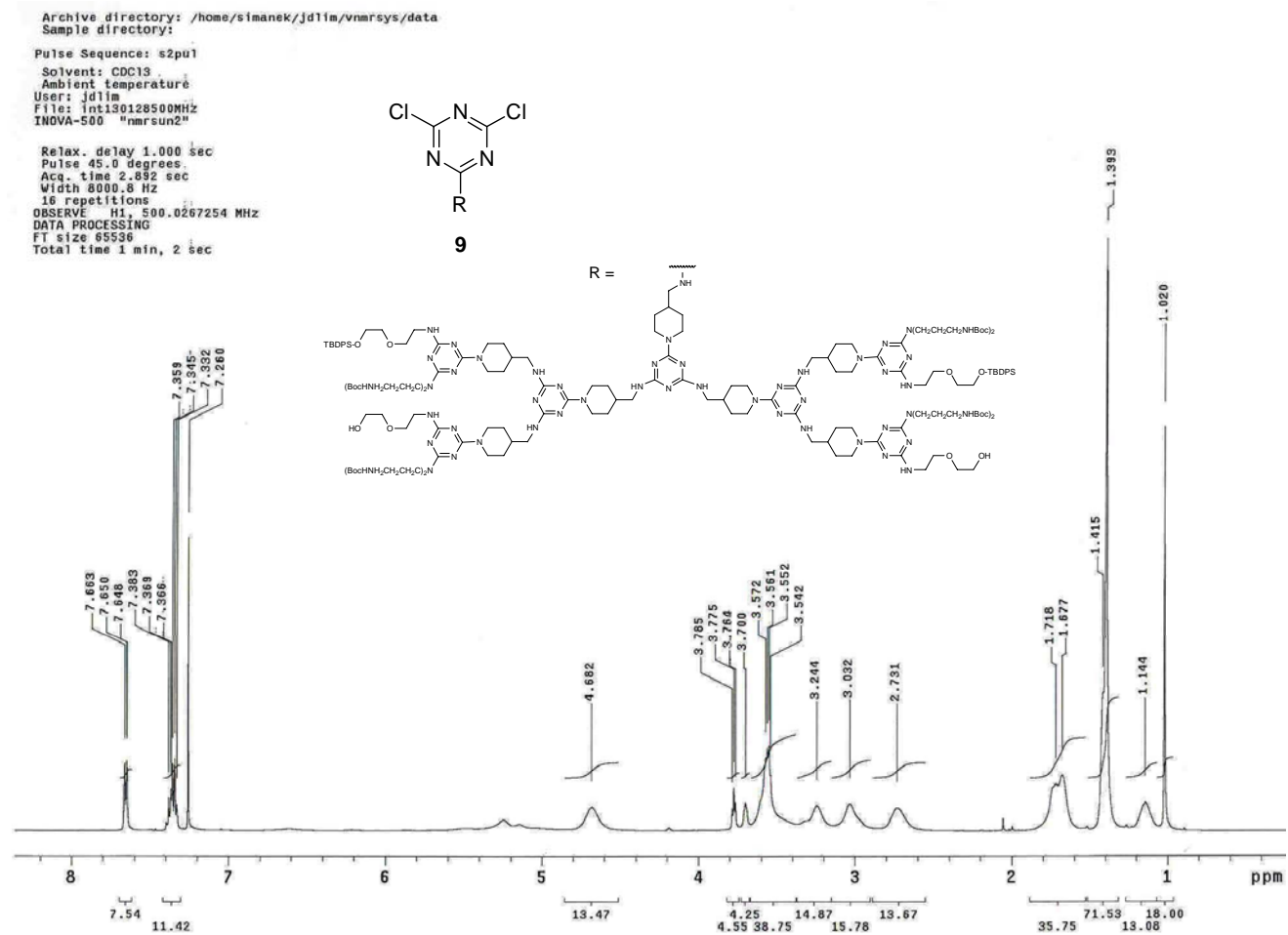


Figure A.8b. The ^1H NMR spectrum of **9**.

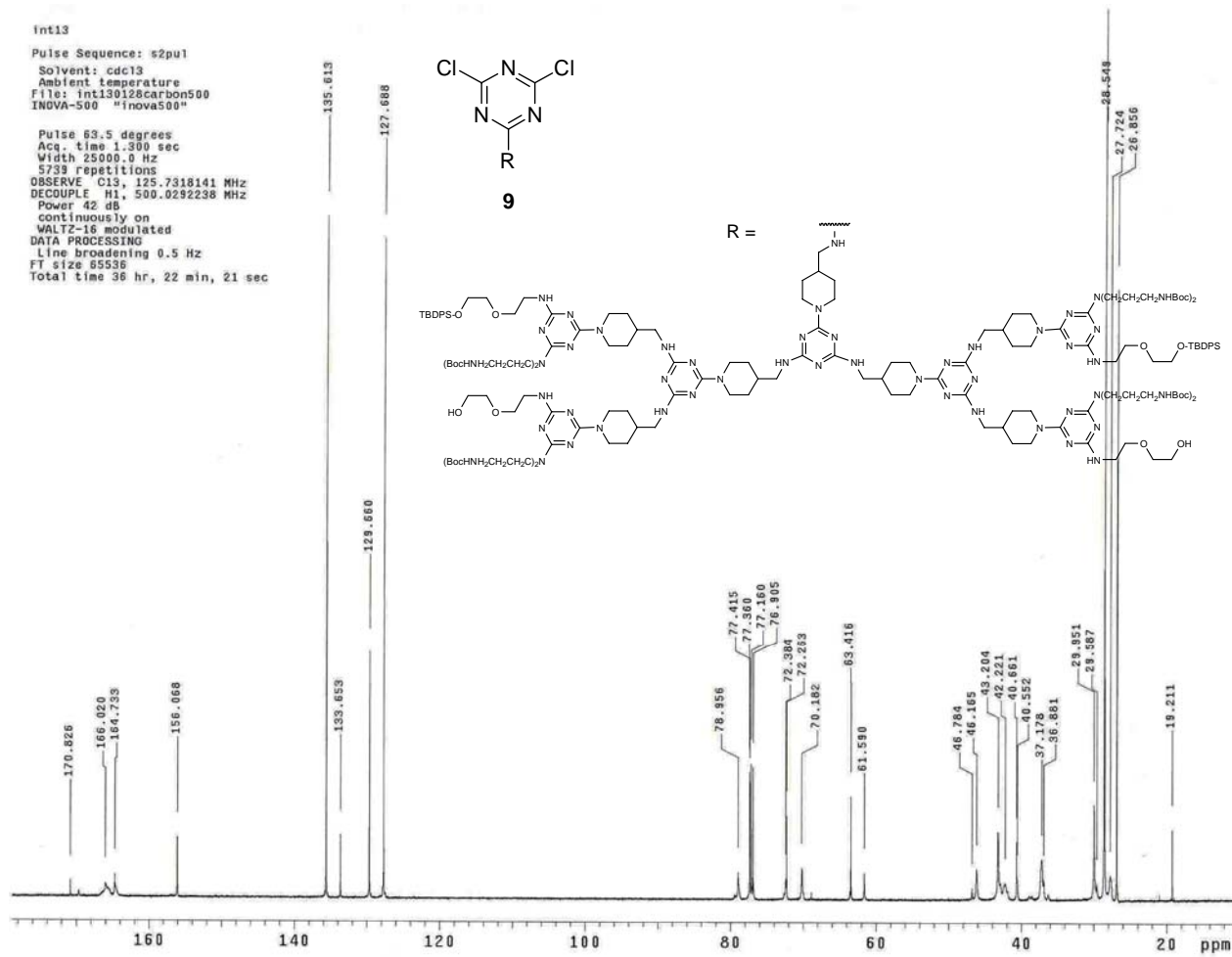


Figure A.8c. The ¹³C NMR spectrum of 9.

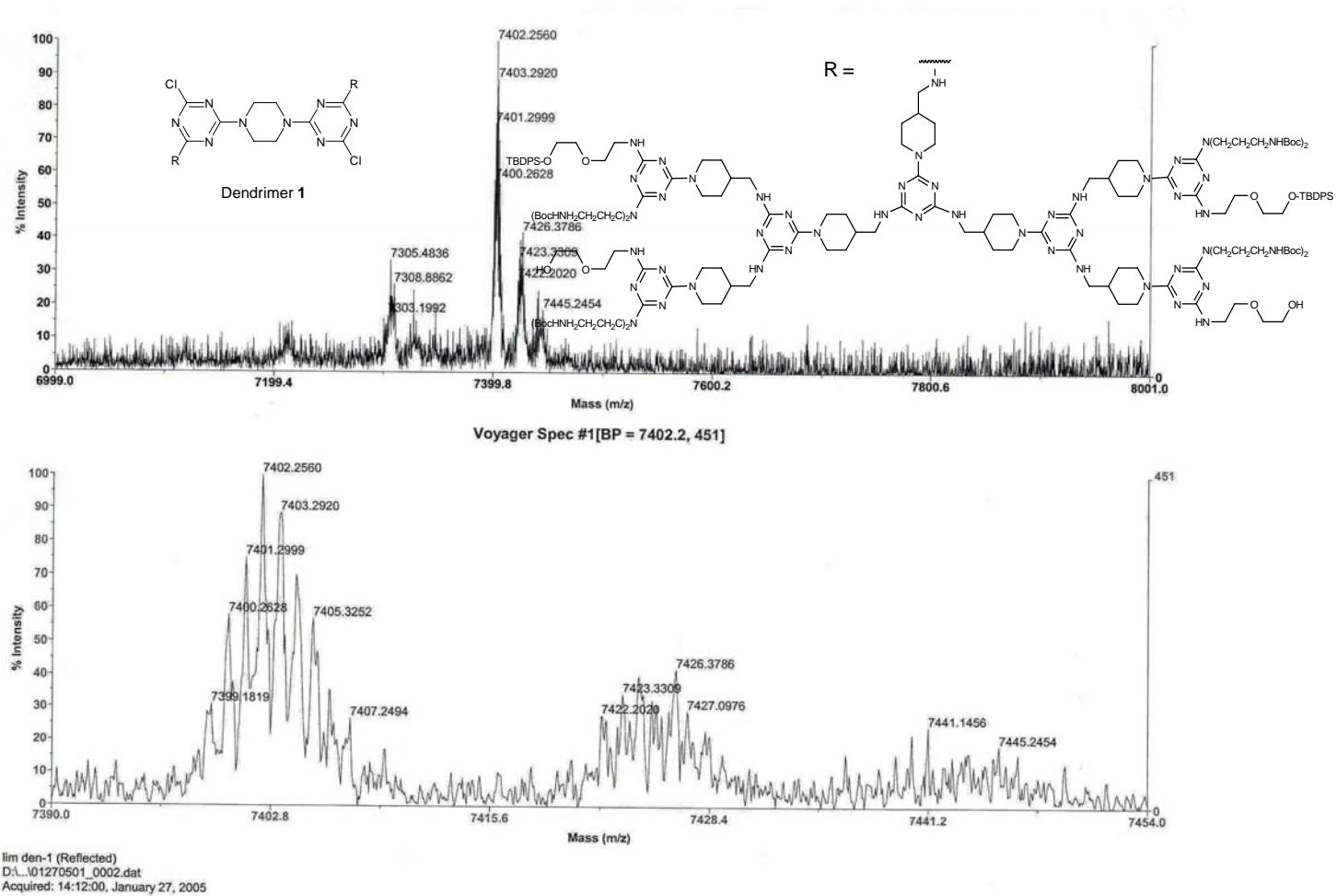


Figure A.9a. The MALDI-TOF mass spectrum of 1.

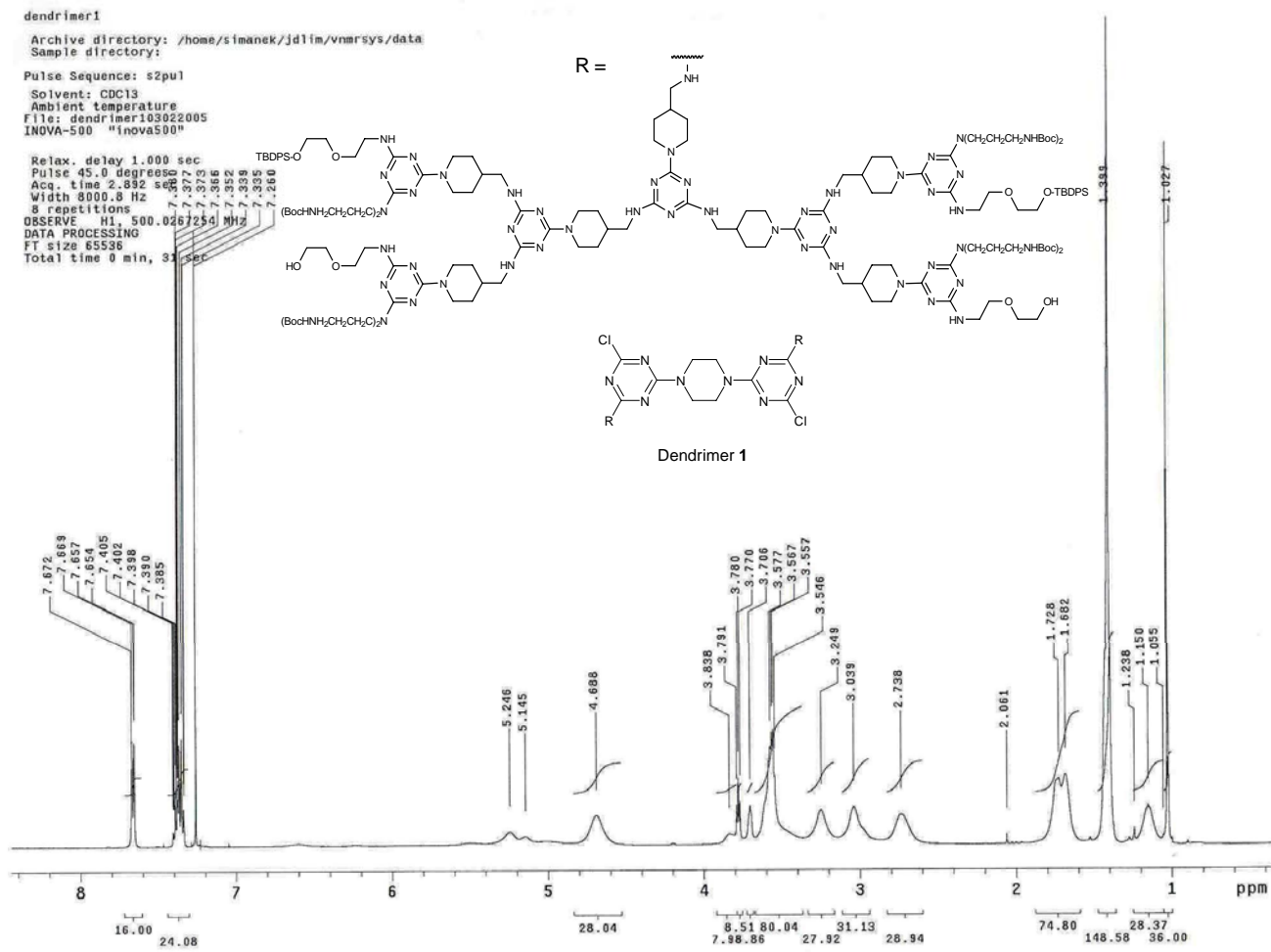


Figure A.9b. The ¹H NMR spectrum of 1.

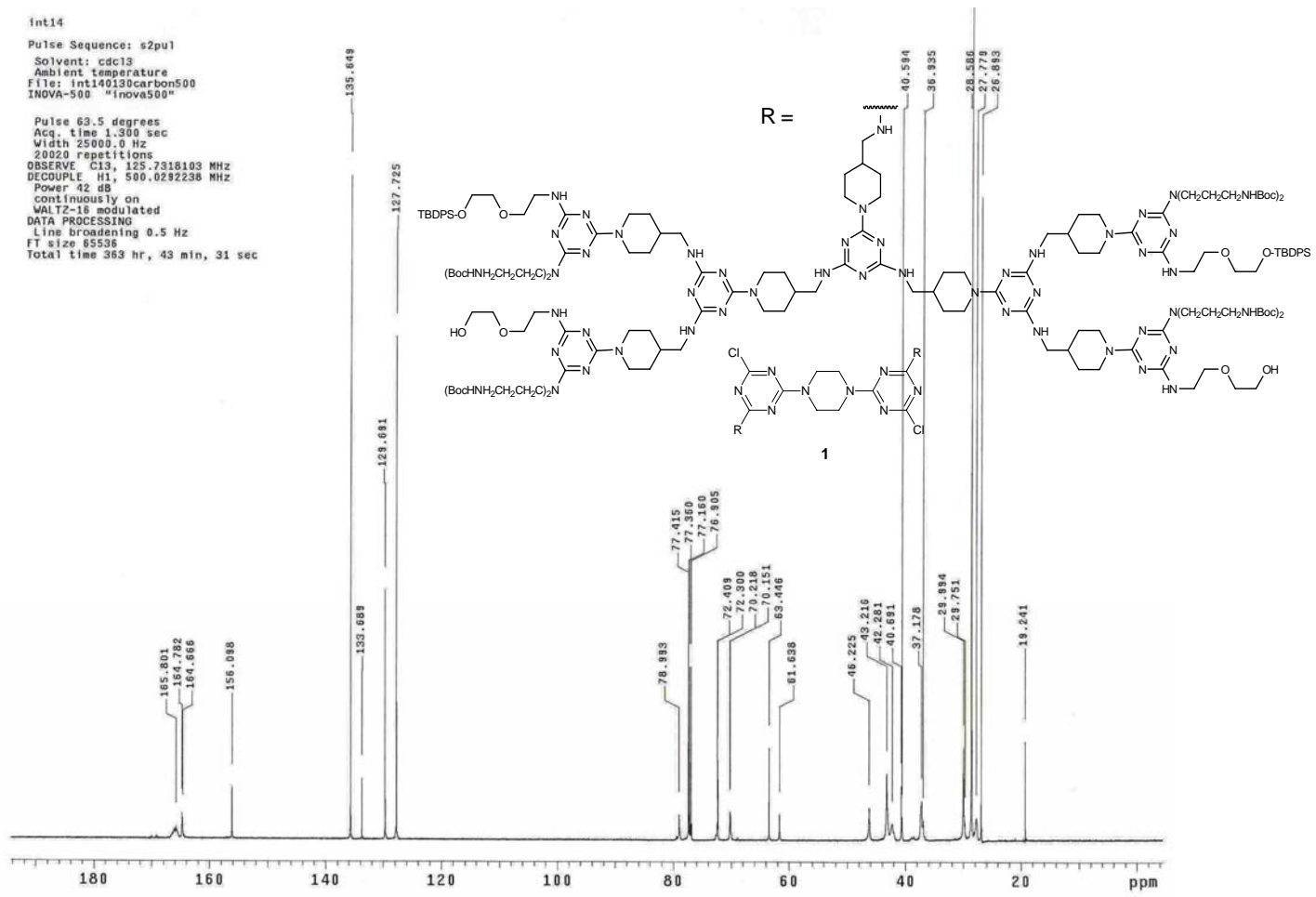


Figure A.9c. The ^{13}C NMR spectrum of **1**.

APPENDIX B
SPECTRA RELEVANT TO CHAPTER III

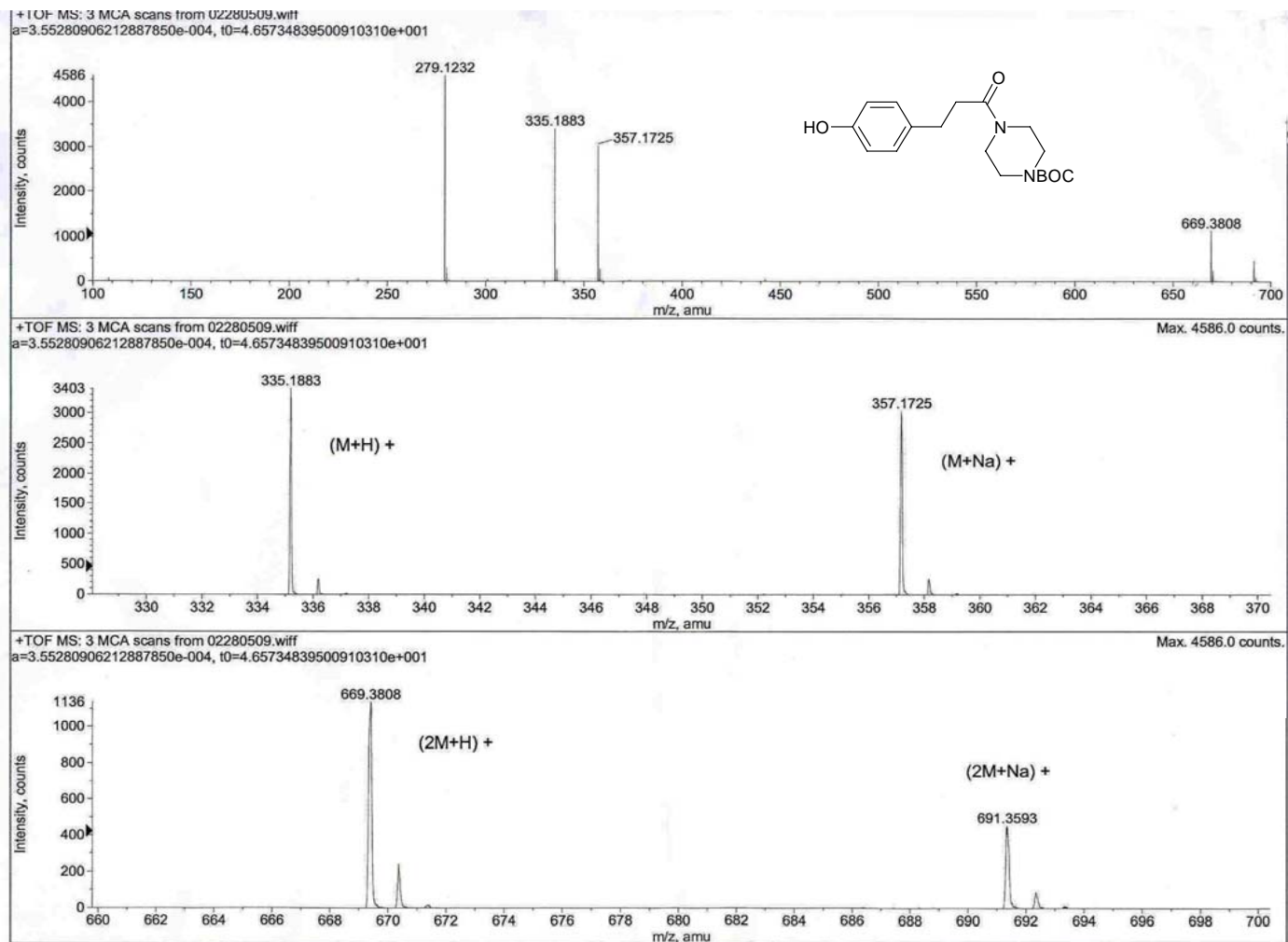


Figure B.1a. The ESI-TOF mass spectrum of **BH-BOC-piperazine**.

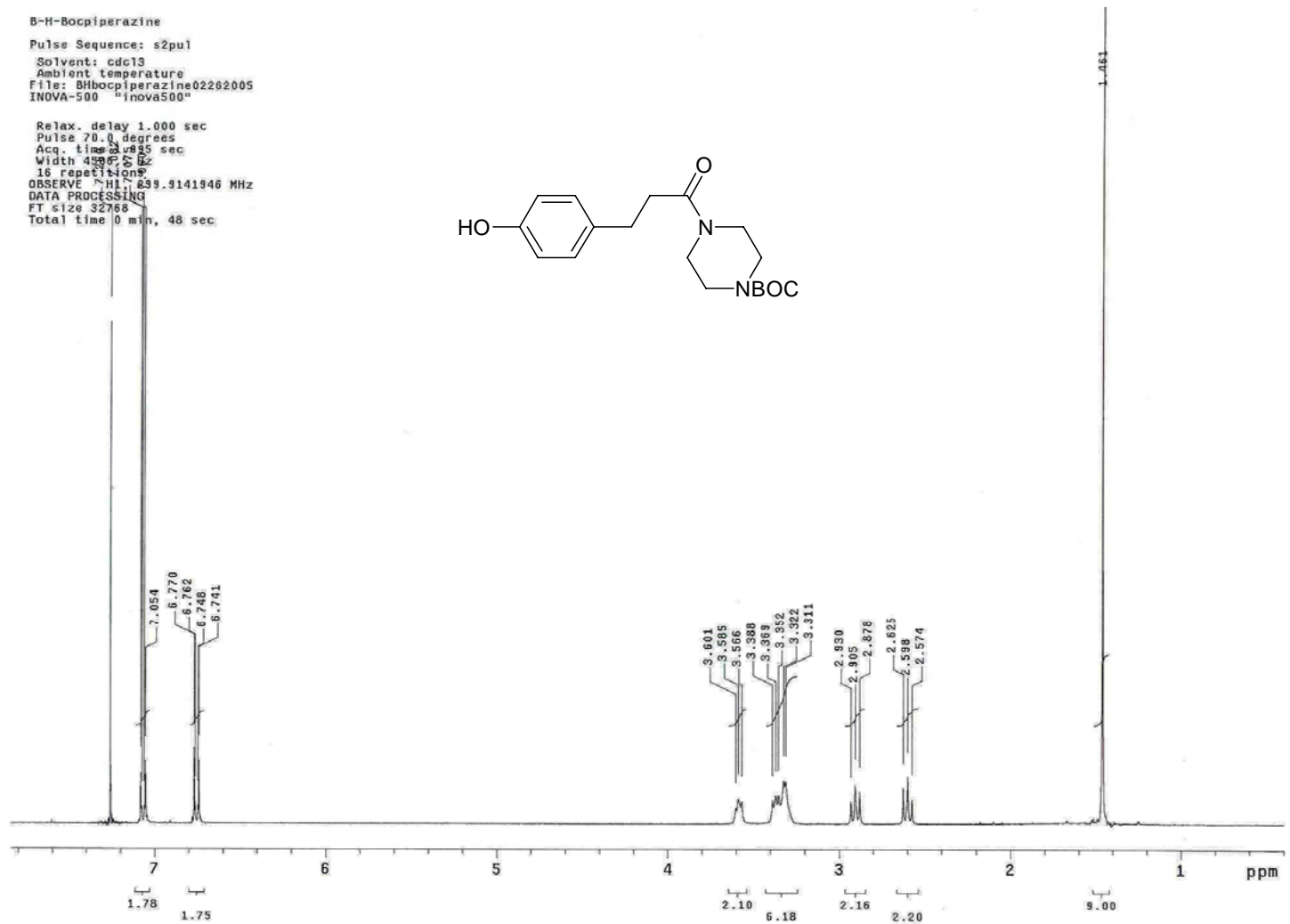


Figure B.1b. The ¹H NMR spectrum of BH-BOC-piperazine.

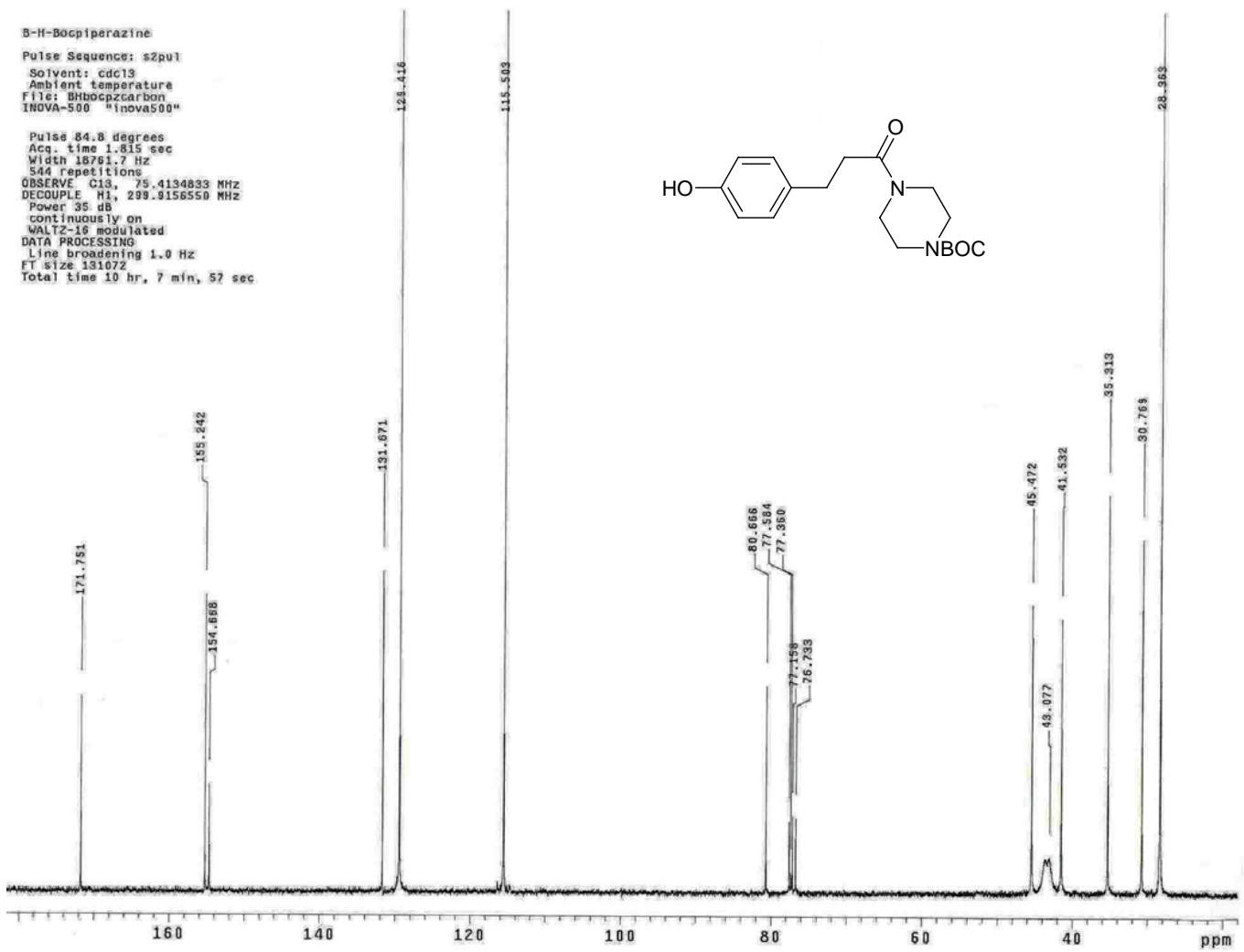


Figure B.1c. The ^{13}C NMR spectrum of BH-BOC-piperazine.

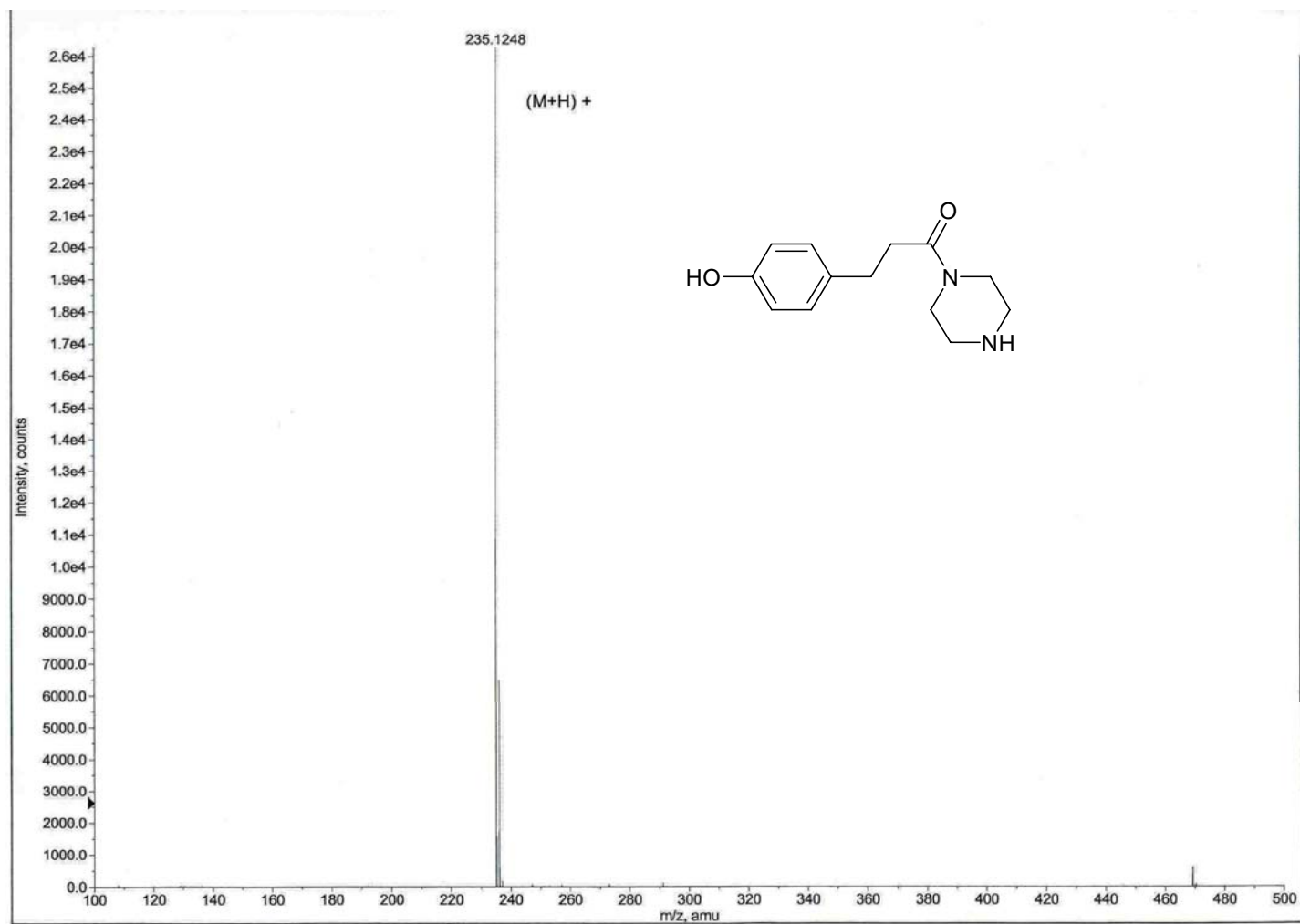


Figure B.2a. The ESI-TOF mass spectrum of **BH-piperazine**.

Pulse Sequence: s2pu1
Solvent: cd3od
Ambient temperature
File: BHpiperazine03012005
INOVA-500 "inova500"

Relax. delay 1.000 sec
Pulse 70.0 degrees
Acq. time 1.995 sec
Width 4506.5 Hz
16 repetitions
OBSERVE H1, 299.9153745 MHz
DATA PROCESSING
FT size 32768
Total time 0 min, 48 sec

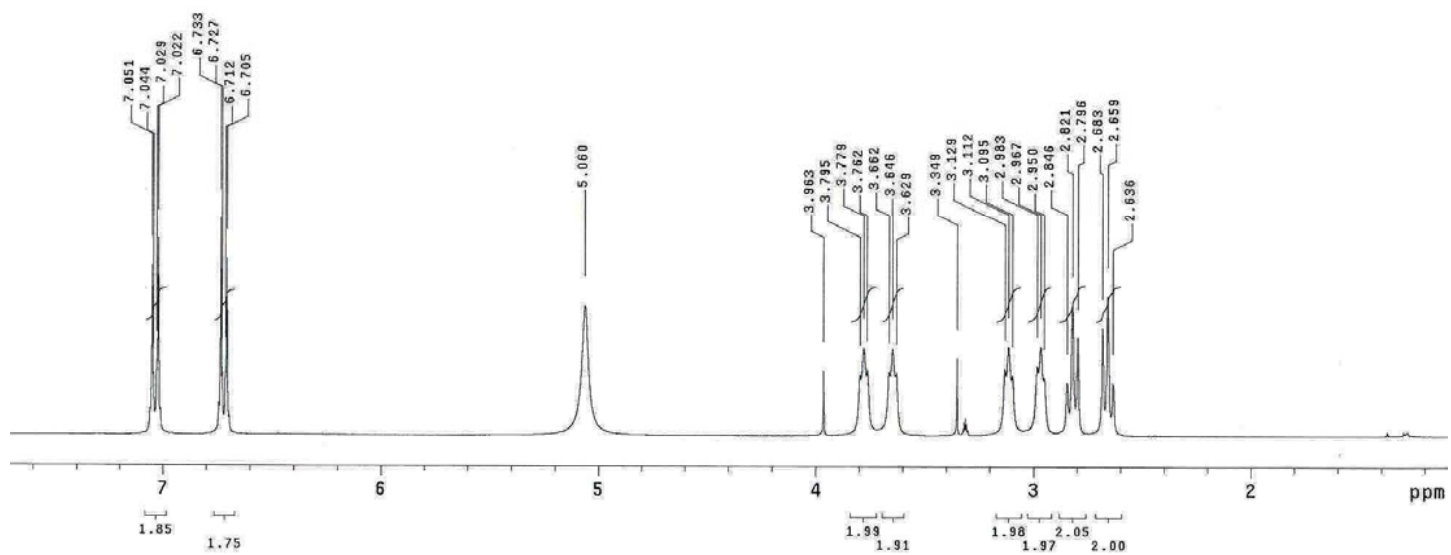
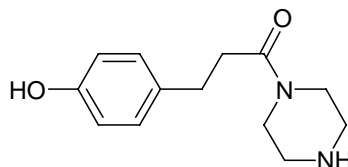


Figure B.2b. The ^1H NMR spectrum of BH-piperazine.

B-H-piperazine
Pulse Sequence: s2pu1
Solvent: cd3od
Ambient temperature
File: BHpiperazinecarbon03012005
INOVA-500 "inova500"

Pulse 84.8 degrees
Acq. time 1.815 sec
Width 18761.7 Hz
138 repetitions
OBSERVE C13, 75.4136791 MHz
DECOUPLE H1, 299.9168366 MHz
Power 35 dB
continuously on
WALTZ-16 modulated
DATA PROCESSING
Line broadening 1.0 Hz
FT size 131072
Total time 31 min, 7 sec

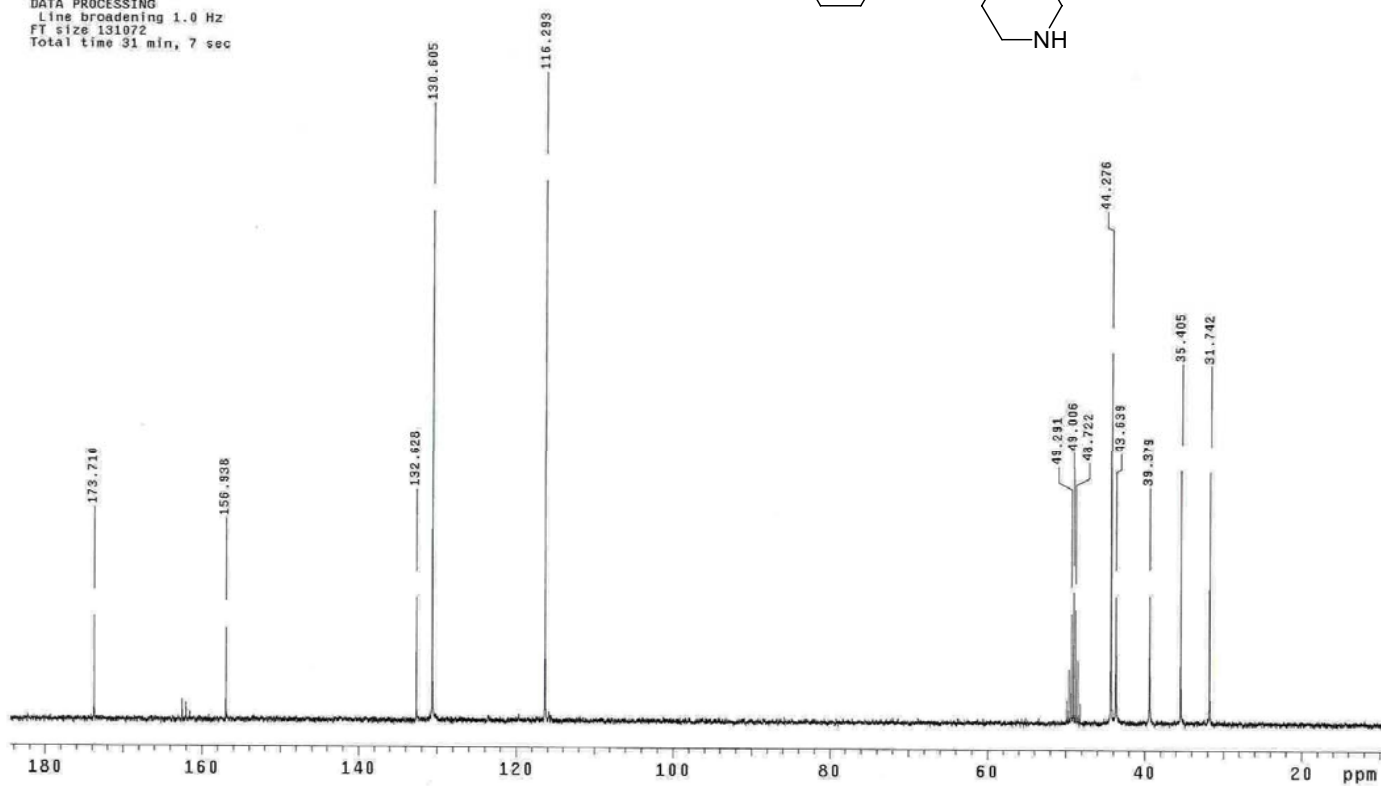
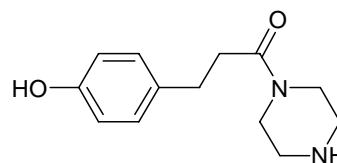


Figure B.2c. The ^{13}C NMR spectrum of BH-piperazine.

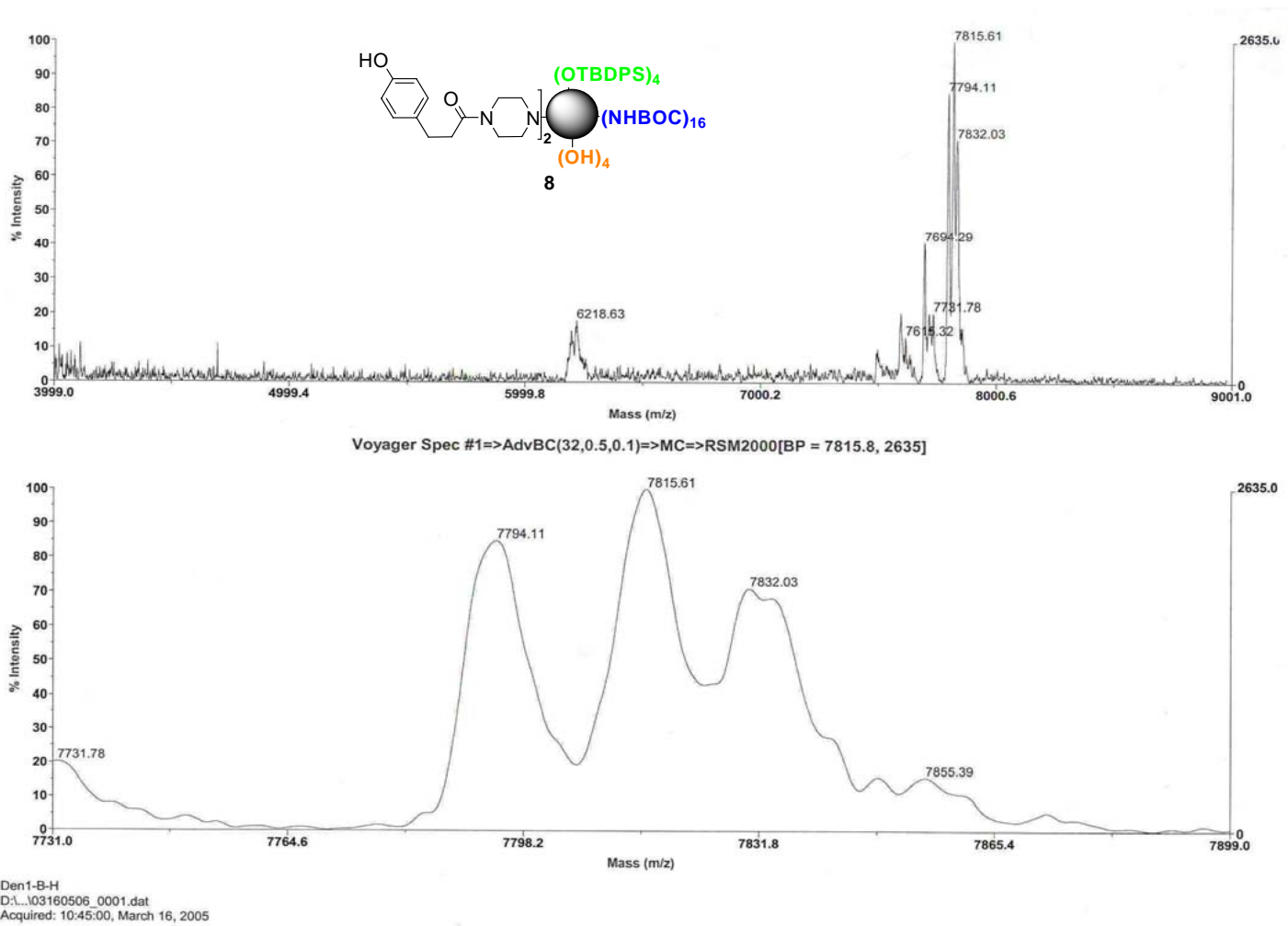


Figure B.3a. The MALDI-TOF mass spectrum of **8**.

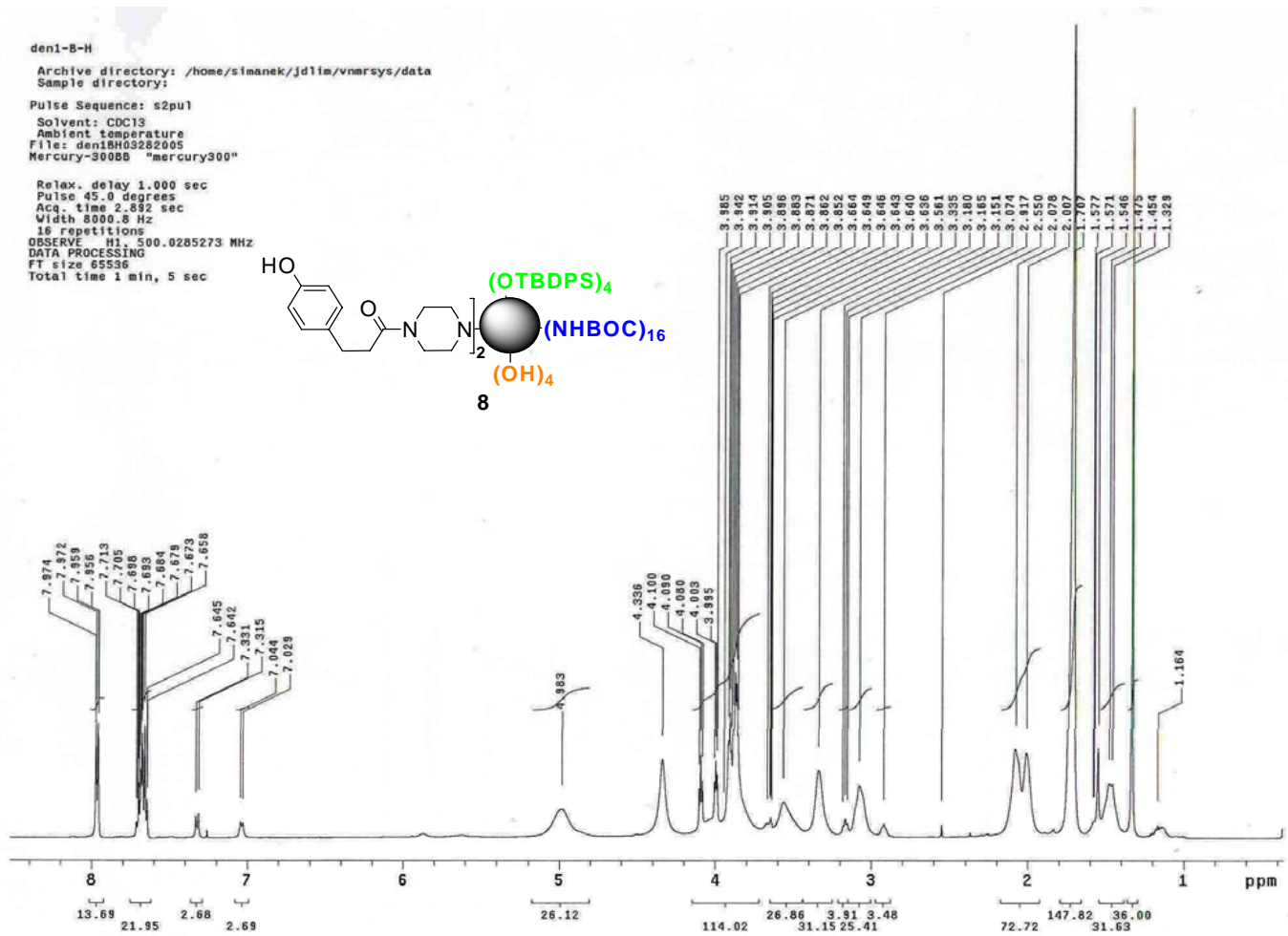


Figure B.3b. The ¹H NMR spectrum of **8**.

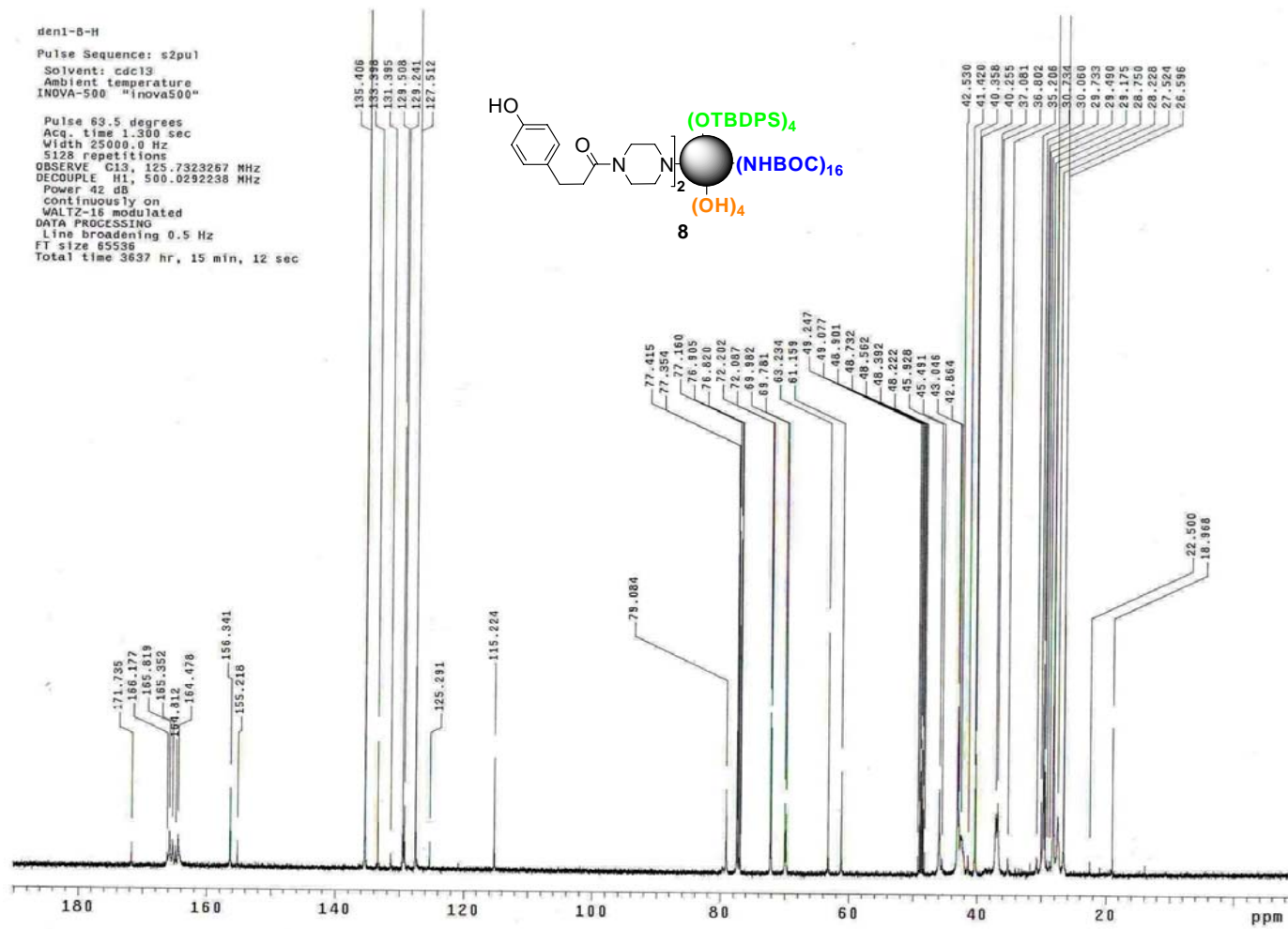
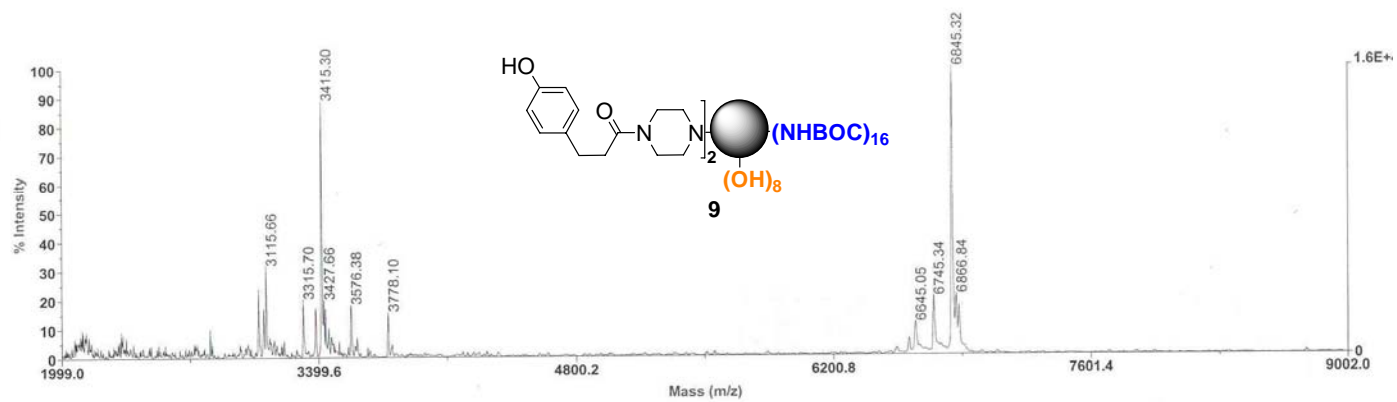
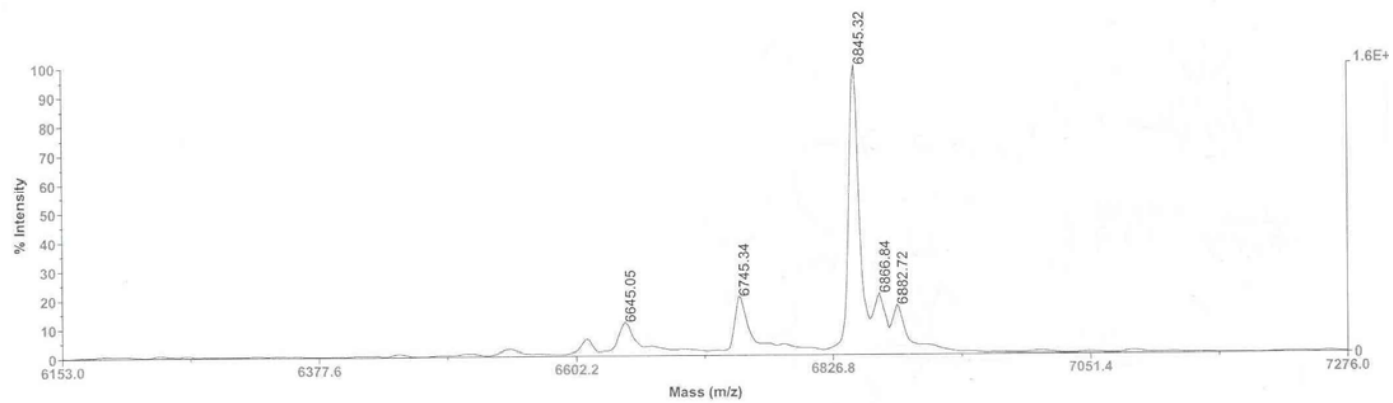


Figure B.3c. The ¹³C NMR spectrum of **8**.



Voyager Spec #1=>AdvBC(32,0.5,0.1)>>RSM2000=>NF0.7=>MC[BP = 6845.5, 15898]



den-10-TBAF-1
D:\...05050511_0001.dat

Figure B.4a. The MALDI-TOF mass spectrum of **9**.

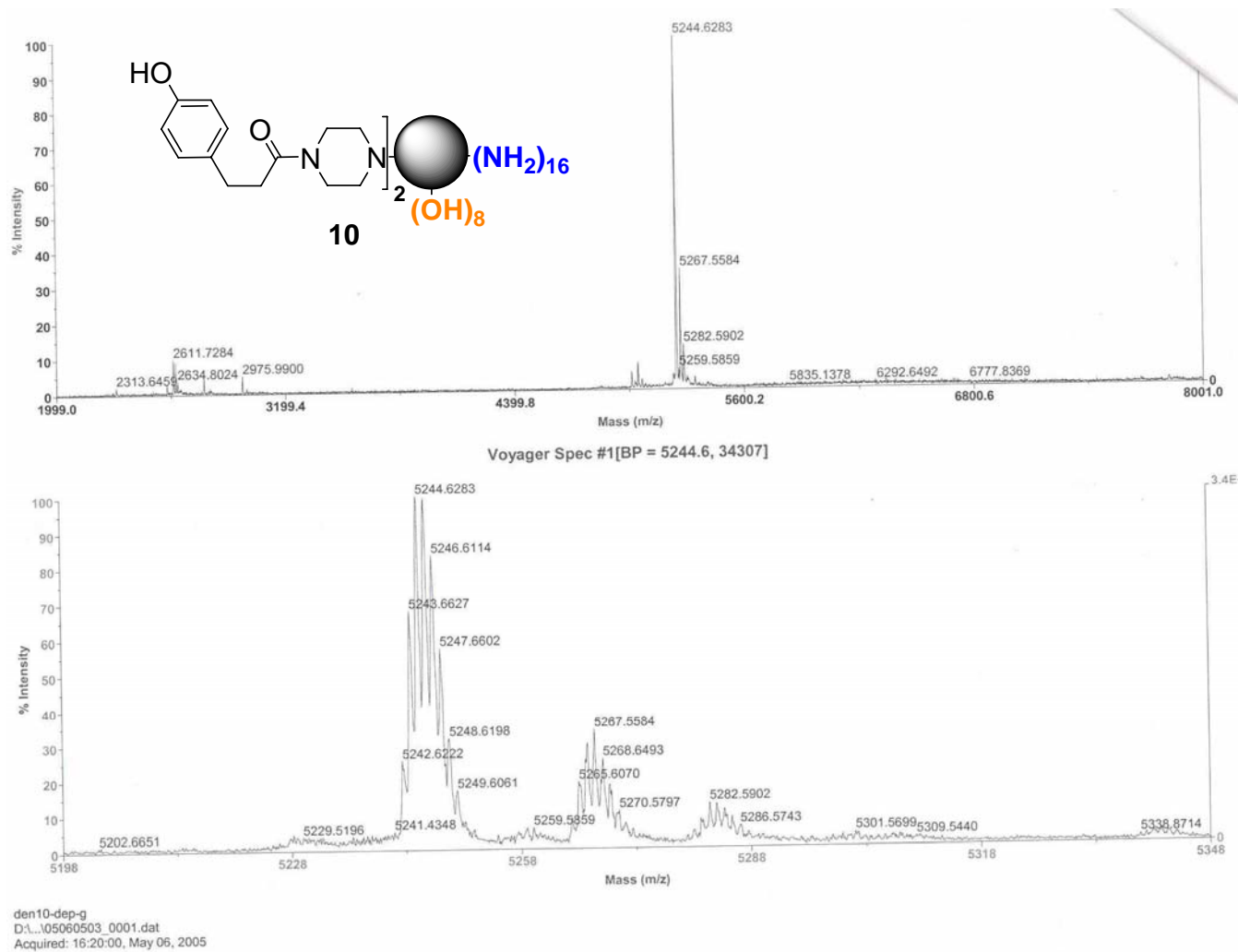


Figure B.5a. The MALDI-TOF mass spectrum of **10**.

Voyager Spec #1=>BC=>AdvBC(32,0.5,0.1)[BP = 7575.9, 23459]

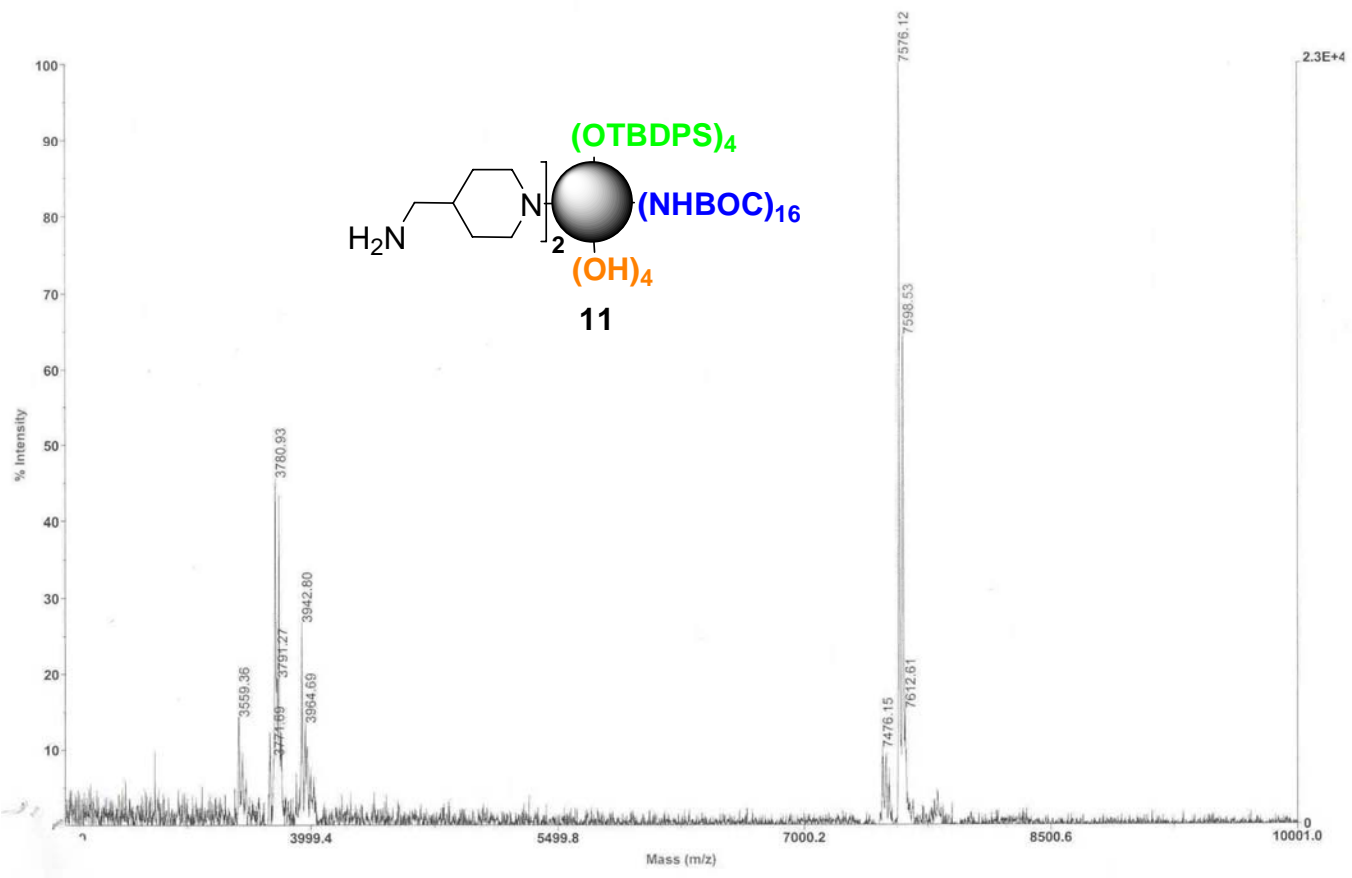


Figure B.6a. The MALDI-TOF mass spectrum of **11**.

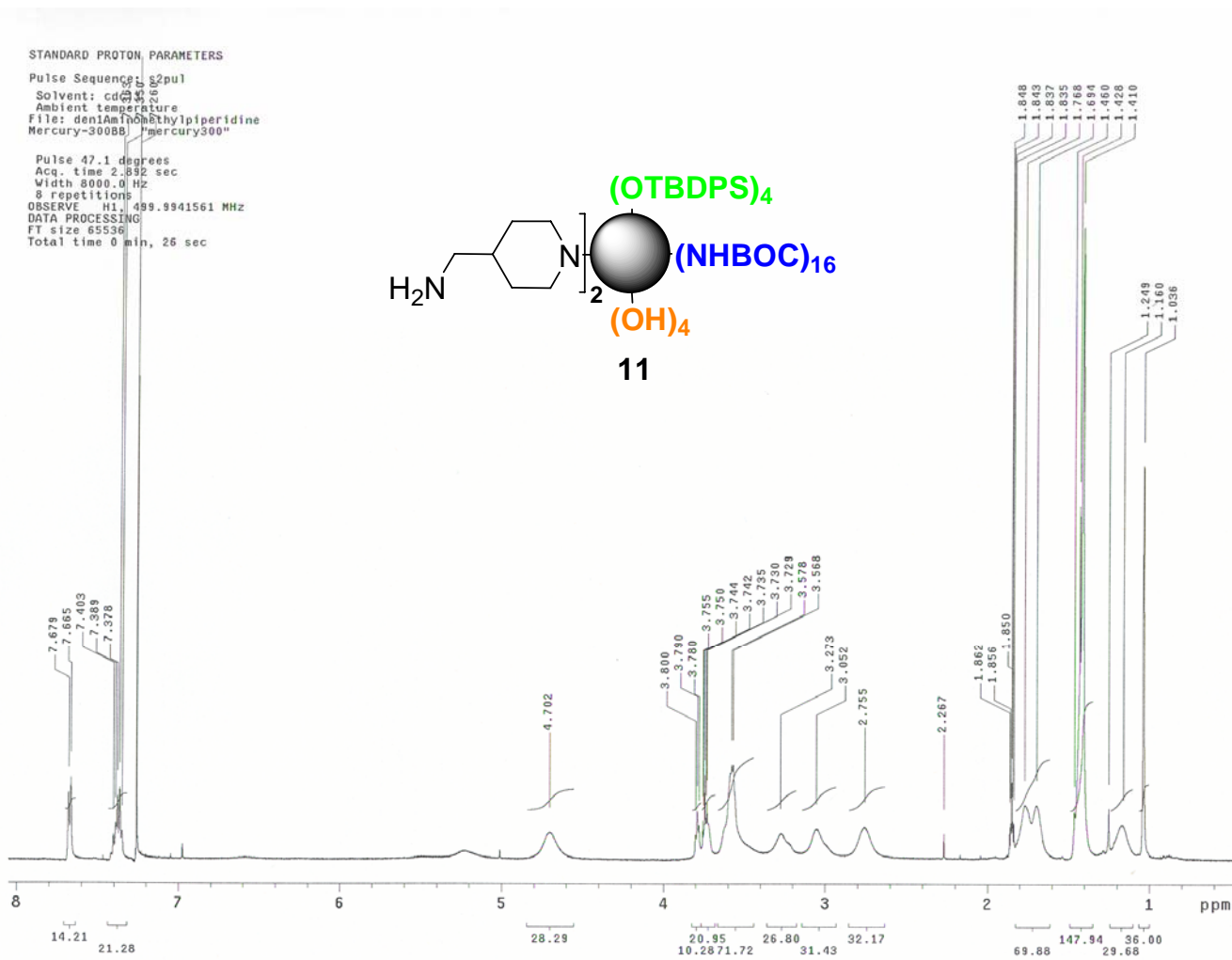


Figure B.6b. The ¹H NMR spectrum of 11.

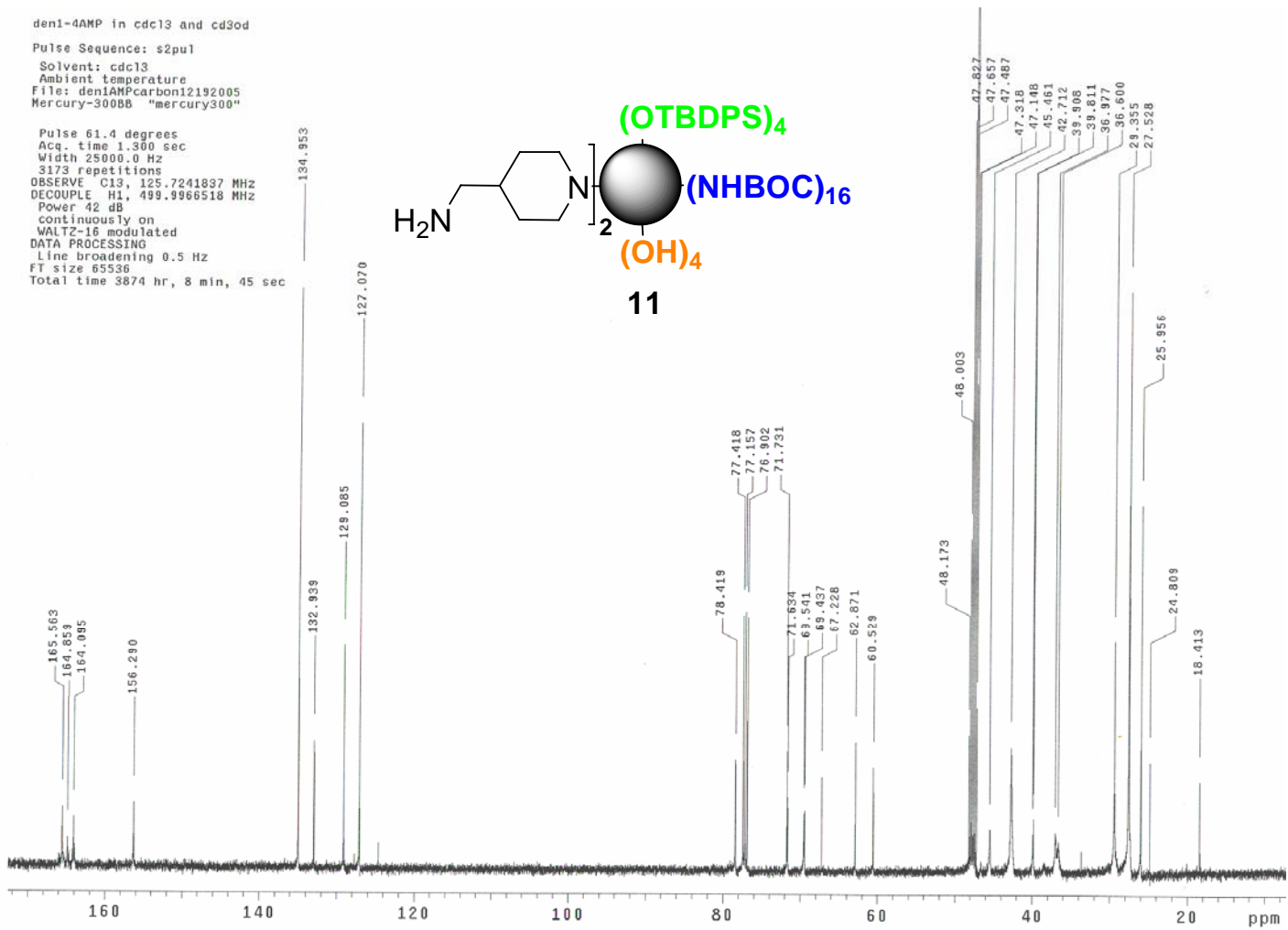


Figure B.6c. The ^{13}C NMR spectrum of **11**.

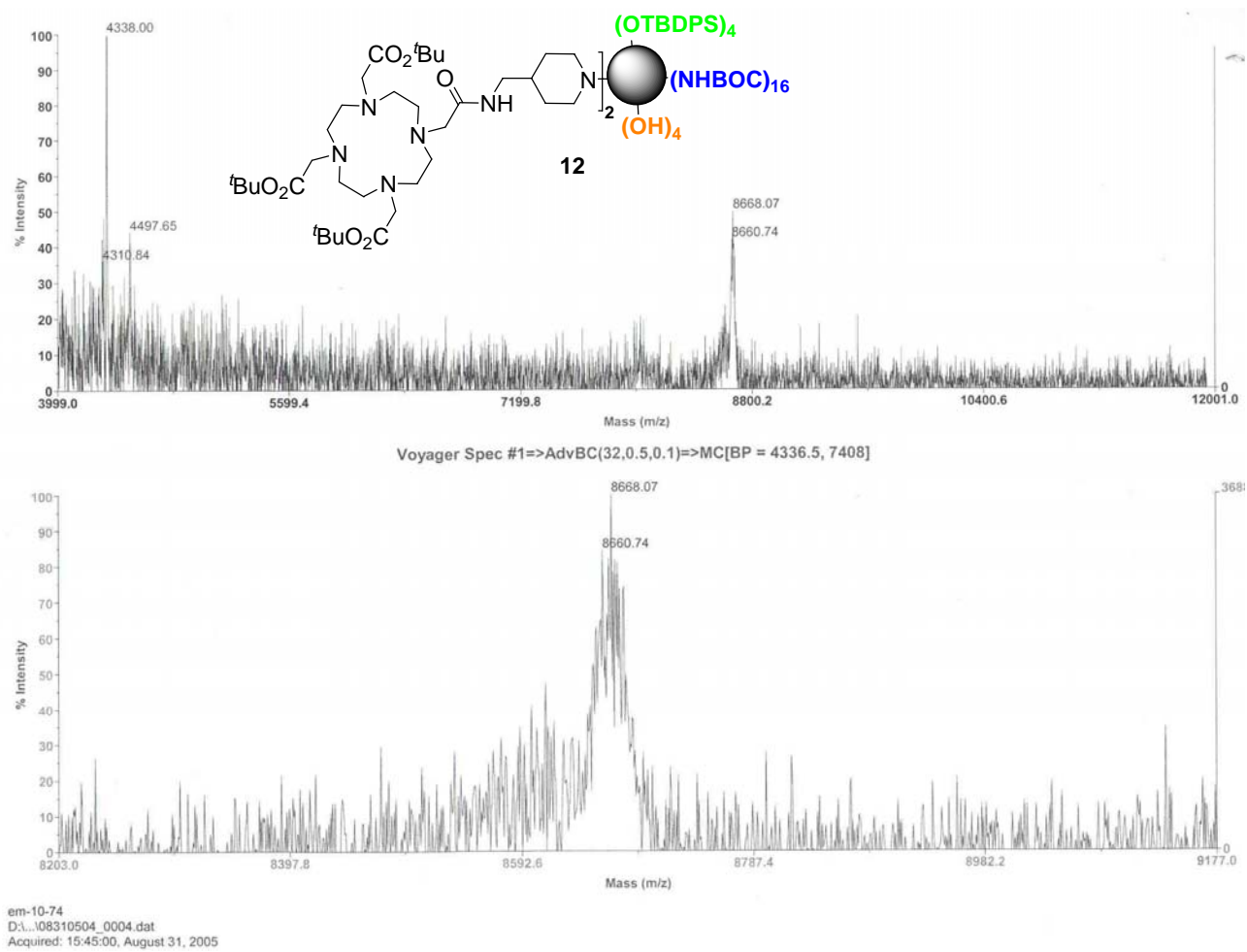


Figure B.7a. The MALDI-TOF mass spectrum of **12**.

Voyager Spec #1[BP = 7752.7, 1372]

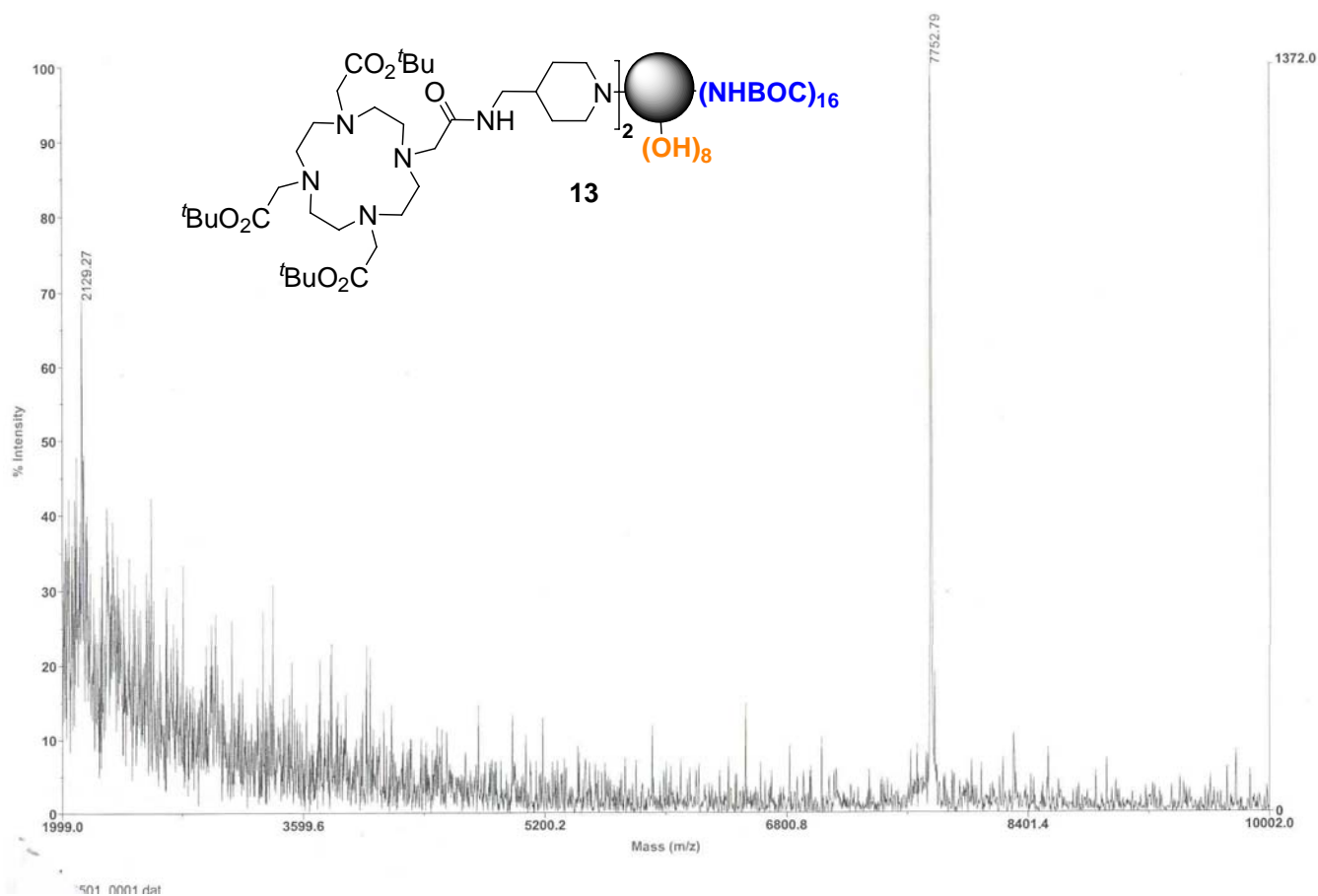


Figure B.8a. The MALDI-TOF mass spectrum of **13**.

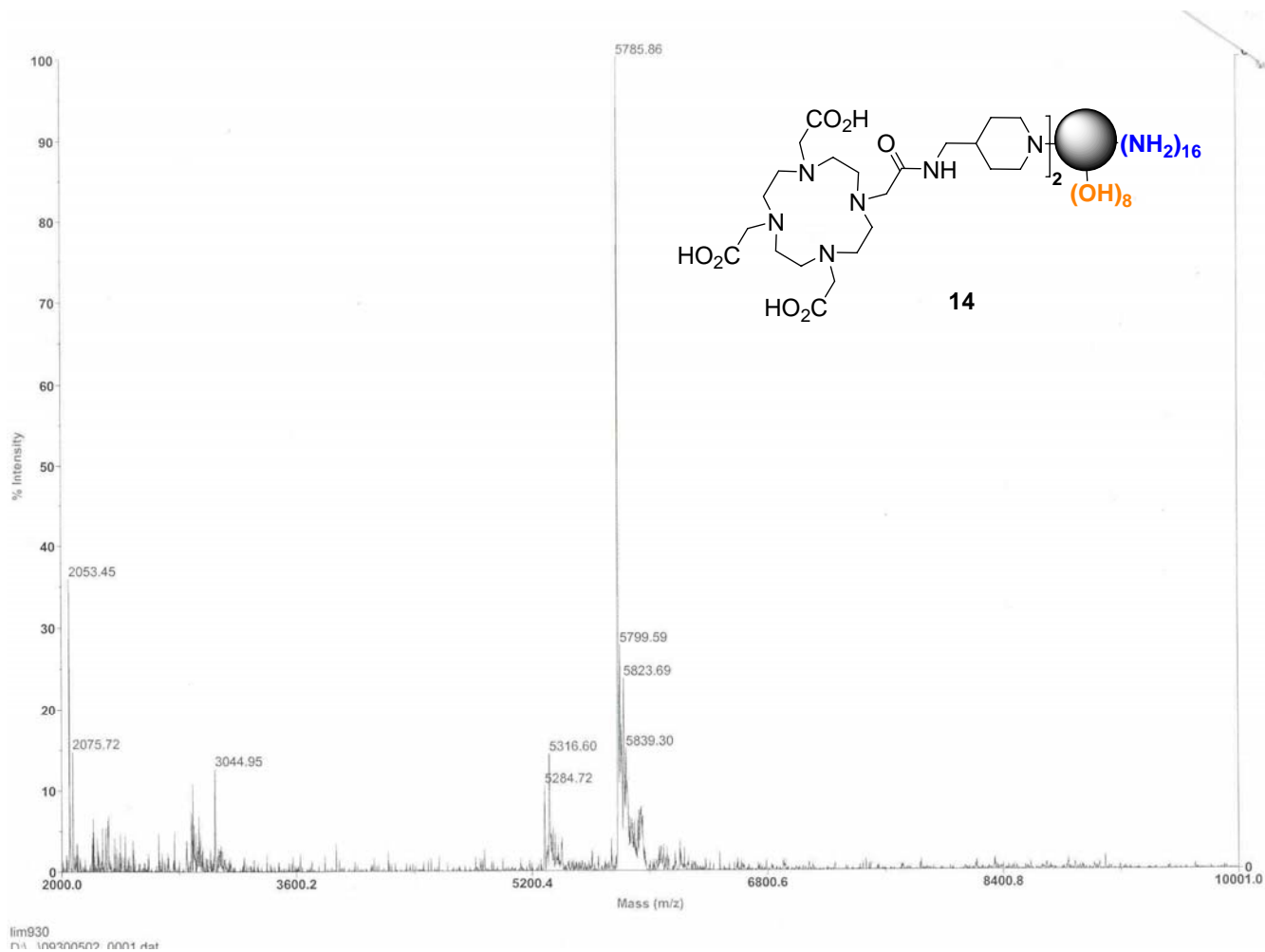


Figure B.9a. The MALDI-TOF mass spectrum of **14**.

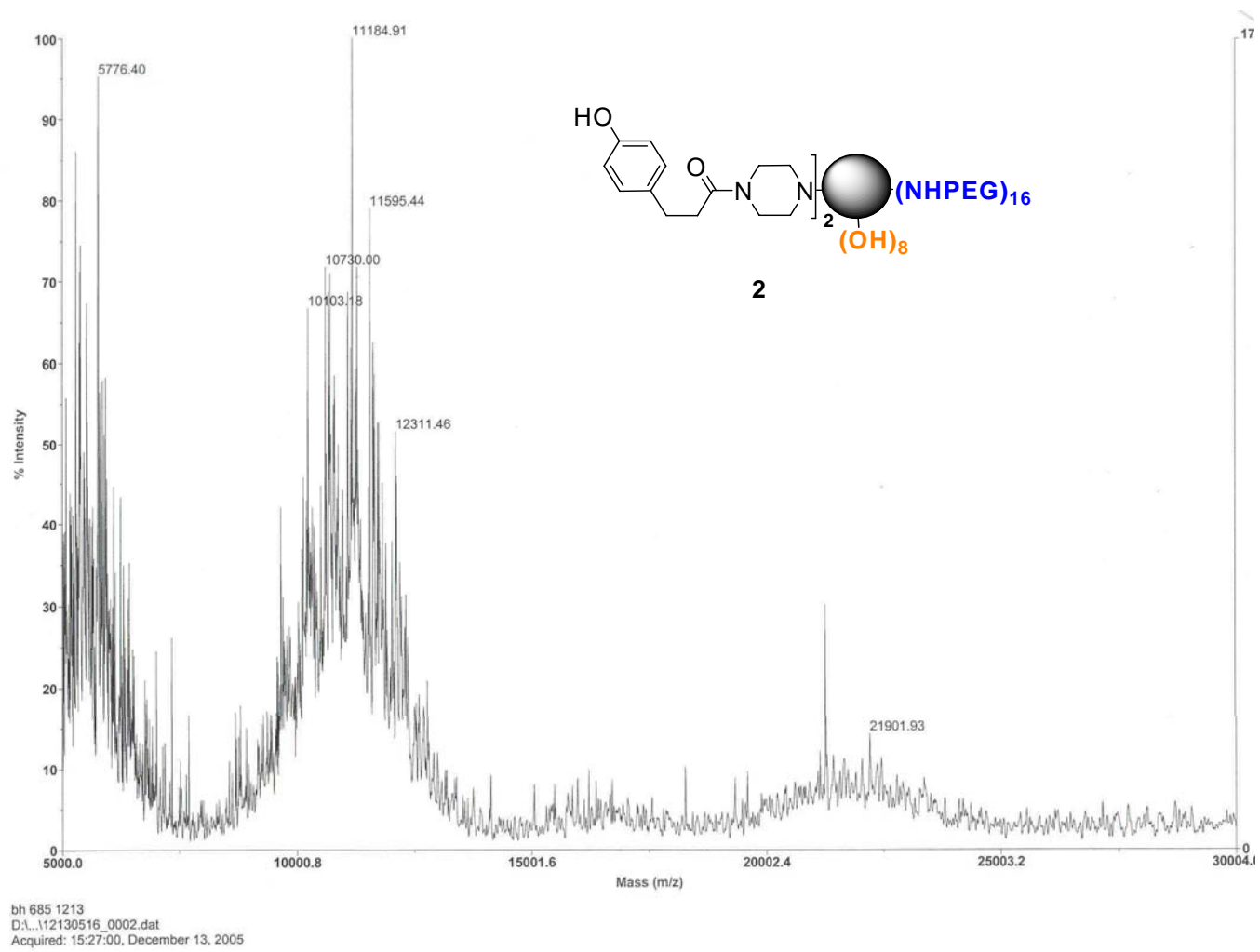


Figure B.10a. The MALDI-TOF mass spectrum of **2**.

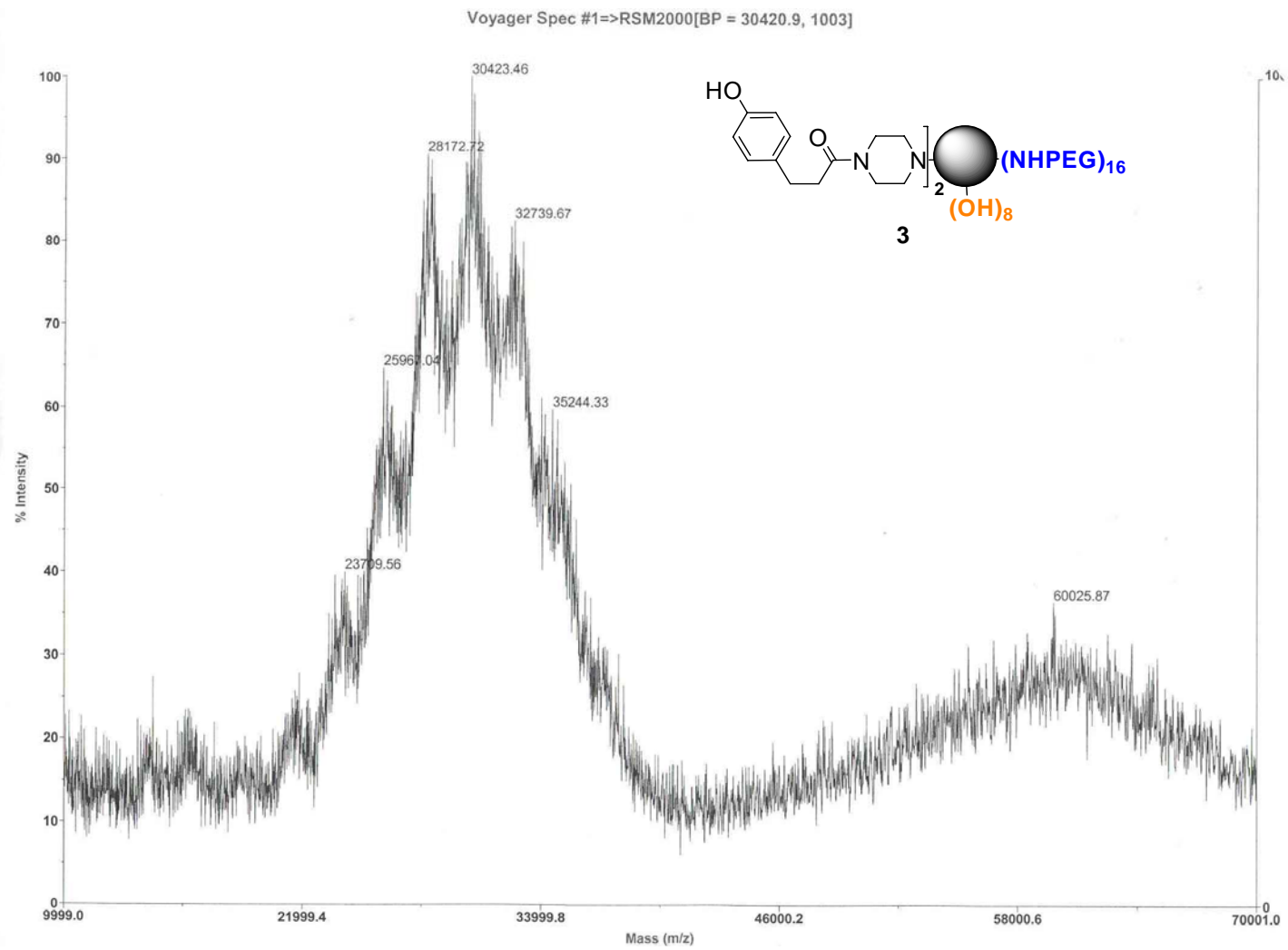


Figure B.11a. The MALDI-TOF mass spectrum of **3**.

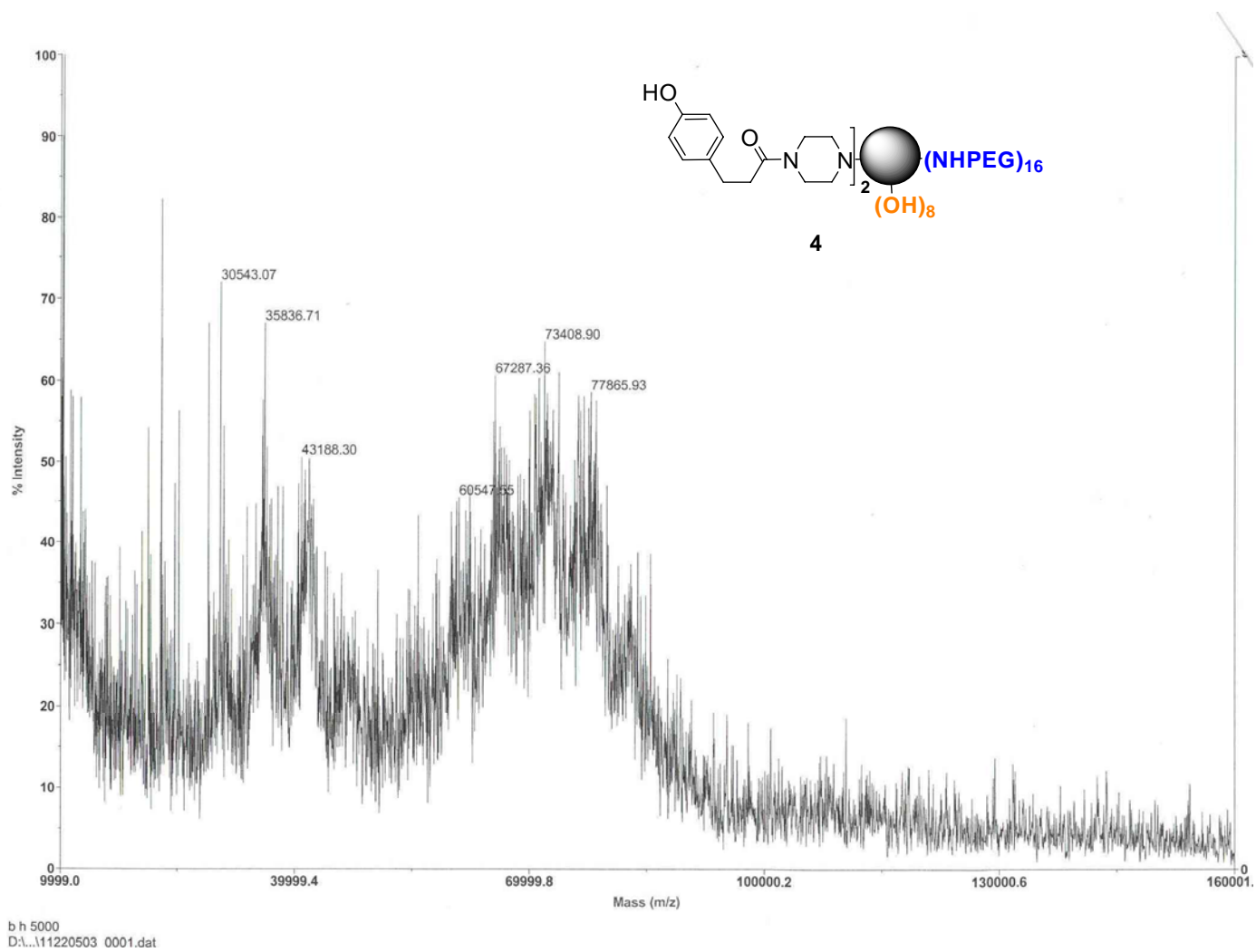


Figure B.12a. The MALDI-TOF mass spectrum of **4**.

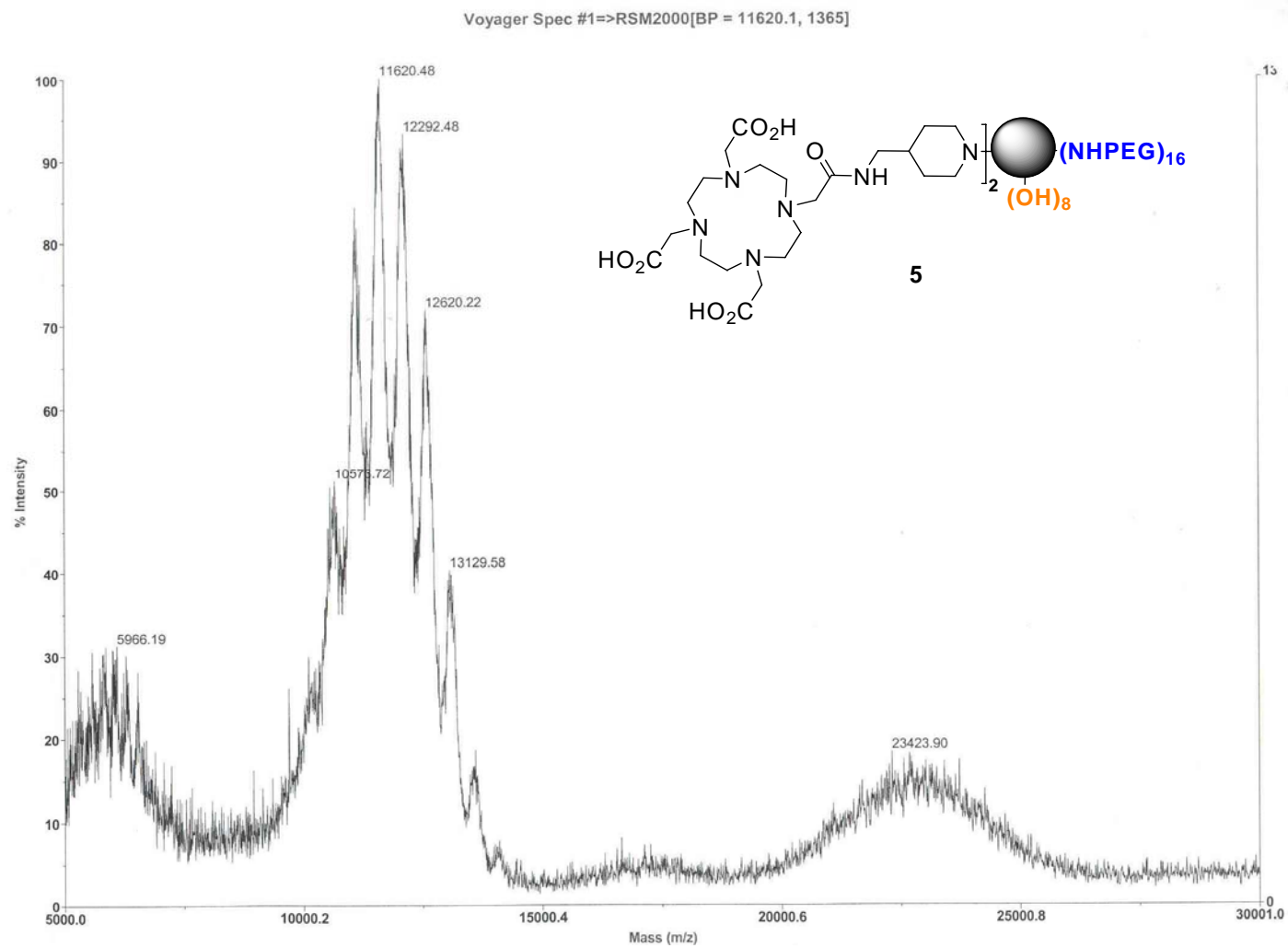


Figure B.13a. The MALDI-TOF mass spectrum of **5**.

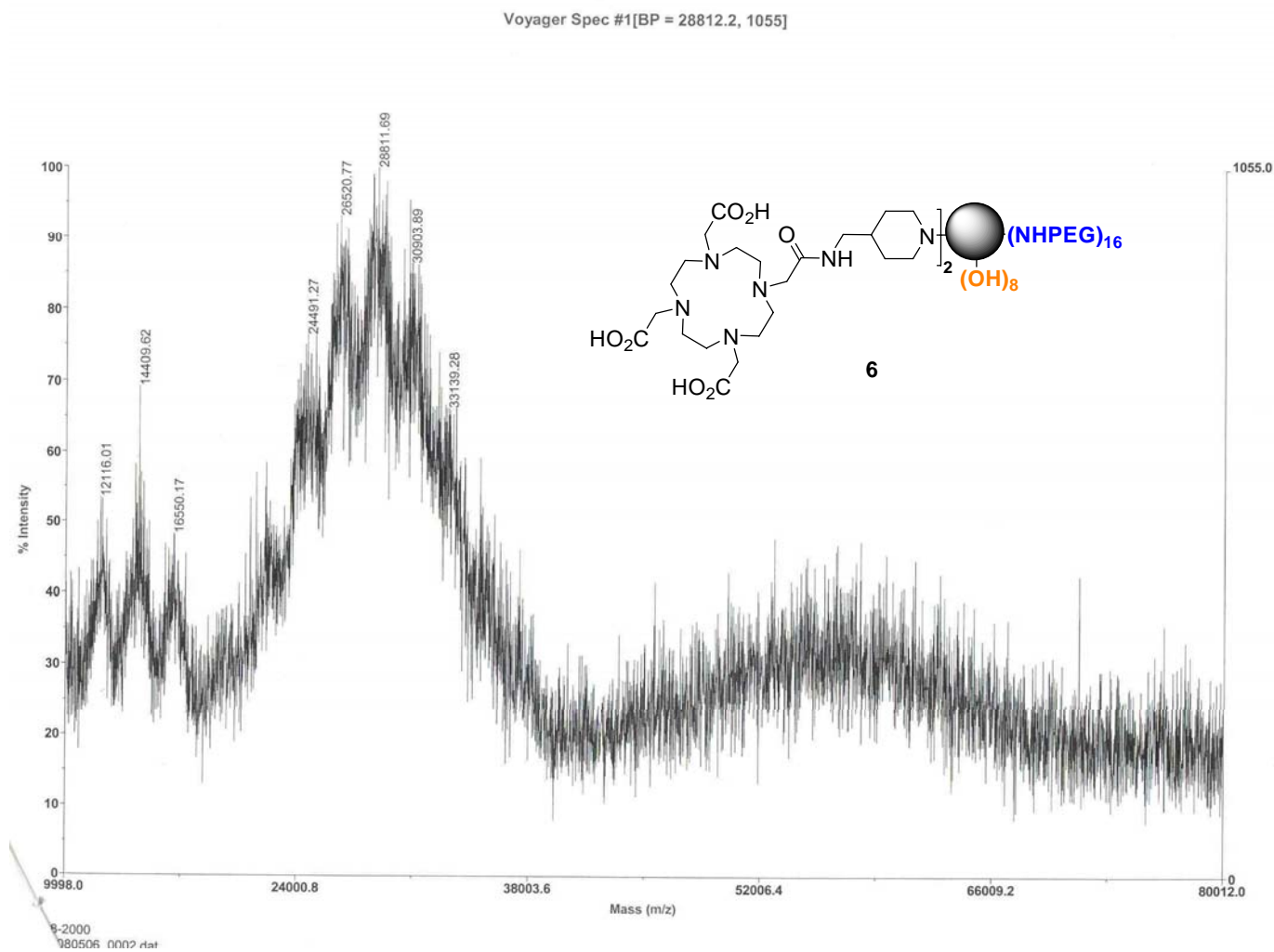


Figure B.14a. The MALDI-TOF mass spectrum of **6**.

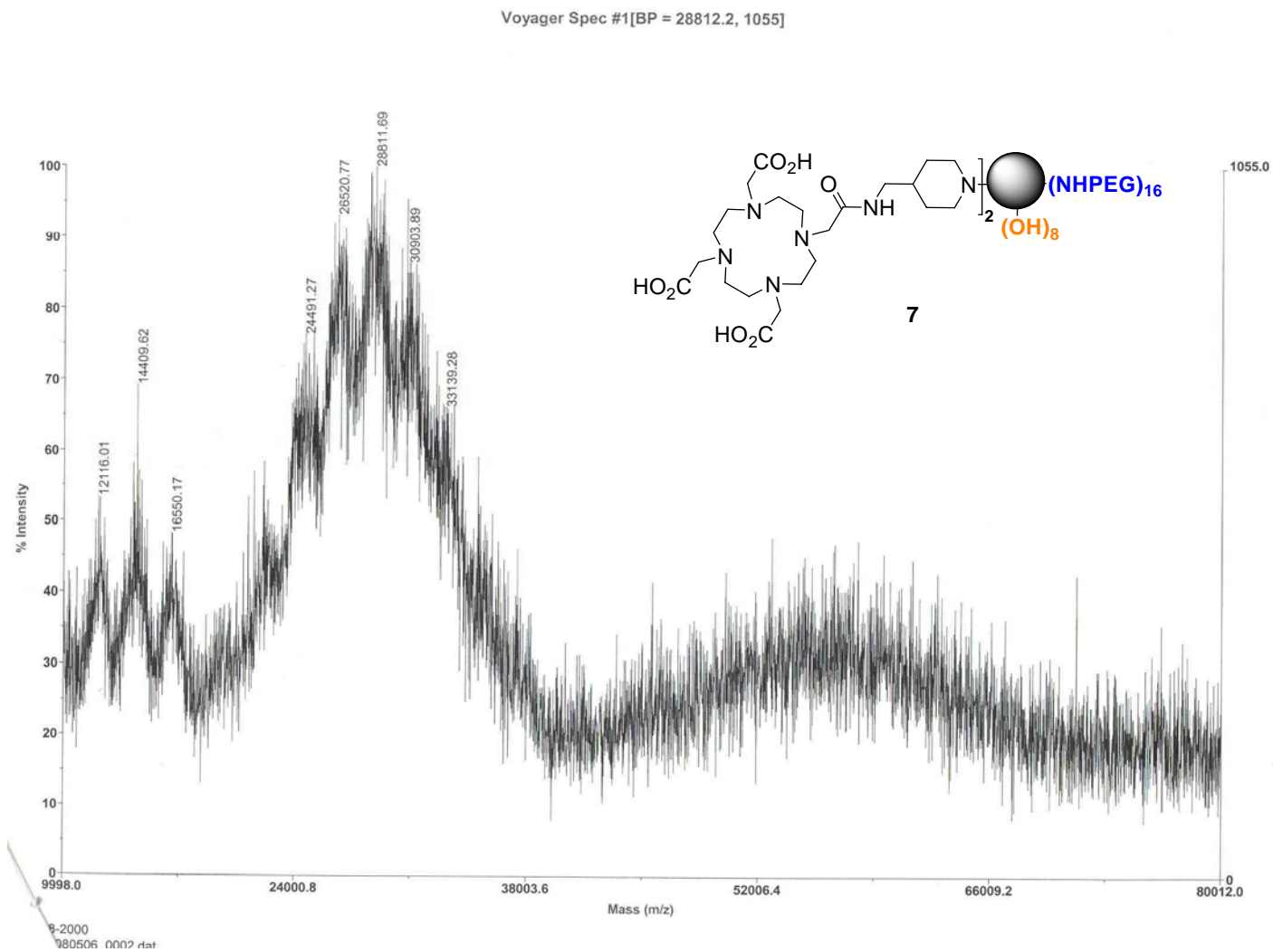


Figure B.15a. The MALDI-TOF mass spectrum of 7.

APPENDIX C
SPECTRA RELEVANT TO CHAPTER IV

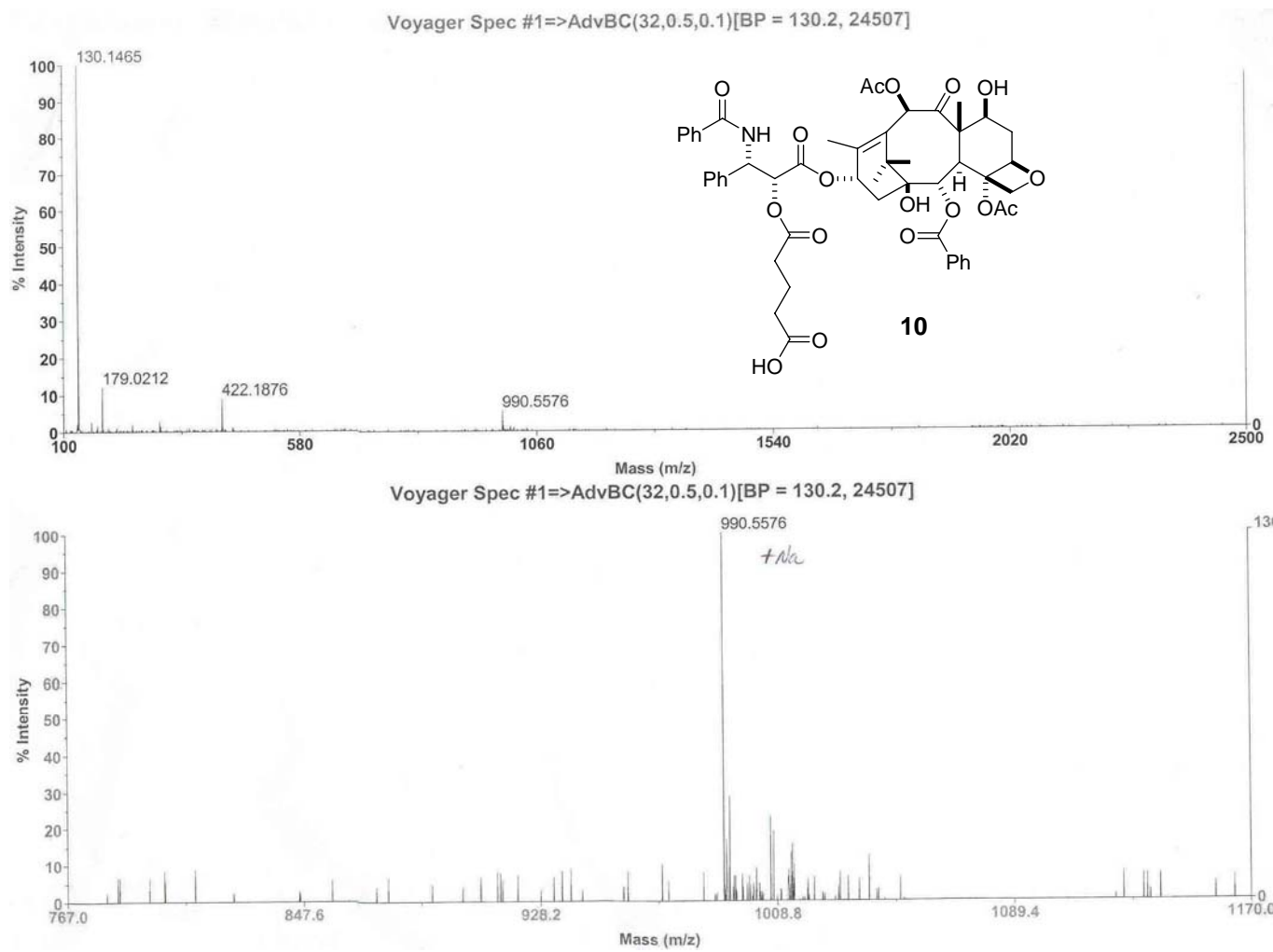


Figure C.1a. The MALDI-TOF mass spectrum of **10**.

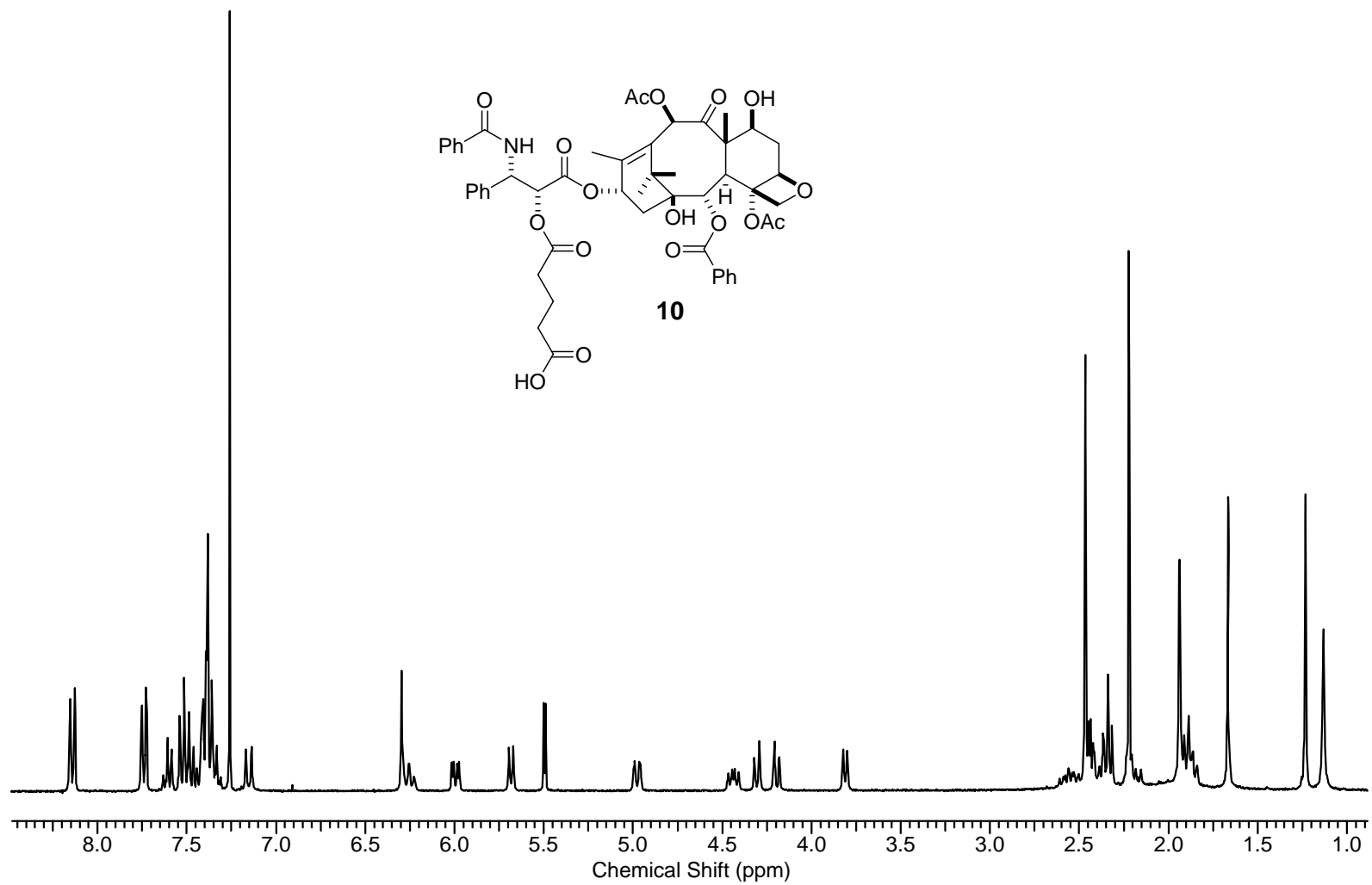


Figure C.1b. The ¹H NMR spectrum of **10**.

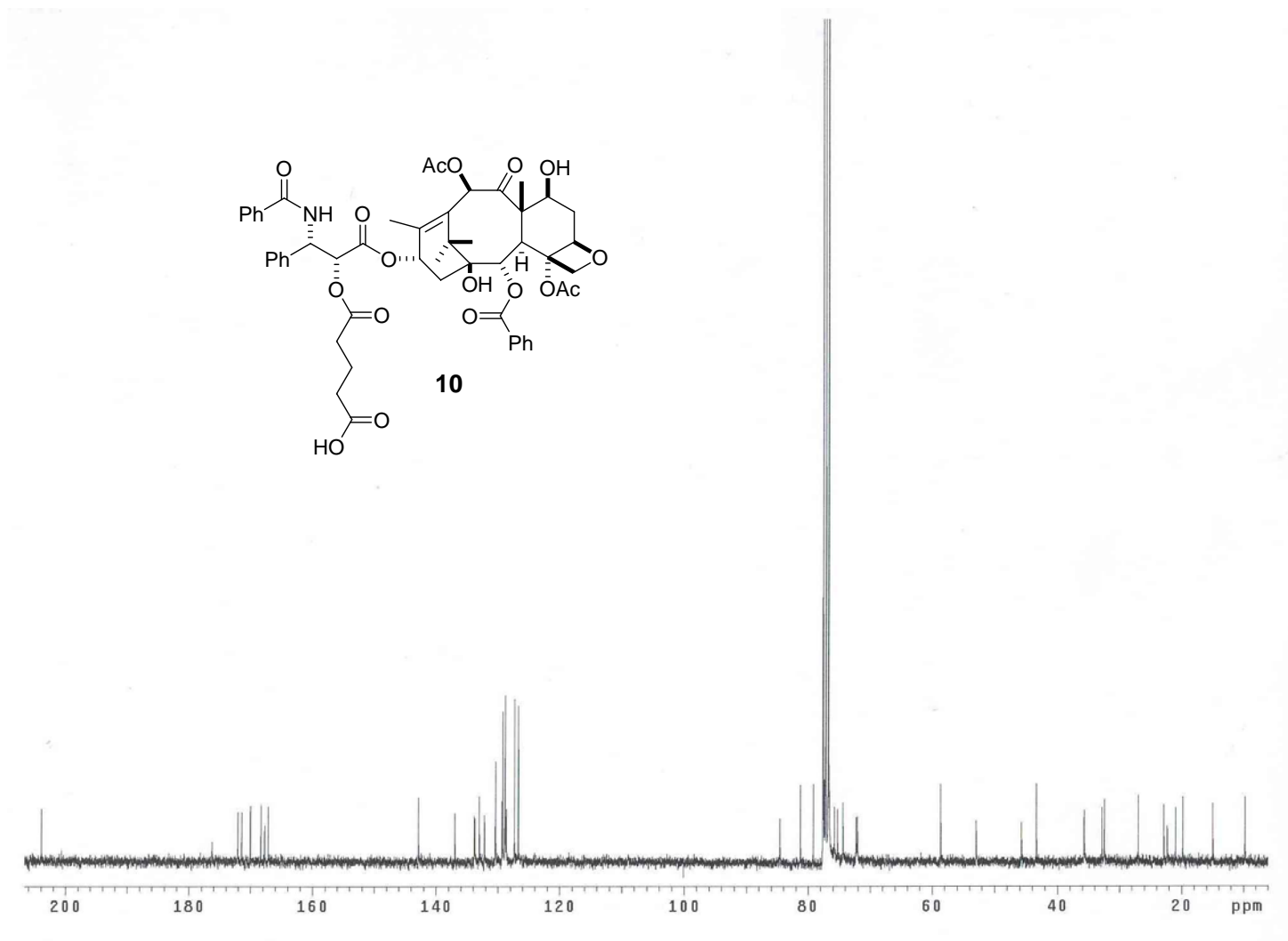


Figure C.1c. The ^{13}C NMR spectrum of **10**.

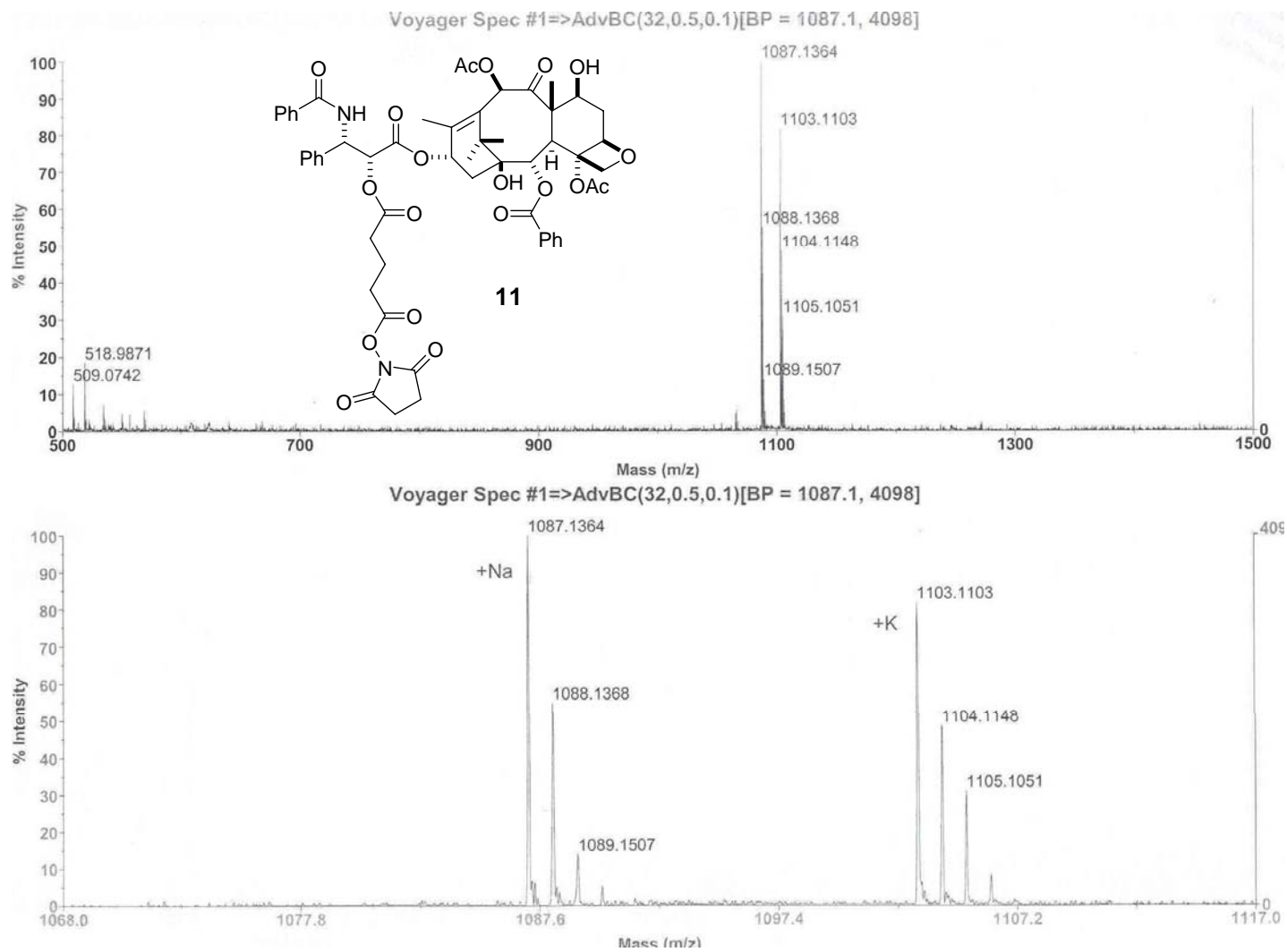


Figure C.2a. The MALDI-TOF mass spectrum of **11**.

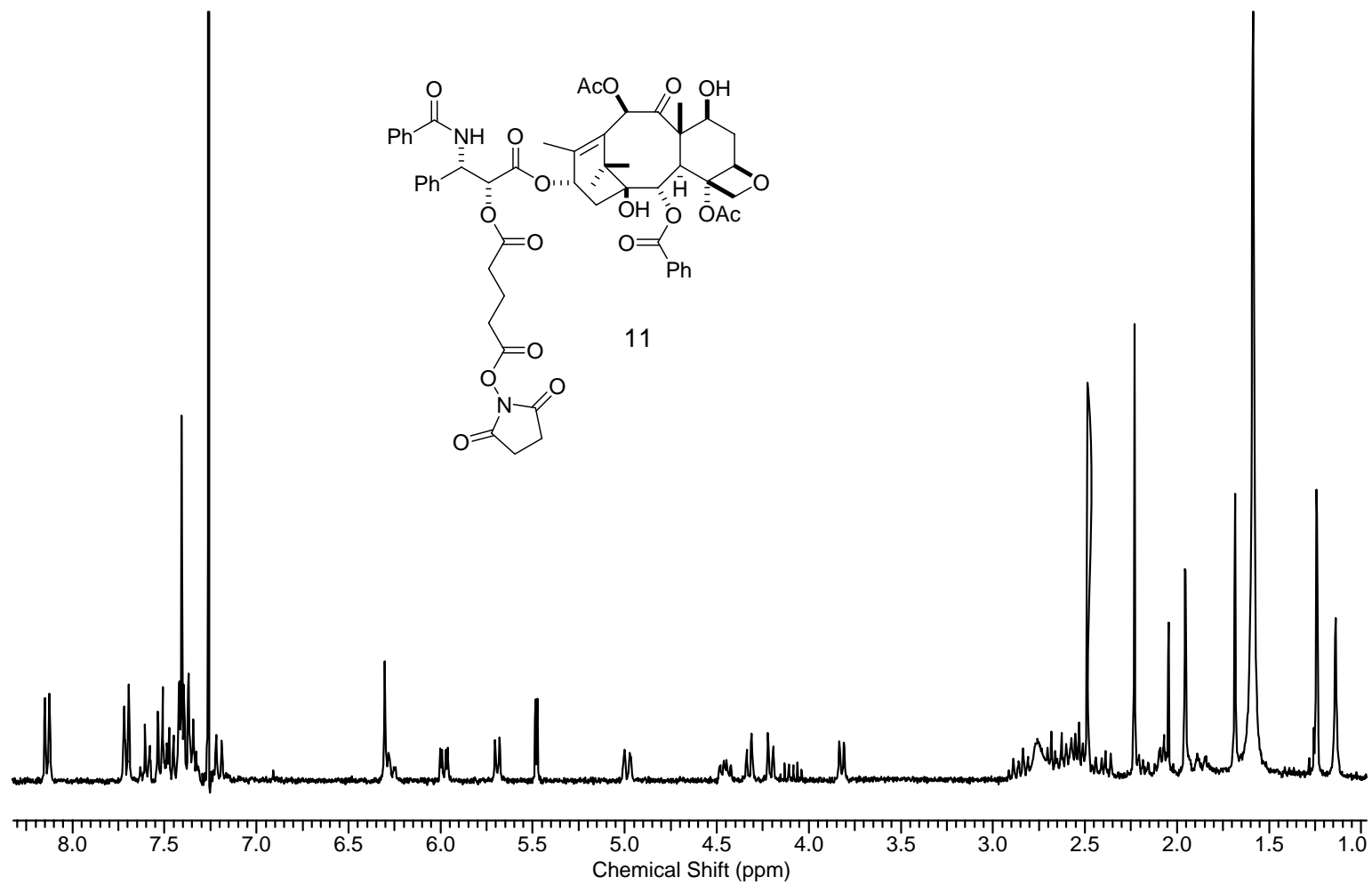


Figure C.2b. The ^1H NMR spectrum of **11**.

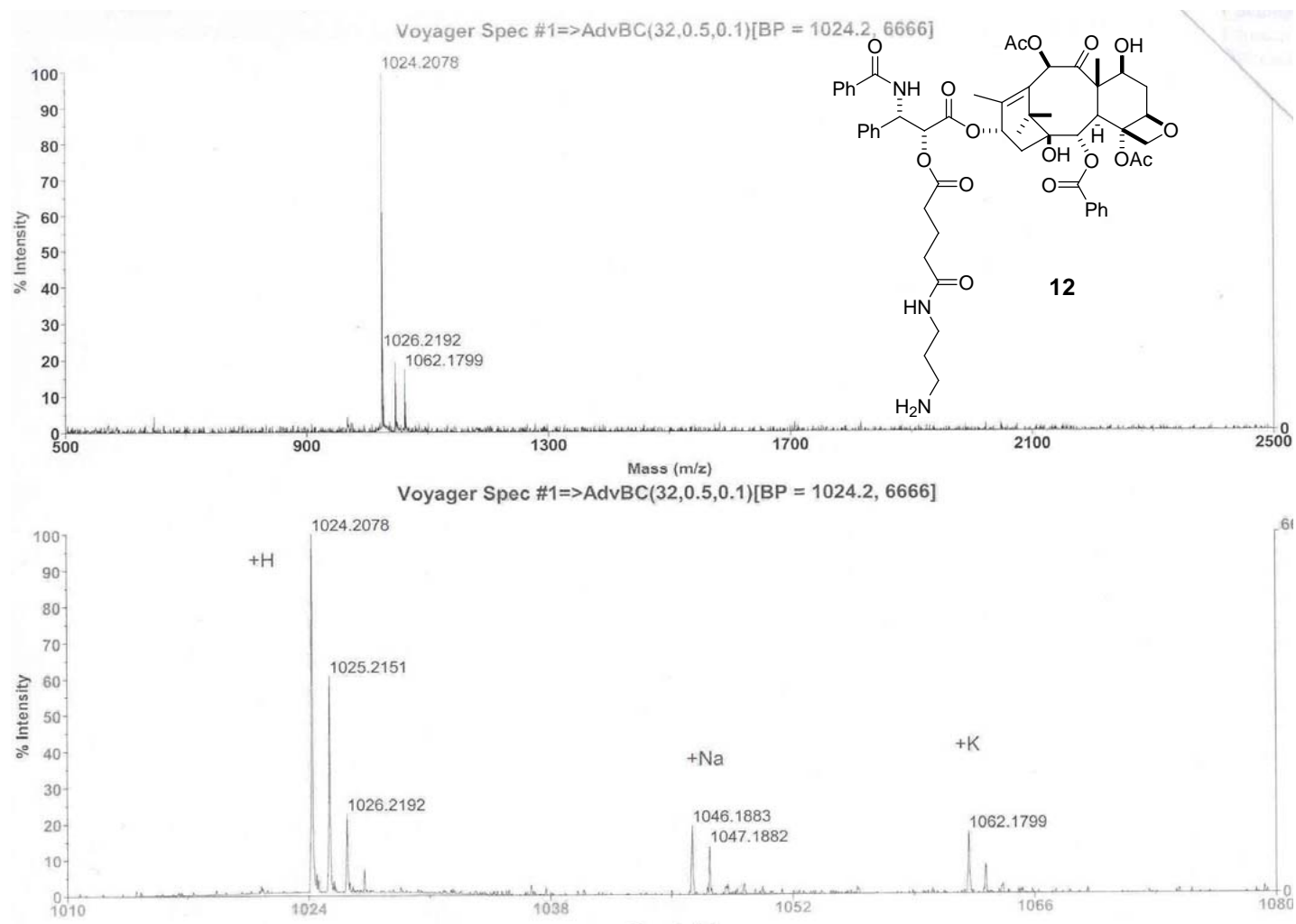


Figure C.3a. The MALDI-TOF mass spectrum of **12**.

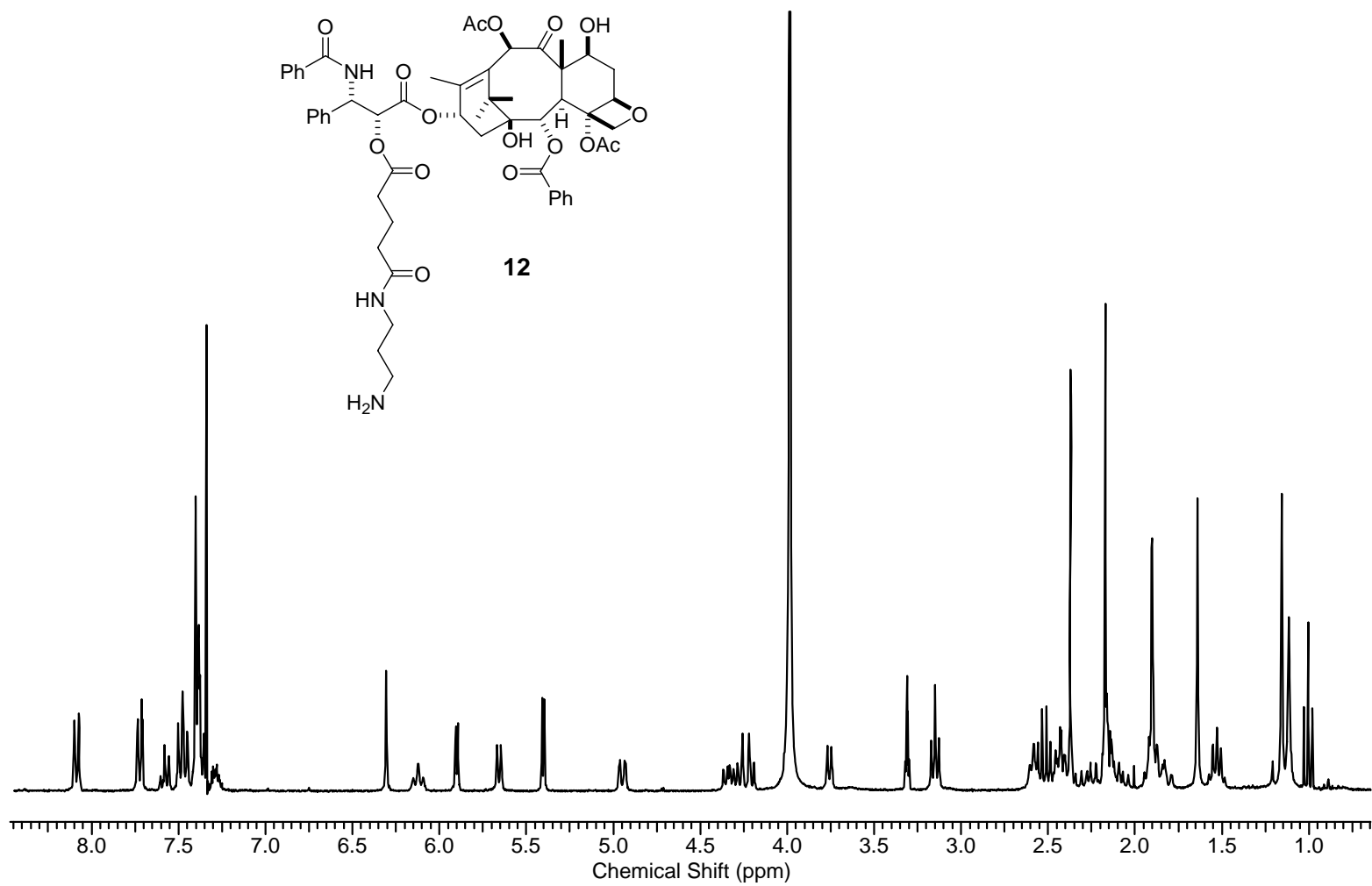


Figure C.3b. The ¹H NMR spectrum of **12**.

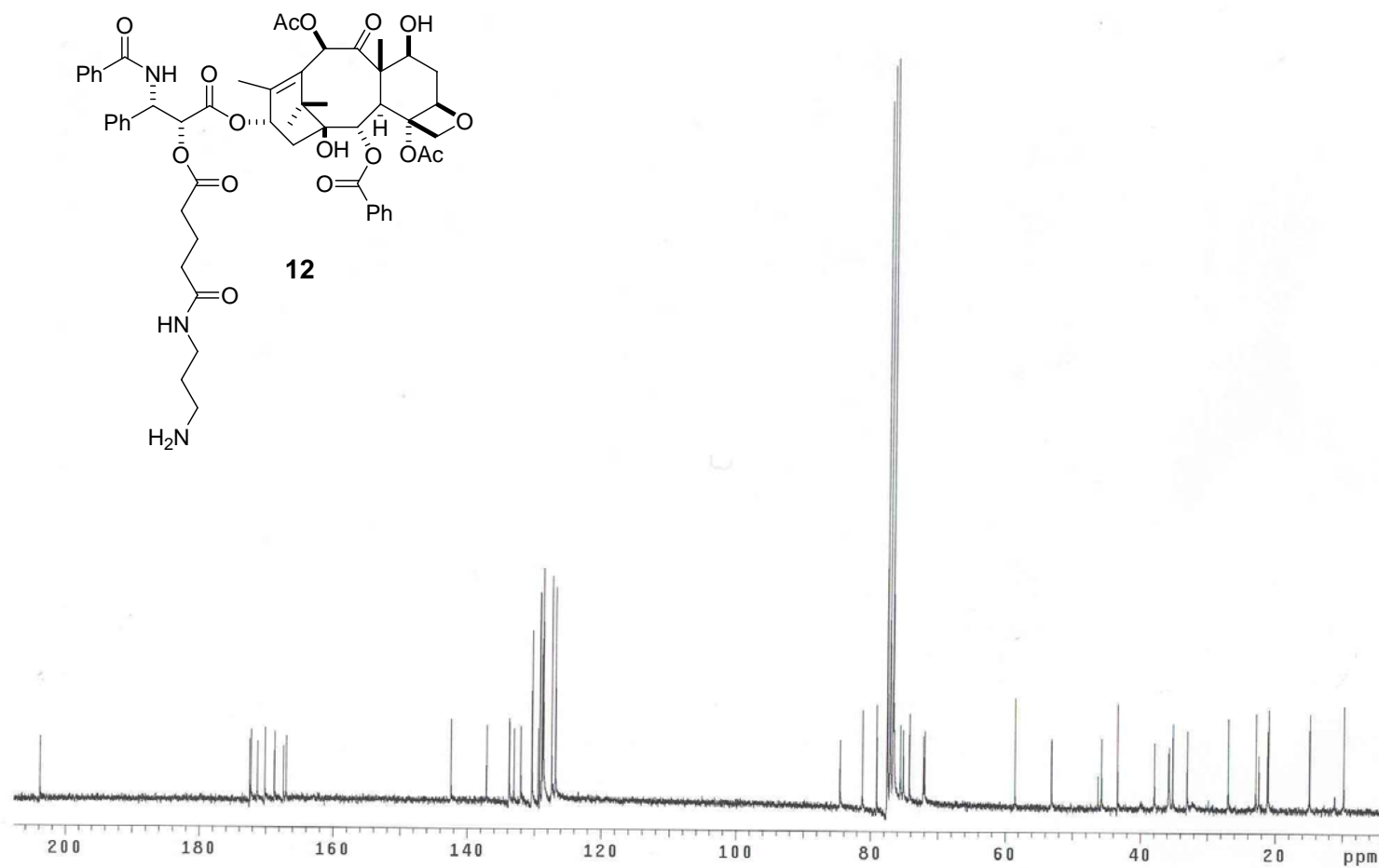


Figure C.3c. The ¹³C NMR spectrum of **12**.

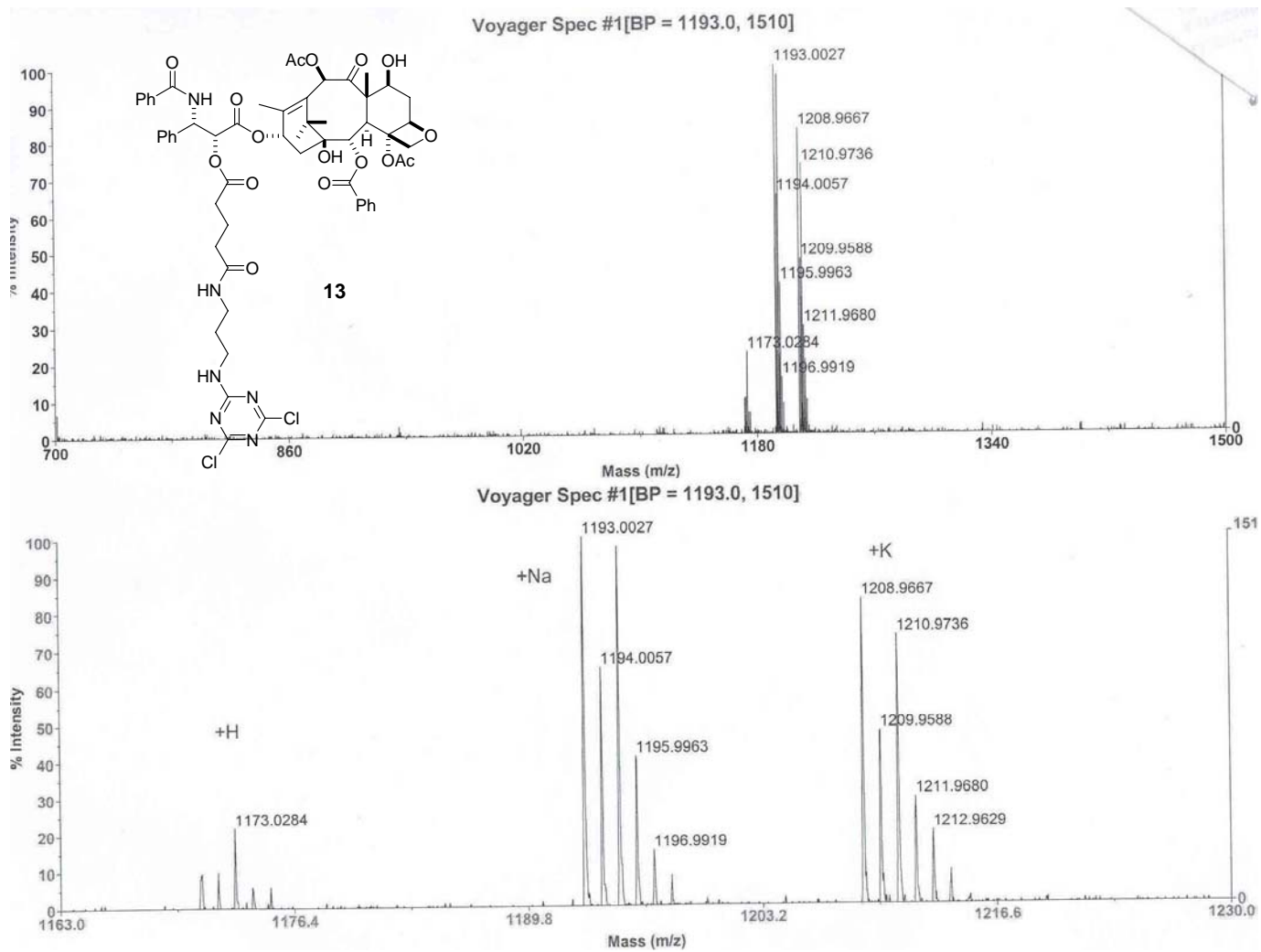


Figure C.4a. The MALDI-TOF mass spectrum of **13**.

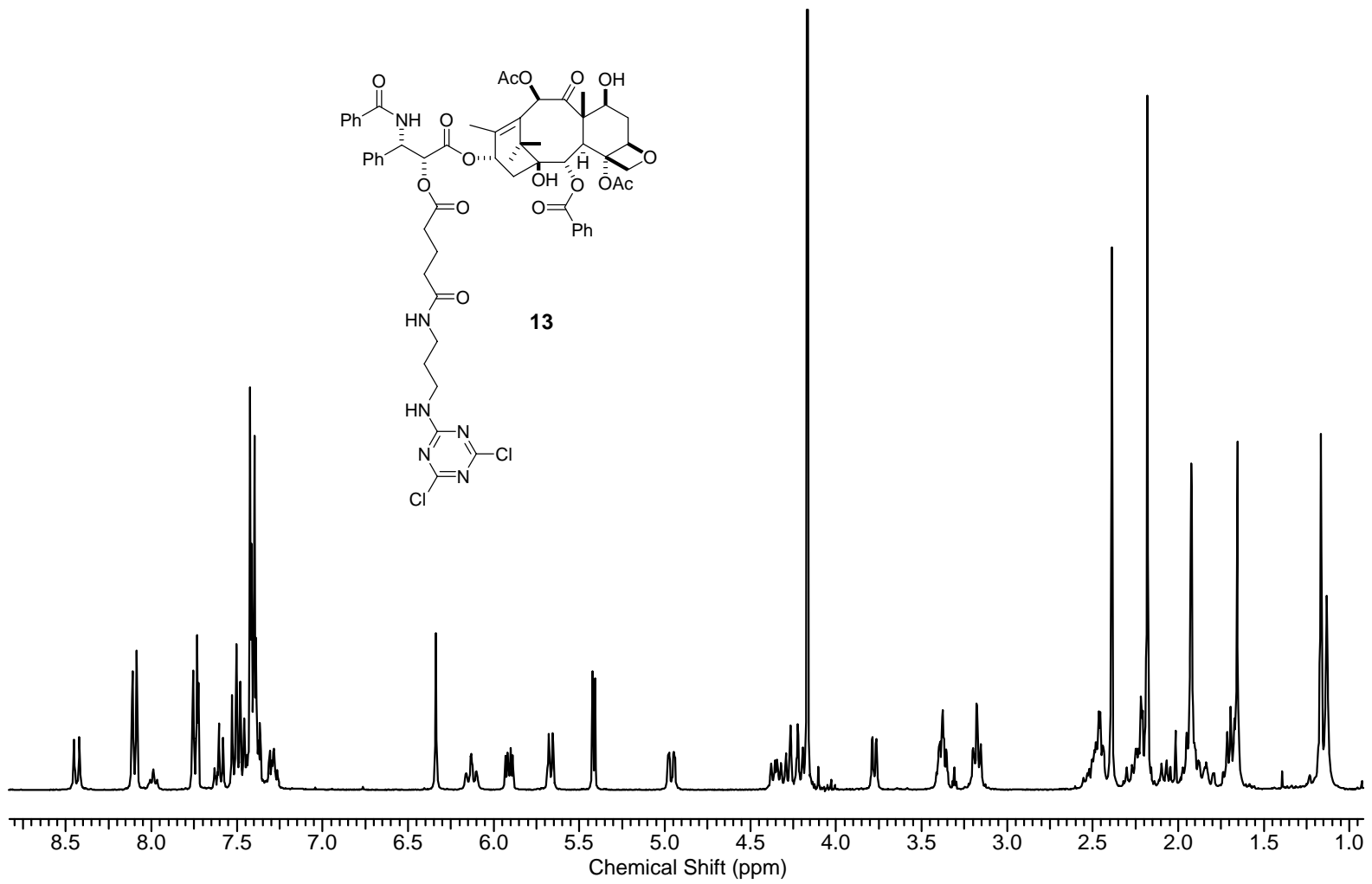


Figure C.4b. The ¹H NMR spectrum of **13**.

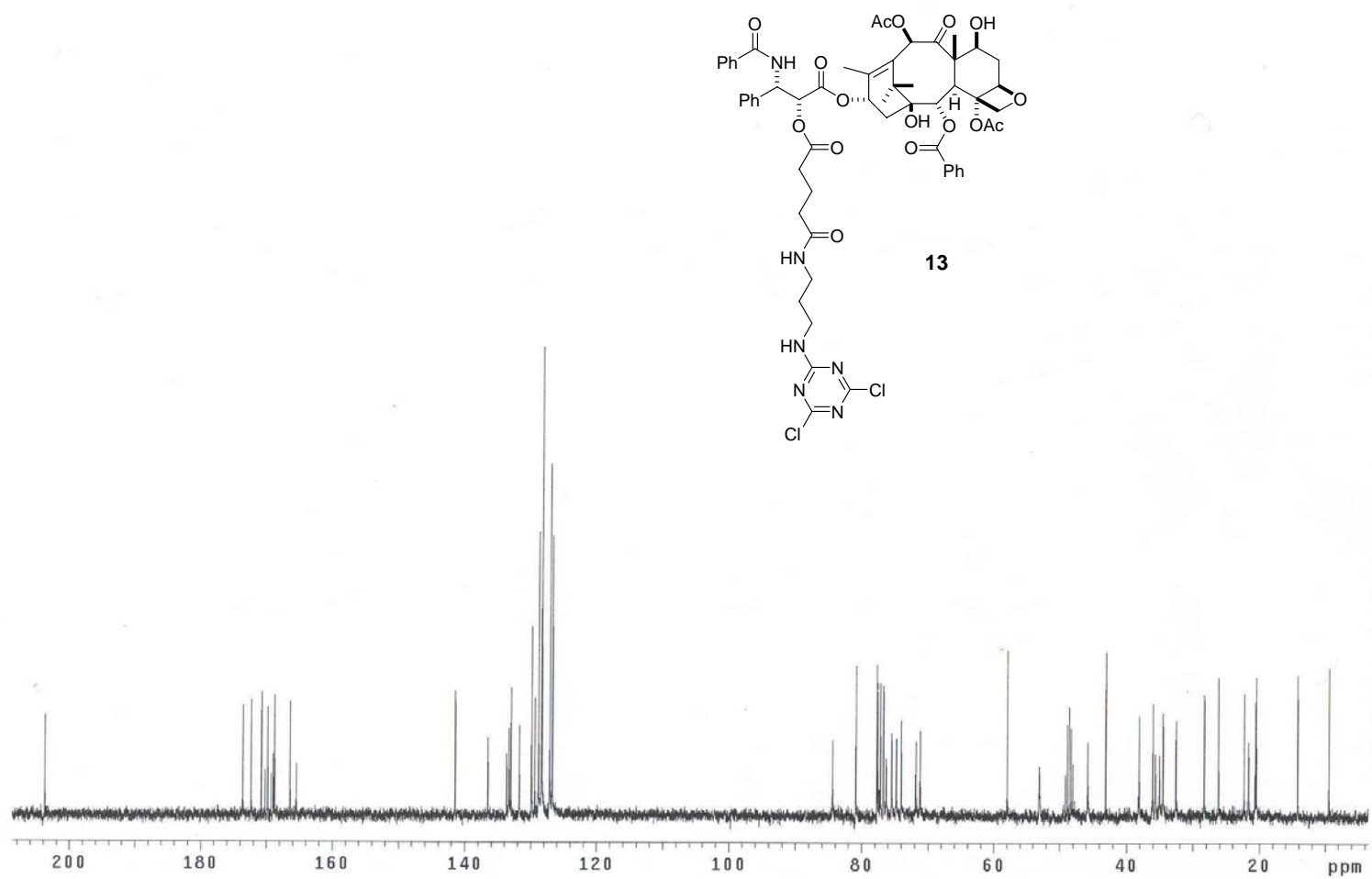


Figure C.4c. The ^{13}C NMR spectrum of **13**.

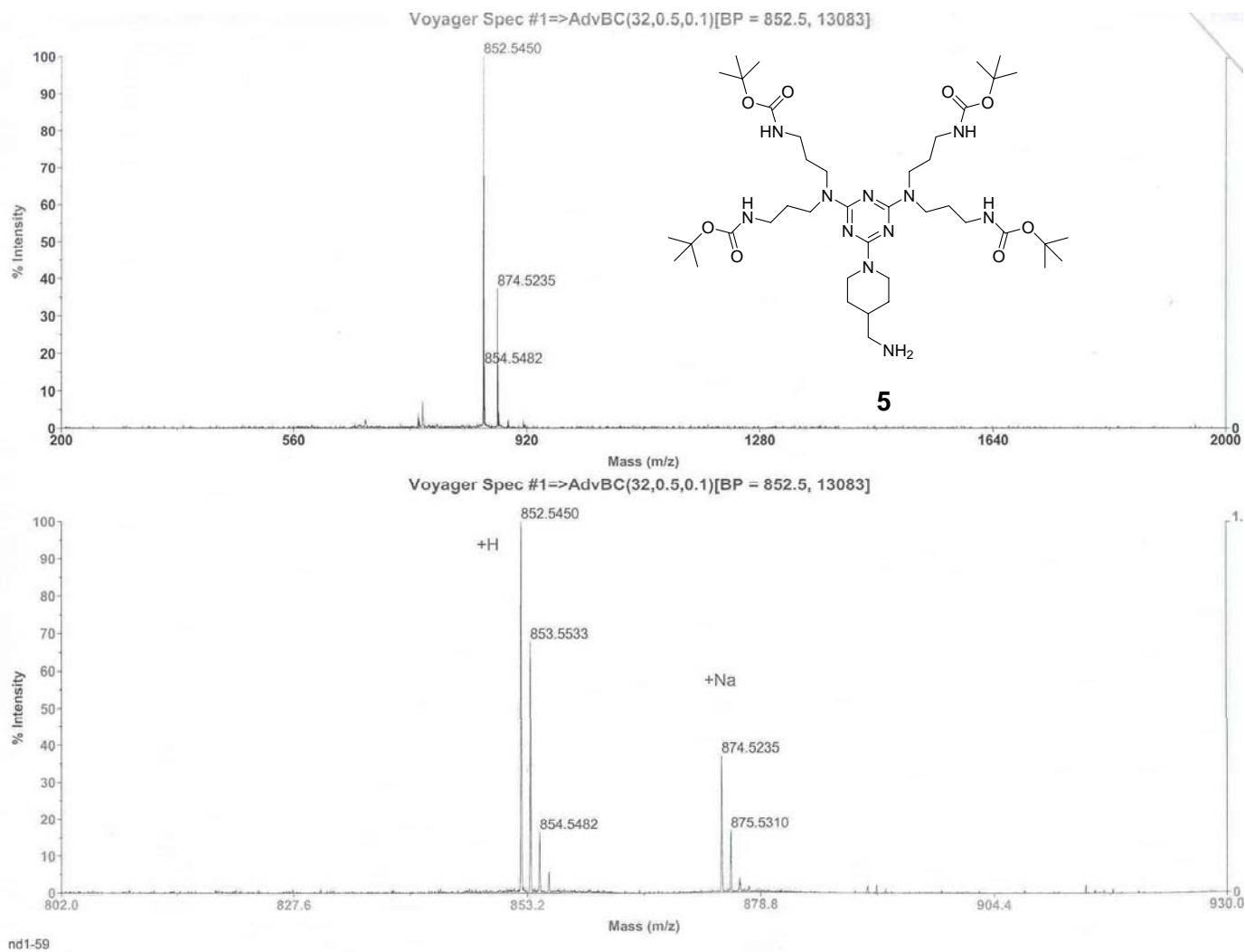


Figure C.5a. The MALDI-TOF mass spectrum of **5**.

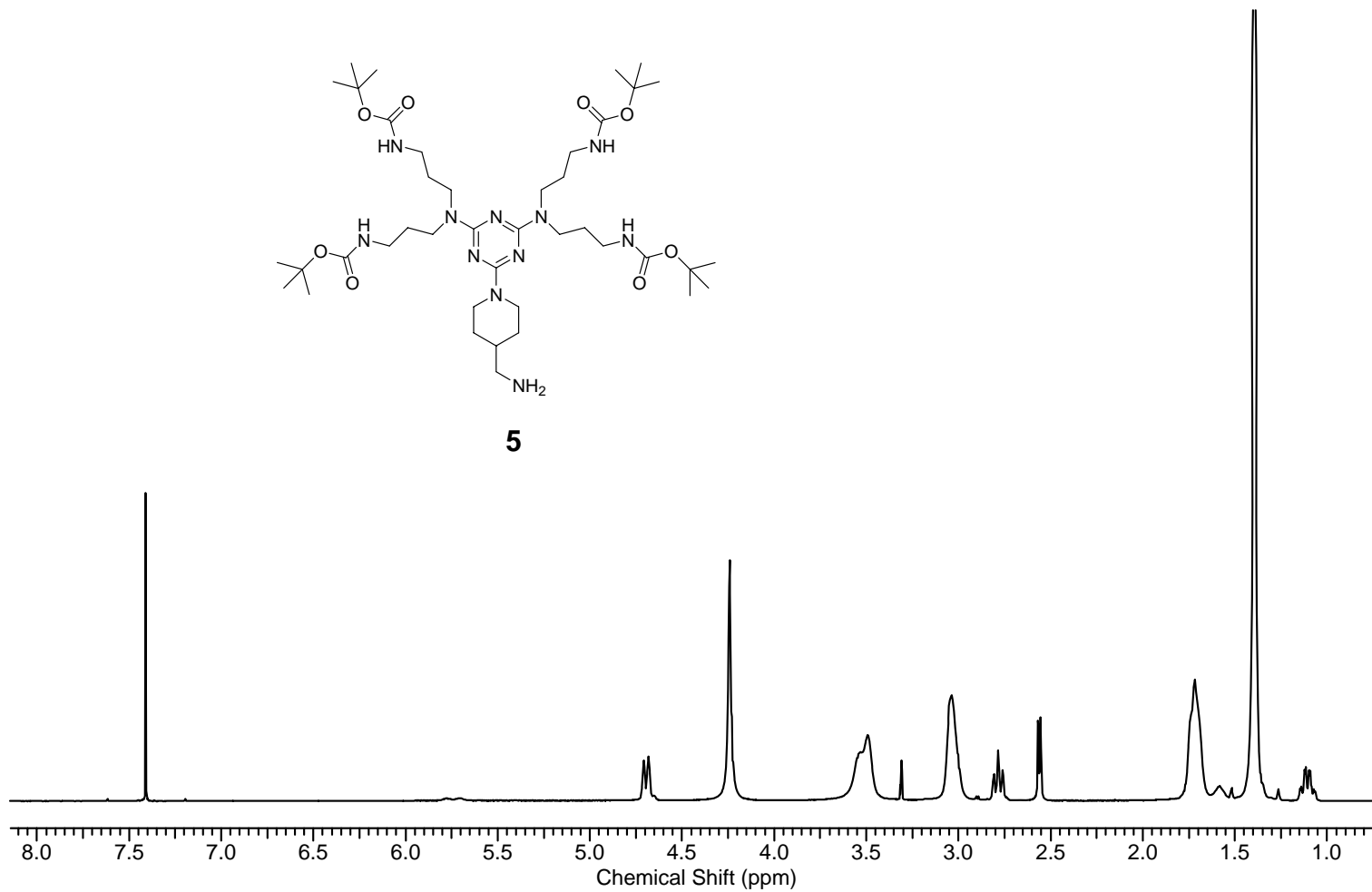
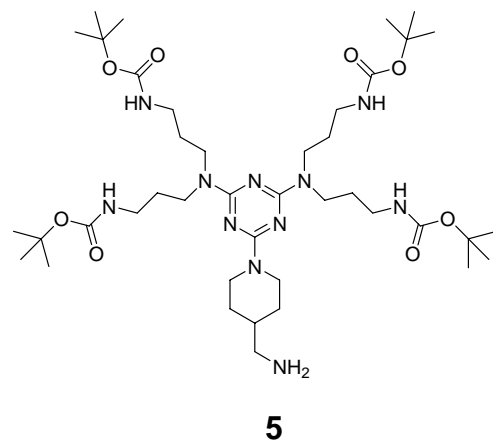


Figure C.5b. The ¹H NMR spectrum of **5**.

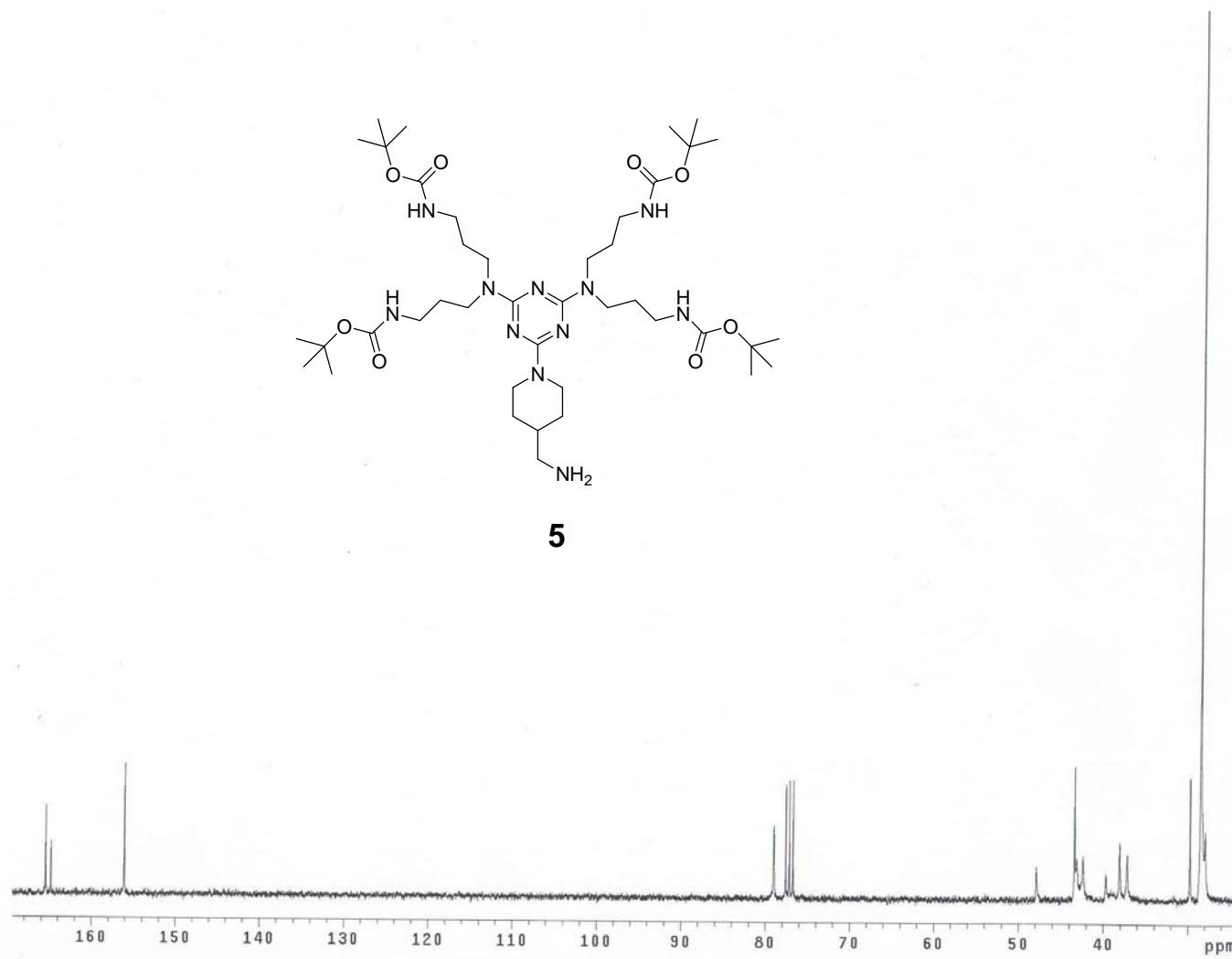


Figure C.5c. The ¹³C NMR spectrum of **5**.

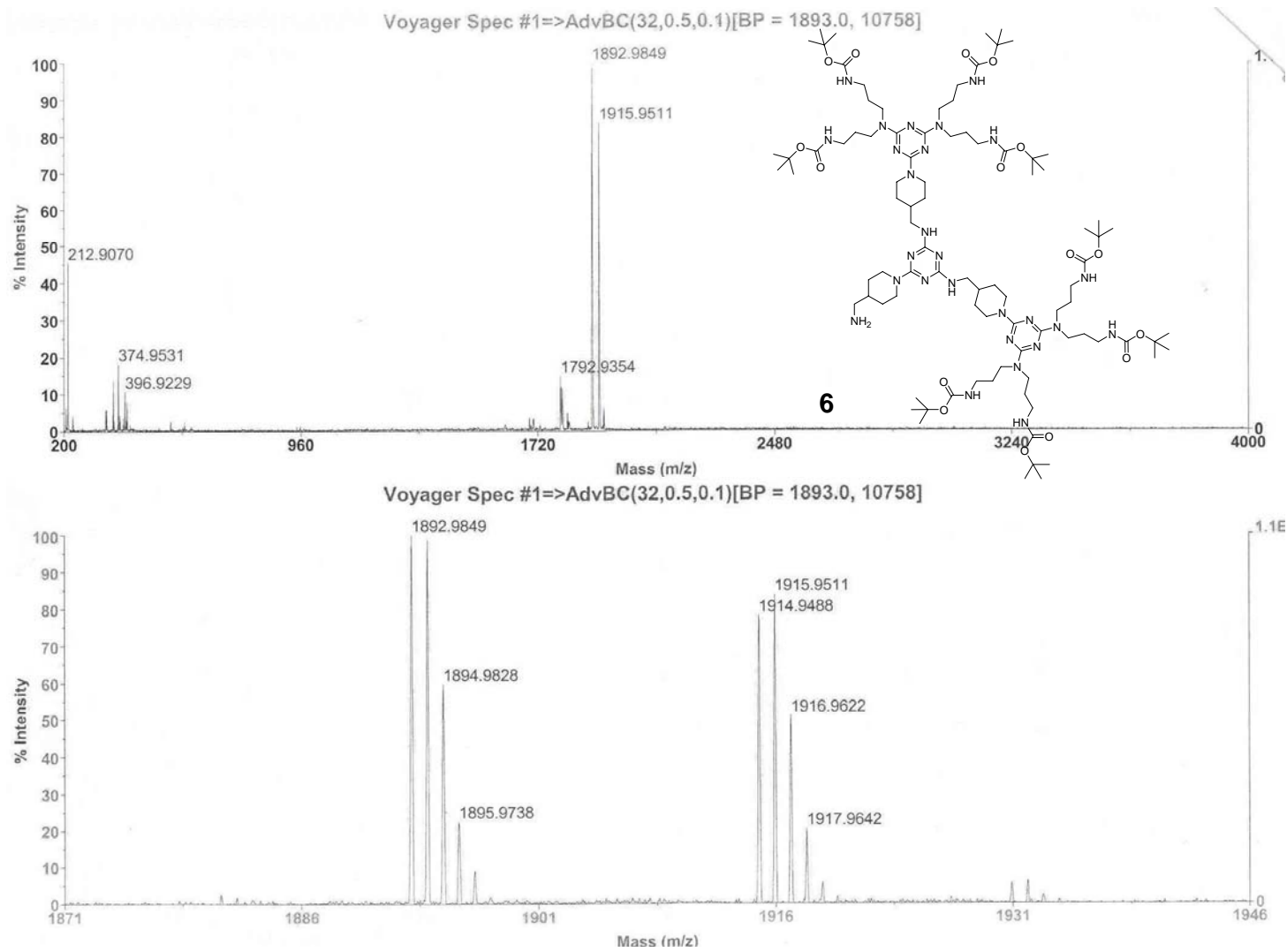


Figure C.6a. The MALDI-TOF mass spectrum of **6**.

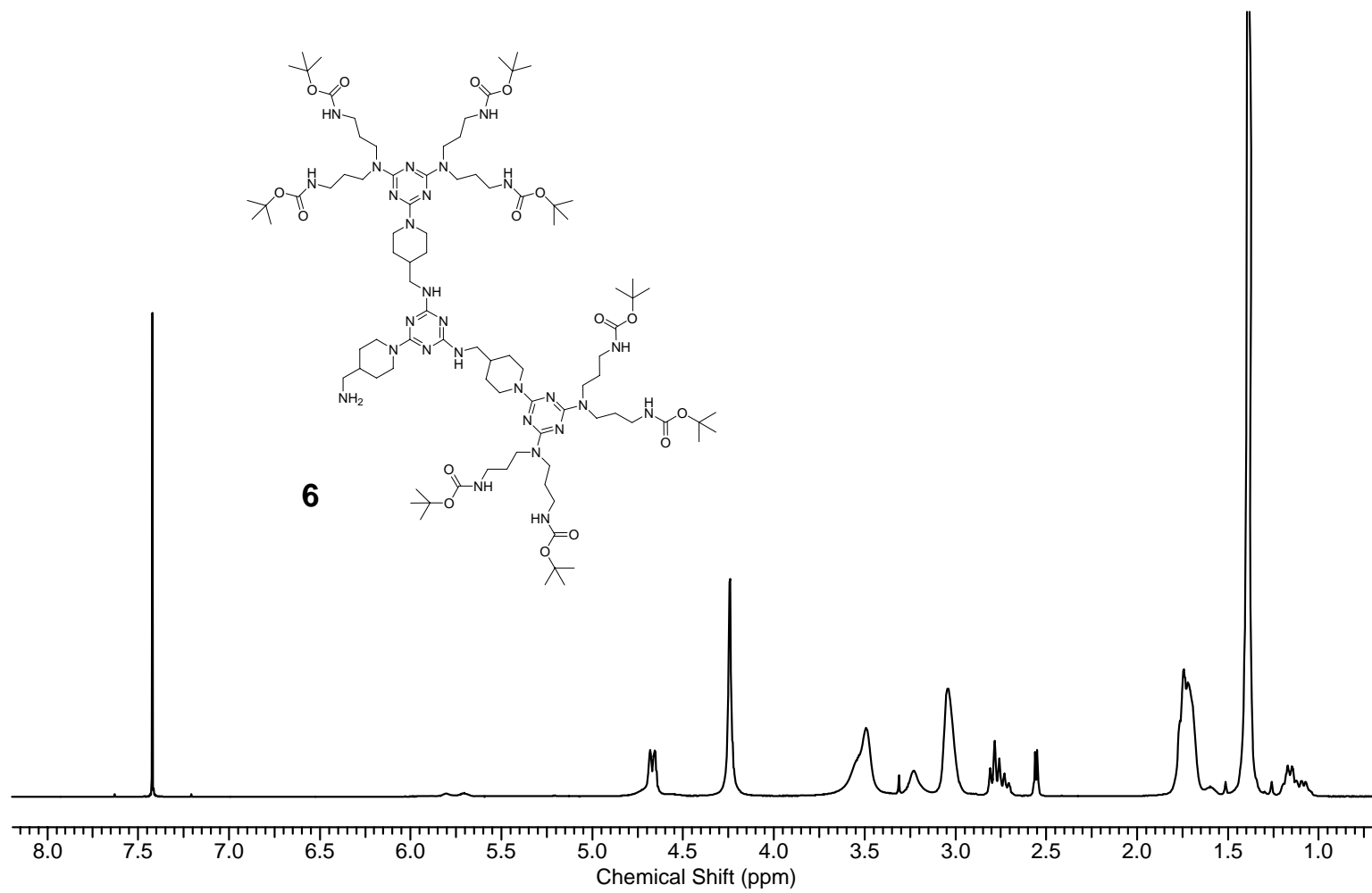


Figure C.6b. The ¹H NMR spectrum of **6**.

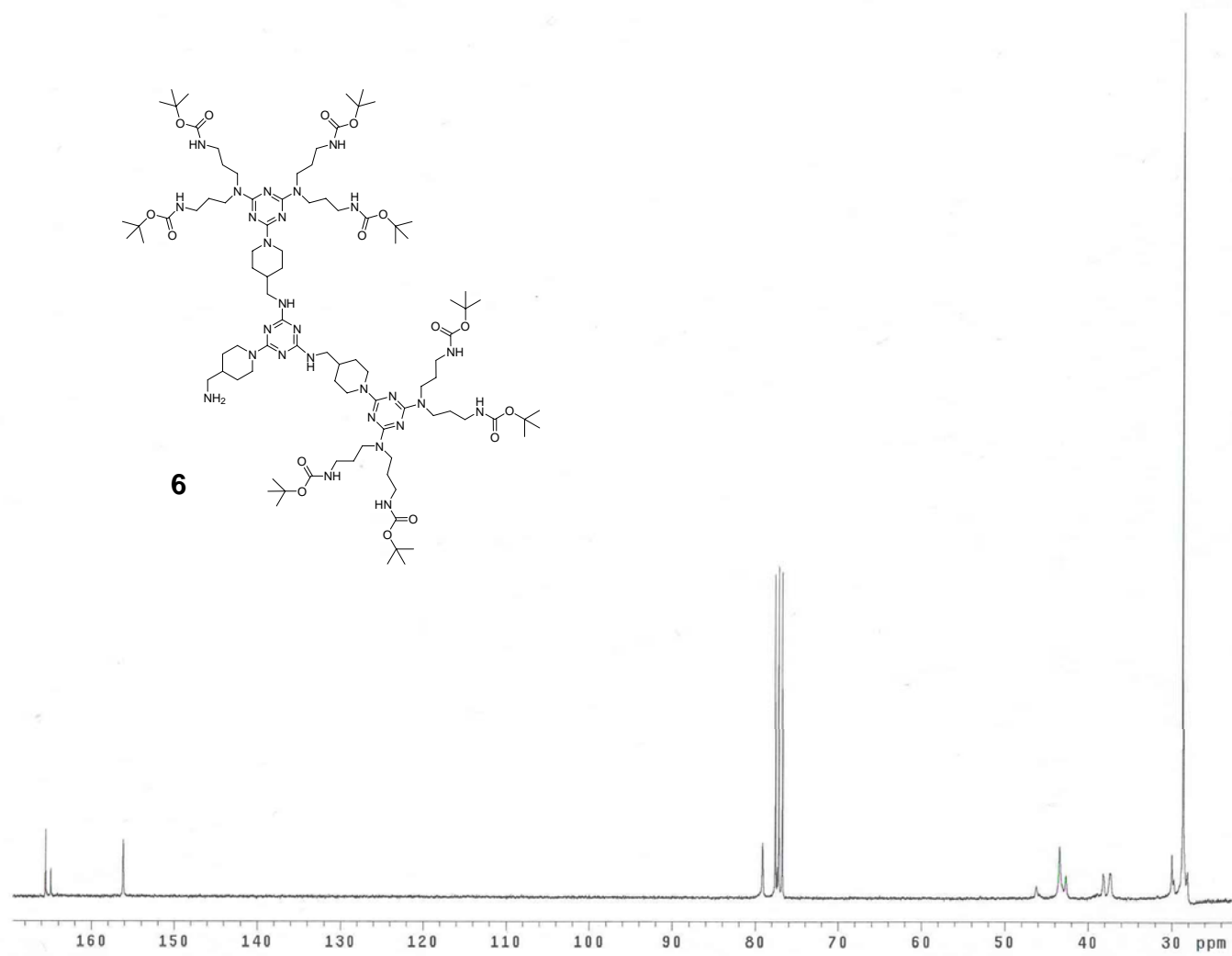


Figure C.6c. The ^{13}C NMR spectrum of **6**.

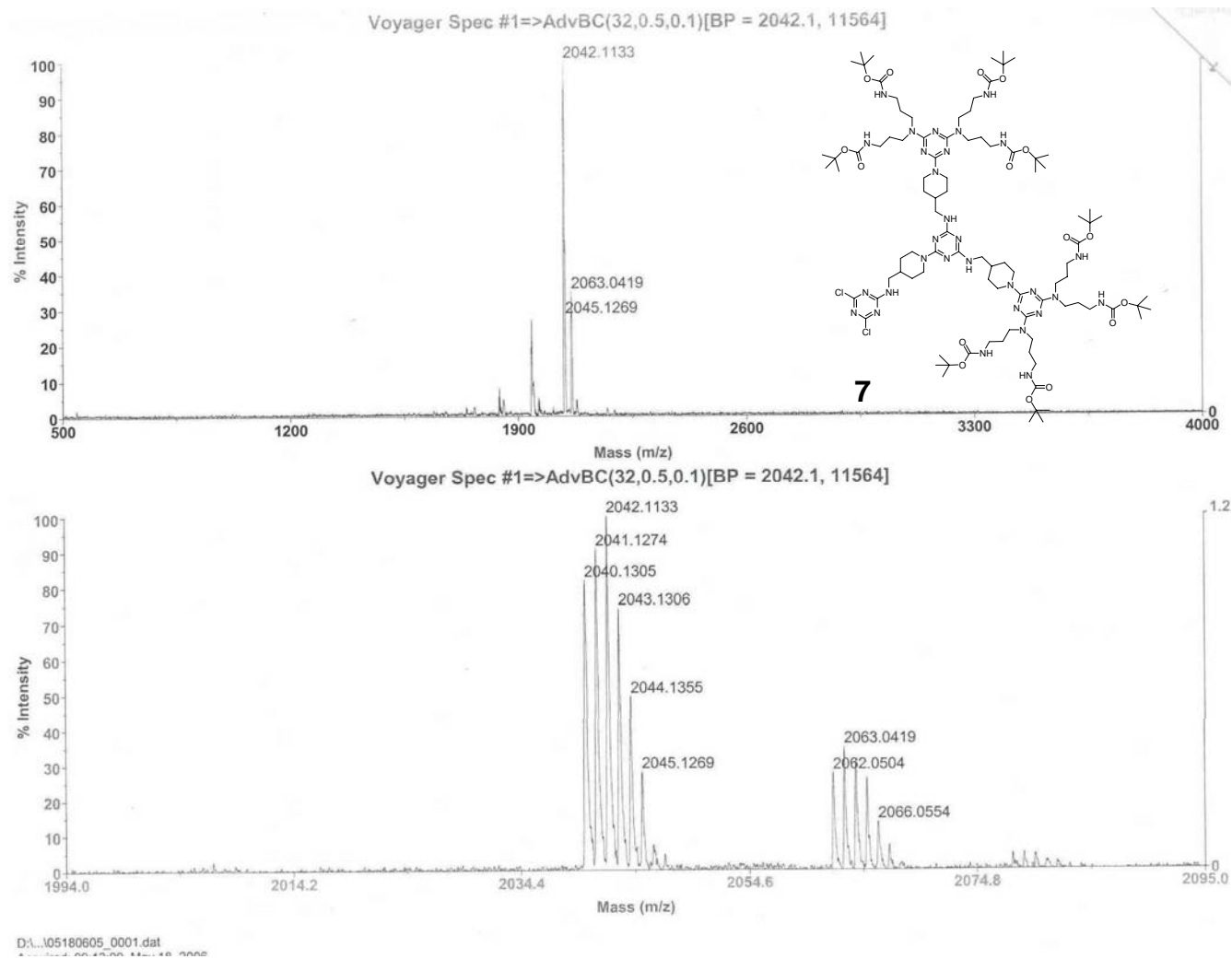


Figure C.7a. The MALDI-TOF mass spectrum of **7**.

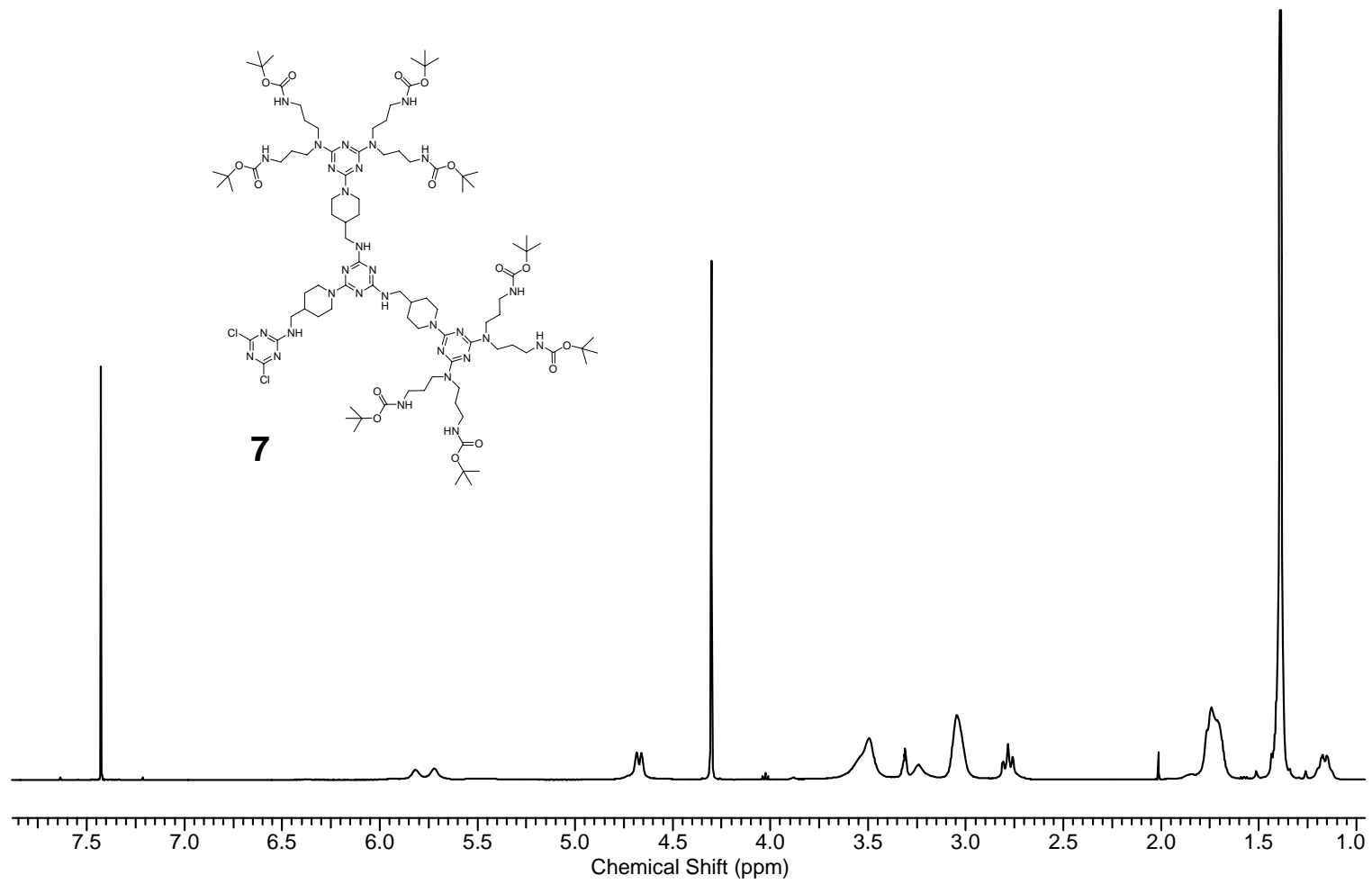


Figure C.7b. The ¹H NMR spectrum of **7**.

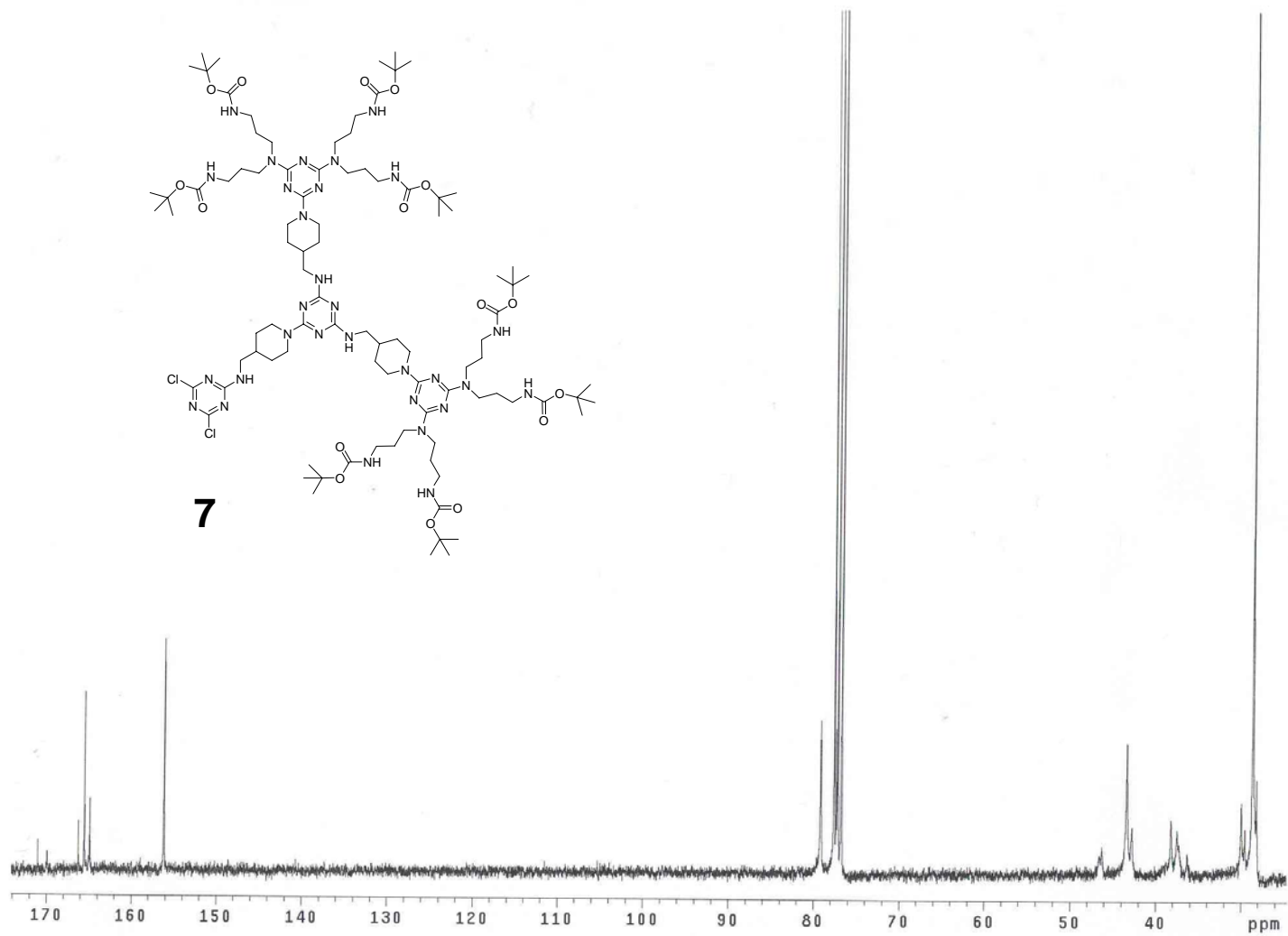


Figure C.7c. The ¹³C NMR spectrum of 7.

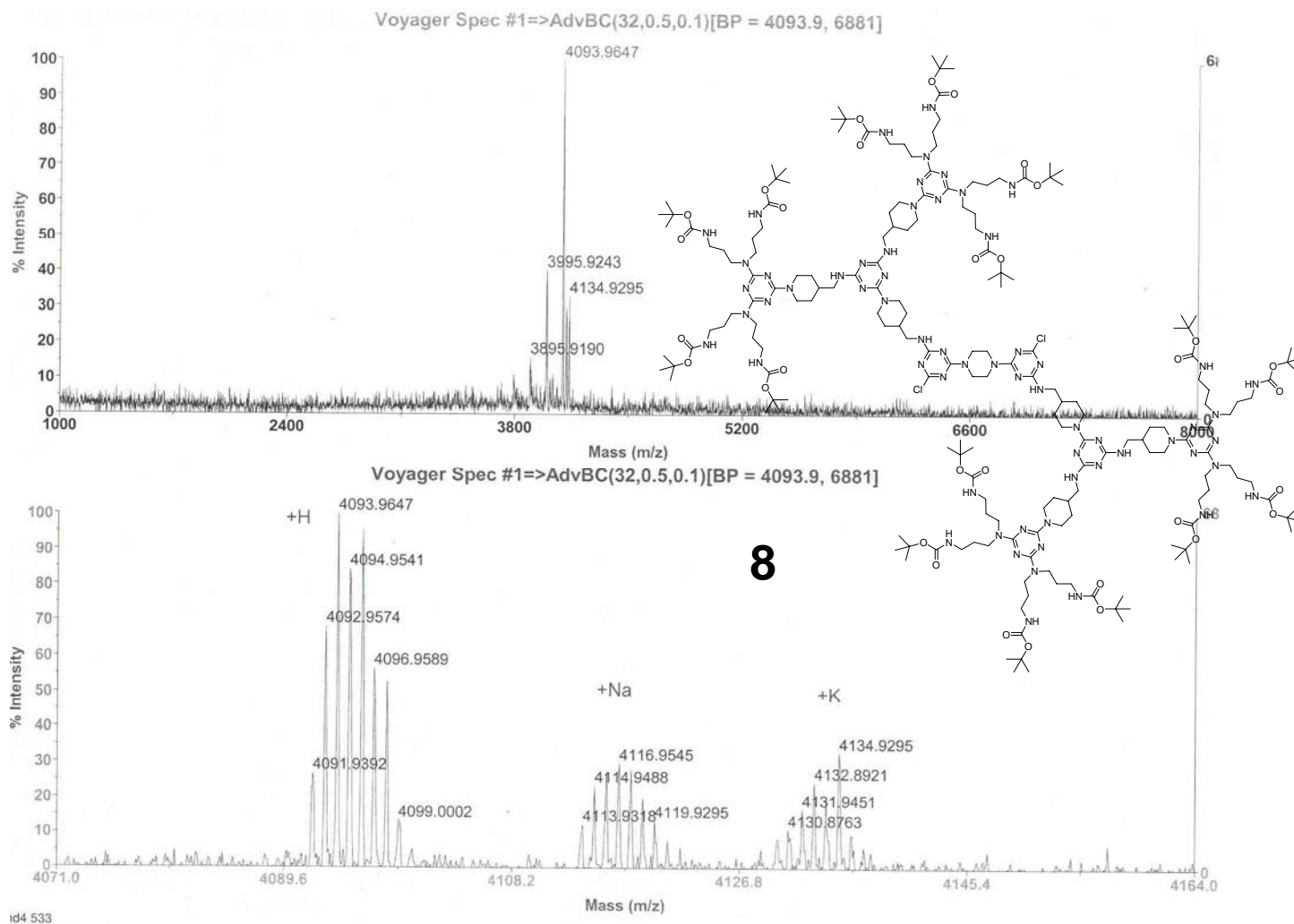


Figure C.8a. The MALDI-TOF mass spectrum of **8**.

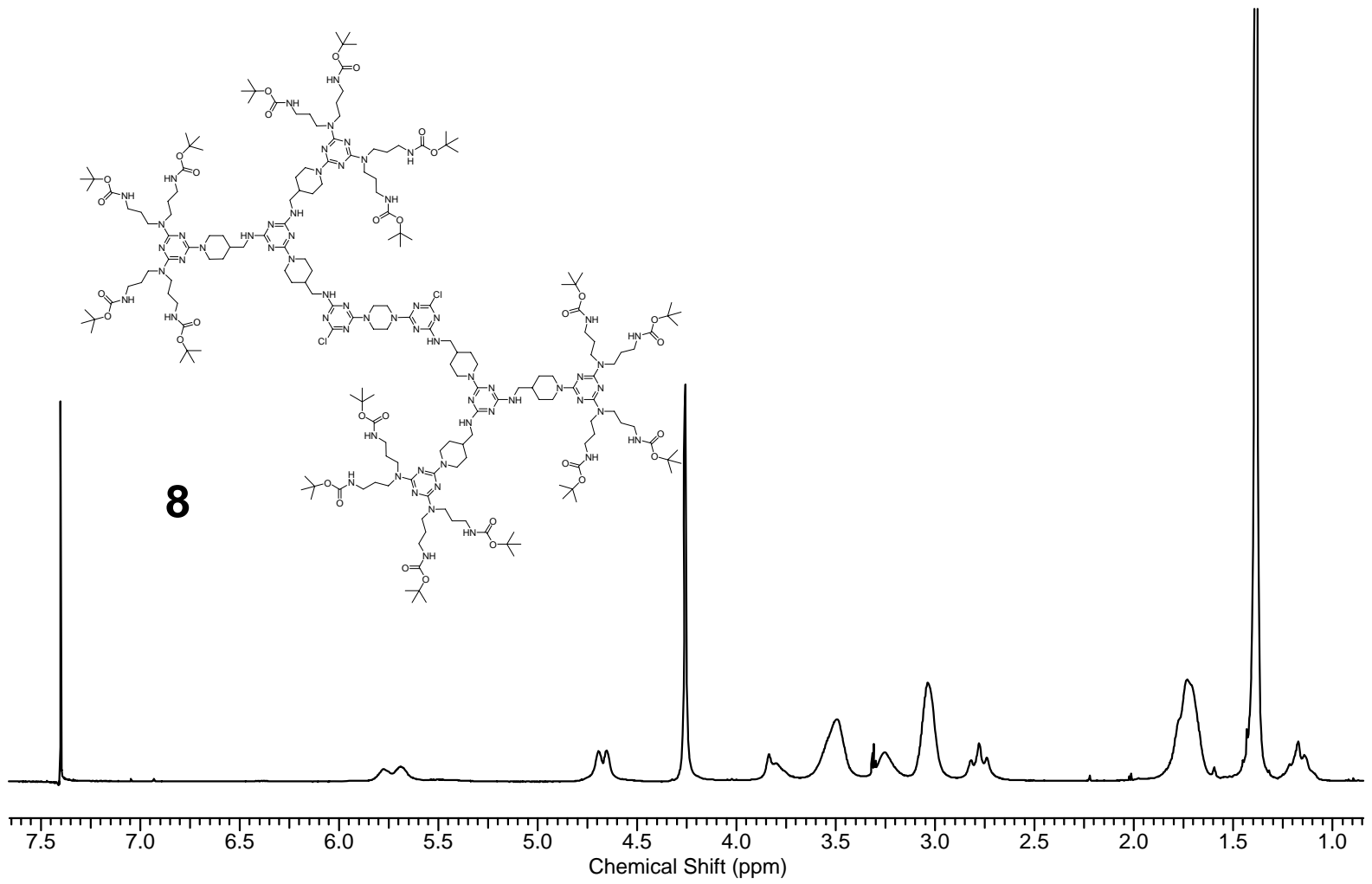


Figure C.8b. The ¹H NMR spectrum of **8**.

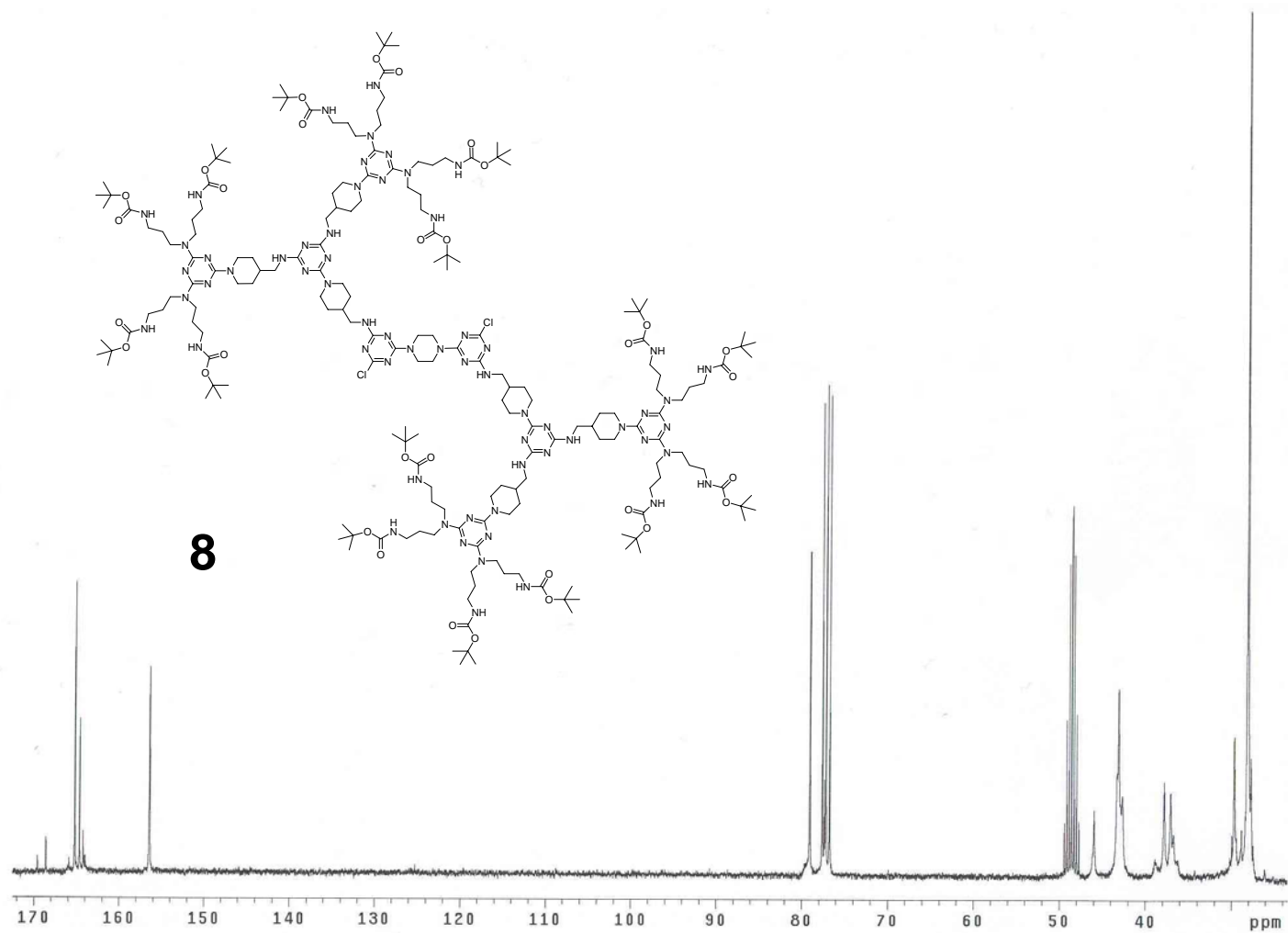


Figure C.8c. The ¹³C NMR spectrum of **8**.

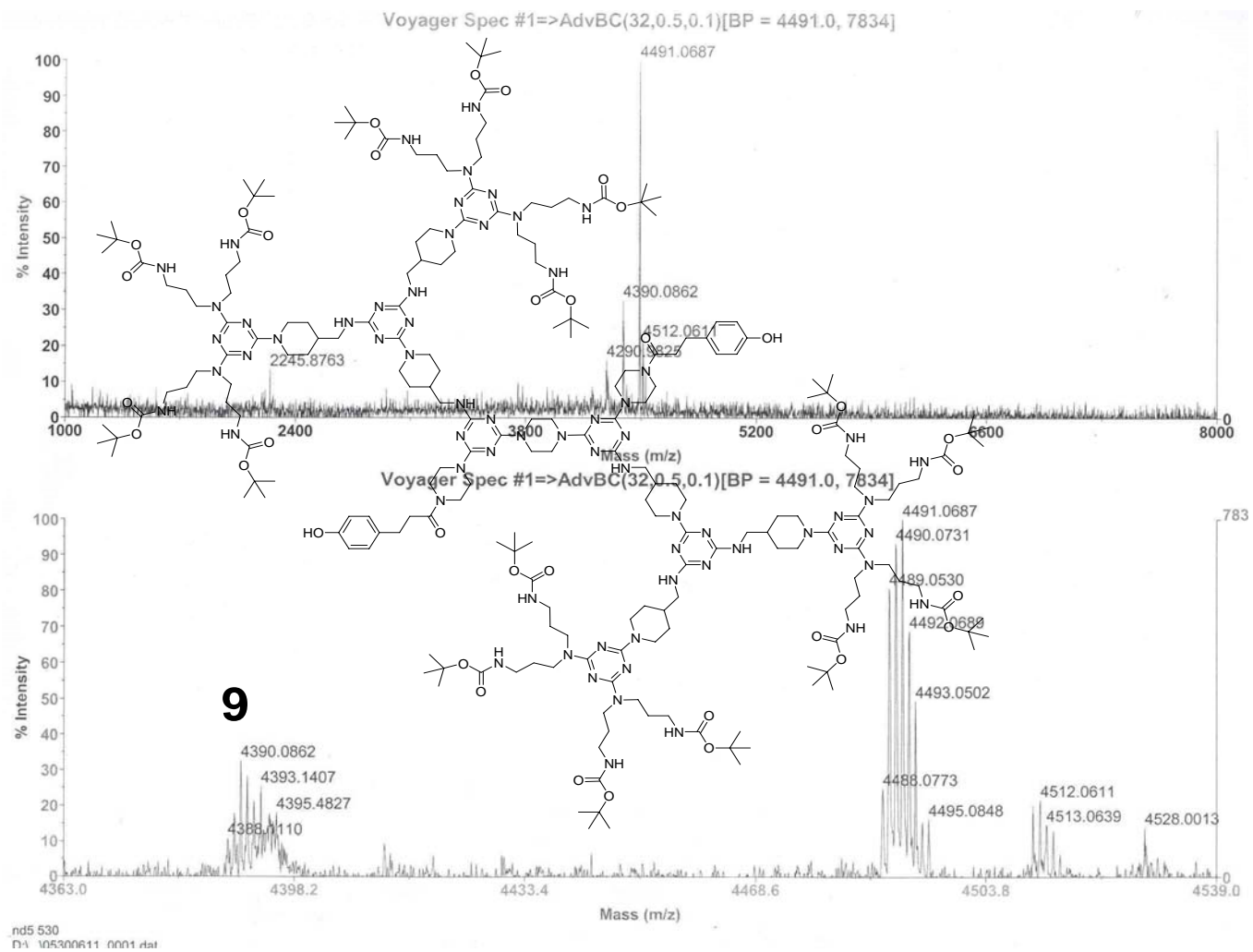


Figure C.9a. The MALDI-TOF mass spectrum of **9**.

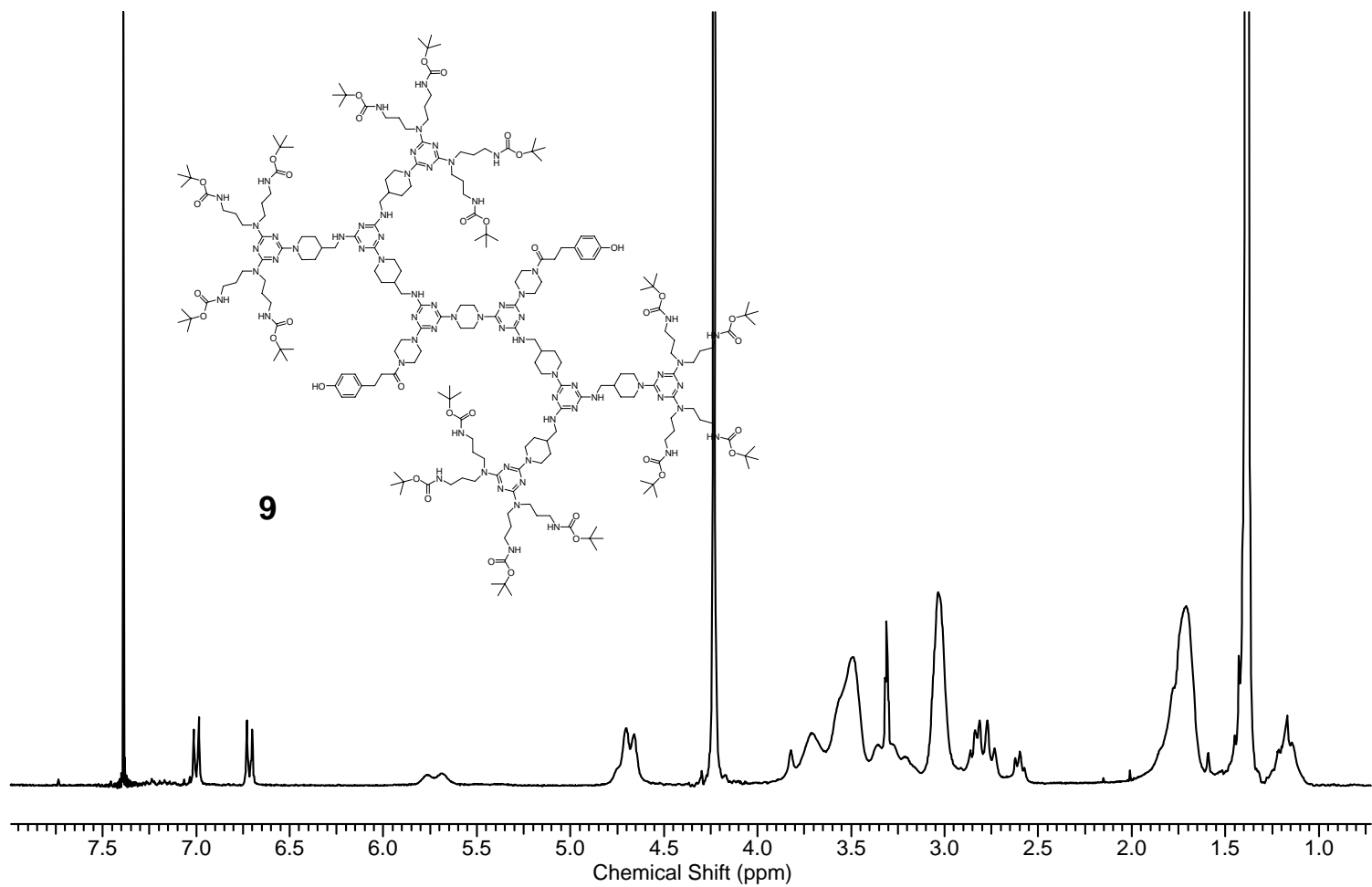


Figure C.9b. The ^1H NMR spectrum of **9**.

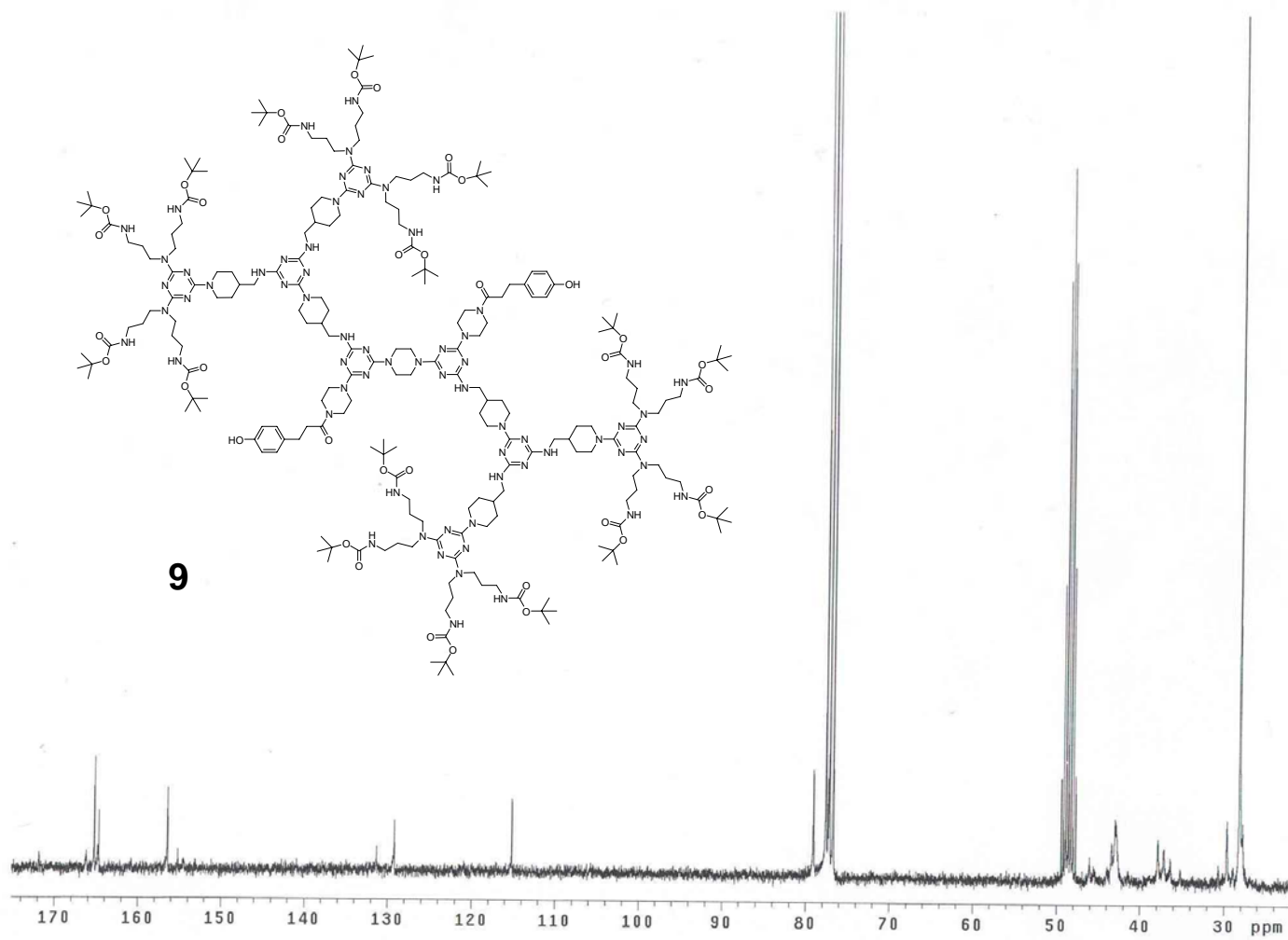


Figure C.9c. The ^{13}C NMR spectrum of **9**.

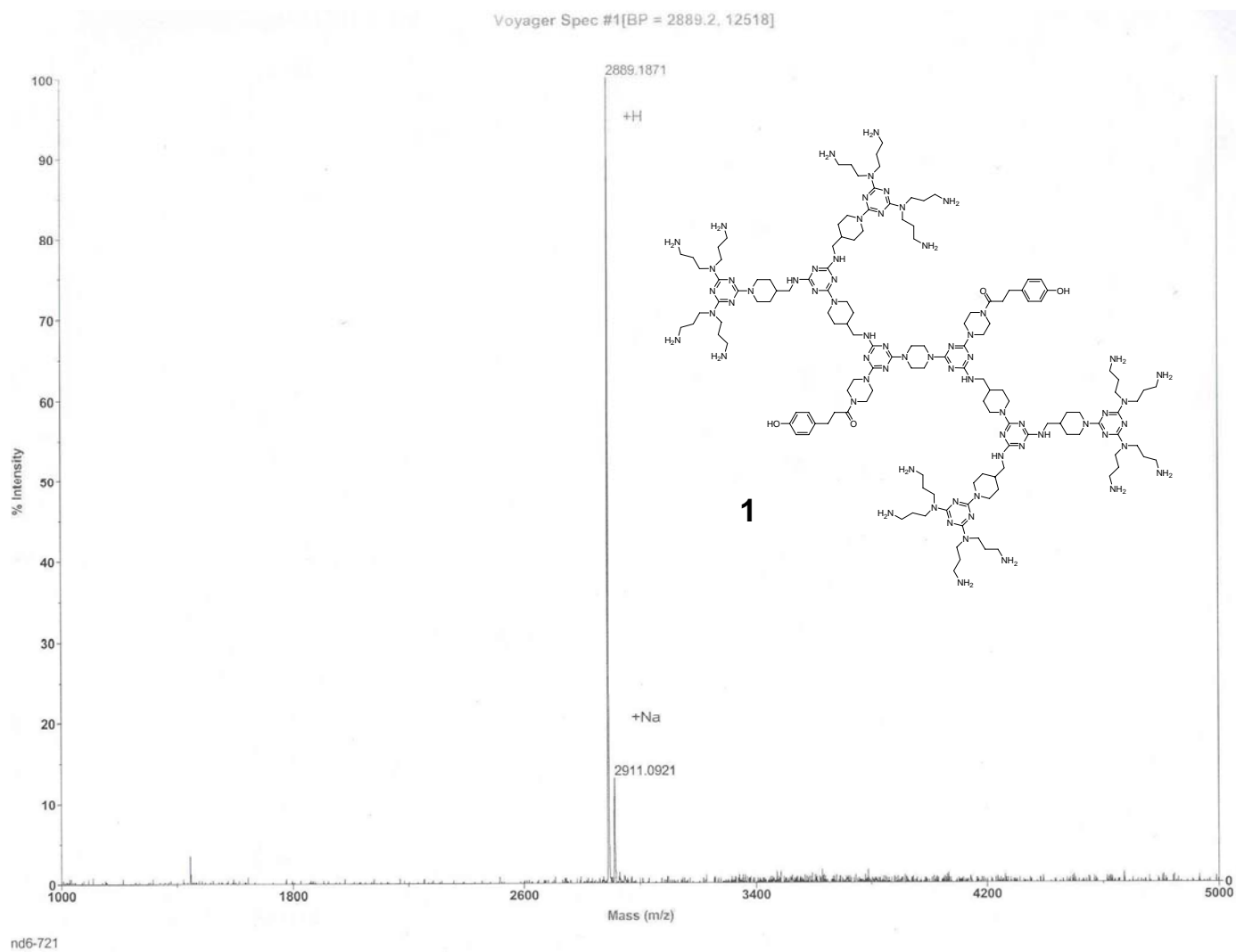


Figure C.10a. The MALDI-TOF mass spectrum of **1**.

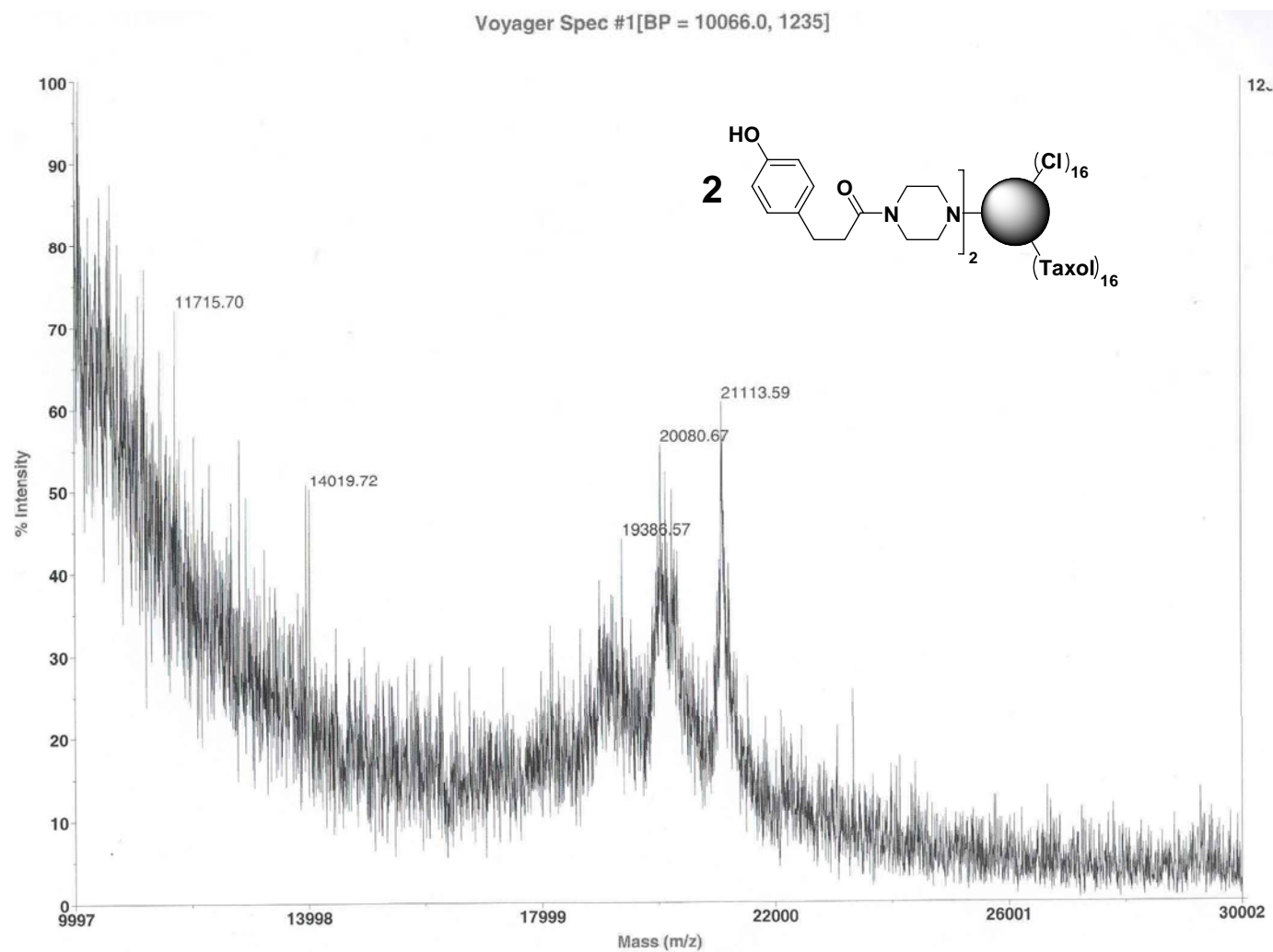


Figure C.11a. The MALDI-TOF mass spectrum of **2**.

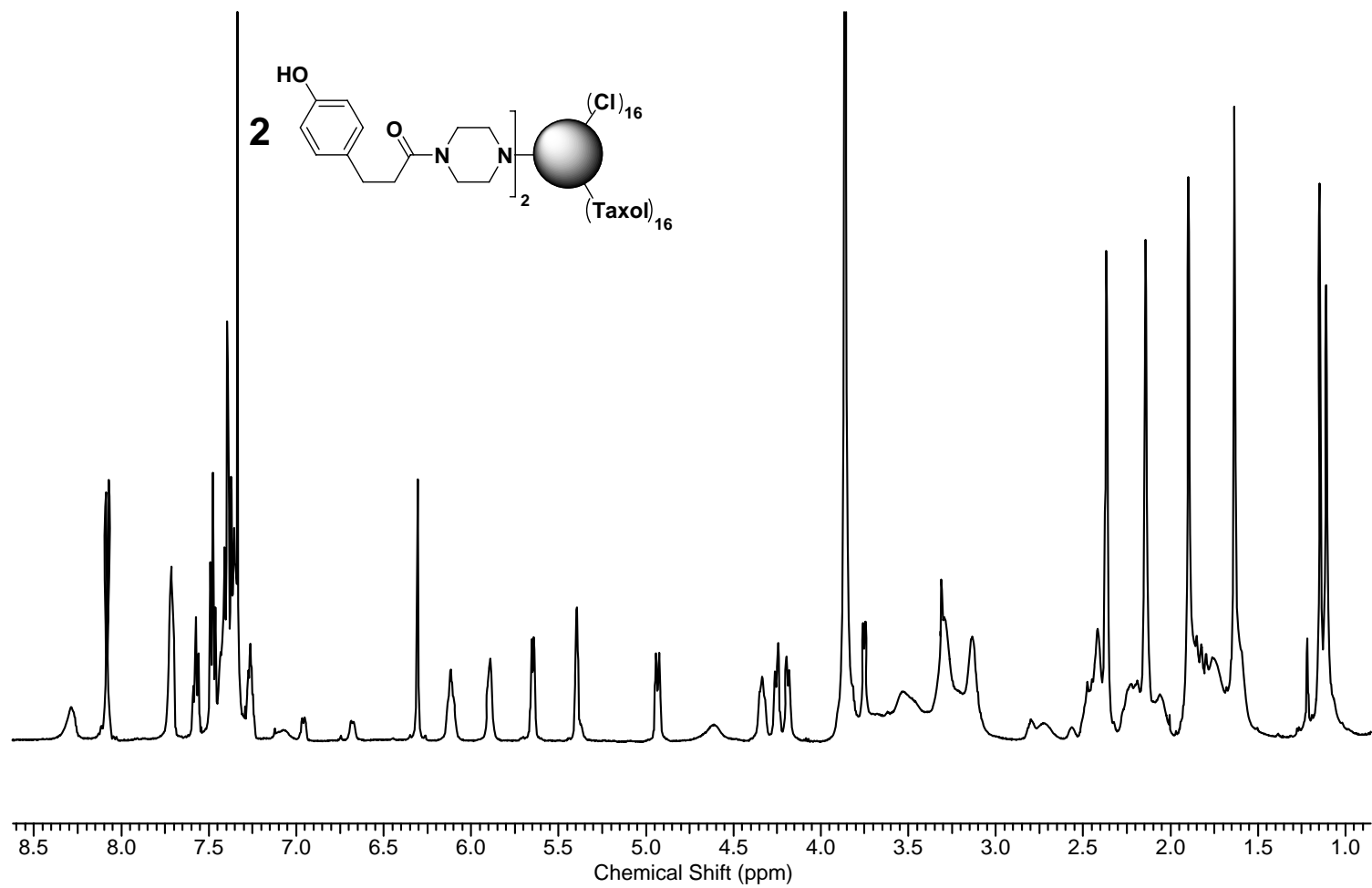


Figure C.11b. The ^1H NMR spectrum of **2**.

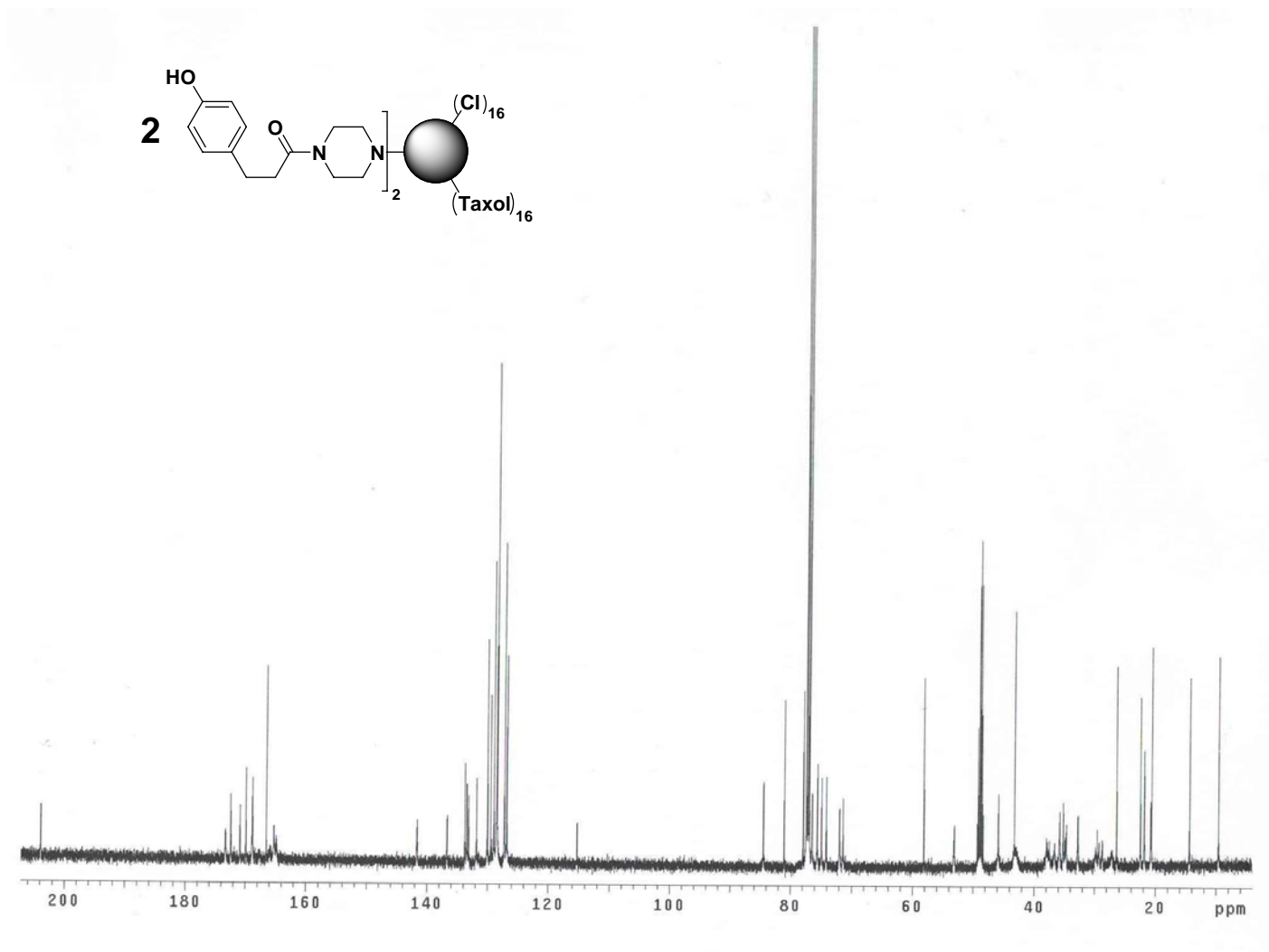


Figure C.11c. The ^{13}C NMR spectrum of **2**.

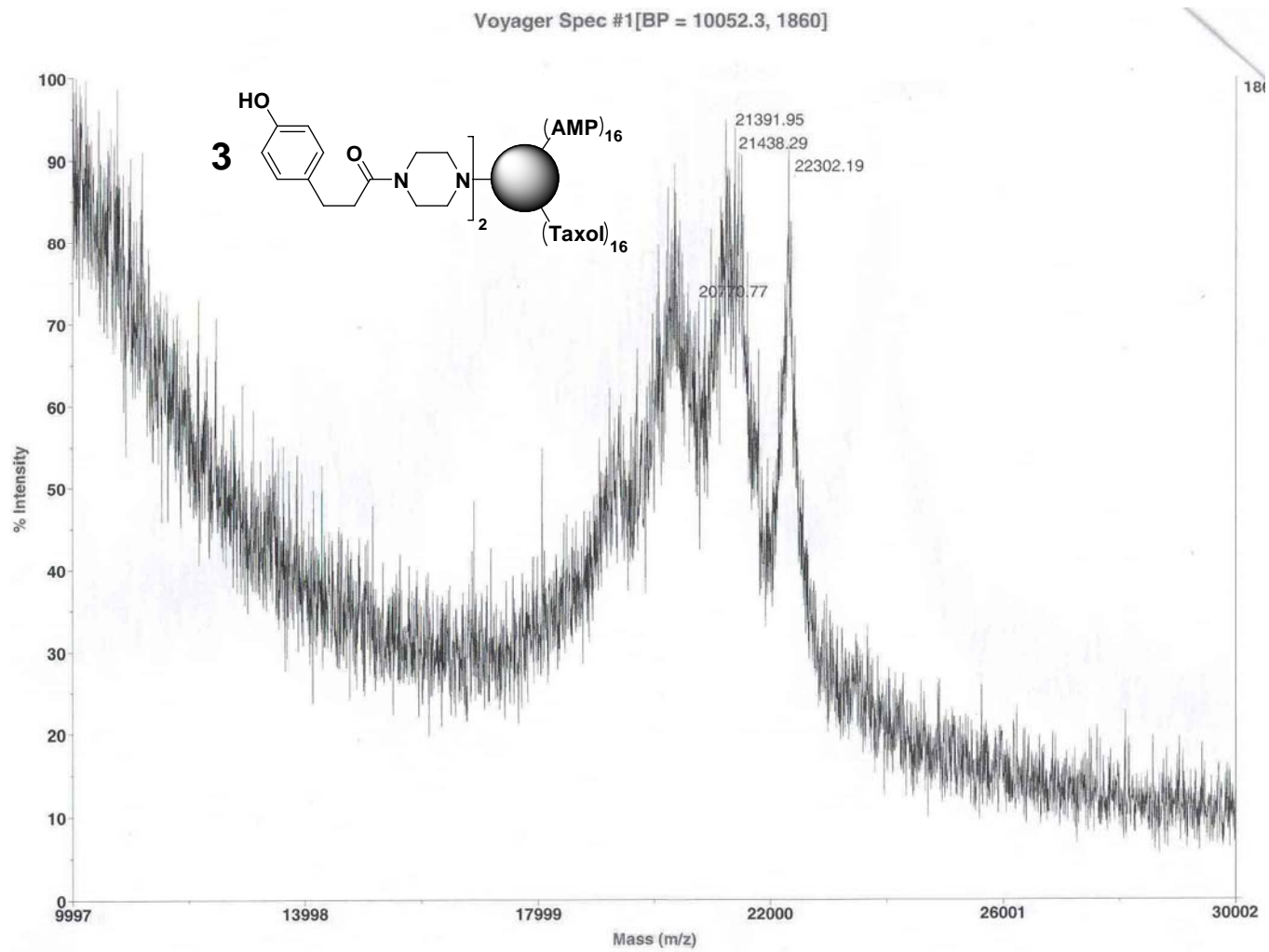


Figure C.12a. The MALDI-TOF mass spectrum of **3**.

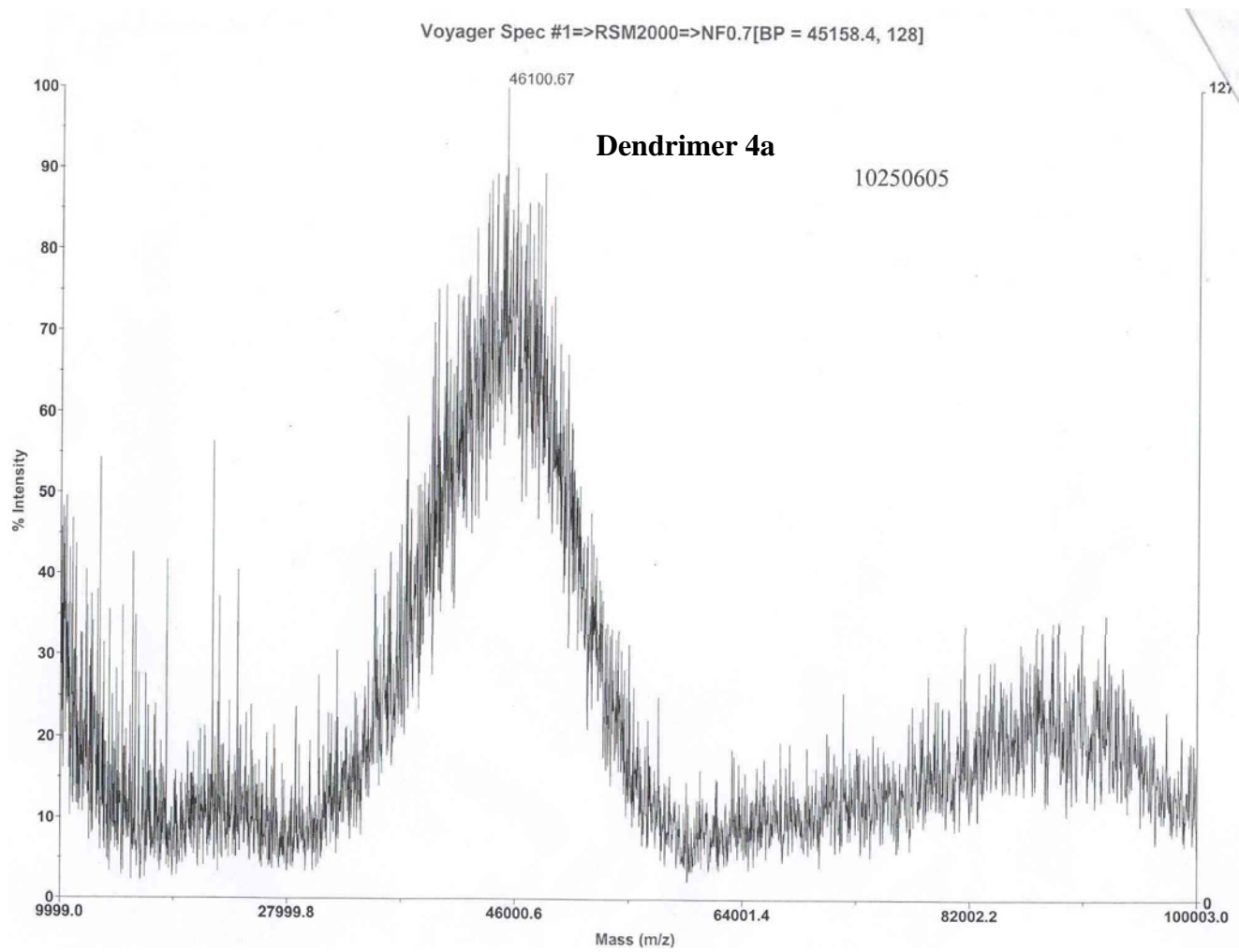


Figure C.13a. The MALDI-TOF mass spectrum of **4a**.

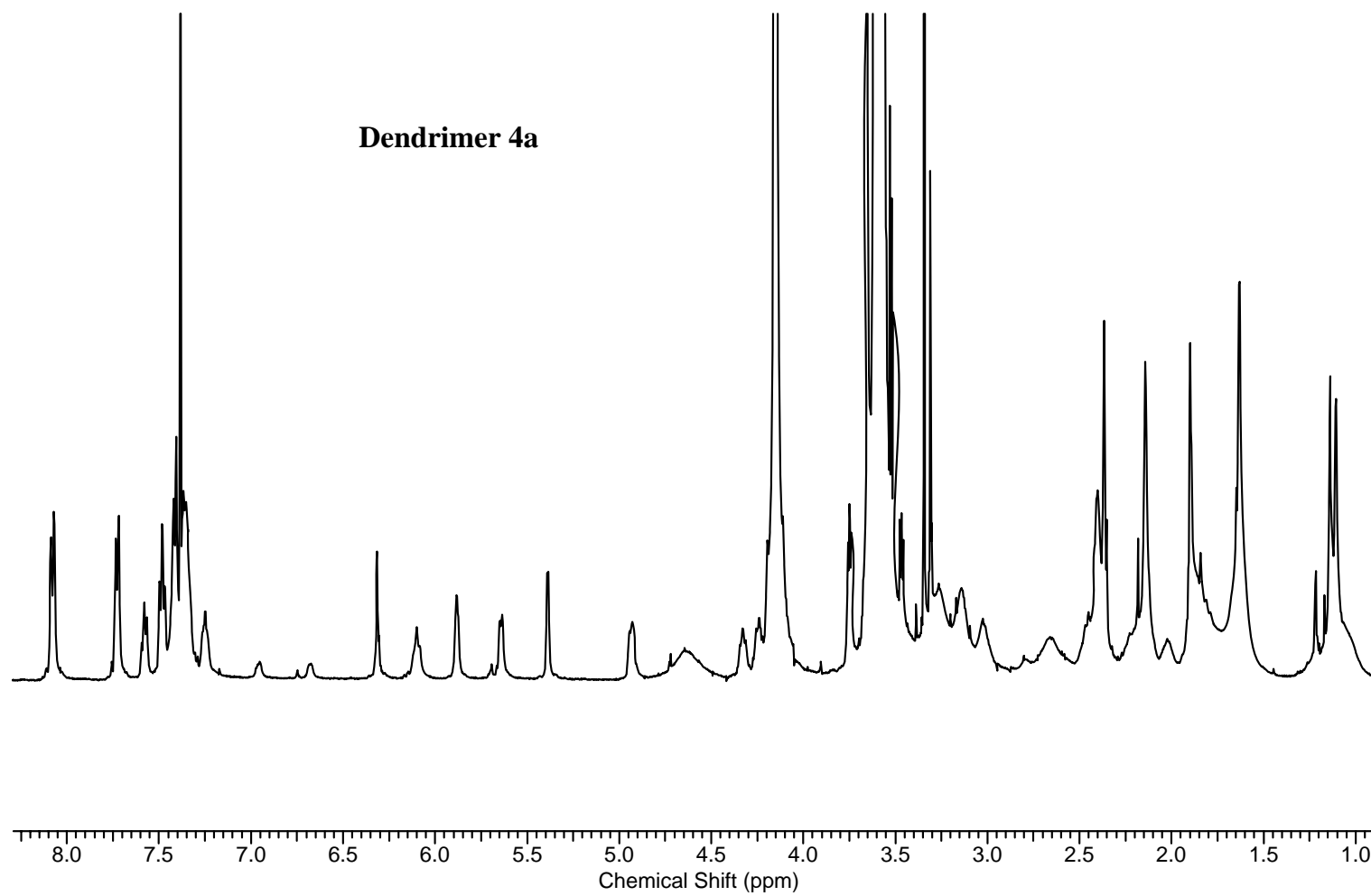


Figure C.13b. The ¹H NMR spectrum of **4a**.

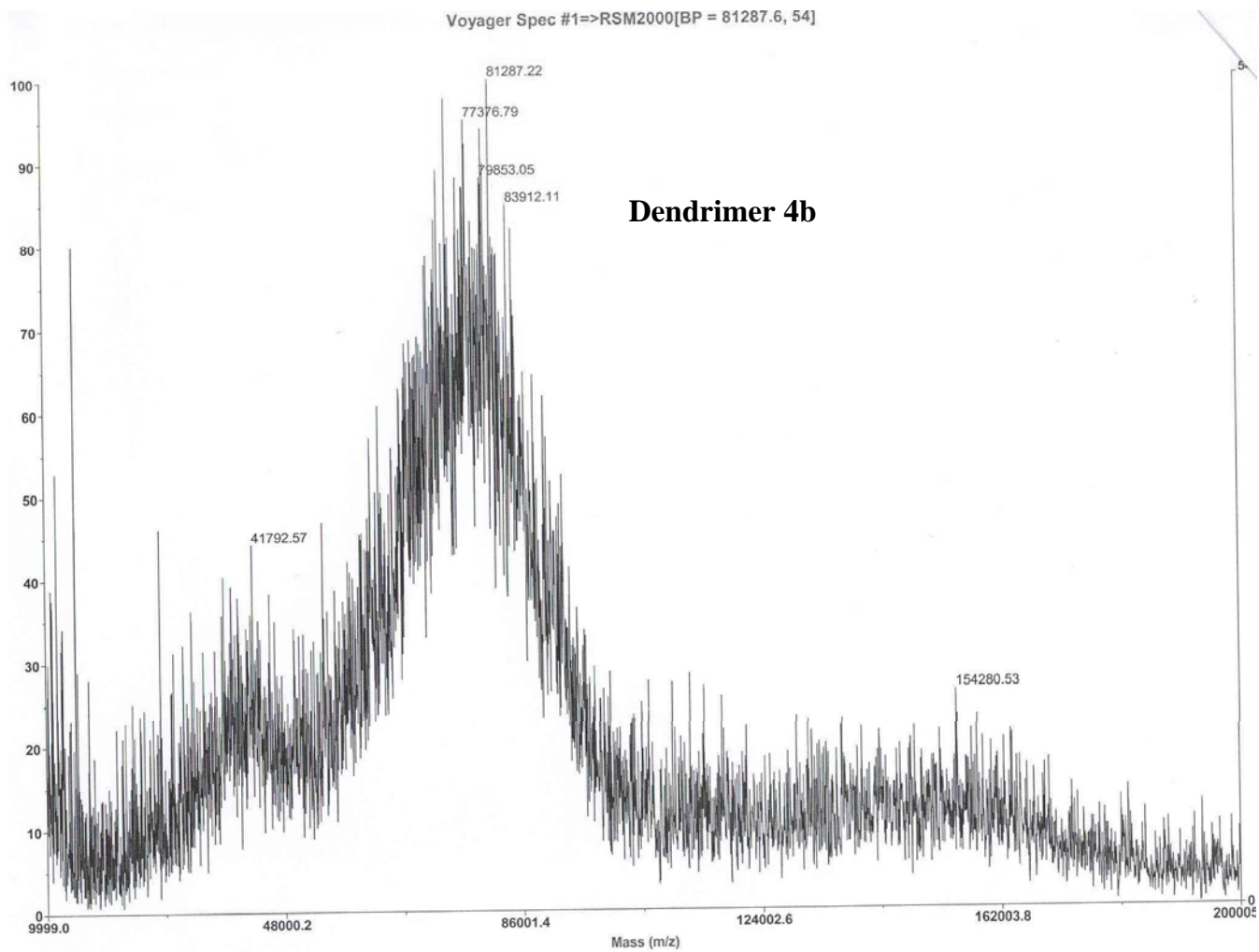


Figure C.14a. The MALDI-TOF mass spectrum of **4b**.

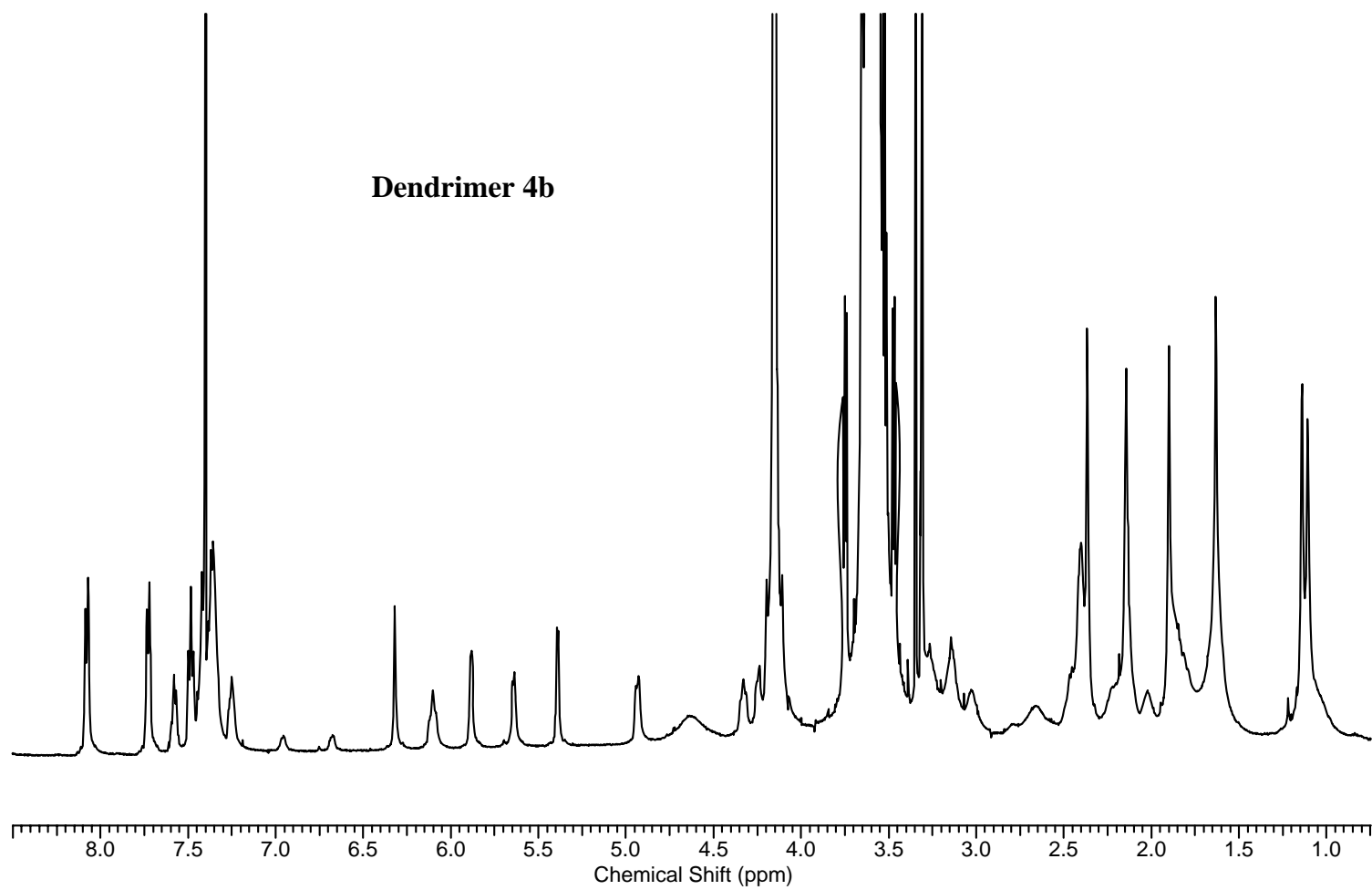


Figure C.14b. The ^1H NMR spectrum of **4b**.

VITA

Name: Jong Doo Lim

Permanent Address: 9-256 Hongeun-2-Dong, Seodaemun-Gu
Seoul, Republic of Korea

Education: Ph.D., Chemistry
Texas A&M University
College Station, TX
August 2007

M.S., Chemistry
Korea University
Seoul, Republic of Korea
February 2001

B.S., Chemistry
Korea University
Seoul, Republic of Korea
February 1999